Balloon Projects

P. de Bernardis

Sapienza Università di Roma - Italy

LiteBIRD Kick-Off Symposium

ISAS/JAXA Tokyo

July 2nd, 2019

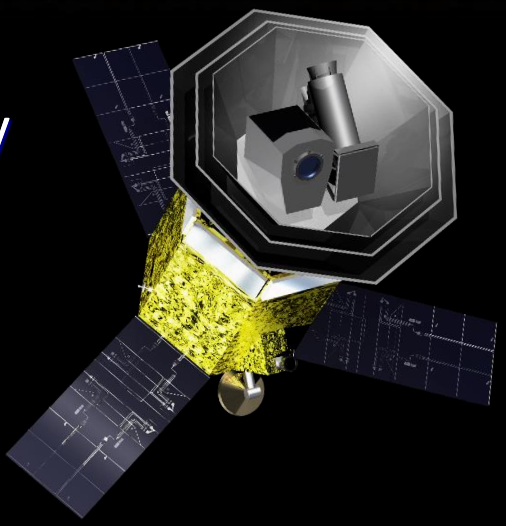

Stratospheric Balloons:

- Near-space carriers able to:
  - Reach ~ 40 km (~ 3 mbar)
  - Stay there for up to 40 days (LDB) and more (ULDB)
  - Lift heavy (2 tons) large payloads (larger than what we can reasonably fly on satellites)
  - Cost roughly 1/100 of a satellite mission
  - Allow for recovery and refly of the payload
- Important for the CMB community:
  - **To carry out sensitive observations at**
    - **high frequency,**
    - **high resolution,**
    - **at the largest angular scales**
  - To qualify instrumentation in preparation of satellite missions
  - To educate young experimentalists !

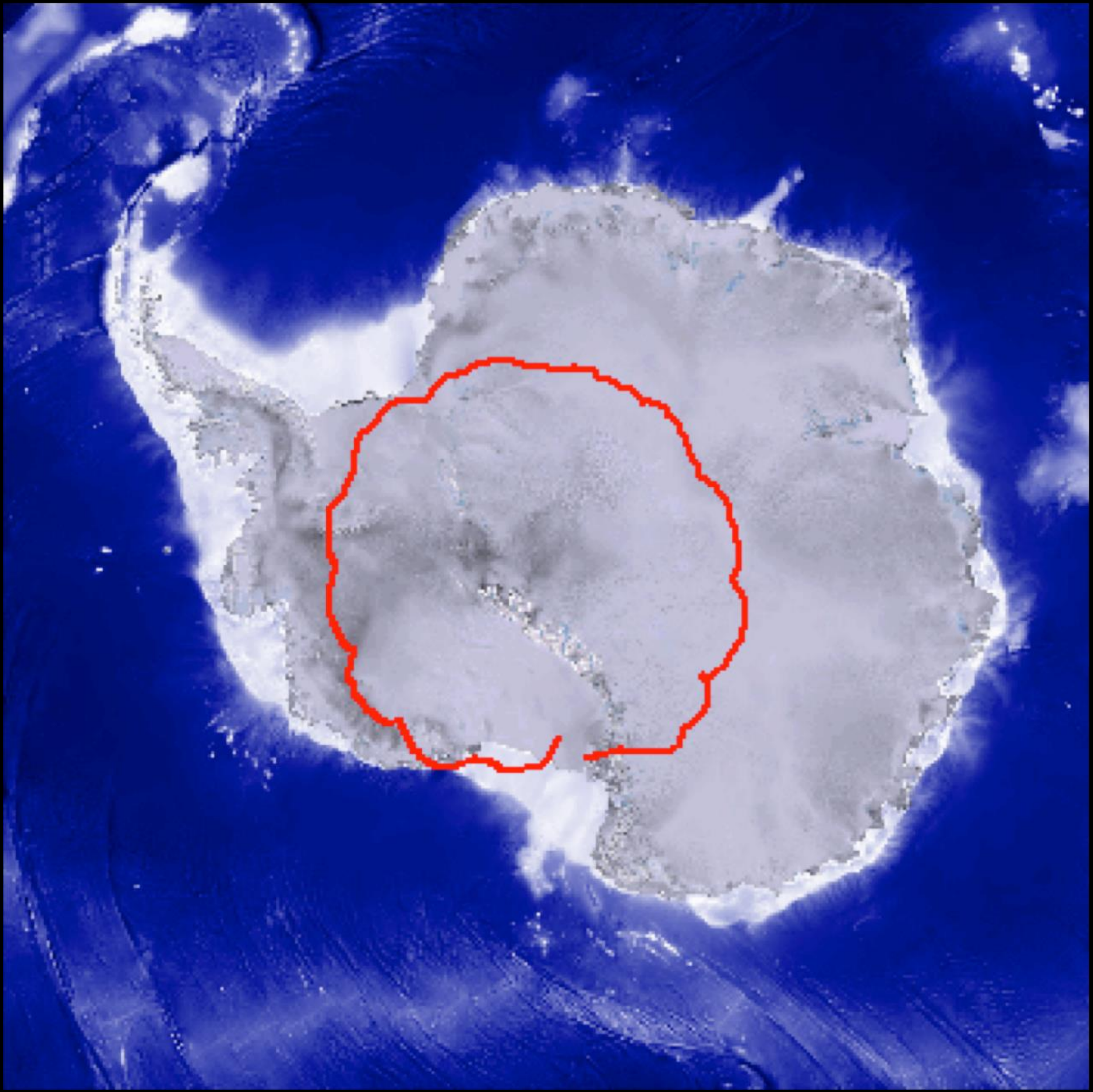

Typical ground-path of a LDB summer flight

Long-duration circumpolar flights (2-4 weeks) for 1-2 tons payloads at 38-40 km altitude

NASA-CSBF :
well established launch facility near McMurdo, Antarctica

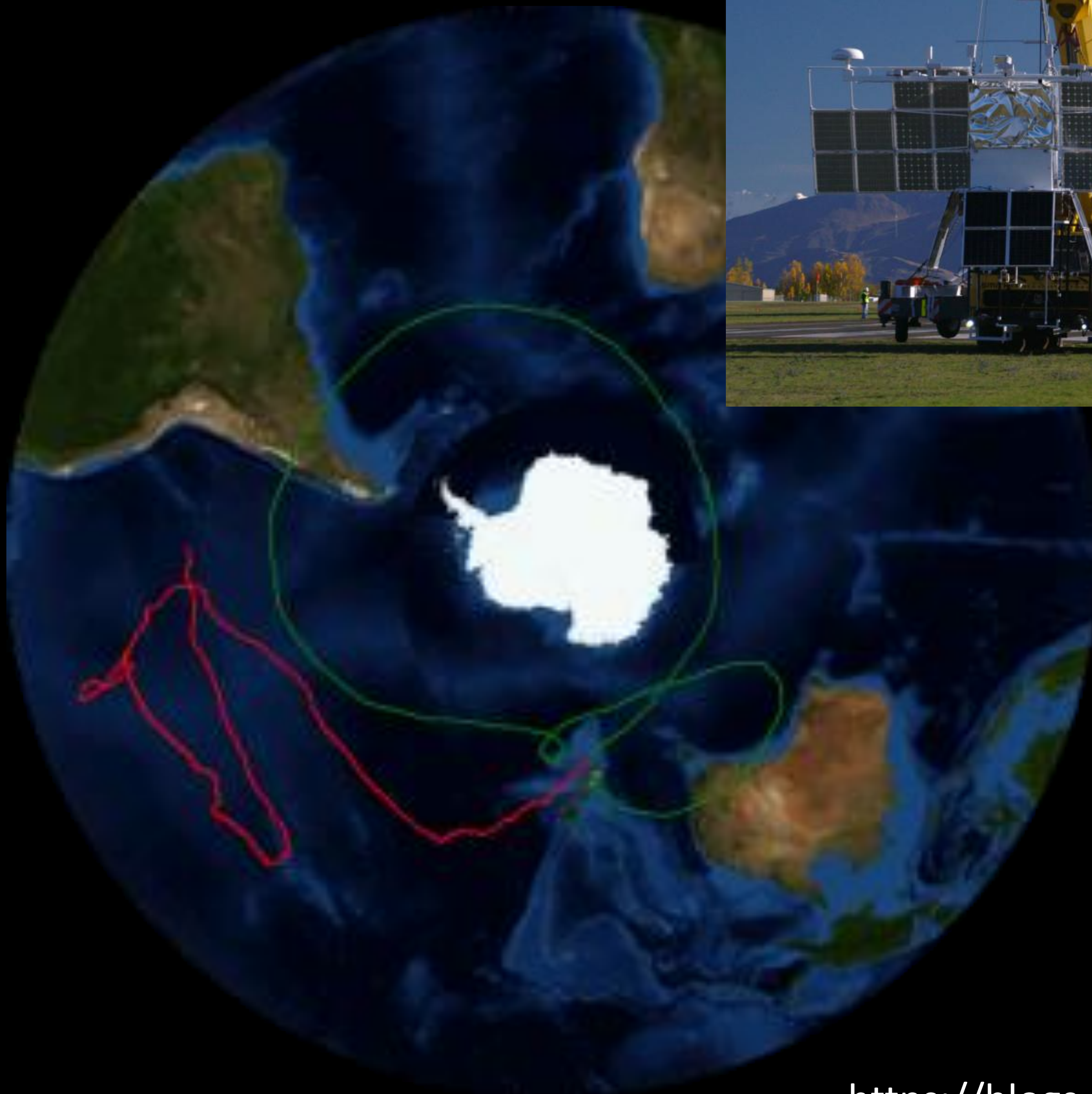

Great progress with super-pressure balloons: COSI payload flown by CSBF in may 2016 for 47 days at altitudes between 33 km and 21 km, with a with a 0.5Mm^3 SPB

ULDB: 30-100 days, 1 ton

https://blogs.nasa.gov/superpressureballoon/

Polar Night Flights

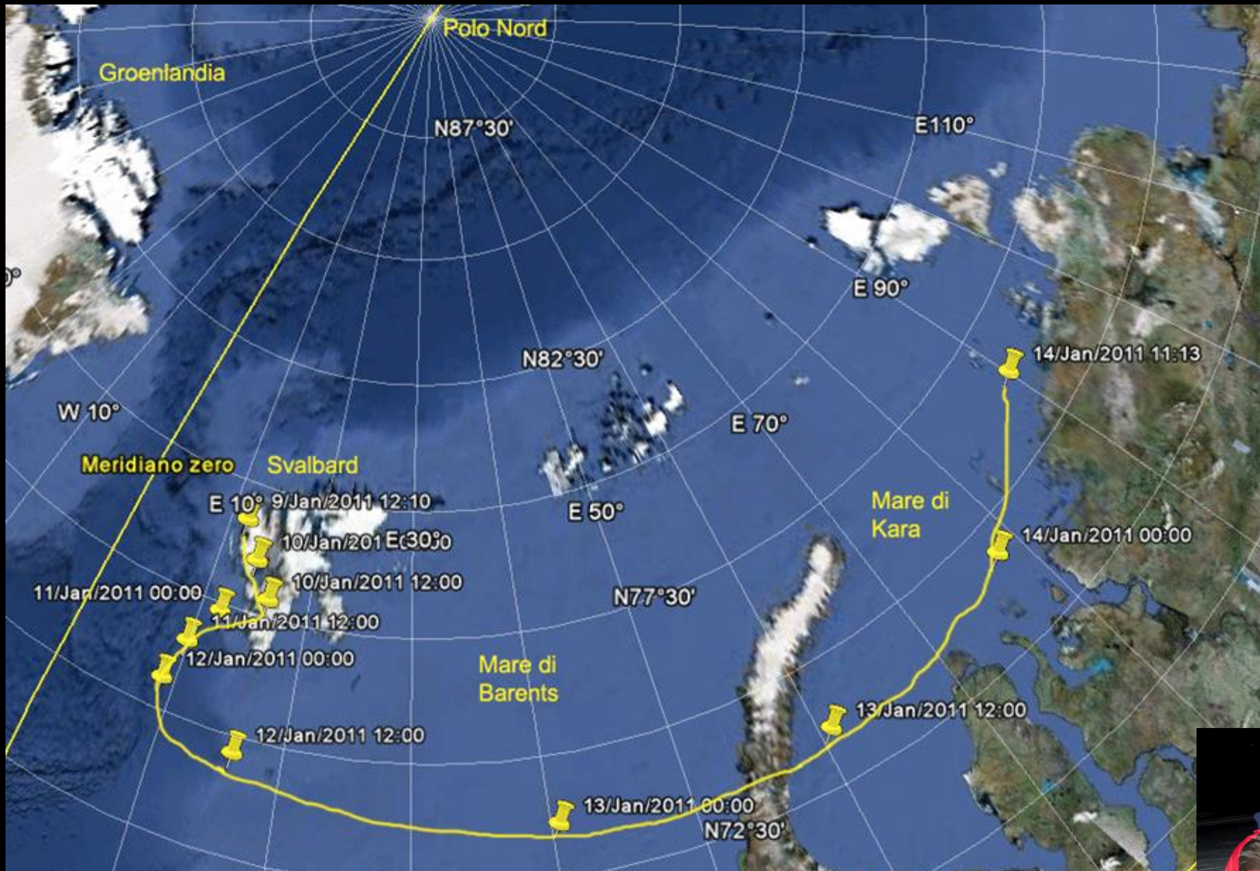

10-20 days winter flights in the Arctic

Stratospheric Balloons:

Disadvantages:

- Stringent limits on mass, power
- Complexity of automation
- Insane integration schedule
- Narrow, and scarce, flight windows
- Risky recovery

Advantage of balloon-borne wrt ground-based: significantly reduced atmospheric emission and fluctuations, mainly at high frequencies

OLIMPO TM
Arctic test
flight, 2014

Atmospheric Emission at different altitudes

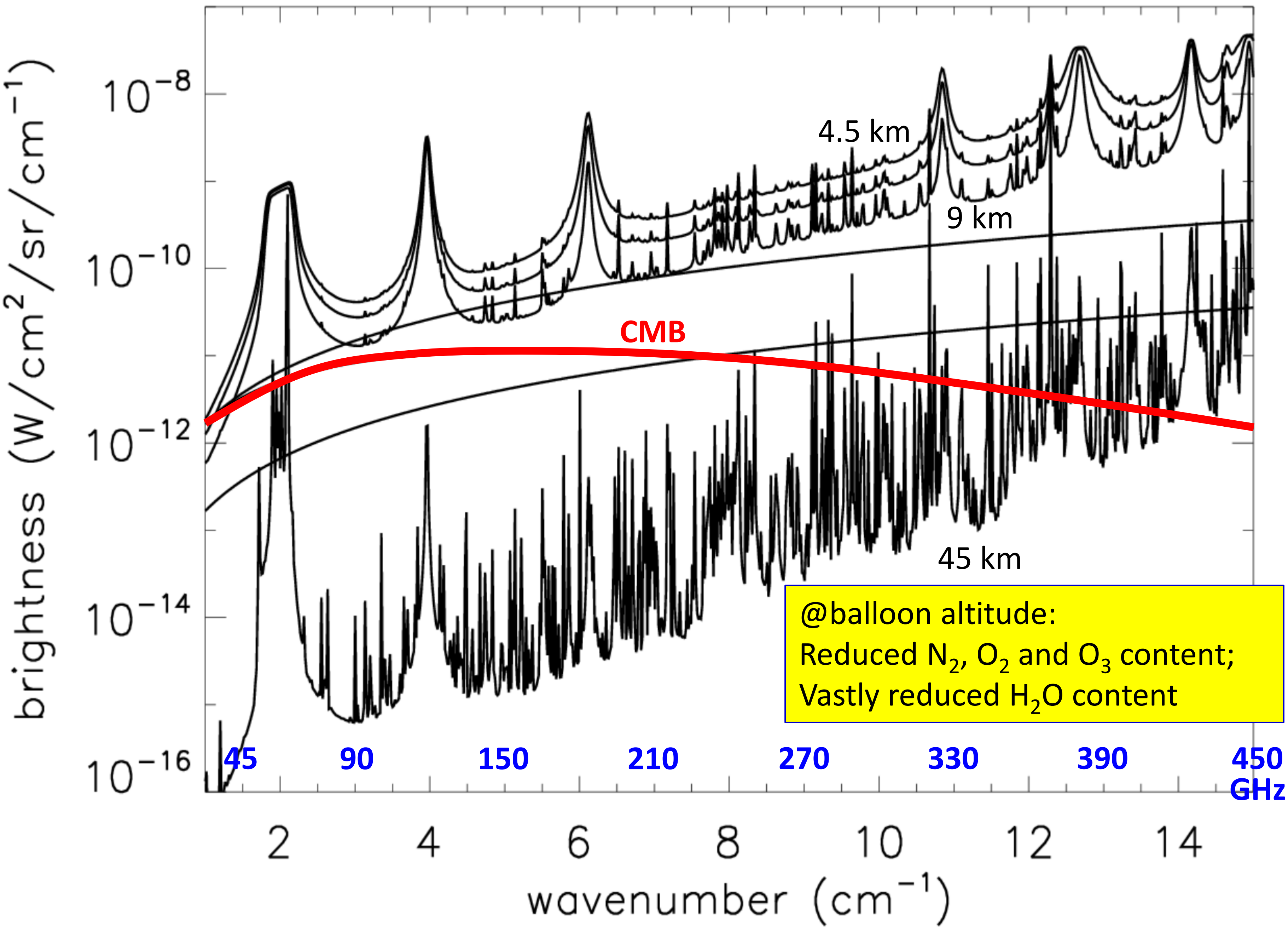

Atmospheric Emission at different altitudes

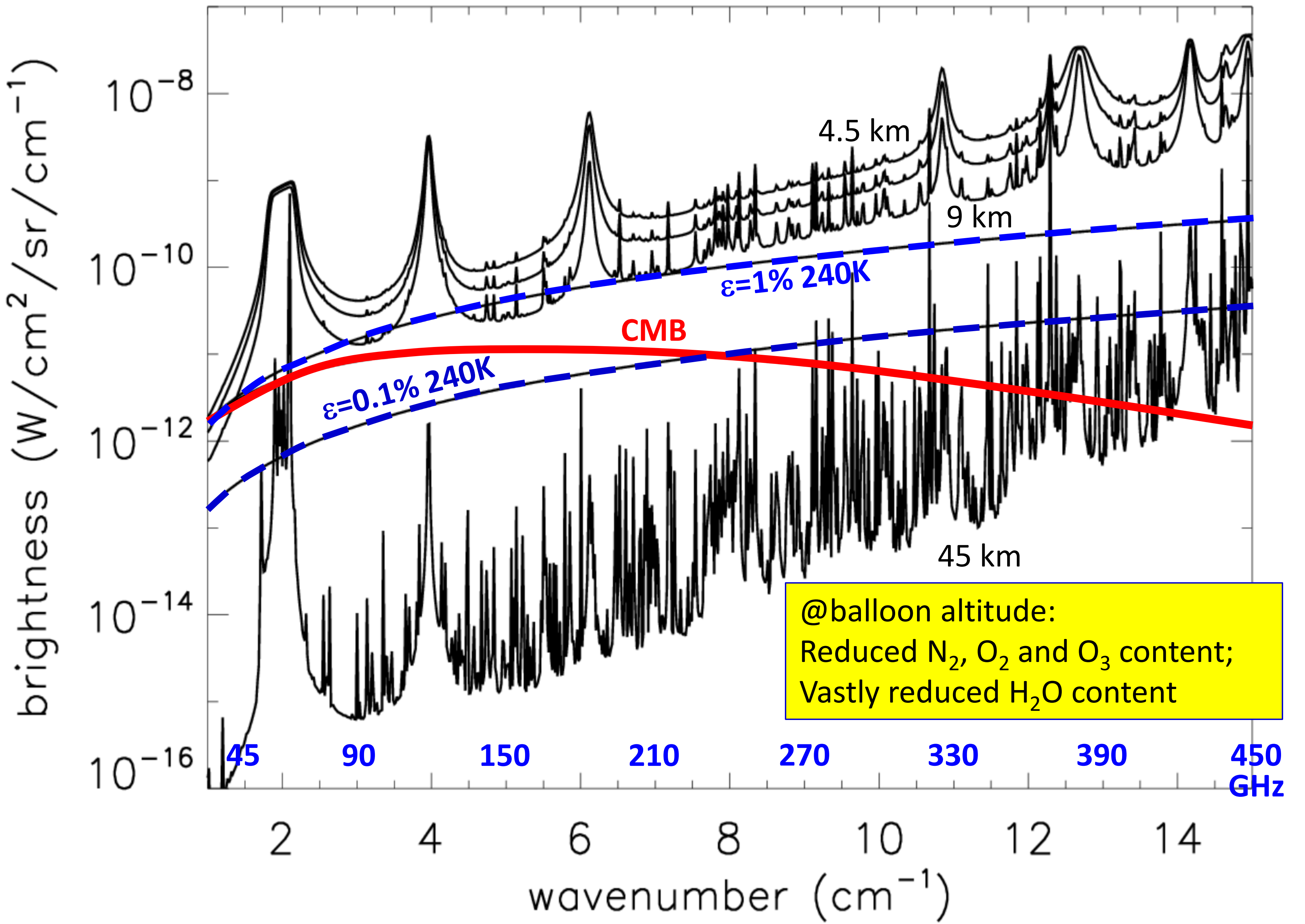

Atmospheric Emission at different altitudes

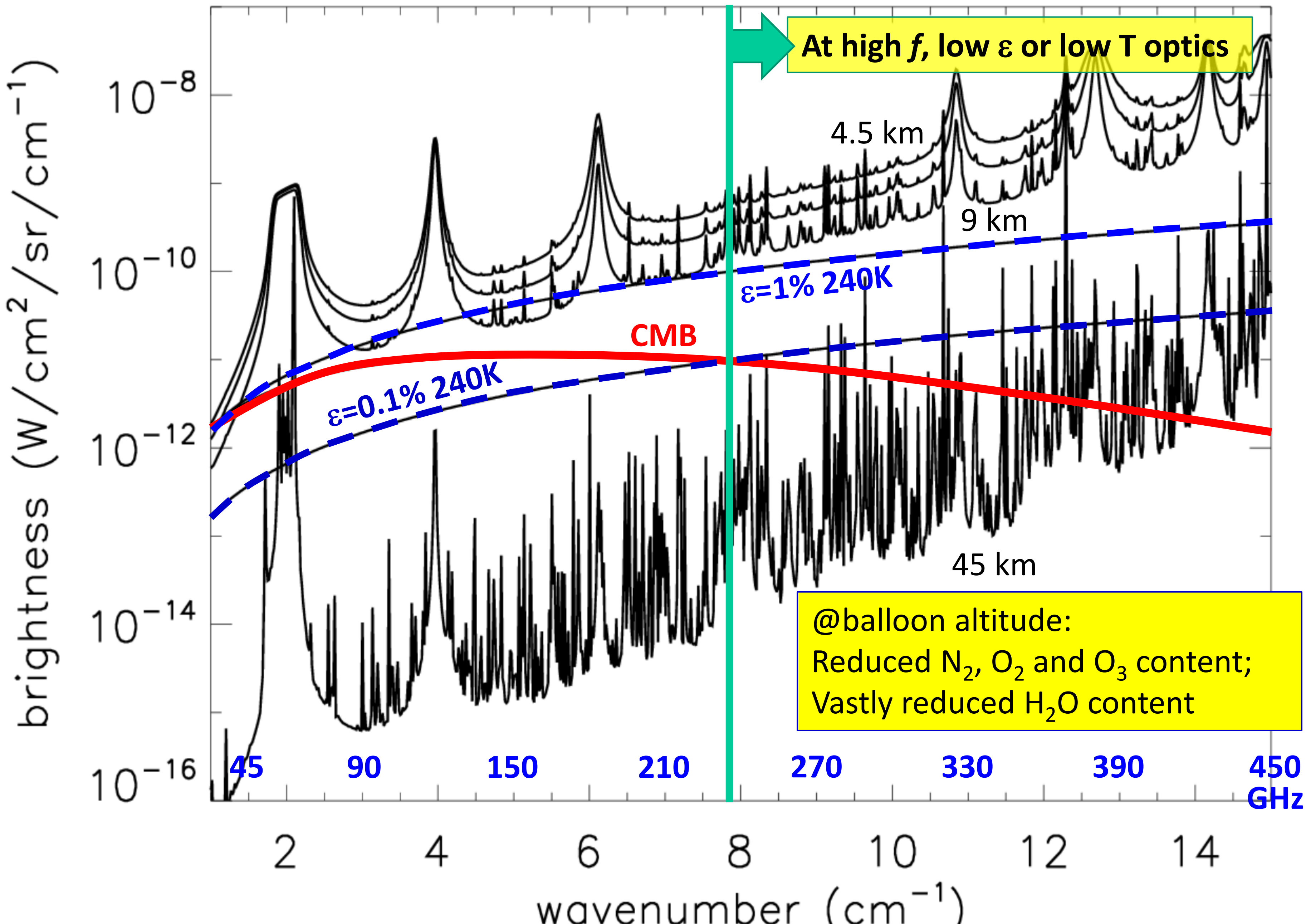

Photon noise from the local environment for CMB observations

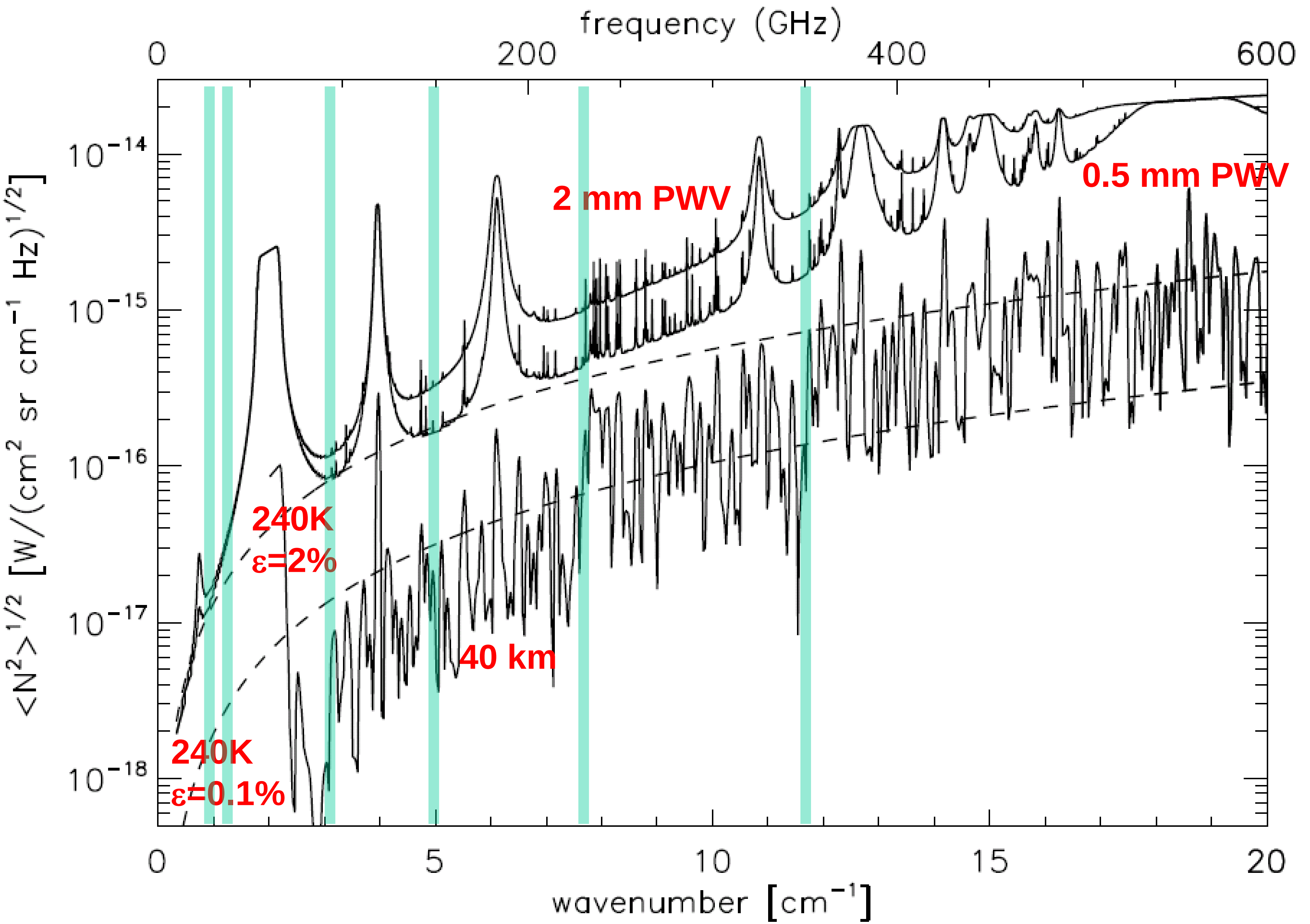

@150 GHz : One day on a balloon …

	GHz	GHz	BKG 4.5km e=0.01	BKG 6.0km e=0.01	BKG 9.0km e=0.01	BKG 45km e=0.001	Space,40K	CMB
0	34	45	2.63	2.14	1.57	0.57	0.53	0.52
1	82	105	5.58	4.39	3.12	0.80	0.70	0.68
2	132	168	8.35	5.95	4.03	0.75	0.59	0.55
3	187	253	26.39	17.08	10.28	0.78	0.47	0.41
4	229	310	39.81	25.70	15.33	0.74	0.33	0.25
5	336	364	27.28	15.65	7.66	0.22	0.05	0.03

pW

	GHz	GHz	NEP 4.5km e=0.01	NEP 6.0km e=0.01	NEP 9.0km e=0.01	NEP 45km e=0.001	Space,40K	CMB
0	34	45	1.06E-017	1.06E-017	7.49E-018	5.51E-018	5.29E-018	5.24E-018
1	82	105	2.57E-017	2.30E-017	1.99E-017	1.00E-017	9.35E-018	9.19E-018
2	132	168	4.10E-017	3.55E-017	2.90E-017	1.22E-017	1.08E-017	1.05E-017
3	187	253	8.78E-017	7.02E-017	5.55E-017	1.51E-017	1.17E-017	1.09E-017
4	229	310	1.20E-016	9.53E-017	7.53E-017	1.63E-017	1.08E-017	9.50E-018
5	336	364	1.13E-016	8.58E-017	5.86E-017	1.02E-017	4.90E-018	3.55E-018

$W/\sqrt{Hz}$

… is like >16 days at the best site on the ground …

@150 GHz : One day on a balloon …

	GHz	GHz	BKG 4.5km e=0.01	BKG 6.0km e=0.01	BKG 9.0km e=0.01	BKG 45km e=0.001	Space,40K	CMB
0	34	45	2.63	2.14	1.57	0.57	0.53	0.52
1	82	105	5.58	4.39	3.12	0.80	0.70	0.68
2	132	168	8.35	5.95	4.03	0.75	0.59	0.55
3	187	253	26.39	17.08	10.28	0.78	0.47	0.41
4	229	310	39.81	25.70	15.33	0.74	0.33	0.25
5	336	364	27.28	15.65	7.66	0.22	0.05	0.03

pW

	GHz	GHz	NEP 4.5km e=0.01	NEP 6.0km e=0.01	NEP 9.0km e=0.01	NEP 45km e=0.001	Space,40K	CMB
0	34	45	1.06E-017	1.06E-017	7.49E-018	5.51E-018	5.29E-018	5.24E-018
1	82	105	2.57E-017	2.30E-017	1.99E-017	1.00E-017	9.35E-018	9.19E-018
2	132	168	4.10E-017	3.55E-017	2.90E-017	1.22E-017	1.08E-017	1.05E-017
3	187	253	8.78E-017	7.02E-017	5.55E-017	1.51E-017	1.17E-017	1.09E-017
4	229	310	1.20E-016	9.53E-017	7.53E-017	1.63E-017	1.08E-017	9.50E-018
5	336	364	1.13E-016	8.58E-017	5.86E-017	1.02E-017	4.90E-018	3.55E-018

$W/\sqrt{Hz}$

… is close to one day in deep space

@350 GHz : One day on a balloon …

	GHz	GHz	BKG 4.5km e=0.01	BKG 6.0km e=0.01	BKG 9.0km e=0.01	BKG 45km e=0.001	Space,40K	CMB	
0	34	45	2.63	2.14	1.57	0.57	0.53	0.52	
1	82	105	5.58	4.39	3.12	0.80	0.70	0.68	
2	132	168	8.35	5.95	4.03	0.75	0.59	0.55	
3	187	253	26.39	17.08	10.28	0.78	0.47	0.41	pW
4	229	310	39.81	25.70	15.33	0.74	0.33	0.25	
5	336	364	27.28	15.65	7.66	0.22	0.05	0.03	

	GHz	GHz	NEP 4.5km e=0.01	NEP 6.0km e=0.01	NEP 9.0km e=0.01	NEP 45km e=0.001	Space,40K	CMB	
0	34	45	1.06E-017	1.06E-017	7.49E-018	5.51E-018	5.29E-018	5.24E-018	
1	82	105	2.57E-017	2.30E-017	1.99E-017	1.00E-017	9.35E-018	9.19E-018	
2	132	168	4.10E-017	3.55E-017	2.90E-017	1.22E-017	1.08E-017	1.05E-017	
3	187	253	8.78E-017	7.02E-017	5.55E-017	1.51E-017	1.17E-017	1.09E-017	$W/\sqrt{Hz}$
4	229	310	1.20E-016	9.53E-017	7.53E-017	1.63E-017	1.08E-017	9.50E-018	
5	336	364	1.13E-016	8.58E-017	5.86E-017	1.02E-017	4.90E-018	3.55E-018	

… is like >100 days at the best site on the ground …

@350 GHz : One day on a balloon …

#	GHz	GHz	BKG 4.5km e=0.01	BKG 6.0km e=0.01	BKG 9.0km e=0.01	BKG 45km e=0.001	Space,40K	CMB
0	34	45	2.63	2.14	1.57	0.57	0.53	0.52
1	82	105	5.58	4.39	3.12	0.80	0.70	0.68
2	132	168	8.35	5.95	4.03	0.75	0.59	0.55
3	187	253	26.39	17.08	10.28	0.78	0.47	0.41
4	229	310	39.81	25.70	15.33	0.74	0.33	0.25
5	336	364	27.28	15.65	7.66	0.22	0.05	0.03

pW

#	GHz	GHz	NEP 4.5km e=0.01	NEP 6.0km e=0.01	NEP 9.0km e=0.01	NEP 45km e=0.001	Space,40K	CMB
0	34	45	1.06E-017	1.06E-017	7.49E-018	5.51E-018	5.29E-018	5.24E-018
1	82	105	2.57E-017	2.30E-017	1.99E-017	1.00E-017	9.35E-018	9.19E-018
2	132	168	4.10E-017	3.55E-017	2.90E-017	1.22E-017	1.08E-017	1.05E-017
3	187	253	8.78E-017	7.02E-017	5.55E-017	1.51E-017	1.17E-017	1.09E-017
4	229	310	1.20E-016	9.53E-017	7.53E-017	1.63E-017	1.08E-017	9.50E-018
5	336	364	1.13E-016	8.58E-017	5.86E-017	1.02E-017	4.90E-018	3.55E-018

$W/\sqrt{Hz}$

… is like 0.25-0.1 days in deep space

@420 GHz : One day on a balloon …

	GHz	GHz	BKG 4.5km e=0.01	BKG 6.0km e=0.01	BKG 9.0km e=0.01	BKG 45km e=0.001	Space,40K	CMB
0	34	45	2.63	2.14	1.57	0.57	0.53	0.52
1	82	105	5.58	4.39	3.12	0.80	0.70	0.68
2	132	168	8.35	5.95	4.03	0.75	0.59	0.55
3	187	253	26.39	17.08	10.28	0.78	0.47	0.41
4	229	310	39.81	25.70	15.33	0.74	0.33	0.25
5	336	364	27.28	15.65	7.66	0.22	0.05	0.03
6	405	435	80.57	57.50	35.28	0.33	0.04	0.01

pW

	GHz	GHz	NEP 4.5km e=0.01	NEP 6.0km e=0.01	NEP 9.0km e=0.01	NEP 45km e=0.001	Space,40K	CMB
0	34	45	1.06E-017	1.06E-017	7.49E-018	5.51E-018	5.29E-018	5.24E-018
1	82	105	2.57E-017	2.30E-017	1.99E-017	1.00E-017	9.35E-018	9.19E-018
2	132	168	4.10E-017	3.55E-017	2.90E-017	1.22E-017	1.08E-017	1.05E-017
3	187	253	8.78E-017	7.02E-017	5.55E-017	1.51E-017	1.17E-017	1.09E-017
4	229	310	1.20E-016	9.53E-017	7.53E-017	1.63E-017	1.08E-017	9.50E-018
5	336	364	1.13E-016	8.58E-017	5.86E-017	1.02E-017	4.90E-018	3.55E-018
6	405	435	2.11E-016	1.78E-016	1.39E-016	1.35E-017	4.44E-018	2.38E-018

$W/\sqrt{Hz}$

… is like >250 days at the best site on the ground …

@420 GHz : One day on a balloon …

	GHz	GHz	BKG 4.5km e=0.01	BKG 6.0km e=0.01	BKG 9.0km e=0.01	BKG 45km e=0.001	Space,40K	CMB
0	34	45	2.63	2.14	1.57	0.57	0.53	0.52
1	82	105	5.58	4.39	3.12	0.80	0.70	0.68
2	132	168	8.35	5.95	4.03	0.75	0.59	0.55
3	187	253	26.39	17.08	10.28	0.78	0.47	0.41
4	229	310	39.81	25.70	15.33	0.74	0.33	0.25
5	336	364	27.28	15.65	7.66	0.22	0.05	0.03
6	405	435	80.57	57.50	35.28	0.33	0.04	0.01

pW

	GHz	GHz	NEP 4.5km e=0.01	NEP 6.0km e=0.01	NEP 9.0km e=0.01	NEP 45km e=0.001	Space,40K	CMB
0	34	45	1.06E-017	1.06E-017	7.49E-018	5.51E-018	5.29E-018	5.24E-018
1	82	105	2.57E-017	2.30E-017	1.99E-017	1.00E-017	9.35E-018	9.19E-018
2	132	168	4.10E-017	3.55E-017	2.90E-017	1.22E-017	1.08E-017	1.05E-017
3	187	253	8.78E-017	7.02E-017	5.55E-017	1.51E-017	1.17E-017	1.09E-017
4	229	310	1.20E-016	9.53E-017	7.53E-017	1.63E-017	1.08E-017	9.50E-018
5	336	364	1.13E-016	8.58E-017	5.86E-017	1.02E-017	4.90E-018	3.55E-018
6	405	435	2.11E-016	1.78E-016	1.39E-016	1.35E-017	4.44E-018	2.38E-018

$W/\sqrt{Hz}$

… is like 0.1-0.03 days in deep space (unless you make a better window)

Additional Considerations

- Atmospheric turbulence increases the advantage of balloons wrt ground
- Space missions longer than LDB and ULDB
- Ground-based measurements also longer (but with lower efficiency)
- Cost for a LDB: way smaller than for a space mission
  - Cost per kg : can use large cryostats, large cold optical systems
  - Cost per m^3: use large shields, large telescopes
- Balloons can have very large ground shields and use the Earth as a giant Sun shield
- Excellent test platforms for new technologies, to be flown later in deep space (BOOMERanG, Archeops vs Panck HFI)

CMB-related science from balloons

with large advantage wrt ground-based experiments:

- High resolution dust polarization & dust-cleaned inflationary and lensing B-modes
- CMB Polarization at very large angular scales
- Spectral measurements of the SZ effect
- Spectral measurements of CIB anisotropy
- Precision measurements of CMB spectrum (in selected frequency bands)
- …

Example: Survey of Dust Polarization

- *f*=270, 350, 420 GHz and up basically cannot be done, at the required level of precision, from the ground.
- 350 GHz is the highest frequency polarized channel of Planck.
- Rough comparison, at 350 GHz:
  - ULDB has shorter observing time than Planck (by a factor 10) -> 0.33 penalty
  - ULDB has higher photon noise than Planck -> 0.3 penalty
  - ULDB can have 100 times more detectors than Planck -> 10 gain
  - ULDB can focus on the cleanest regions of the sky -> 10 gain
- So ULDB can be ~ 10x10x0.3x0.33 ~ 10 times more sensitive than Planck in a selected clean region at 350 GHz.
- ULDB can provide the missing info for polarization at *f*>350 GHz.
- In addition, ULDB can use a polarization modulator, which was not present on Planck, potentially improving the control of systematic effects and the final accuracy.

Current / Pending Balloons for CMB-related science

Missions Recently Flown	survey area [sky fraction]	frequencies [GHz]	resolution [arcmin]
EBEX (2012/13)	0.2	150/250/410	8/5/5
Spider (2014/15)	0.1	94/150	42/28
PILOT (2015)	<0.01	1200/545	3
Piper (2017)	0.8	200	36
OLIMPO (N.LDB 2018)	0.01	140-220-340-450	2/4
Missions Planned	**survey area [sky fraction]**	**frequencies [GHz]**	**resolution [arcmin]**
Spider (LDB 2020)	0.1	94-285 (3)	42-15
OLIMPO (S.LDB 2021)	0.01	140-220-340-450	2/4
LSPE (N.LDB 2020)	0.25	44-240 (4)	85-20
Missions in Preparation	**survey area [sky fraction]**	**frequencies [GHz]**	**resolution [arcmin]**
Piper (2020)	0.8	200-600 (4)	36-12
BLAST-TNG (2020)	< 0.01	1200, 860, 600	1
EBEX-IDS	0.035	150-360 (7)	8-3
BFORE	0.23	270-600 (3)	4
BSIDE	0.05	600-700	7

The Balloon-borne Large Aperture Submillimeter Telescope
BLAST

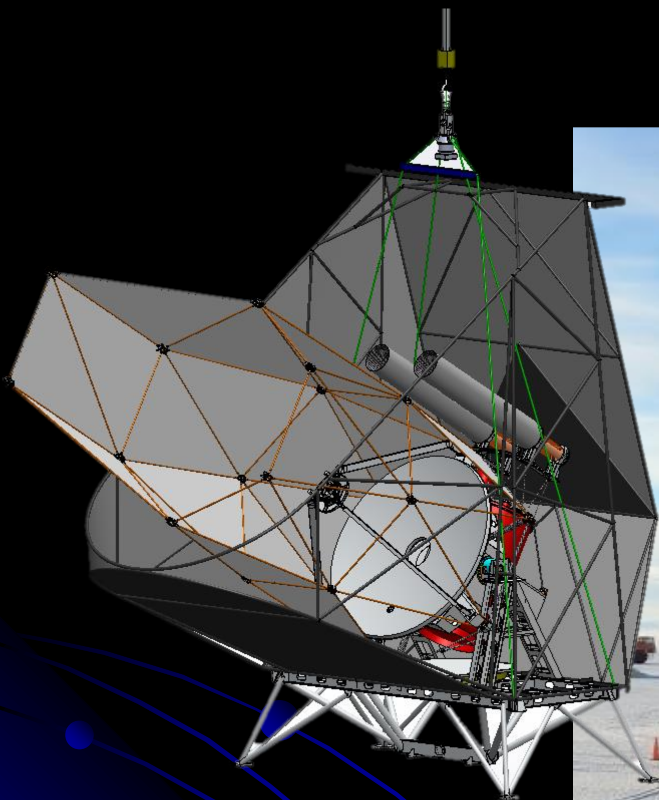

PI Marc Devlin (UPenn)
https://sites.northwestern.edu/blast/

SPECIFICATIONS:

- 2.5 meter Carbon Fiber Mirror
- **2200 KID detectors**
    - 250, 350 and 500 μm
    - Polarization Sensitive
    - 280 mK
- 22 arcsec resolution at 250 μm
- 28 day flight!

Science:

- Polarized dust emission **in star forming regions** in our Galaxy.
- Polarized dust emission in low dust regions for CMB polarization foregrounds.

Flight from Antarctica: December 2019

Polarized Instrument for Long-wavelength Observation of the Tenuous interstellar medium

PILOT

PI J.P. Bernard (IRAP Toulouse)
http://pilot.irap.omp.eu/PAGE_PILOT/index.html/

SPECIFICATIONS:

- 0.9 meter aperture telescope
- **2048 bolometers**
  - 240 and 550 μm
  - Polarization Sensitive with cryogenic HWP
  - 280 mK
- 1.9' resolution at 250 μm
- See Mangilli et al. Astro-ph/1804.05645
- Flown by CNES (Timmins)

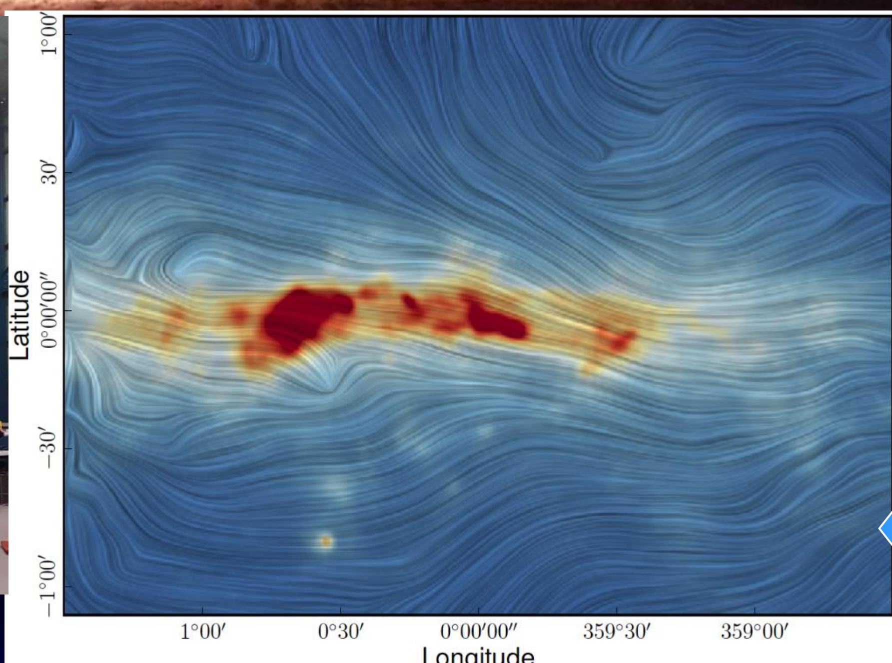

Science:

- a balloon-borne experiment to study the polarized emission arising from dust grains present in the diffuse interstellar medium in our Galaxy.
- See Mangilli et al. (2019) arXiv:1901.06196 for first science results.

The E and B EXperiment

EBEX

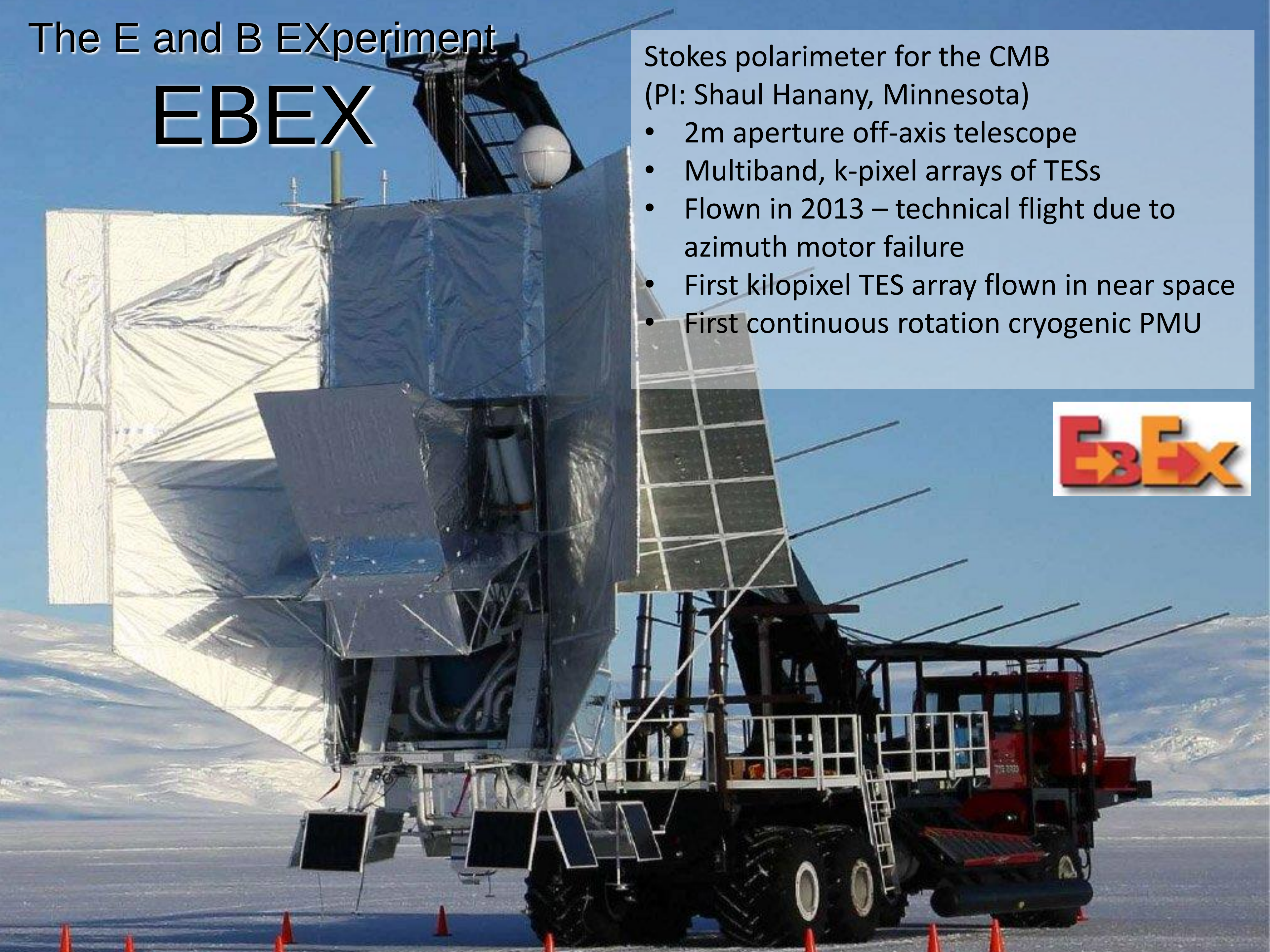

Stokes polarimeter for the CMB
(PI: Shaul Hanany, Minnesota)

- 2m aperture off-axis telescope
- Multiband, k-pixel arrays of TESs
- Flown in 2013 – technical flight due to azimuth motor failure
- First kilopixel TES array flown in near space
- First continuous rotation cryogenic PMU

Telescope

effective focal length	198 cm
aperture diameter	105 cm
PR focal length	80 cm
∠ between PR and SR axes	12.77°
PR offset	100 cm
SR semi-major axis length, a	110.2 cm
SR semi-minor axis length, b	98.21 cm
SR conic constant, K	-0.2059
SR opening half-angle	52°
PR maximum size	1.5 × 1.8 m
SR maximum size	1.2 × 1.3 m

Cold Optics

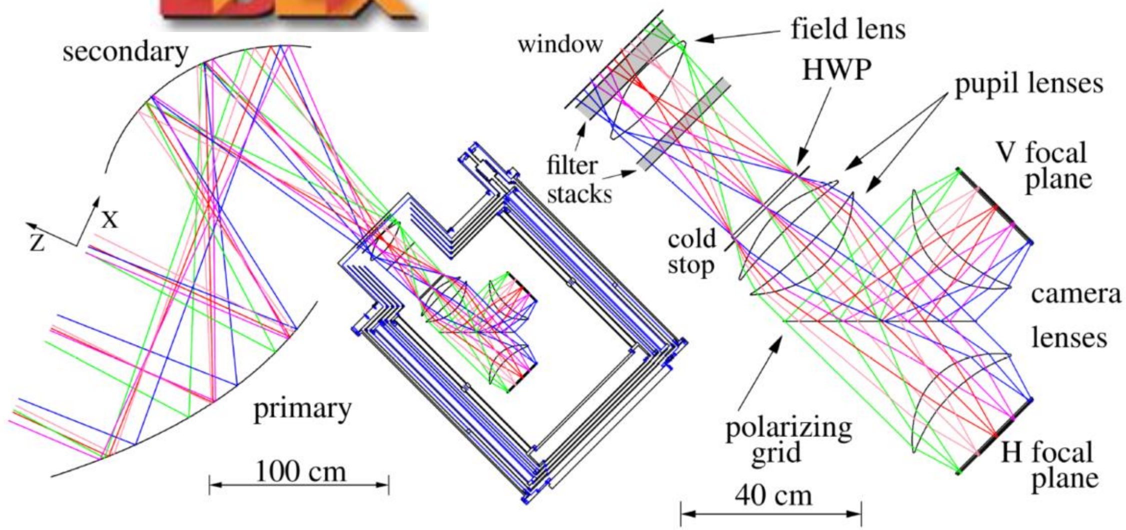

Focal Planes

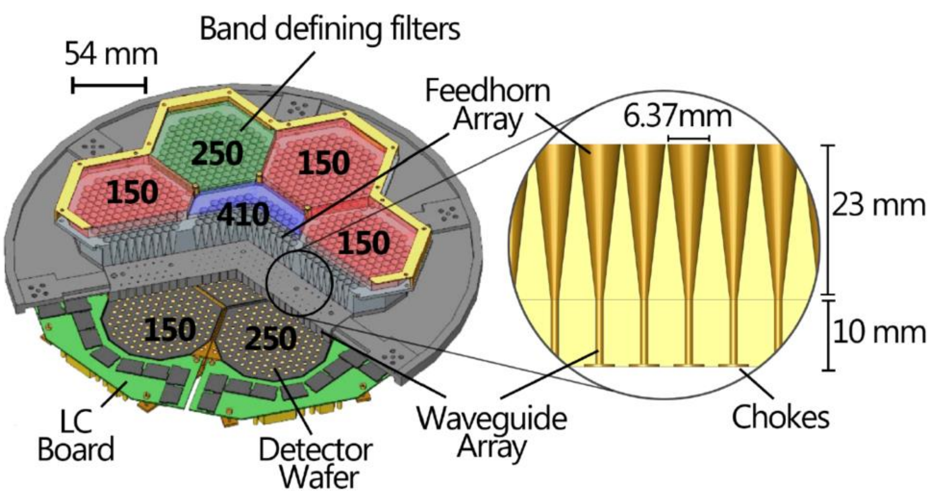

The EBEX Collaboration *et al* 2018 *ApJS* **239** 7
The EBEX Collaboration *et al* 2018 *ApJS* **239** 8

TES Detectors

	Count of	Frequency (GHz) 150	250	410	Total
1	detectors on wafers	1120	560	280	1960
2	maximum detectors to read out	992	496	254	1742
3	detectors which passed warm electrical & visual inspections	908	455	232	1595
4	channels wired to detectors which passed warm electrical & visual inspections	861	447	213	1521
5	detectors which passed the 0.8 K network analysis test	805	430	187	1422
6	detectors after SQUID failures removed	773	414	155	1342
7	detectors after noise polluters removed	676	371	133	1180
8	detectors with successful flight IV curves	504	342	109	955

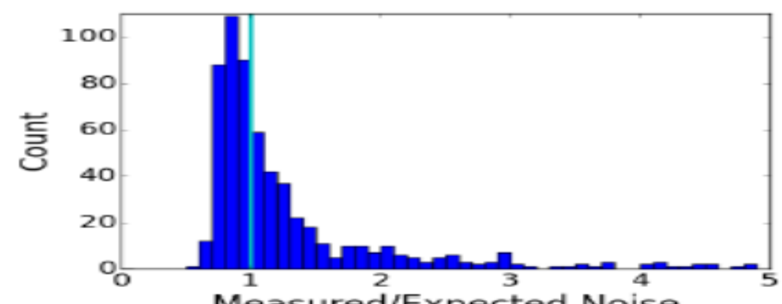

The EBEX Collaboration *et al* 2018 *ApJS* **239** 7

Excellent in-flight performance of the cryogenic continuously rotating HWP polarization modulator

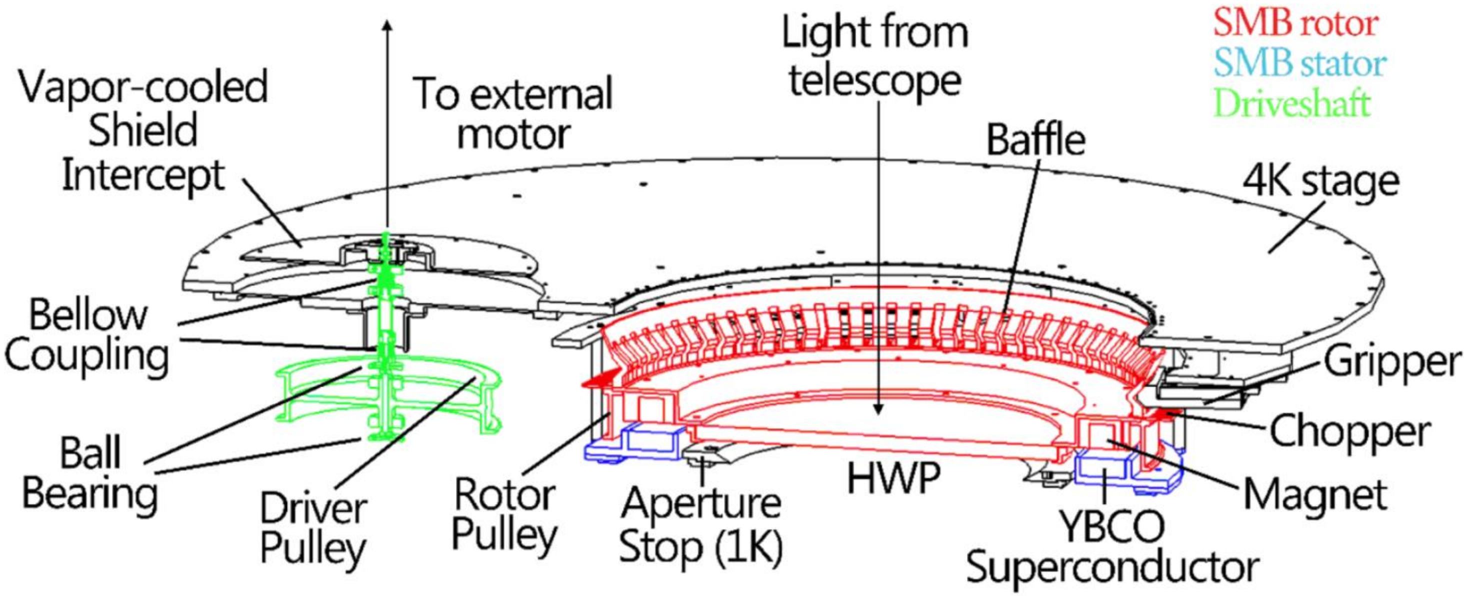

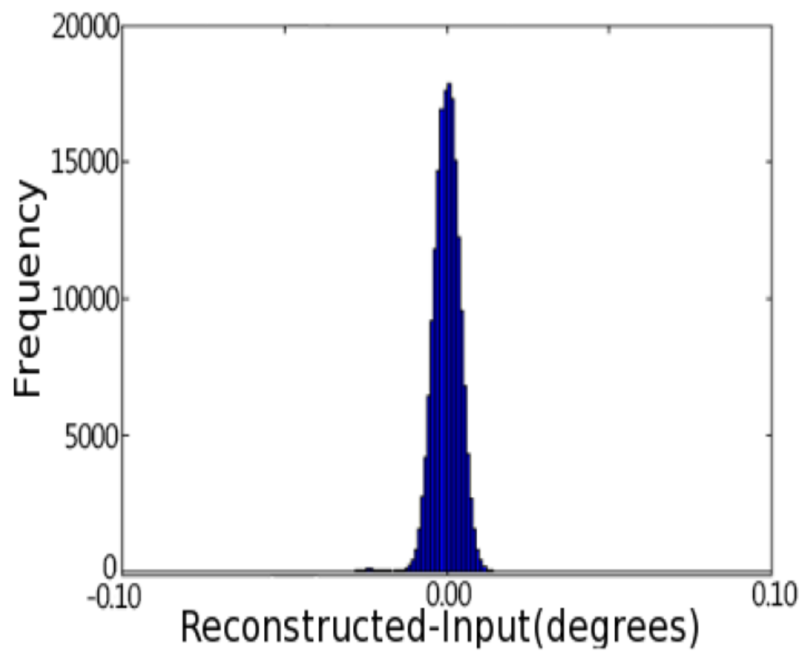

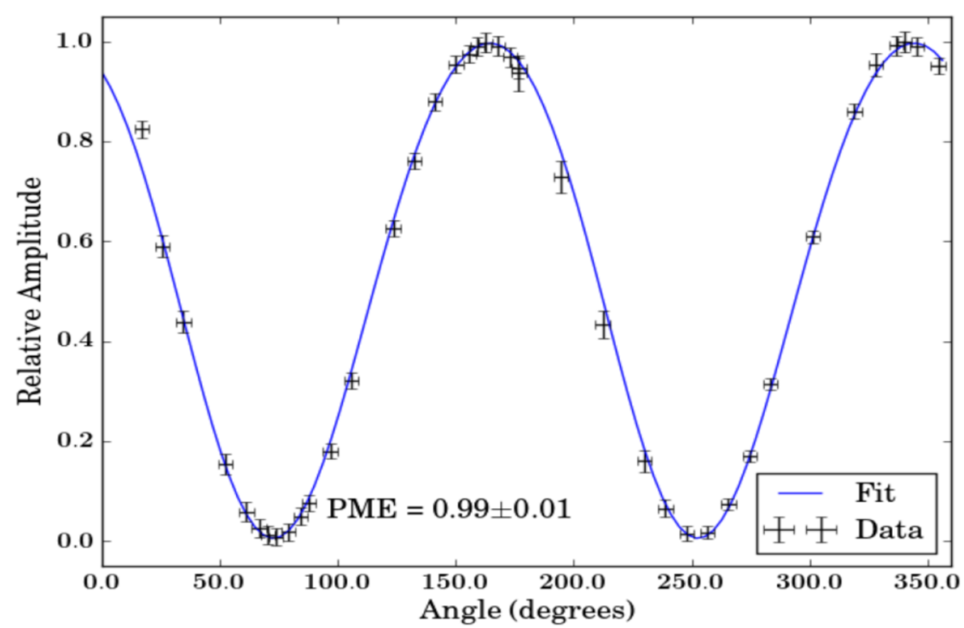

2013 Flight

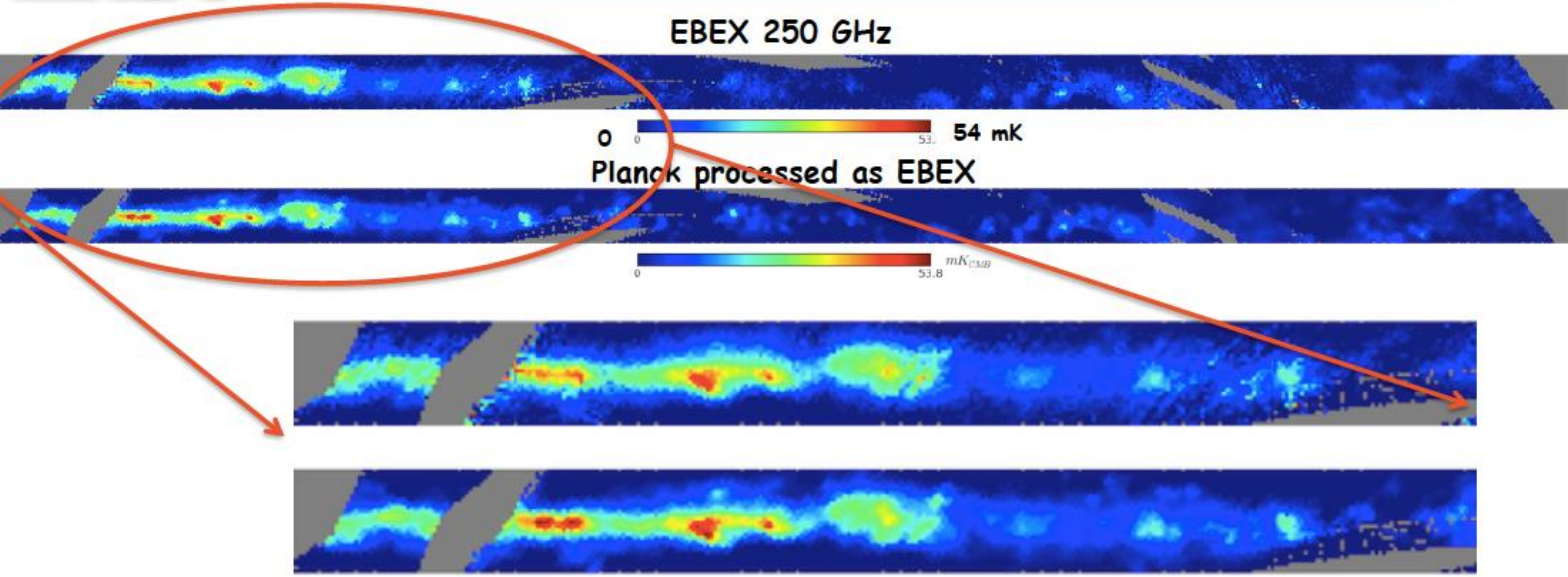
EBEX 250 GHz
0
54 mK
Planck processed as EBEX
53.8
mK_{CMB}

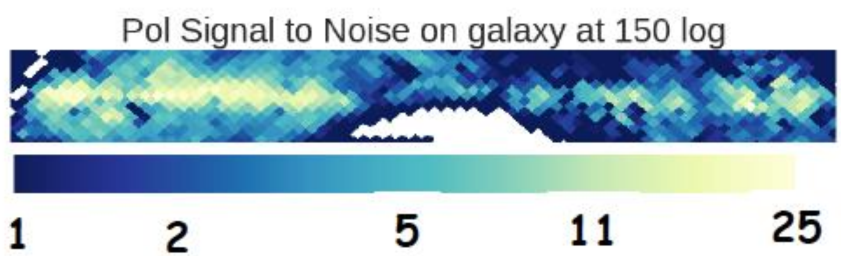
Pol Signal to Noise on galaxy at 150 log
1
2
5
11
25

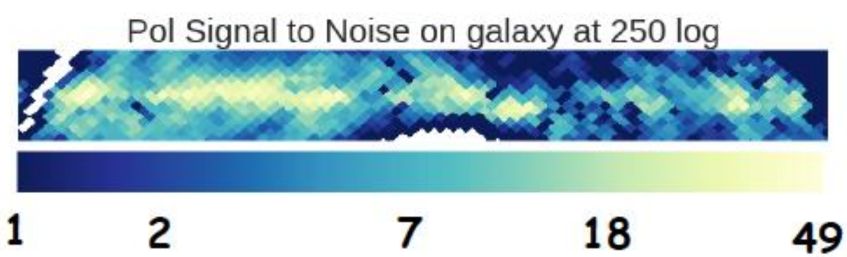
Pol Signal to Noise on galaxy at 250 log
1
2
7
18
49

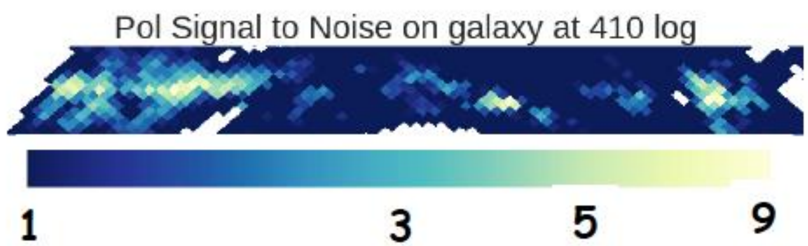
Pol Signal to Noise on galaxy at 410 log
1
3
5
9

IDS Instrument, Baseline (2018)

- PI: S. Hanany, Minnesota
- 1.5 m aperture
- FWHM of 7.2’ at 150 GHz
- 20 day flight observing 1500 deg^2
- 3 band multichroic pixels
- Total map depth of 4 μK arcmin
- Constraints by IDS + ground based data
  - r < 0.003 (2σ), simple foreground model
  - r < 0.01 (2σ) and unbiased, complex foregrounds

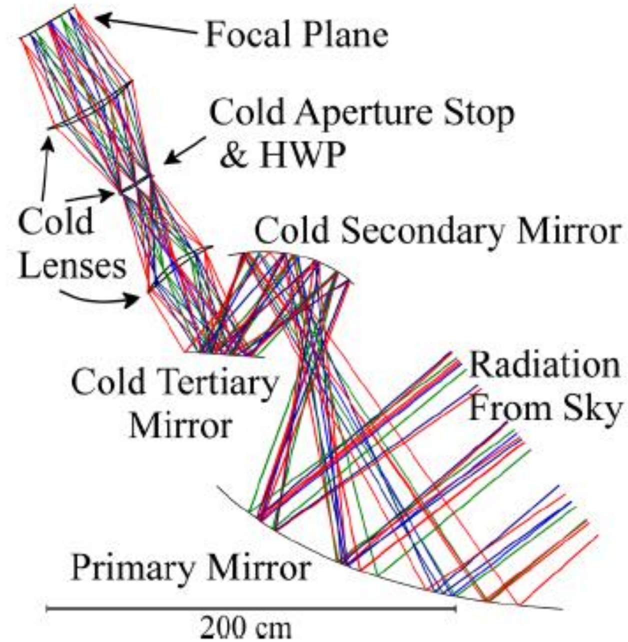

Pixel Type	Center Frequency (GHz)	FWHM (arcmin)	NET/detector ($\mu K\sqrt{sec}$)[a]	Detectors (#)	Array NET ($\mu K\sqrt{sec}$)[a]
Low-Frequency (2316 pixels)	150/180[b]	7.2/6.0	142/148	2316/2316	2.95/3.08
	250	4.4	248	3202	4.38
	320	3.6	498	2648	9.68
High-Frequency (1680 pixels)	220	4.9	219	3360	3.78
	280	3.9	361	3360	6.23
	360	3.2	956	3360	16.5
Total				20562	

[a] Thermodynamic units; multiply by $\sqrt{2}$ for Stokes Q, U
[b] Half of the pixels are 150 GHz, the other half 180 GHz (see Section 1.6.2)

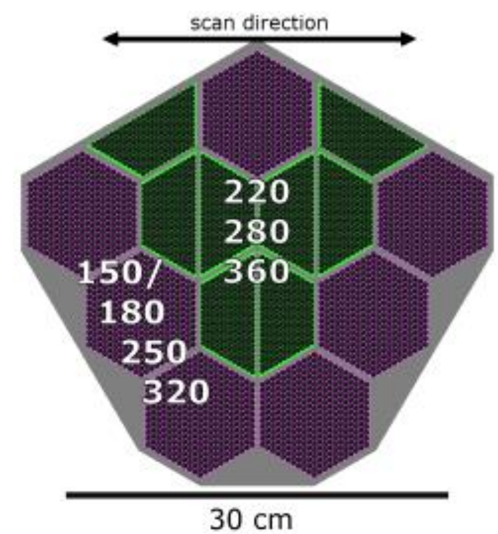

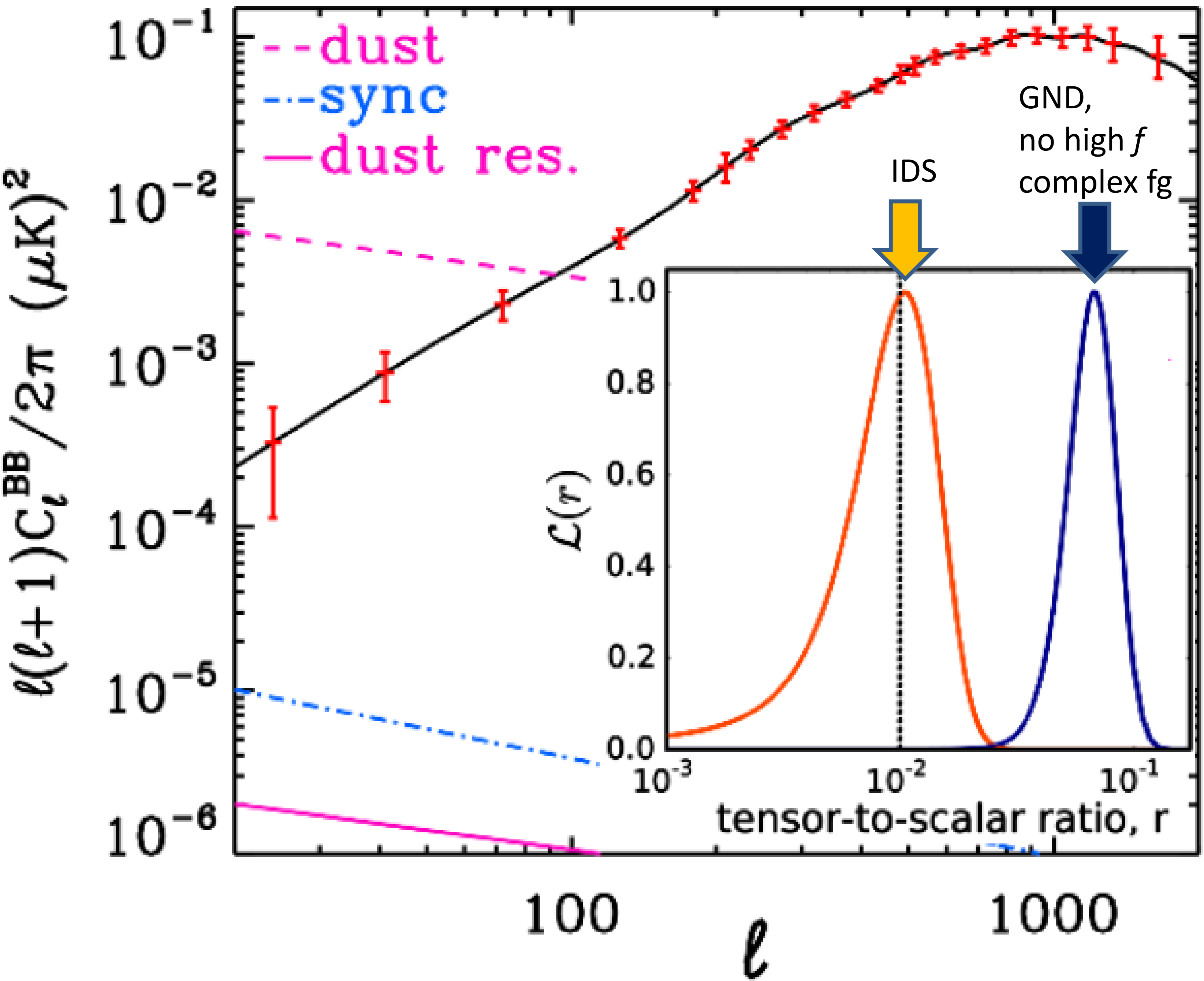

$\ell(\ell+1)C_\ell^{BB}/2\pi\ (\mu K)^2$
ℓ
--dust
-·-sync
—dust res.
IDS
GND,
no high f
complex fg
$\mathcal{L}(r)$
tensor-to-scalar ratio, r

IDS Instrument, New Concept (2019)

- 0.40 m aperture
- FWHM of 20’ at 150 GHz
  - Ensures 270 GHz matches BICEP at 150 GHz
- 30 day flight observing 1500 deg^2
- Total map depth of 2.4 μK arcmin
- Smaller, simpler design adaptable to NZ ULDB flight, allowing τ measurement

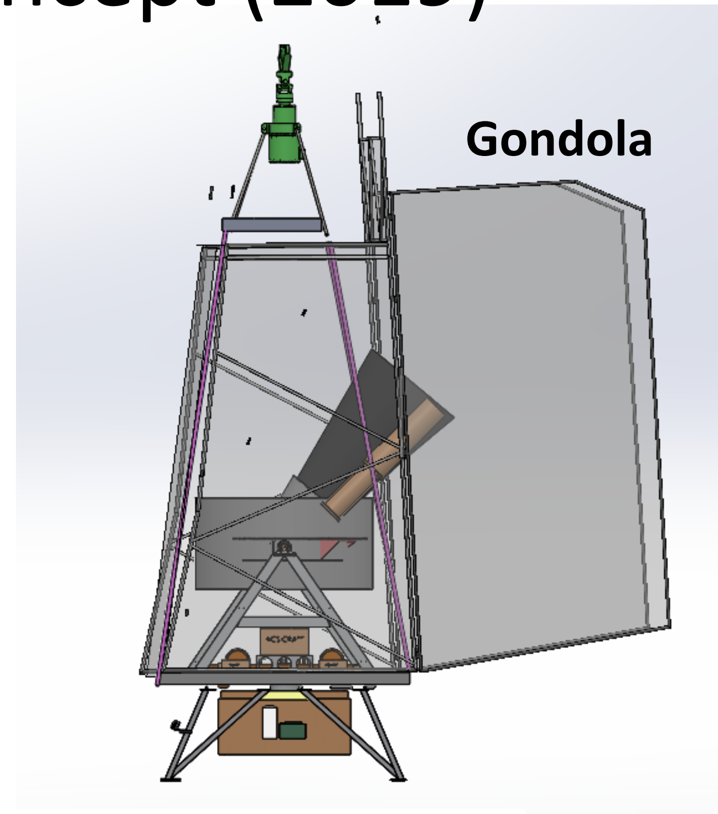

Band GHz	FWHM arcmin	Bolo NET uK_{CMB} rt(s)	# Bolos	Array NET uK_{CMB} rt(s)
180	17	79	1000	2.5
220	13.0	126	3000	2.4
270	10.7	209	3000	3.8
320	9.8	344	3000	6.3
370	8.4	702	3000	12.8
			12000	

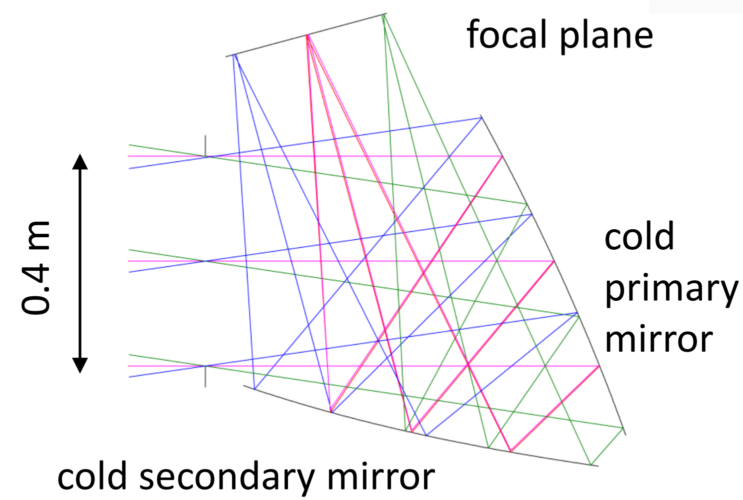

cryogenic systems for ULDB

- LDB cryogenic systems, based on liquid cryogens (LN, Lhe) have a target hold time of 1 month and a mass at the launch of the order of 300 kg (see e.g. Masi et al. Cryogenics, 38, 319-324, 1998, Coppolecchia et al. 2019)
- To exploit the longer flight duration (order of 100 days) of a ULDB and cope with the reduced payload mass compliance of sealed balloons, longer duration and lighter cryostats must be optimized.
- Solutions are possible either using cryogenic fluids:
  - A long lifetime balloon-borne cryostat and magnetic refrigerator J. O. Gundersen et al. 2013, Advances in Cryogenic Engineering, Quan-Sheng Shu et al. Eds. Springer
- or using hybrid systems with mechanical coolers for the intermediate temperature stage (useful for large windows).

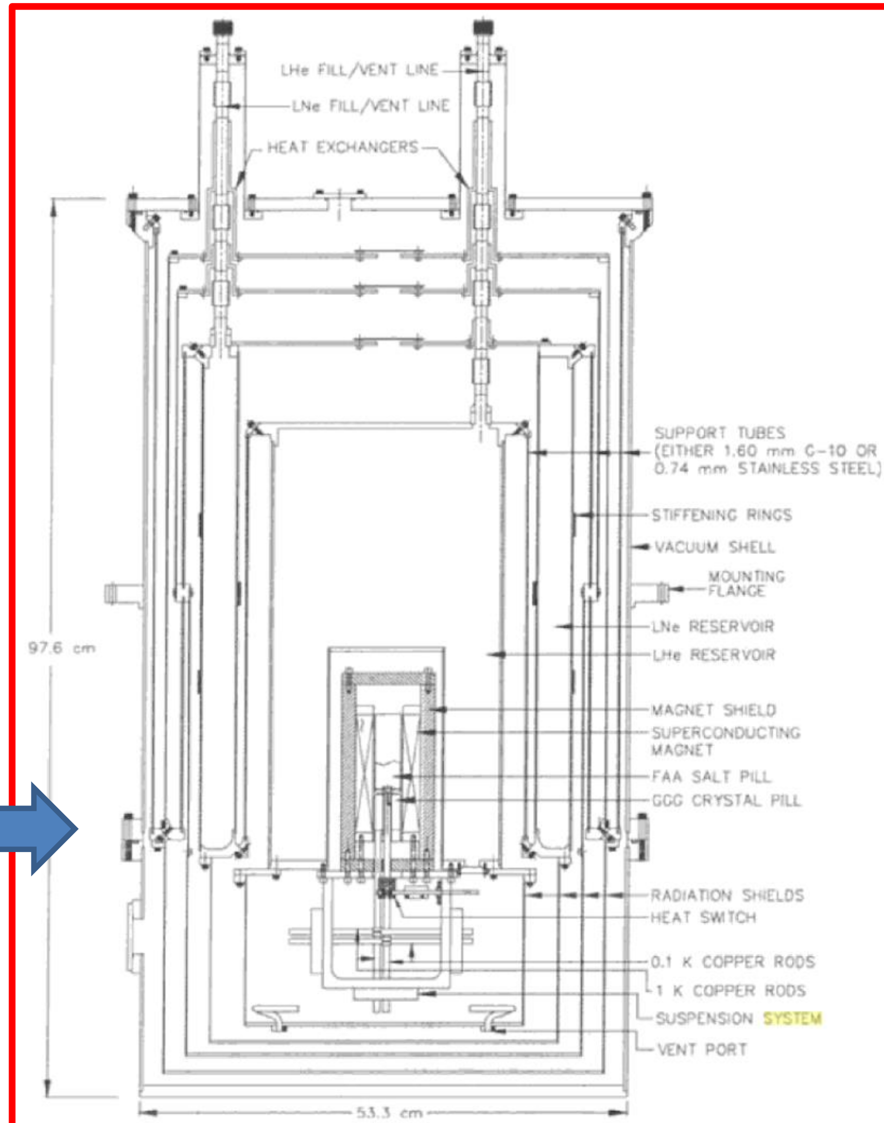

SPIDER

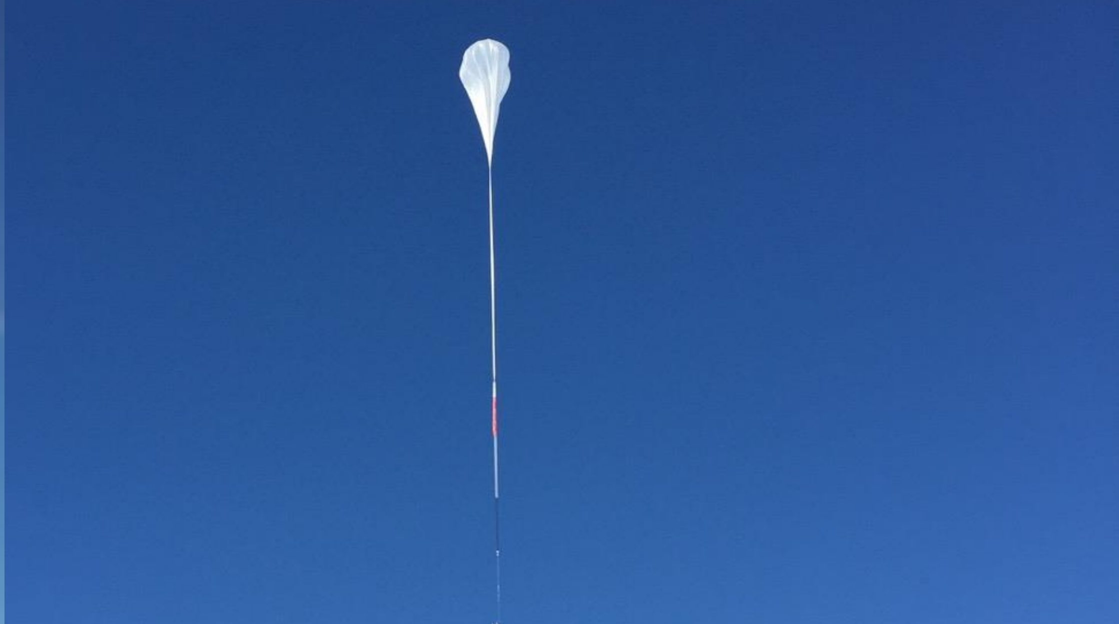

- Balloon-borne CMB polarization survey with multi-wavelength, large format bolometer arrays.
- PI Bill Jones (Princeton)
- First payload flown in 2015.
- 100, 150, 273 GHz FPUs
- Stepped cryogenic HWPs (~12h)

Spider 2015: Overview

Sky coverage	About 10 %
Scan rate (az, sinusoid)	3.6 deg/s at peak
Polarization modulation	Stepped cryogenic HWP
Detector type	Antenna-coupled TES
Multipole range	$10 < \ell < 300$
Observation time	16 days at 36 km
Limits on r†	0.03

† Ignoring all foregrounds, at 99% confidence

	Frequency [GHz]	
	94	150
Telescopes	3	3
Bandwidth [GHz]	22	36
Optical efficiency	30-45%	30-50%
Angular resolution* [arcmin]	42	28
Number of detectors†	652 (816)	1030 (1488)
Optical background‡ [pW]	≤ 0.25	≤ 0.35
Instrument NET† [μK·rts]	6.5	5.1

*FWHM. †Only counting those currently used in analysis
‡Including sleeve, window, and baffle

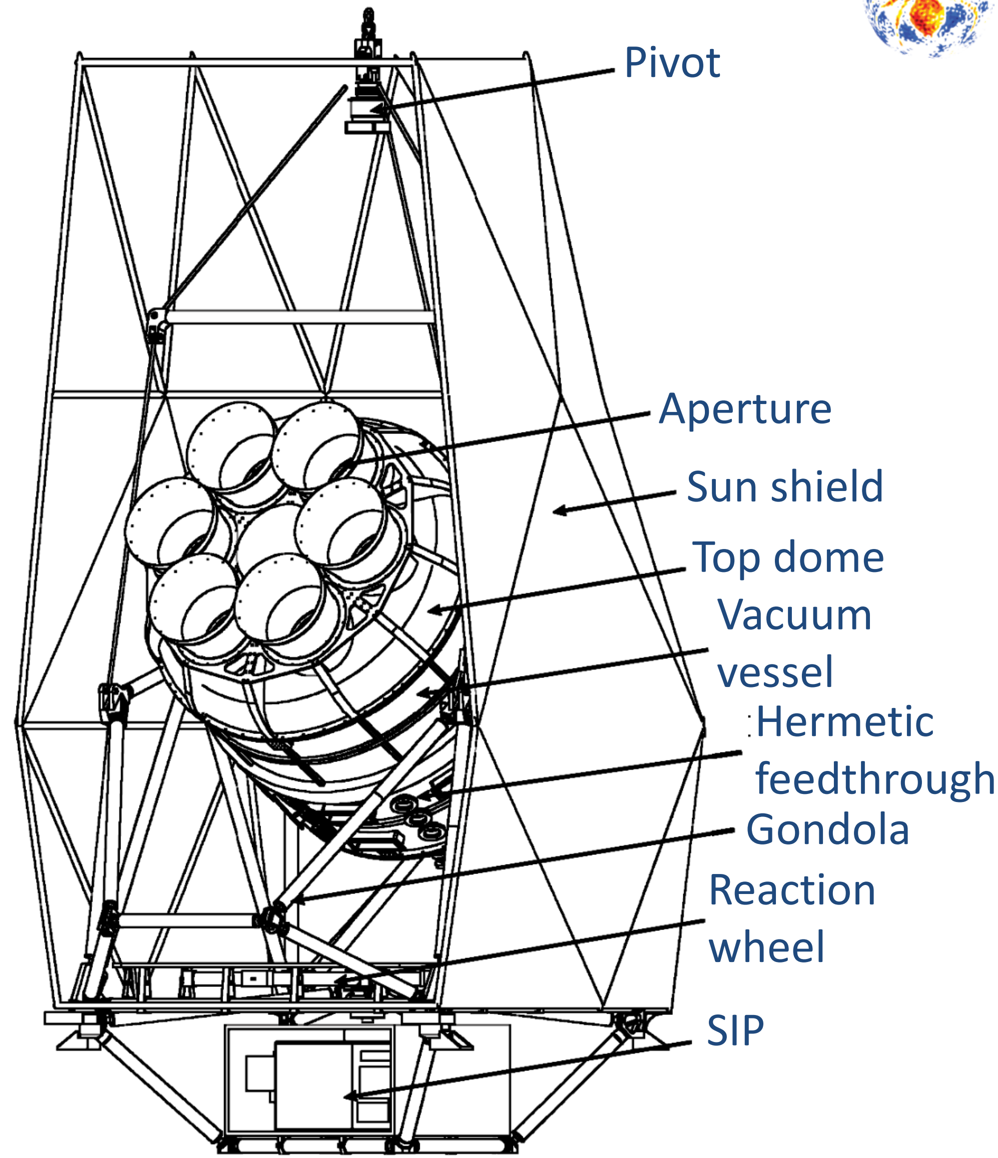

SPIDER

2015 Payload:

6 X

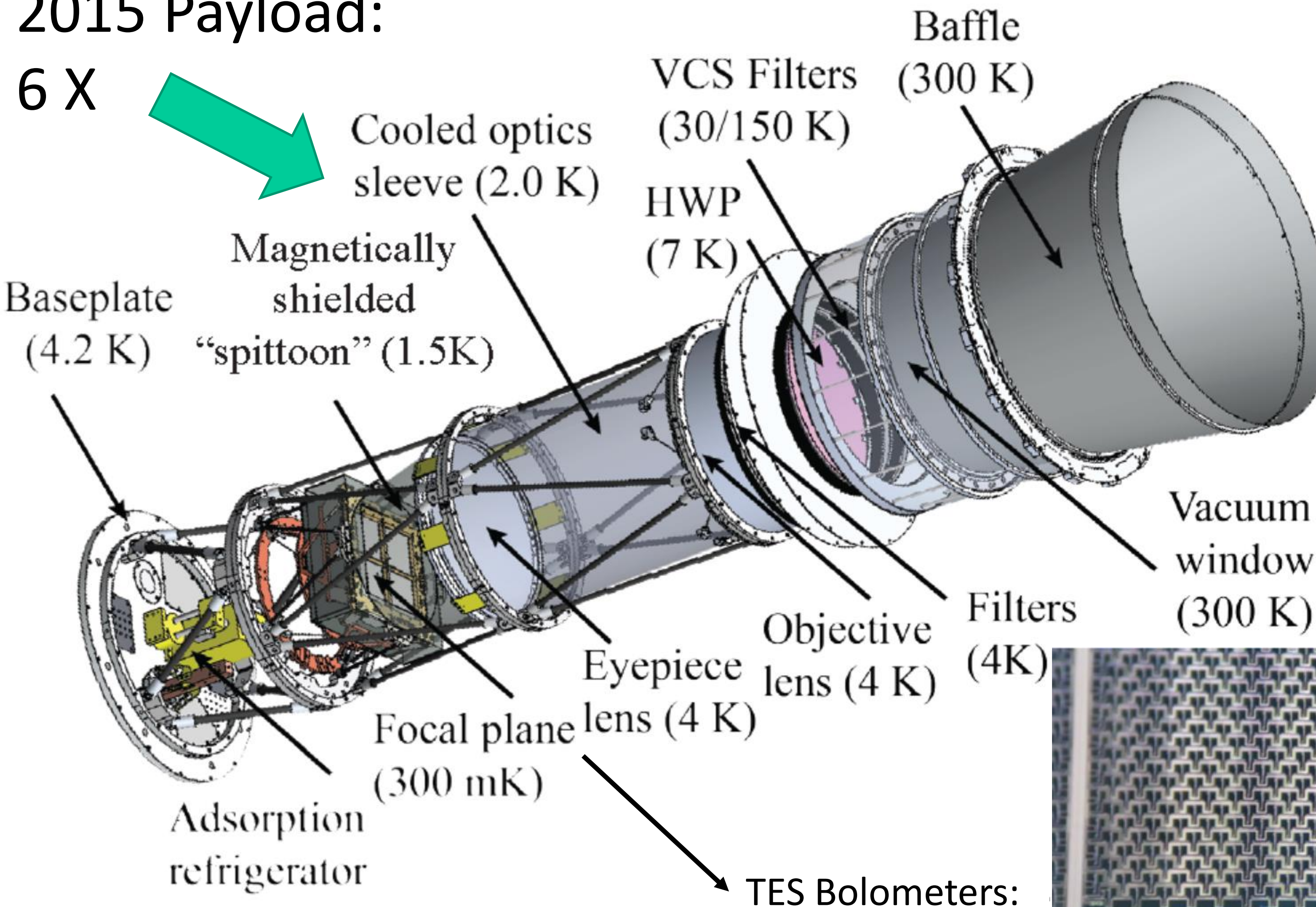

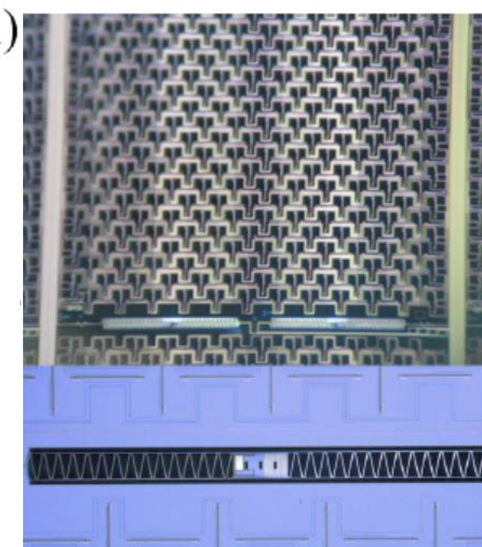

See e.g. Gualtieri et al. arXiv:1711.10596

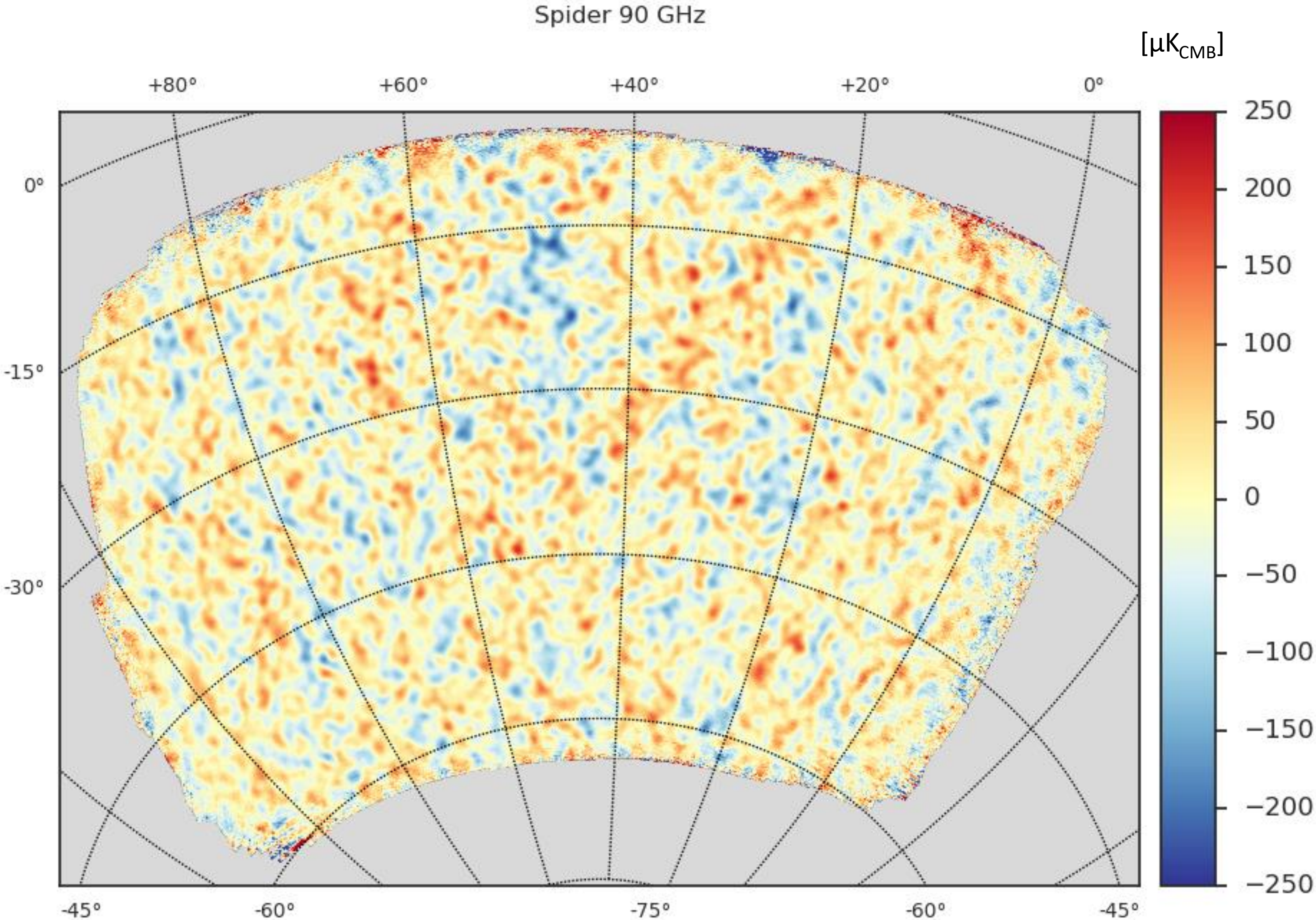
Spider 90 GHz
[μK_CMB]
+80°
+60°
+40°
+20°
0°
0°
-15°
-30°
-45°
-60°
-75°
-60°
-45°
250
200
150
100
50
0
−50
−100
−150
−200
−250

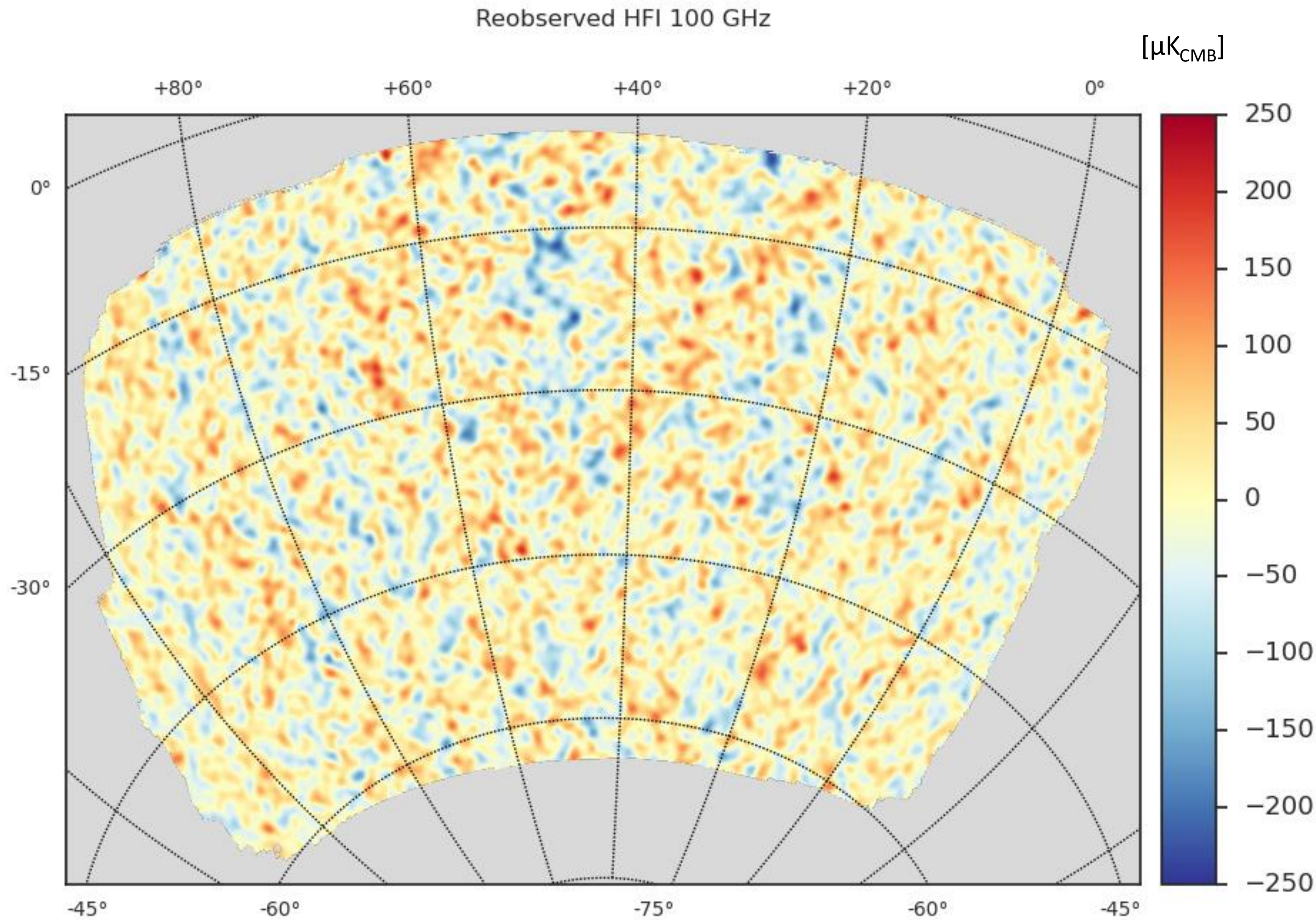
Reobserved HFI 100 GHz
[μK$_{CMB}$]
+80°
+60°
+40°
+20°
0°
0°
-15°
-30°
-45°
-60°
-75°
-60°
-45°
250
200
150
100
50
0
−50
−100
−150
−200
−250

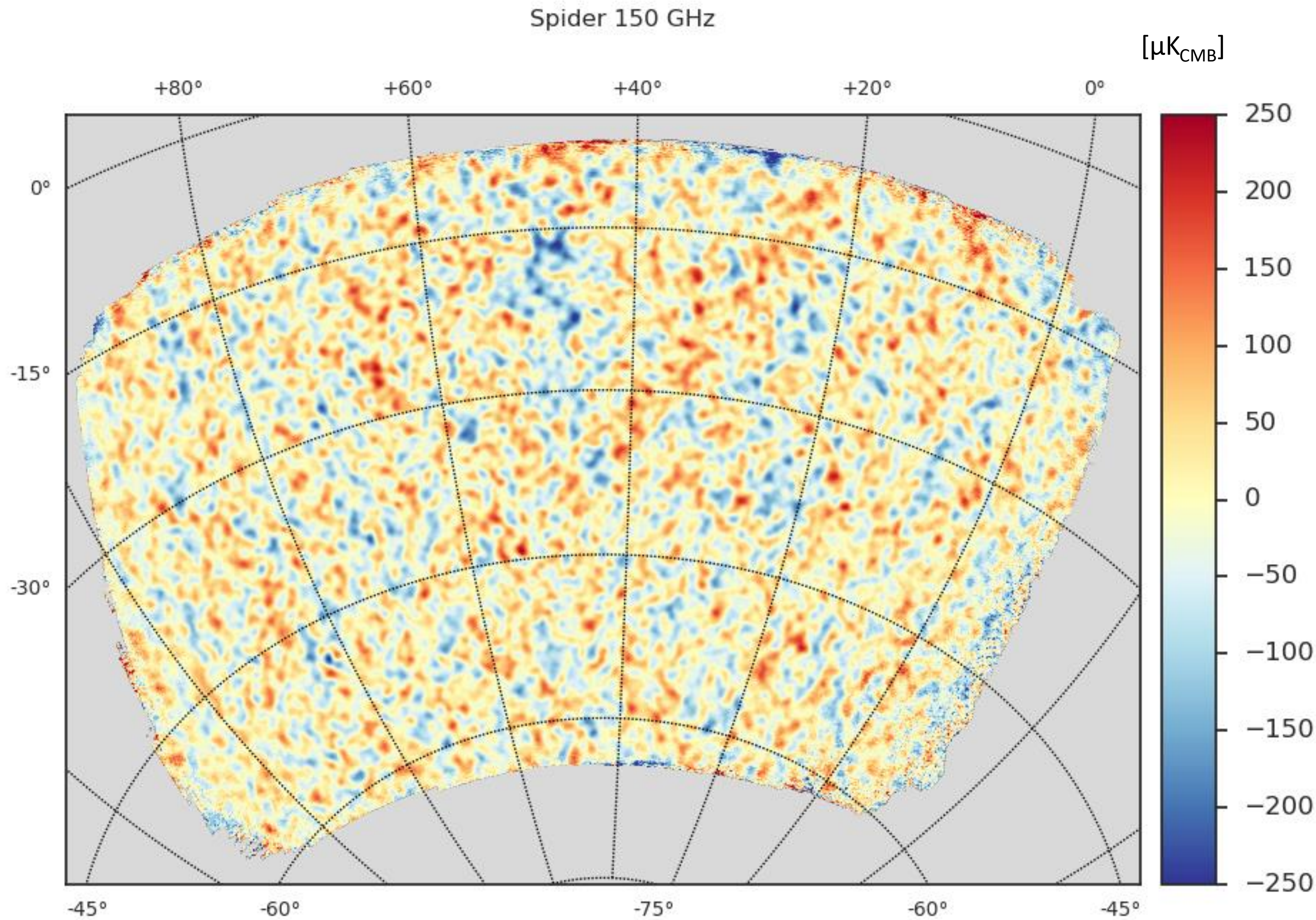
Spider 150 GHz
[μK$_{CMB}$]
+80°
+60°
+40°
+20°
0°
0°
-15°
-30°
-45°
-60°
-75°
-60°
-45°
250
200
150
100
50
0
−50
−100
−150
−200
−250

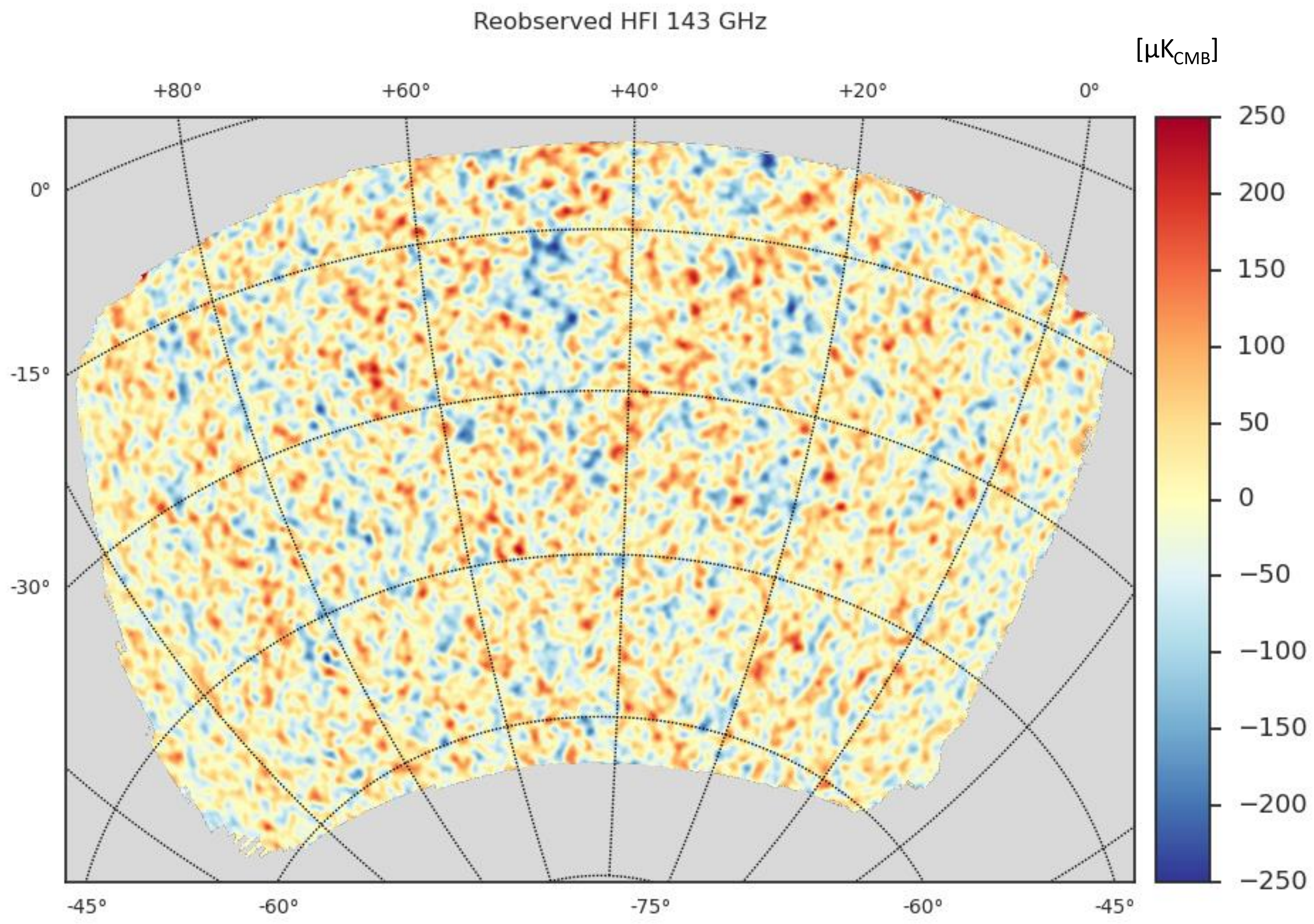

Reobserved HFI 143 GHz
[μK_CMB]
+80°
+60°
+40°
+20°
0°
0°
-15°
-30°
-45°
-60°
-75°
-60°
-45°
250
200
150
100
50
0
−50
−100
−150
−200
−250

Stacking hot spots : SPIDER

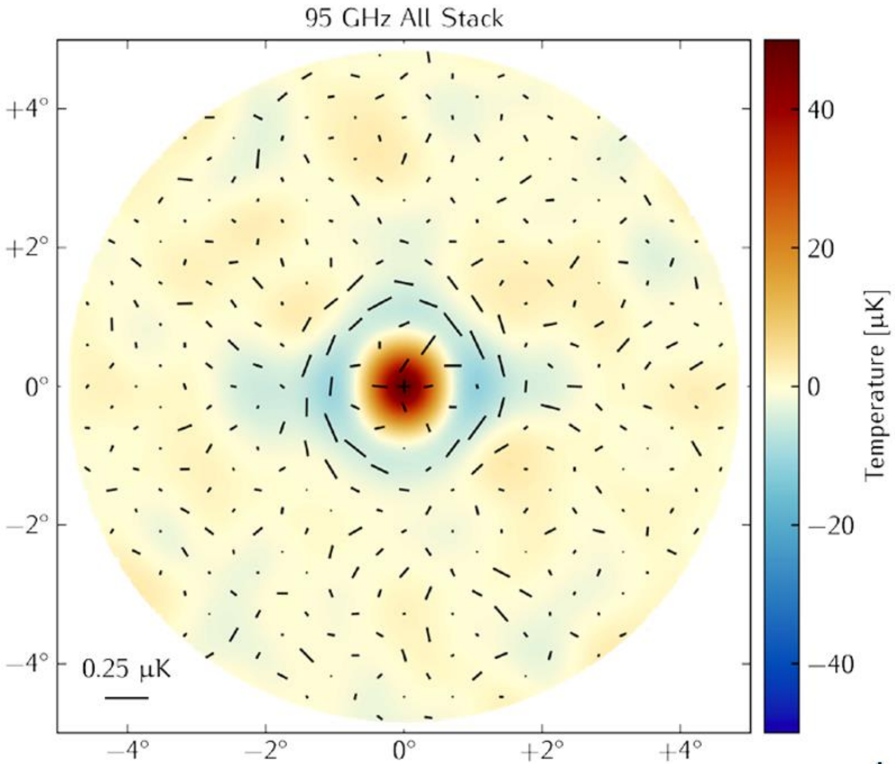

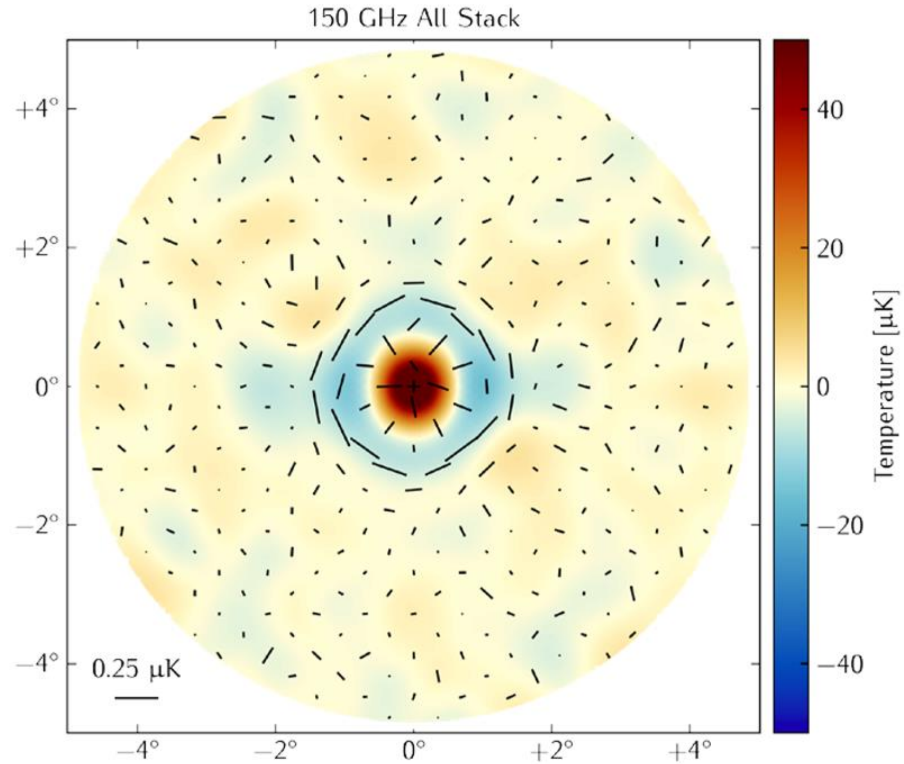

PRELIMINARY

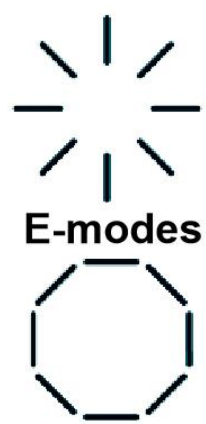

E-modes

PRELIMINARY

SCAR AAA Chiang Mai
Aug 3 2017

Lorenzo Moncelsi

SPIDER

- Data analysis on-going. First science results:
  - Instrument sensitive to circular polarization via the non-ideality of the HWP (!)
  - Upper limits to Circular Polarization of the CMB. M. Nagy et al. Ap.J. **844**, 151 (2017)

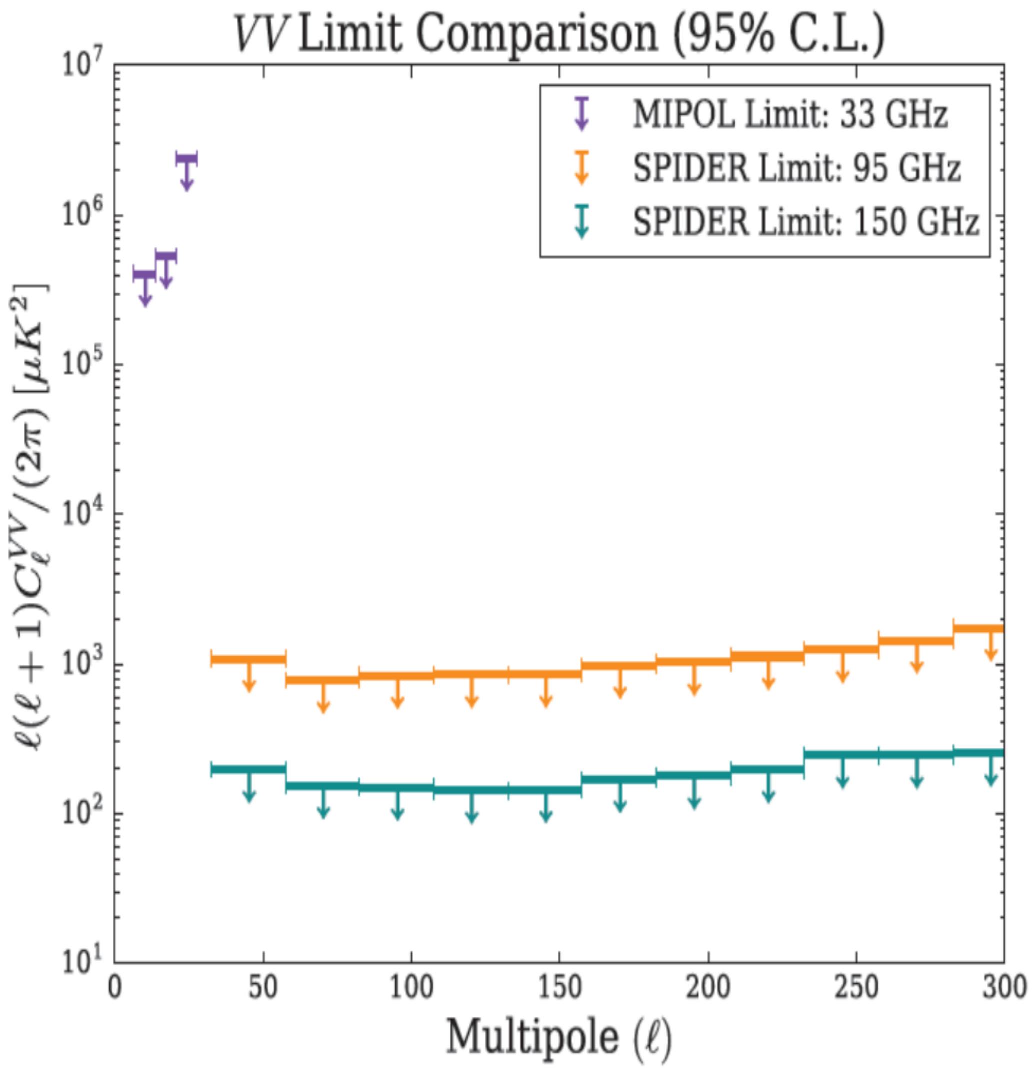

SPIDER

- 2015 data analysis on-going
- New payload fully integrated in the Princeton high-bay
- 3 x 512 detector 285 GHz FPUs
- 2x 94 GHz FPUs
- 1x 150 GHz FPU
- To be flown in dec. 2020.

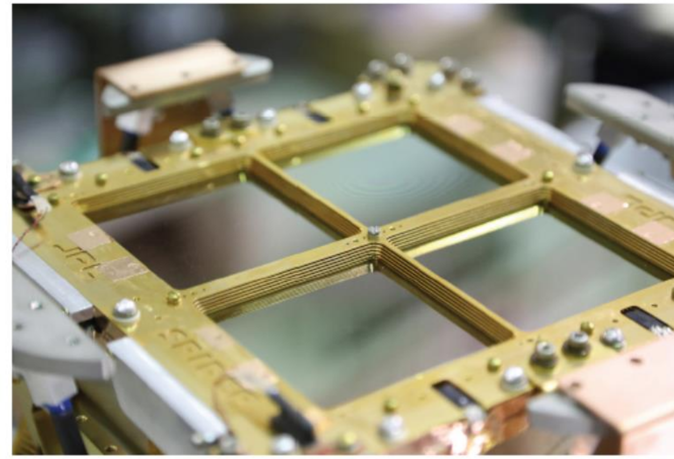

SPIDER focal plane, showing 4 silicon detector tiles under quartz AR coats

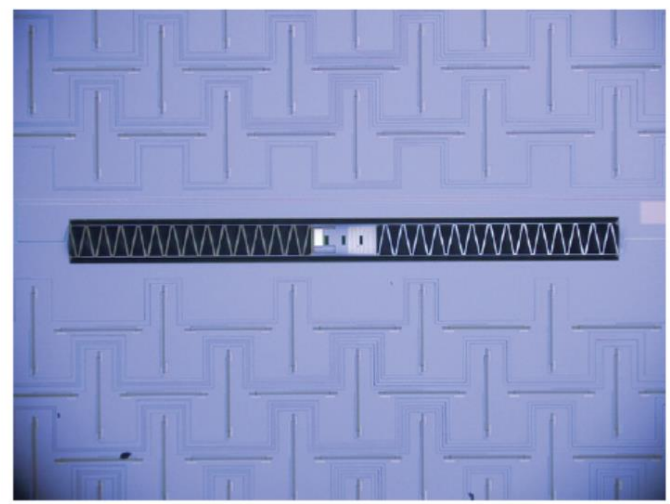

Bolometer suspended on meandered SiN legs, surrounded by slot antenna array

OLIMPO

- The OLIMPO experiment is a first attempt at spectroscopic measurements of CMB anisotropy.
- A large (2.6m aperture) balloon-borne telescope with a 4-bands photometric array and a plug-in room temperature spectrometer (150, 250, 350, 460 GHz).
- Similar resolution as SPT in the high frequency bands
- http://olimpo.roma1.infn.it
- **Main scientific targets:**
  - **SZ effect in clusters –> unbiased estimates of cluster parameters**
  - **Spectrum of CMB anisotropy –> anisotropic spectral distortions**

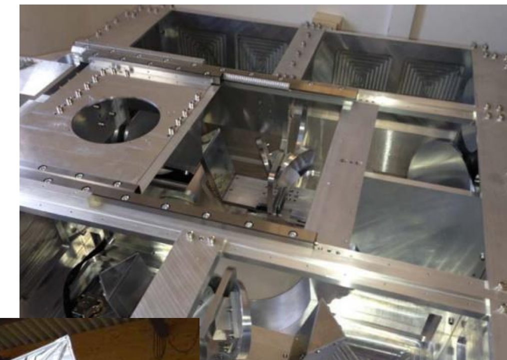

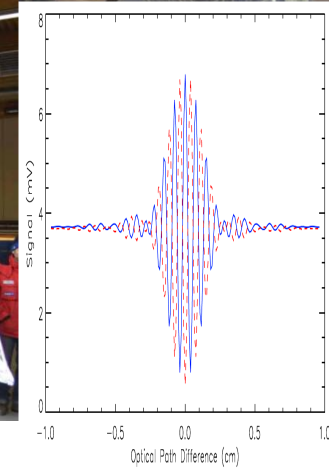

Sunyaev-Zeldovich effect in clusters of galaxies

- Inverse Compton Effect for CMB photons against charged particles in the hot gas of clusters (same as y-type distortion)
- Cluster optical depth: $\tau = n\sigma\ell$

  ℓ = a few Mpc = 10^{25} cm

  $n < 10^{-3}$ cm^{-3}

  $\sigma = 6.65\text{x}10^{-25}$ cm^2

- So $\tau = n\sigma\ell < 0.01$: there is a 1% likelihood that a CMB photon crossing the cluster is scattered by an electron
- $E_{electron} >> E_{photon}$, so the electron transfers energy to the photon. To first order, the energy gain of the photon is

$$\boxed{\frac{\Delta\nu}{\nu} = \frac{kT_e}{m_e c^2} \approx \frac{5keV}{500keV} = 0.01}$$

- The resulting CMB temperature anisotropy is

$$\boxed{\frac{\Delta T}{T} \approx \tau \frac{\Delta\nu}{\nu} \approx 0.01 \times 0.01 = 10^{-4}}$$

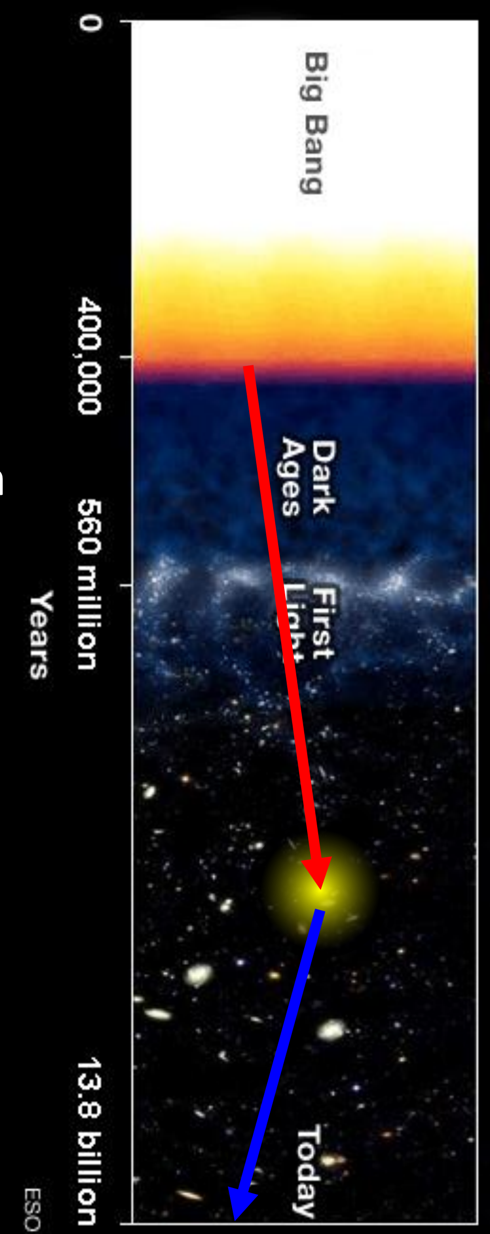

Sunyaev R., Zeldovich Y.B., 1972, Comm. Astrophys. Space Phys., 4, 173
Birkinshaw M., 1999, Physics Reports, 310, 97-195

Sunyaev-Zeldovich effect

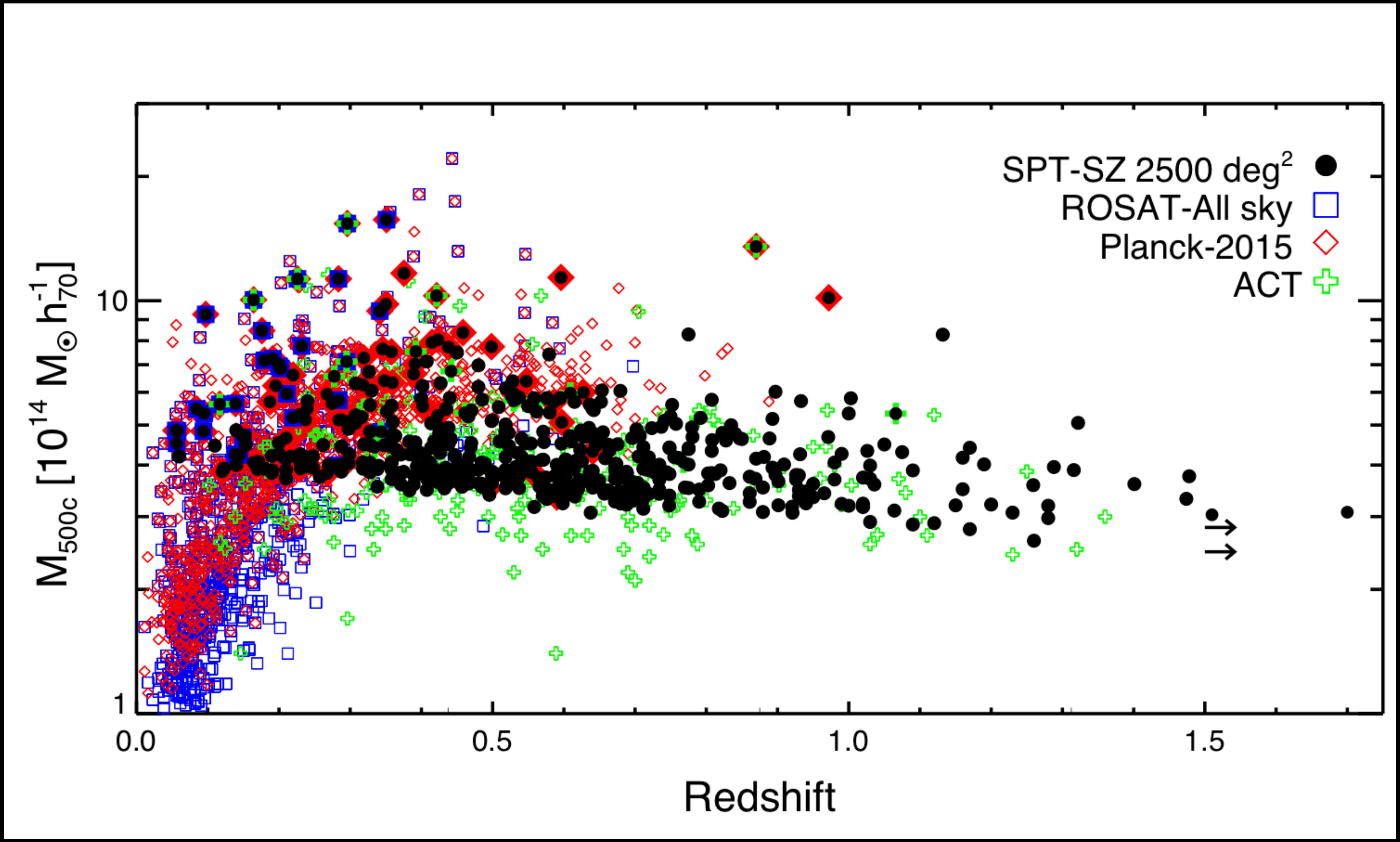

- The comptonization of CMB photons crossing clusters of galaxies has been measured for thousands of clusters, with masses ranging from 10^{14} to 2×10^{15} M_{sun}. The high-redshift, large mass limit is sampled optimally by large telescopes as ACT (Atacama) and SPT (at the south pole). Potentially, many more clusters can be measured ! (see below)

A&A 538, A86 (2012)
DOI: 10.1051/0004-6361/201118062

Astronomy & Astrophysics

Low-resolution spectroscopy of the Sunyaev-Zel'dovich effect and estimates of cluster parameters

P. de Bernardis[1,2], S. Colafrancesco[3,4], G. D'Alessandro[1], L. Lamagna[1,2], P. Marchegiani[3], S. Masi[1,2], and A. Schillaci[1,2]

[1] Dipartimento di Fisica, Università di Roma "La Sapienza", Roma, Italy
e-mail: paolo.debernardis@roma1.infn.it
[2] INFN Sezione di Roma 1, Roma, Italy
[3] INAF – Osservatorio Astronomico di Roma, Monte Porzio Catone, Italy
[4] School of Physics, University of the Witwatersrand, Johannesburg Wits 2050, South Africa

Received 9 September 2011 / Accepted 8 November 2011

ABSTRACT

Context. The Sunyaev-Zel'dovich (SZ) effect is a powerful tool for studying clusters of galaxies and cosmology. Large mm-wave telescopes are now routinely detecting and mapping the SZ effect in a number of clusters, measure their comptonisation parameter and use them as probes of the large-scale structure and evolution of the universe.
Aims. We show that estimates of the physical parameters of clusters (optical depth, plasma temperature, peculiar velocity, non-thermal components etc.) obtained from ground-based multi-band SZ photometry can be significantly biased, owing to the reduced frequency coverage, to the degeneracy between the parameters and to the presence of a number of independent components larger than the number of frequencies measured. We demonstrate that low-resolution spectroscopic measurements of the SZ effect that also cover frequencies >270 GHz are effective in removing the degeneracy.
Methods. We used accurate simulations of observations with lines-of-sight through clusters of galaxies with different experimental configurations (4-band photometers, 6-band photometer, multi-range differential spectrometer, full coverage spectrometers) and dif-

OLIMPO

- Long Duration Balloon experiment for mm & sub-mm astronomy
- Operates from the stratosphere - launch from Svalbard
- Cassegrain telescope, 2.6m aperture
- Multifrequency arrays of bolometers
- Low resolution spectrometer

ch	ν_{eff} [GHz]	$\Delta\nu_{FWHM}$ [GHz]	Res. [']
I	148.4	21.5	4.2
II	215.4	20.6	2.9
III	347.7	33.1	1.8
IV	482.9	54.2	1.8

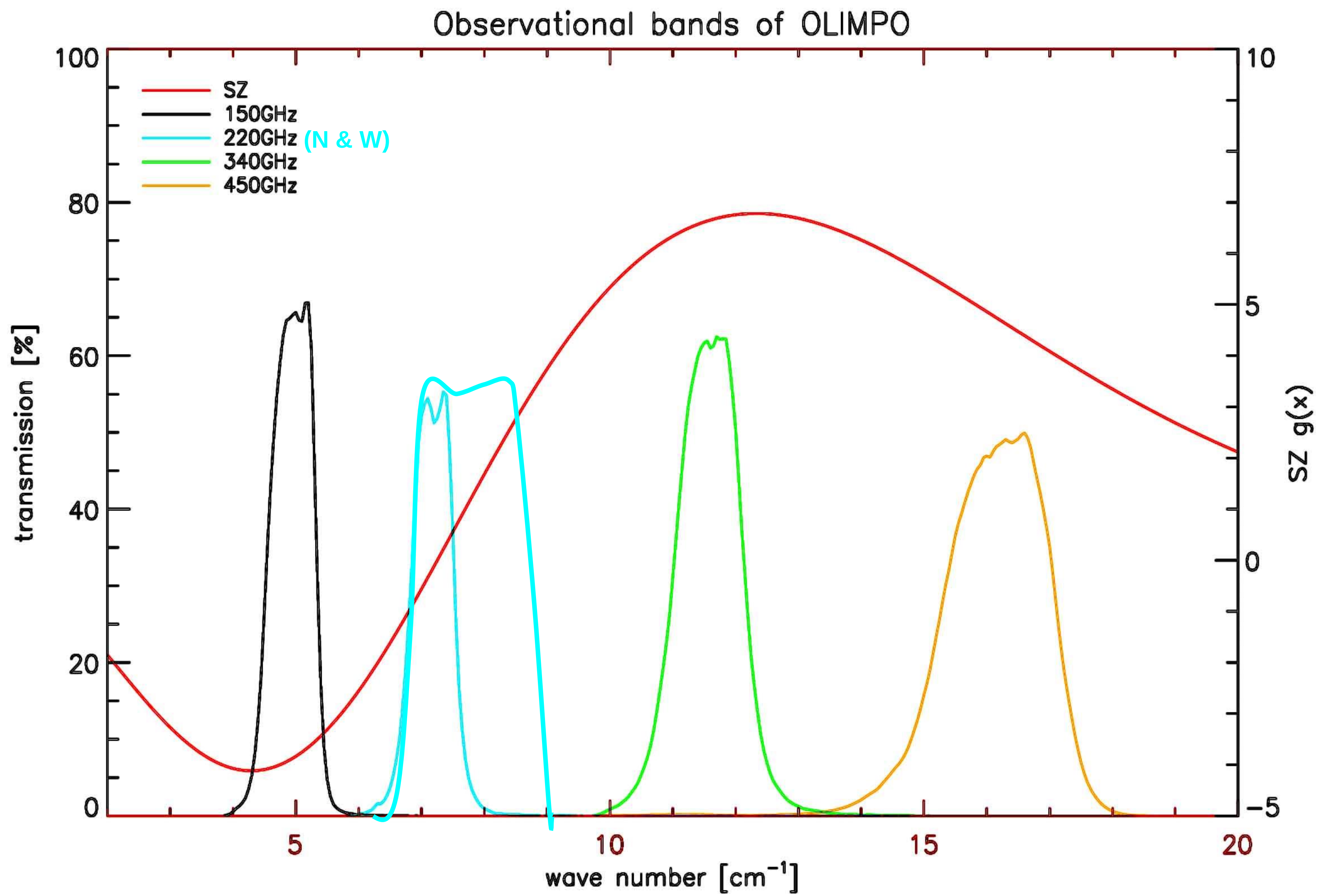
Observational bands of OLIMPO
SZ
150GHz
220GHz (N & W)
340GHz
450GHz
100
80
60
40
20
0
transmission [%]
10
5
0
−5
SZ g(x)
5
10
15
20
wave number [cm^{-1}]

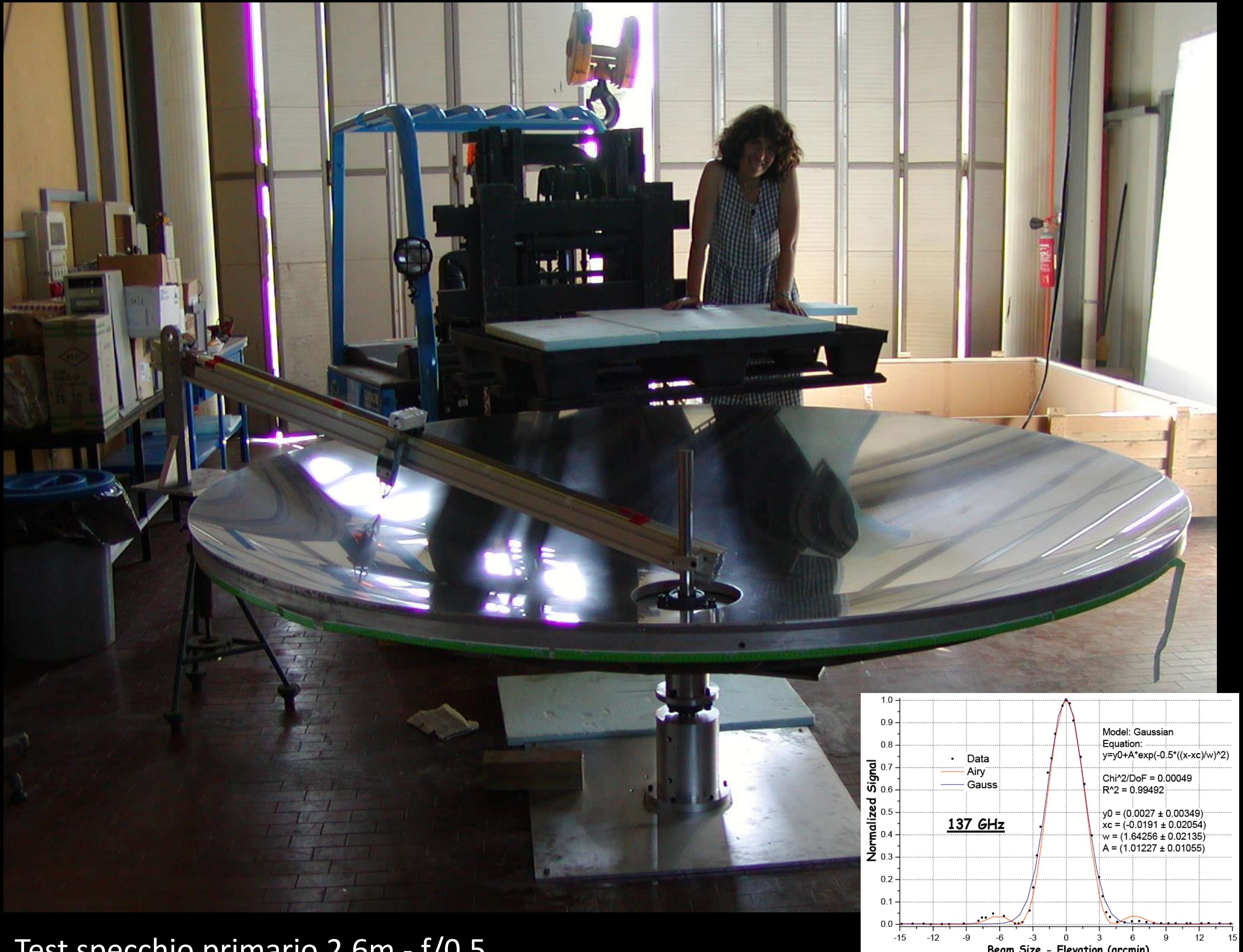

Test specchio primario 2.6m - f/0.5

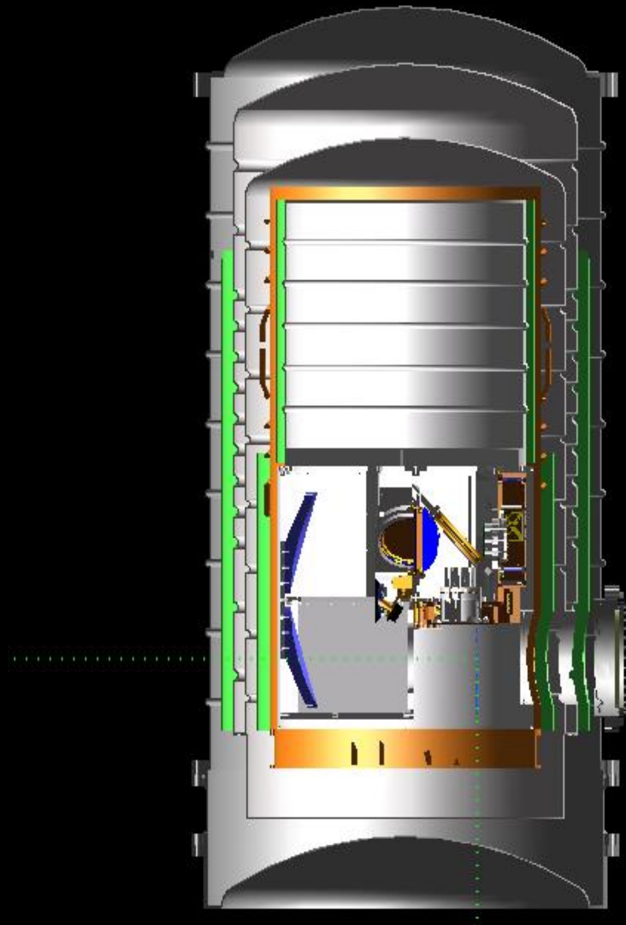

0.3K cryostat (made in Sapienza)
65L superfluid ^{4}He
70L liquid N
40LSTP ^{3}He refrigerator
50L experimental volume
Hold time – 15 days @ 0.3K

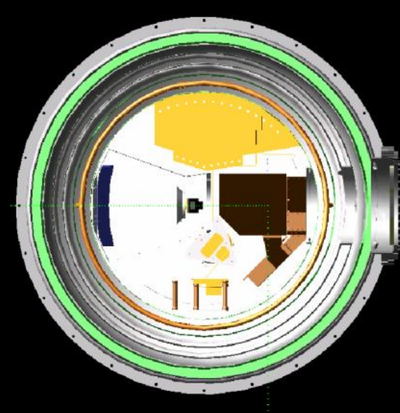

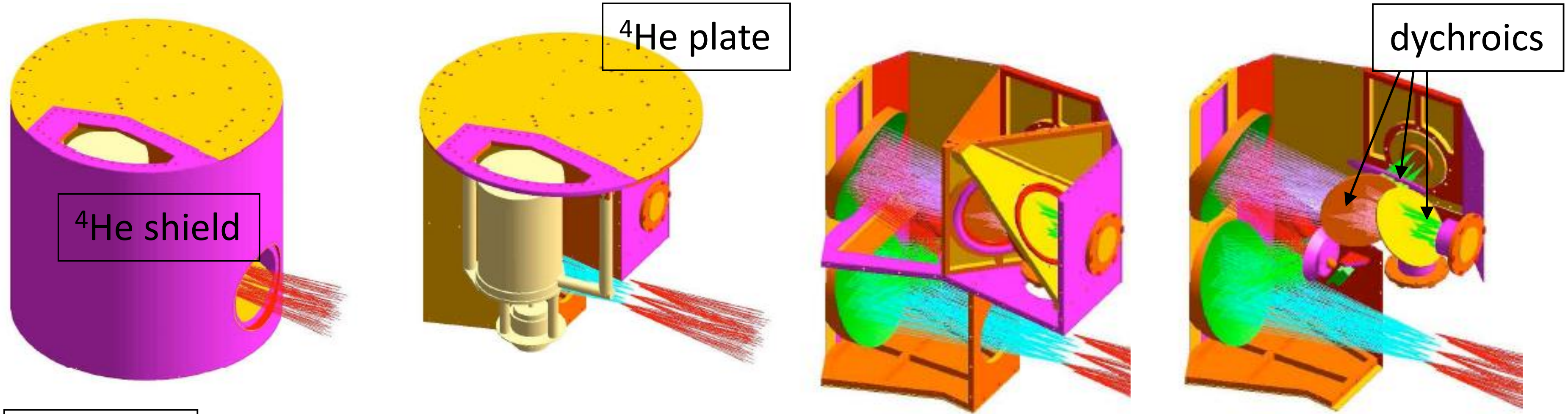

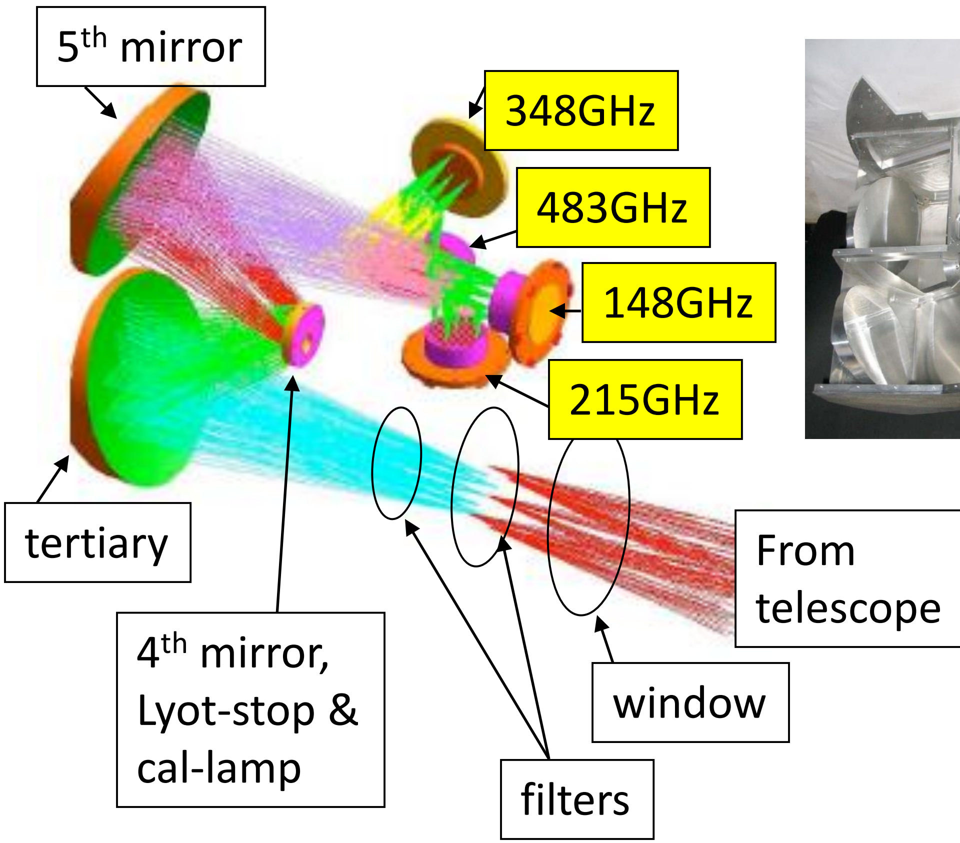

OLIMPO: Cold Optics and Arrays

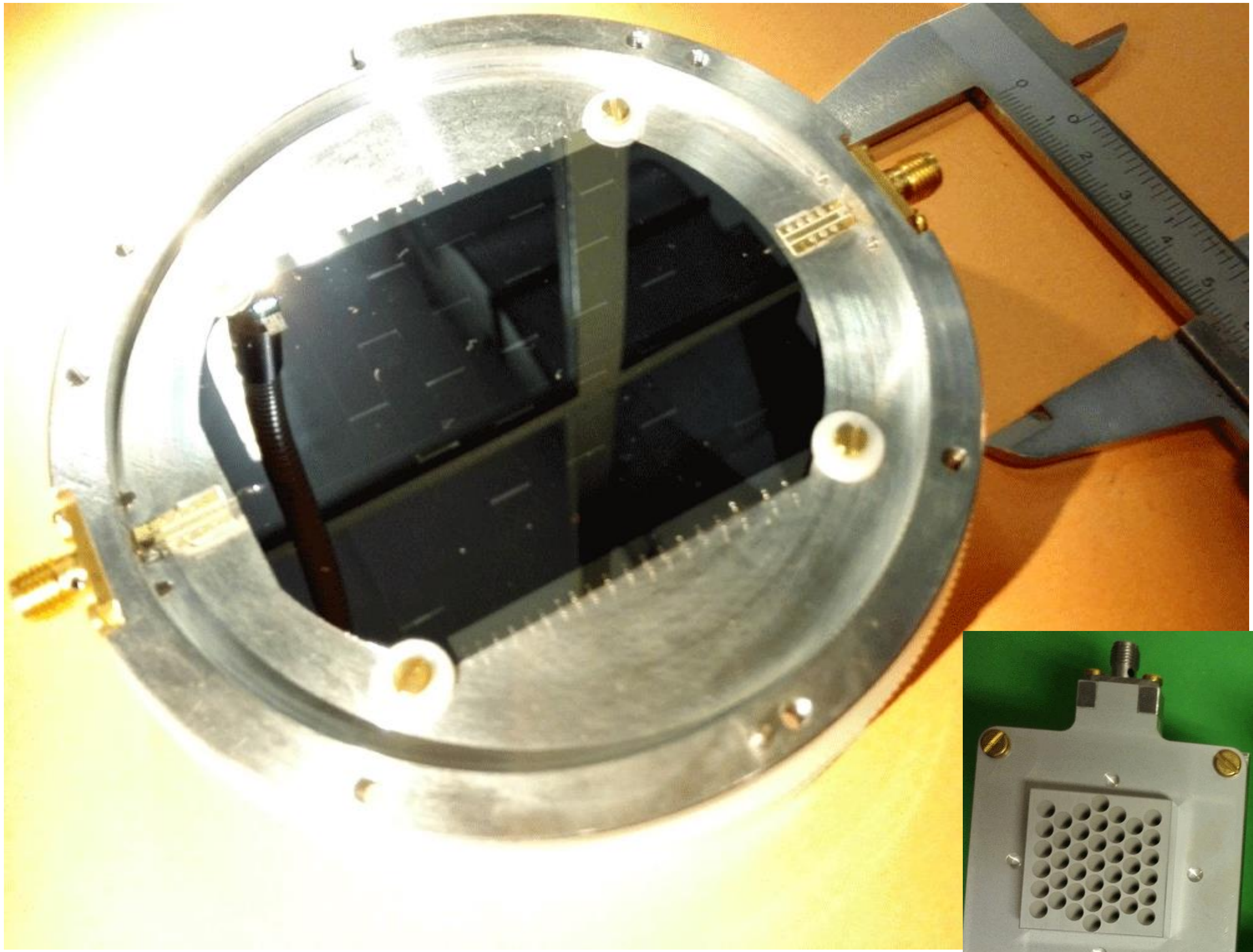

OLIMPO
Kinetic Inductance
Detectors

AL LEKIDs @
140, 200, 340, 480 GHz

100-600 MHz res.

CNR-IFN + Sapienza

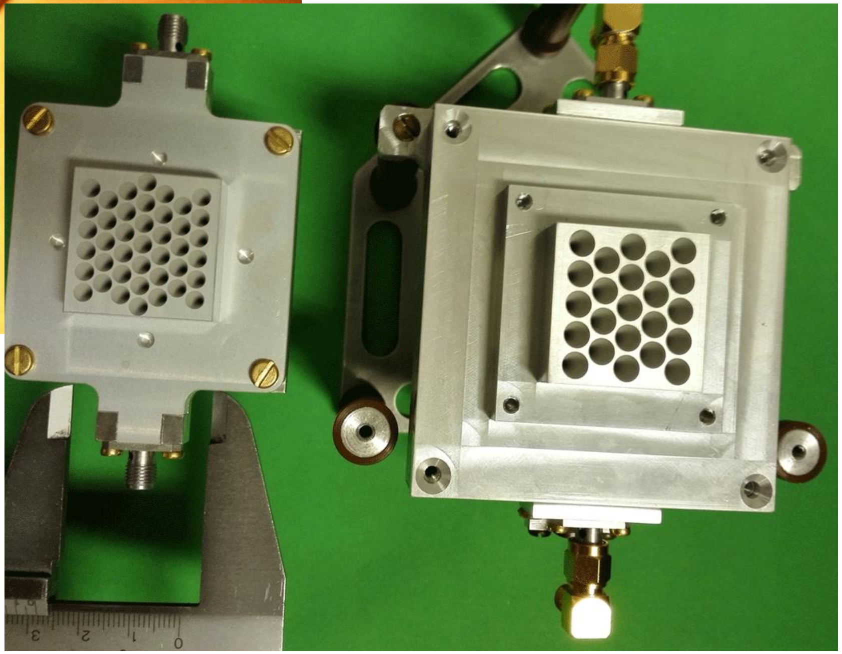

SAPIENZA
UNIVERSITÀ DI ROMA

IFN

OLIMPO's DIFFERENTIAL SPECTROMETER

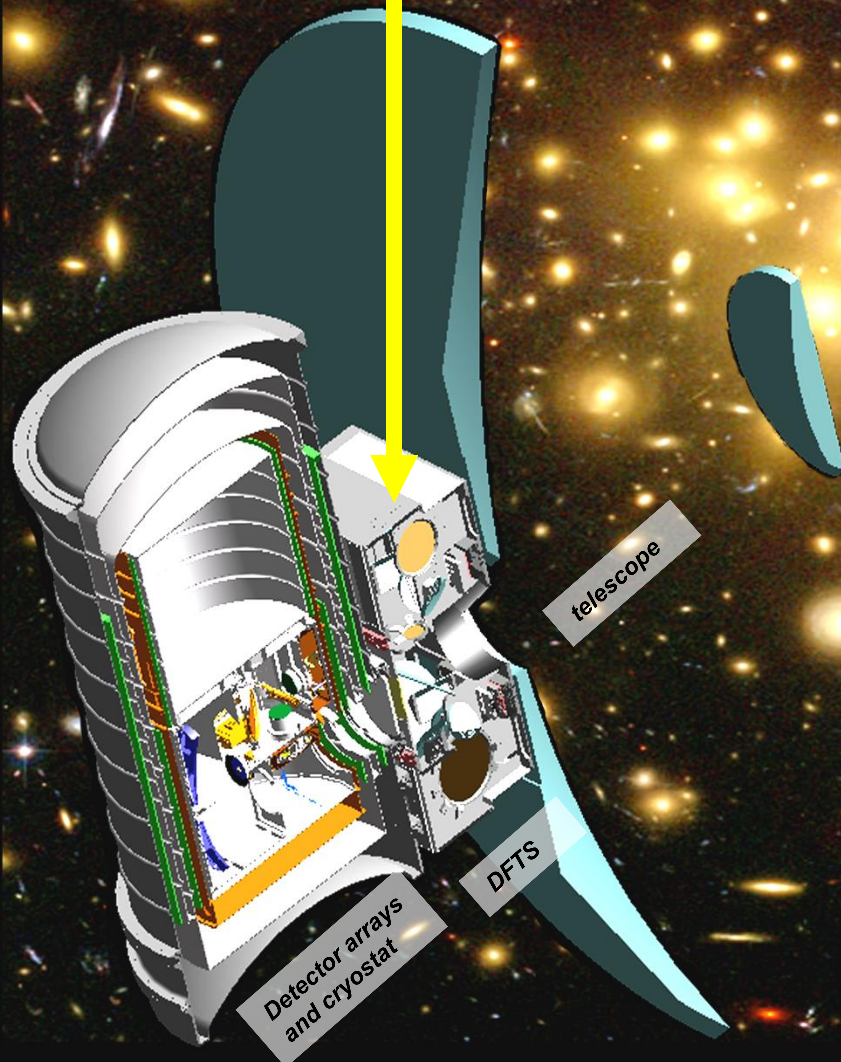

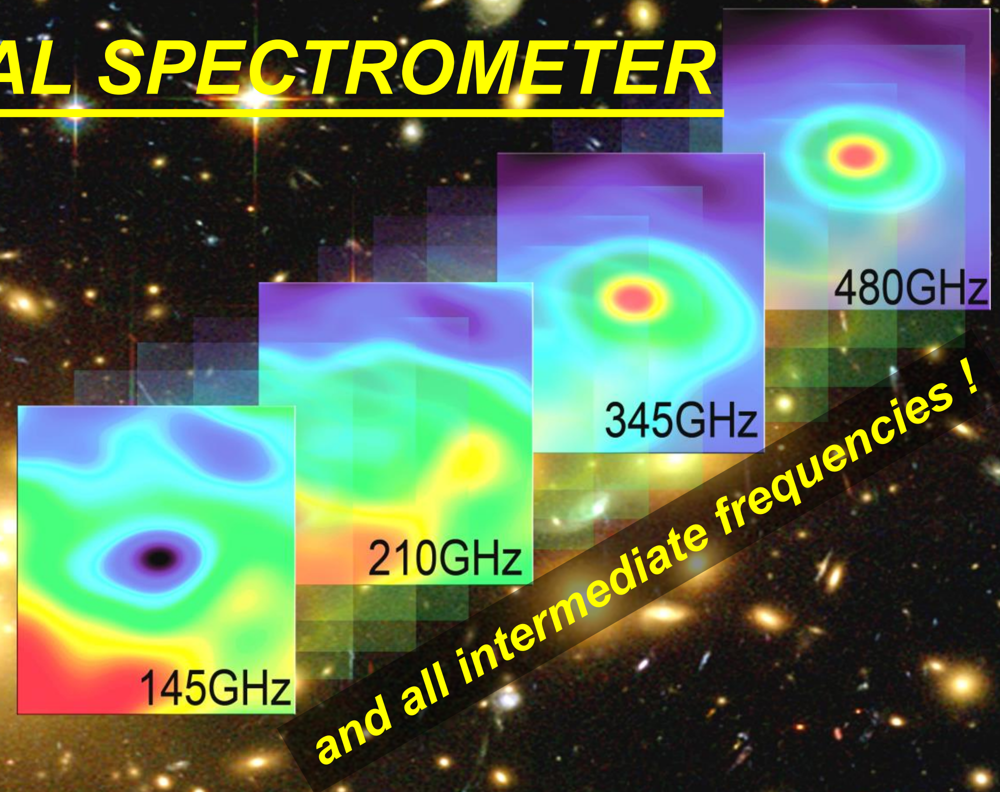

A Differential Fourier Transform Spectrometer (DFTS).
Similar to COBE-FIRAS but…
.. rather than measuring the brightness difference between the sky and an internal blackbody, it measures the **brightness difference between two directions in the sky**

- **The instrument is based on a double Martin Puplett Interferometer configuration to avoid the loss of half of the signal.**
- **A wedge mirror splits the sky image in two halves I_a and I_b, used as input signals for both inputs of the two FTS's.**
- **In the FTSs the beam to be analyzed is split in two halves, and a variable optical path difference is introduced.**

Olimpo Telescope

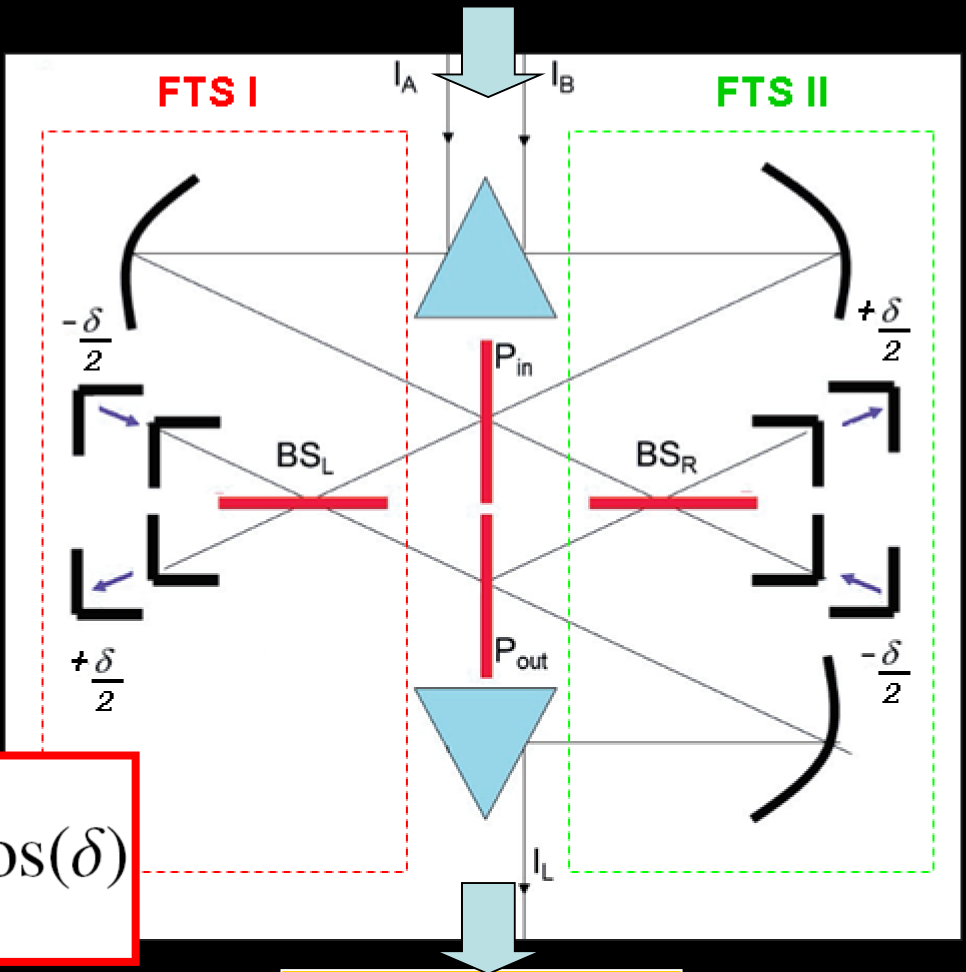

Olimpo Cryostat

See Schillaci et al. A&A 565, A125, 2014 for a detailed description of the instrument. The output brightness is

$$I_L = \frac{1}{2}(I_a + I_b) + \frac{1}{2}(I_a - I_b)\cos(\delta)$$

δ = variable phase shift, introduced by the variable optical path difference.

Only the *difference* between the two input brightnesses is modulated by the variable optical path difference.

A&A 565, A125 (2014)
DOI: 10.1051/0004-6361/201423631

Astronomy & Astrophysics

Efficient differential Fourier-transform spectrometer for precision Sunyaev-Zel'dovich effect measurements

Alessandro Schillaci[1], Giuseppe D'Alessandro[1], Paolo de Bernardis[1], Silvia Masi[1], Camila Paiva Novaes[2], Massimo Gervasi[3], and Mario Zannoni[3]

[1] Dipartimento di Fisica, Università di Roma "La Sapienza", Roma, Italy
e-mail: alessandro.schillaci@roma1.infn.it
[2] Divisão de Astrofísica, Instituto Nacional de Pesquisas Espaciais, São José dos Campos, SP, Brazil
[3] Dipartimento di Fisica G. Occhialini, Universitá Milano Bicocca, Milano, Italy

Received 13 February 2014 / Accepted 11 April 2014

ABSTRACT

Context. Precision measurements of the Sunyaev-Zel'dovich effect in clusters of galaxies require excellent rejection of common-mode signals and wide frequency coverage.
Aims. We describe an imaging, efficient, differential Fourier transform spectrometer (FTS), optimized for measurements of faint brightness gradients at millimeter wavelengths.
Methods. Our instrument is based on a Martin-Puplett interferometer (MPI) configuration. We combined two MPIs working synchronously to use the whole input power. In our implementation the observed sky field is divided into two halves along the meridian, and each half-field corresponds to one of the two input ports of the MPI. In this way, each detector in the FTS focal planes measures the difference in brightness between two sky pixels, symmetrically located with respect to the meridian. Exploiting the high common-mode rejection of the MPI, we can measure low sky brightness gradients over a high isotropic background.
Results. The instrument works in the range $\sim$1–20 cm^{-1} (30–600 GHz), has a maximum spectral resolution 1/(2 OPD) = 0.063 cm^{-1} (1.9 GHz), and an unvignetted throughput of 2.3 cm^{2}sr. It occupies a volume of $0.7 \times 0.7 \times 0.33$ m^3 and has a weight of 70 kg. This design can be implemented as a cryogenic unit to be used in space, as well as a room-temperature unit working at the focus of suborbital and ground-based mm-wave telescopes. The first in-flight test of the instrument is with the OLIMPO experiment on a stratospheric balloon; a larger implementation is being prepared for the Sardinia radio telescope.

Key words. cosmic background radiation – instrumentation: spectrographs – techniques: spectroscopic – galaxies: clusters: general

The real thing….
and measured interferograms

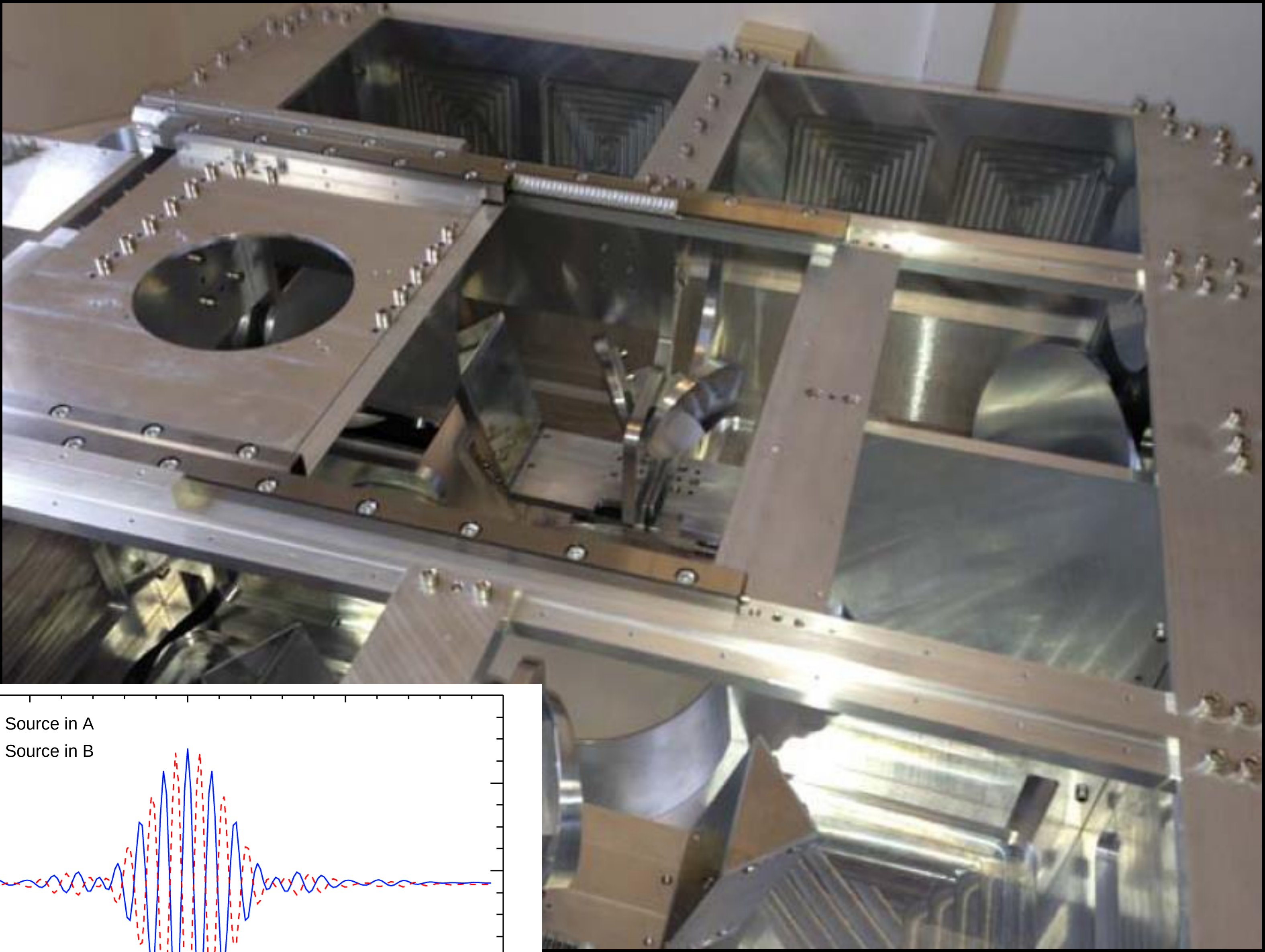

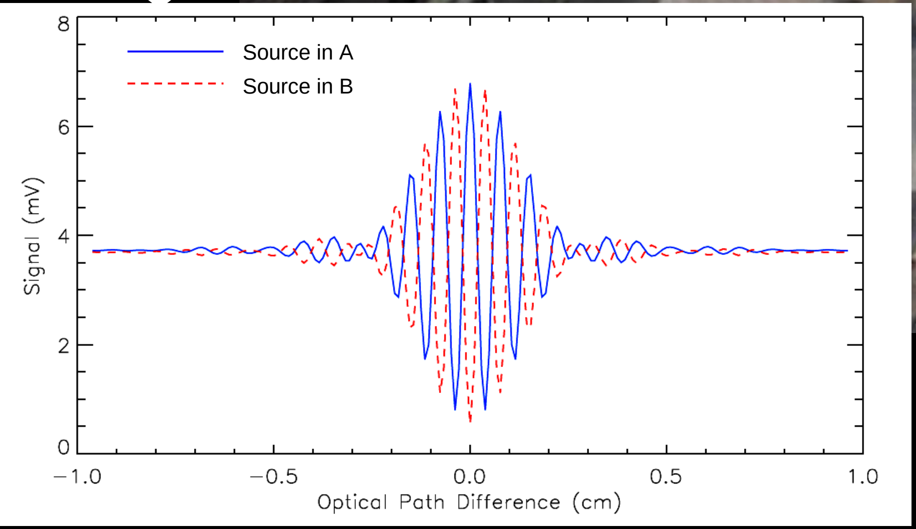

CMRR

- The differential signal (SZ) is much smaller than the common mode, which is CMB + instrument emissivity (a few %) + residual atmosphere.
- We have measured the common-mode rejection ratio of the FTS using custom temperature-controlled blackbody sources at the two entrance ports of the FTS.
- It turns out that the CMRR of our DFTS is <-55dB
- This means that the offset is less than the SZ signal in OLIMPO, and will be much less than the SZ signal in a cryogenic/space implementation.

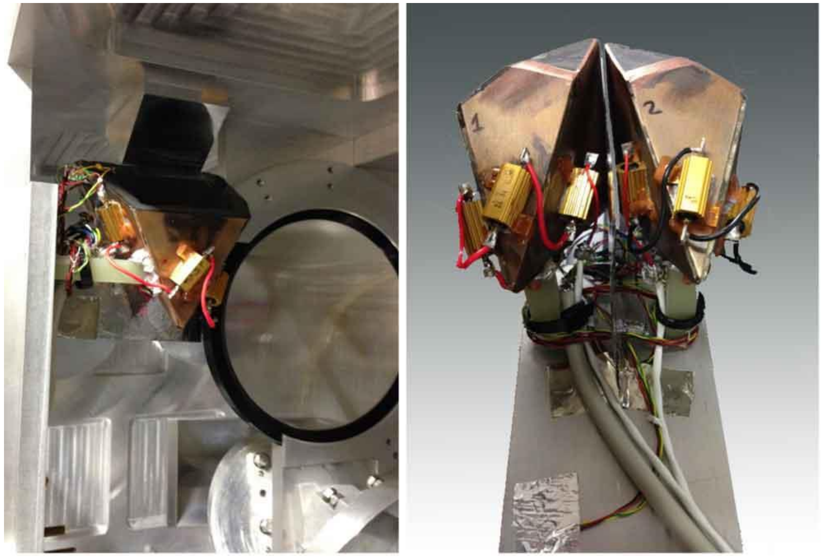

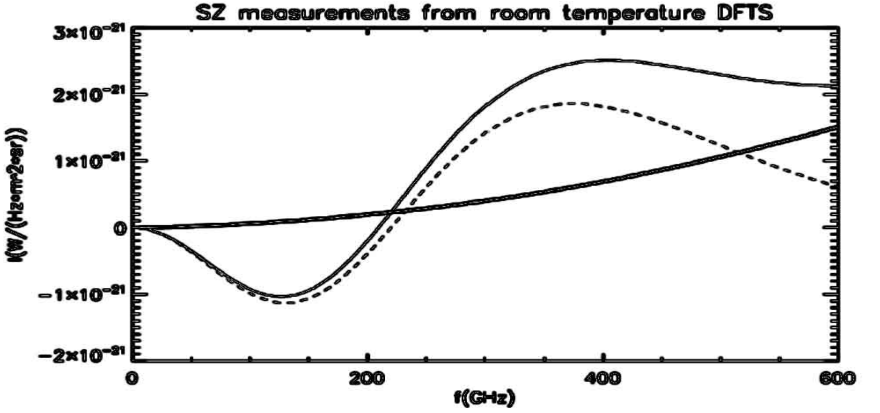

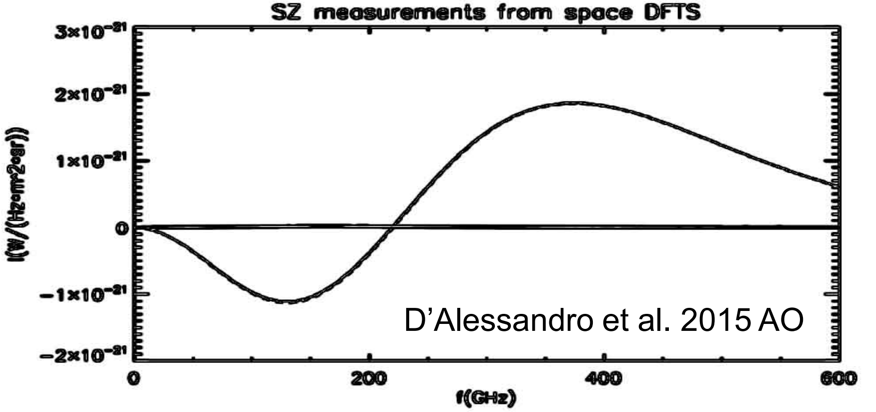

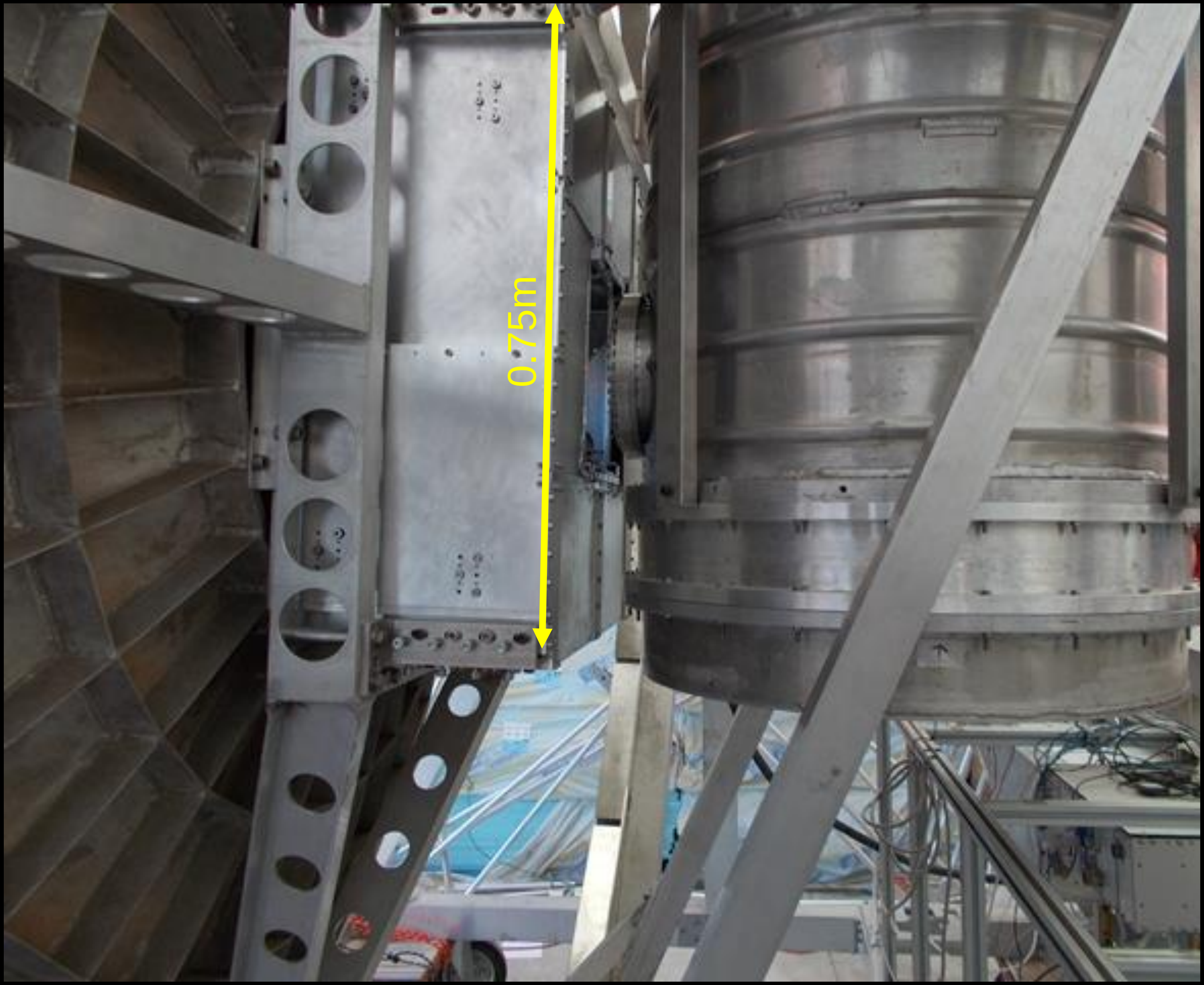

Telescope / primary mirror DFTS cryostat / detectors arrays

Main components of OLIMPO integrated on the payload

Observation Program

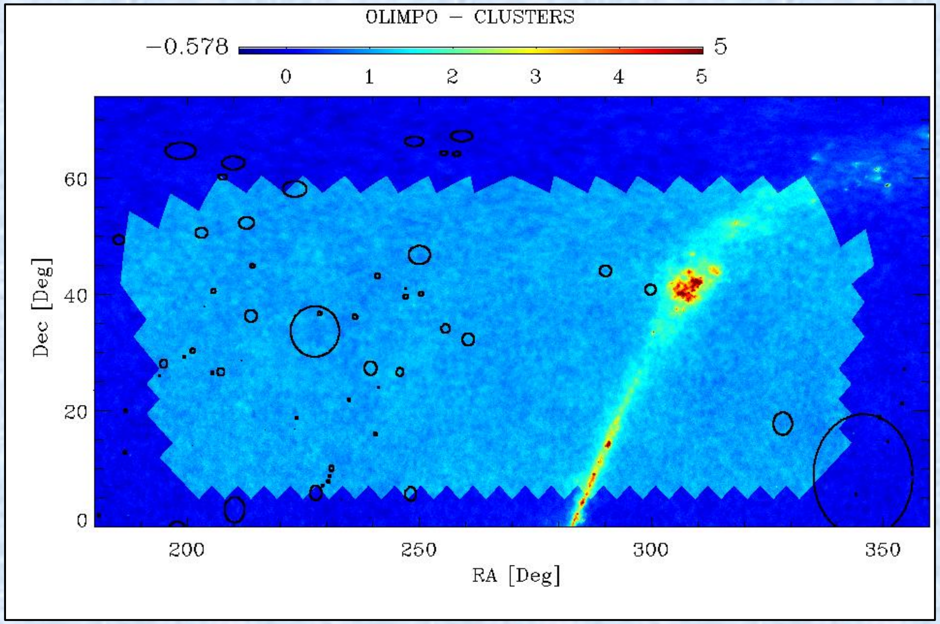

ind	ID	RA	Dec	TIME	frac	NAME
0	1	212.83	52.2	18000	1	3C295CLUSTER
1	40	194.95	27.98	3600	0	ABELL1656
2	43	203.13	50.51	3600	1	ABELL1758
3	44	205.48	26.37	3600	1	ABELL1775
4	45	207.25	26.59	3600	1	ABELL1795
5	48	216.72	16.68	18000	1	ABELL1913
6	49	223.18	16.75	11360.88	1.27	ABELL1983
7	50	223.63	18.63	18000	1	ABELL1991
8	51	223.21	58.05	5640.53	1.28	ABELL1995
9	53	227.56	33.53	18000	1	ABELL2034
10	54	229.19	7	3600	1	ABELL2052
11	55	230.76	8.64	3600	1	ABELL2063
12	56	234.95	21.77	3600	1	ABELL2107
13	57	236.25	36.06	18000	1	ABELL2124
14	58	239.57	27.23	3600	1	ABELL2142
15	59	240.57	15.9	3600	1	ABELL2147
16	61	247.04	40.91	18000	1	ABELL2197
17	62	247.15	39.52	3600	1	ABELL2199
18	63	248.19	5.58	3600	1	ABELL2204
19	65	250.09	46.69	3600	1	ABELL2219
20	66	255.68	34.05	7230	1.49	ABELL2244
21	69	260.62	32.15	18000	1	ABELL2261
22	70	290.19	43.96	3600	1	ABELL2319
23	71	328.39	17.67	3600	1	ABELL2390
24	98	241.24	23.92	13045.75	1.1	AWM4
25	100	299.87	40.73	18000	1	CYGNUSA
26	101	201.2	30.19	18000	1	GHO1322+3027
27	102	241.11	43.08	18000	1	GHO1602+4312
28	107	230.46	7.71	3600	1	MKW03S
29	120	228.61	36.61	18000	1	MS1512.4+3647
30	121	245.9	26.56	13147.05	1.1	MS1621.5+2640
31	128	201.15	13.93	18000	0	NGC5129GROUP
32	134	199.34	29.19	18000	1	RDCSJ1317+2911
33	143	231.17	9.96	18000	1	RXJ1524.6+0957
34	150	211.73	28.57	18000	1	WARPJ1406.9+2834
35	151	213.8	36.2	18000	1	WARPJ1415.1+3612
36	161	194.02	25.95	18000	0	[VMF98]128
37	162	203.74	37.84	18000	1	[VMF98]139
38	163	205.71	40.47	18000	1	[VMF98]148
39	164	214.12	44.78	18000	1	[VMF98]158
40	165	250.47	40.03	18000	1	[VMF98]184

- In a circumpolar summer long duration flight (>200h) we plan to observe 40 selected clusters and to perform a blind deep integration on a clean sky region
- We have optimized the observation plan distributing the integration time among the different targets according to their brightness and diurnal elevation.

- OLIMPO launched at 07:09 GMT, 14/Jul/2018, Longyearbyen (Svalbard)
- Great performance of Kinetic Inductance Detector Arrays, Telescope and Spectrometer.
- First Validation of KIDs in space conditions
- TM/TC problems (only LOS TM/TC contact) -> successful technical flight

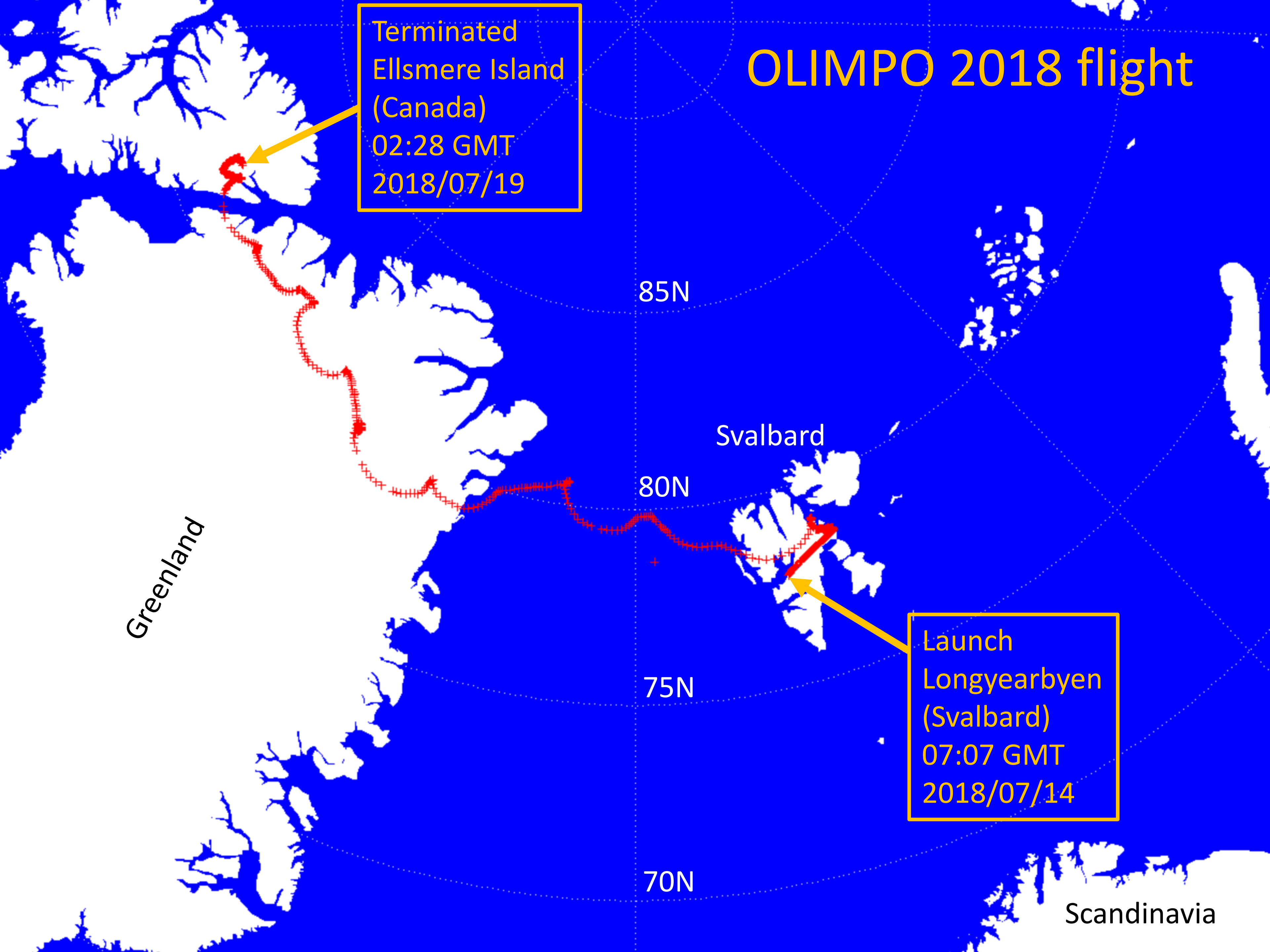
OLIMPO 2018 flight
Terminated
Ellsmere Island
(Canada)
02:28 GMT
2018/07/19
Launch
Longyearbyen
(Svalbard)
07:07 GMT
2018/07/14
Svalbard
Greenland
Scandinavia
85N
80N
75N
70N

OLIMPO: Kinetic Inductance Detectors

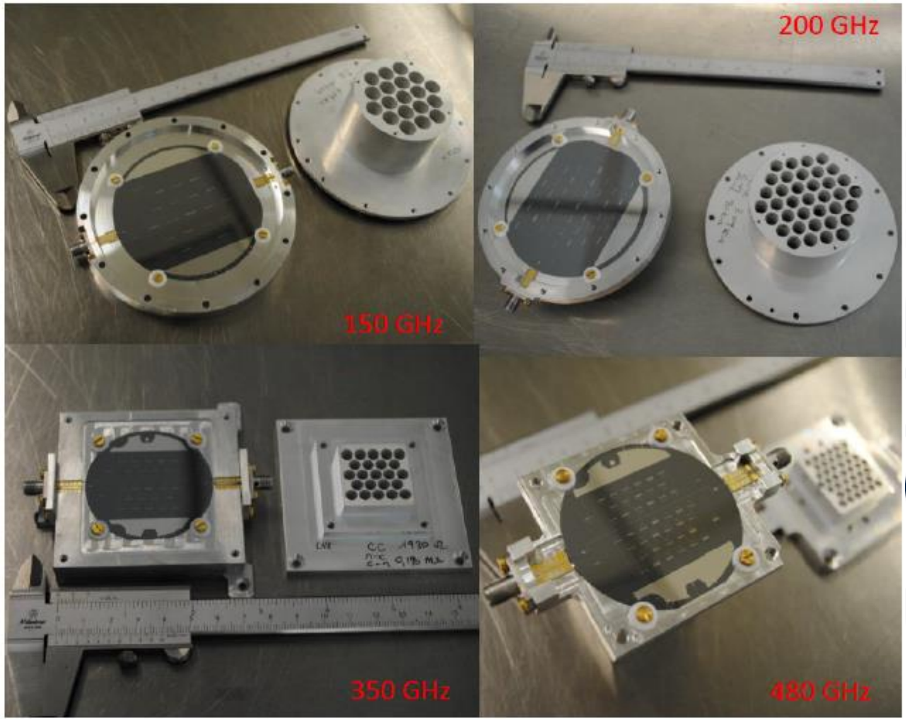

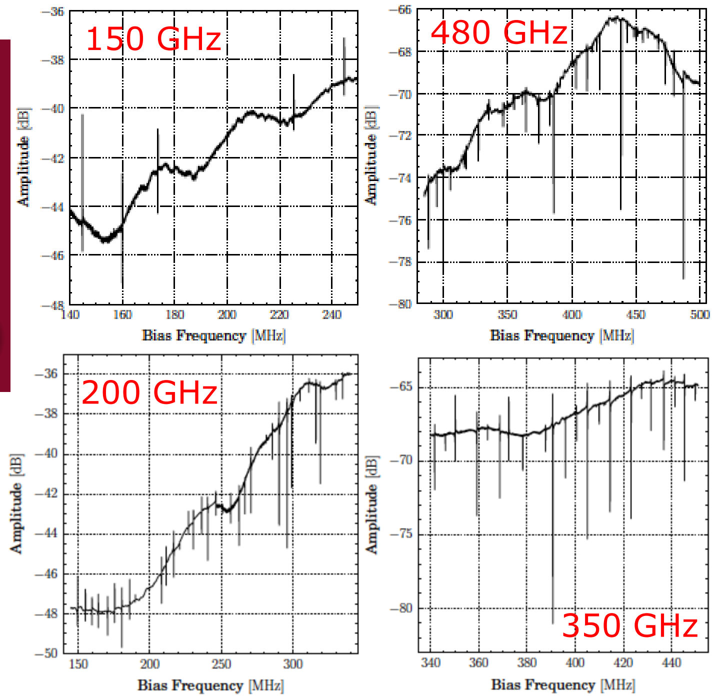

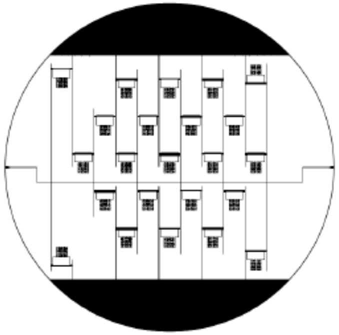

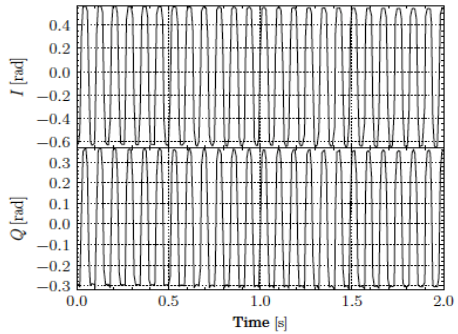

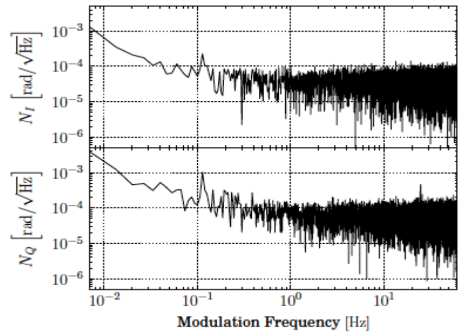

Channel	NET_{RJ} $[mK/\sqrt{Hz}]$
150 GHz	0.180
200 GHz	0.145
350 GHz	0.288
480 GHz	0.433

typical NET

See Paiella et al. (2019) JCAP01(2019)039

Kinetic Inductance Detectors : in-flight performance

Calibration lamp signals (10 mK optical stimulator) as in-flight calibration transfer

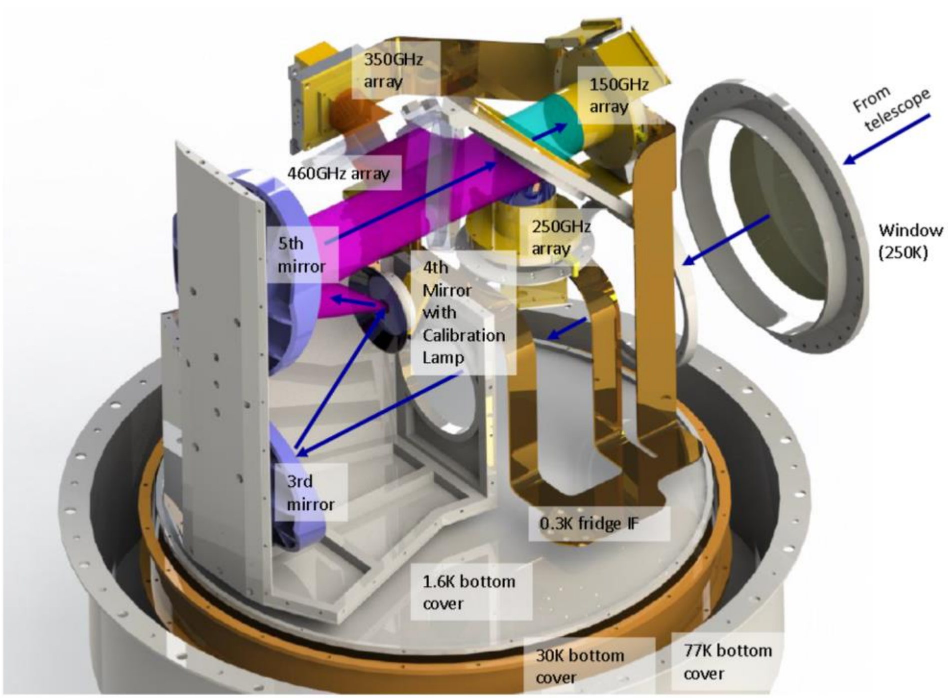

Figure 4. Sketch of the OLIMPO cryogenic reimaging optics (3[rd] mirror, 4[th] mirror, 5[th] mirror, dichroics and detector arrays). The cryogenic liquid tanks and many parts of the outer shell and shields have been hidden to show the optical system. The calibration lamp is located in the center of the 4[th] mirror, which is the Lyot stop of the optical system, and close to the *foci* of the 3[rd] and 5[th] mirrors. The beam from the calibration lamp, illuminating the four detector arrays is also shown. The path of the chief ray coming from the telescope and reaching the 150 GHz array is indicated by the blue arrows. For scale, the diameter of the 1.6 K L^4He tank is 45 cm.

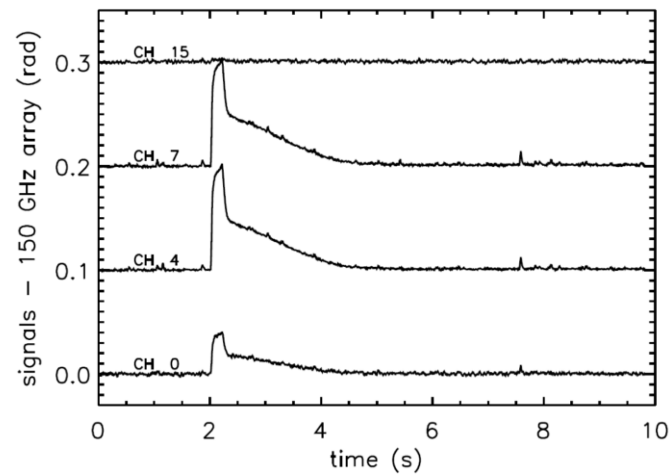

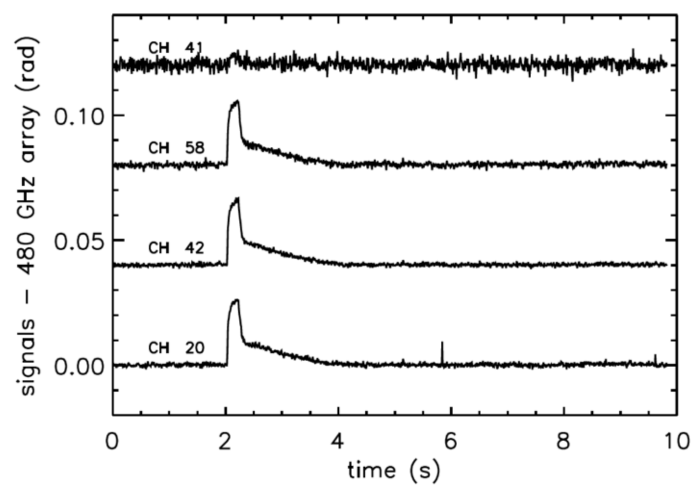

agenzia spaziale italiana

See Masi et al. (2019) JCAP07(2019)003

Kinetic Inductance Detectors : in-flight performance

Response of KIDs to cosmic rays in the stratospheric environment – first test ever

Time ordered data

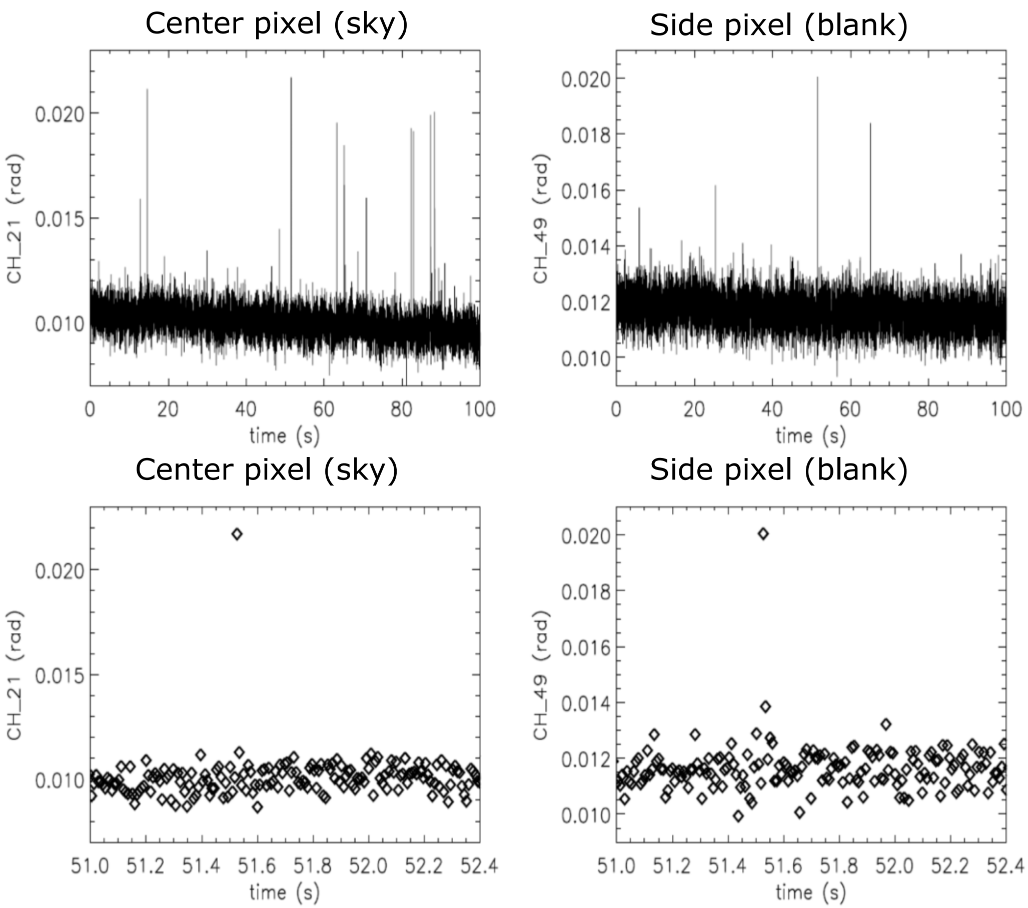

460 GHz array

Histograms

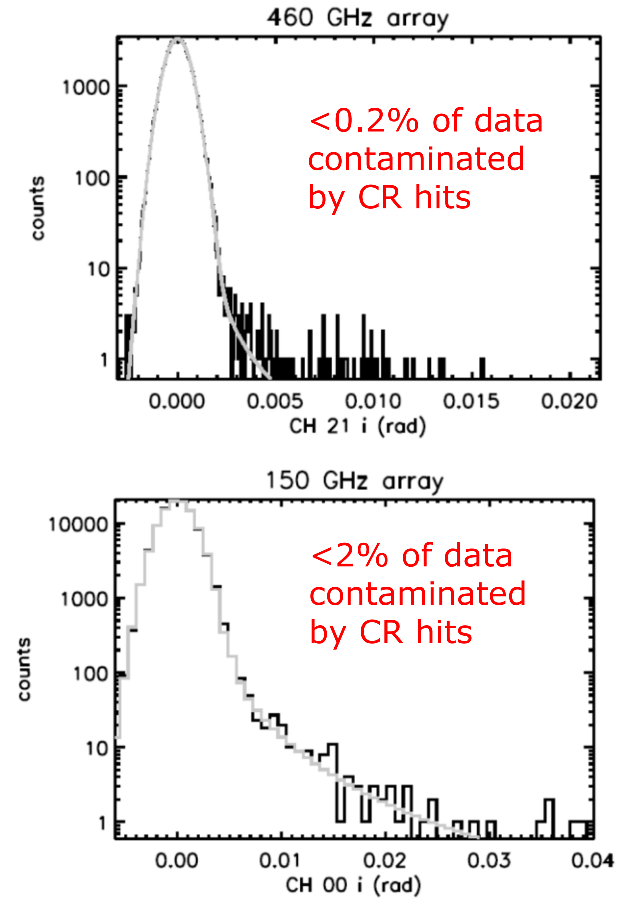

See Masi et al. (2019) JCAP07(2019)003

Expected results from science flight

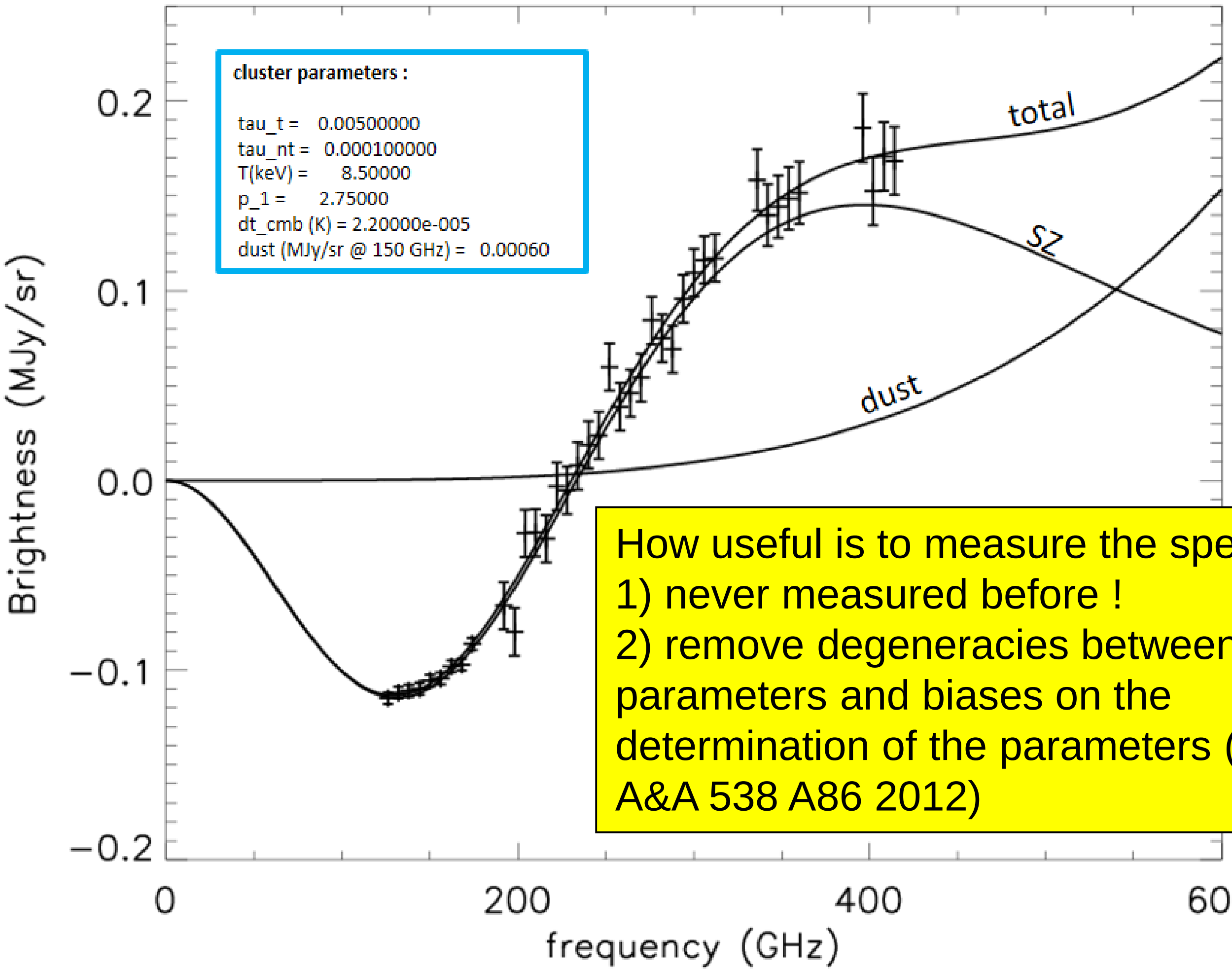

How useful is to measure the spectrum ?
1) never measured before !
2) remove degeneracies between cluster parameters and biases on the determination of the parameters (see A&A 538 A86 2012)

agenzia spaziale italiana

After this first successful technical flight,
the OLIMPO team has applied for an Antarctic science flight

LSPE

the Large-Scale Polarization Explorer

Paolo de Bernardis,
Università La Sapienza, Roma, Italy
for the LSPE collaboration

MI
GE
PI
FE
RM1
RM2

Peter	Ade	University of Cardiff
Giorgio	Amico	Dip. Fisica Sapienza & INFN Roma1
Alessandro	Baldini	INFN Pisa
Paola	Battaglia	Dip. Fisica Università di Milano
Elia Stefano	Battistelli	Dip. Fisica Sapienza & INFN Roma1
Alessandro	Baù	Dip. Fisica Università di Milano Bicocca
Carlo	Bemporad	INFN Pisa
Marco	Bersanelli	Dip. Fisica Università di Milano
Michele	Biasotti	Dip. Fisica Uni. Genova & INFN Genova
Andrea	Boscaleri	IFAC - CNR Firenze
Alessandro	Buzzelli	Università di Roma TorVergata & INFN Roma2
Paolo	Cabella	Università di Roma TorVergata & INFN Roma2
Francesco	Cavaliere	Dip. Fisica Università di Milano
Valentina	Ceriale	Dip. Fisica Uni. Genova & INFN Genova
Eugenia	Coccia	Dip. Fisica Tor Vergata & INFN Roma2
Gabriele	Coppi	Dip. Fisica Sapienza & INFN Roma1
Alessandro	Coppolecchia	Dip. Fisica Sapienza & INFN Roma1
Dario	Corsini	Dip. Fisica Uni. Genova & INFN Genova
Angelo	Cruciani	Dip. Fisica Sapienza & INFN Roma1
Francesco	Cuttaia	INAF - IASF Bologna
Antonello	D'Addabbo	Dip. Fisica Sapienza & INFN Roma1
Giuseppe	D'Alessandro	Dip. Fisica Sapienza & INFN Roma1
Paolo	de Bernardis	Dip. Fisica Sapienza & INFN Roma1
Giancarlo	De Gasperis	Università di Roma TorVergata & INFN Roma2
Matteo	De Gerone	Dip. Fisica Uni. Genova & INFN Genova
Marco	De Petris	Dip. Fisica Sapienza & INFN Roma1
Francesco	Del Torto	Dip. Fisica Università di Milano
Alessandro	Di Marco	Università di Roma TorVergata & INFN Roma2
Viviana	Fafone	Dip. Fisica Tor Vergata & INFN Roma2
Lorenzo	Fiorineschi	Dip. Ing. Ind. Uni. Firenze
Flavio	Fontanelli	Dip. Fisica Uni. Genova & INFN Genova
Francesco	Forastieri	Università di Ferrara & INFN Ferrara
Christian	Franceschet	Dip. Fisica Università di Milano
Luca	Galli	INFN Pisa
Flavio	Gatti	Dip. Fisica Uni. Genova & INFN Genova
Massimo	Gervasi	Dip. Fisica Università di Milano Bicocca
Anna	Gregorio	Department of Physics - University of Trieste
Daniele	Grosso	Dip. Fisica Uni. Genova & INFN Genova
Alessandro	Gruppuso	INAF/IASF Bologna & INFN Bologna
Riccardo	Gualtieri	Dip. Fisica Sapienza & INFN Roma1
Victor	Haynes	University of Manchester
Marco	Incagli	INFN Pisa
Nicoletta	Krachmalnicoff	Dip. Fisica Università di Milano
Luca	Lamagna	Dip. Fisica Sapienza & INFN Roma1
Massimiliano	Lattanzi	Università di Ferrara & INFN Ferrara
Bruno	Maffei	University of Manchester
Davide	Maino	Dip. Fisica Università di Milano
Tommaso	Marchetti	Dip. Fisica Sapienza & INFN Roma1
Silvia	Masi	Dip. Fisica Sapienza & INFN Roma1
Aniello	Mennella	Dip. Fisica Università di Milano
Diego	Molinari	Università di Ferrara & INFN Ferrara
Gianluca	Morgante	INAF - IASF Bologna
Federico	Nati	Dip. Fisica Sapienza & INFN Roma1
Paolo	Natoli	Università di Ferrara & INFN Ferrara
Ming Wah	Ng	University of Manchester
Luca	Pagano	Dip. Fisica Sapienza & INFN Roma1
Alessandro	Paiella	Dip. Fisica Sapienza & INFN Roma1
Andrea	Passerini	Dip. Fisica Università di Milano Bicocca
Oscar	Peverini	IEIIT - CNR - Torino
Francesco	Piacentini	Dip. Fisica Sapienza & INFN Roma1
Lucio	Piccirillo	University of Manchester
Giampaolo	Pisano	University of Cardiff
Sara	Ricciardi	INAF - IASF Bologna
Paolo	Rissone	Dip. Ing. Ind. Uni. Firenze
Alessio	Rocchi	Dip. Fisica Tor Vergata & INFN Roma2
Giovanni	Romeo	INGV - Roma
Maria	Salatino	Dip. Fisica Sapienza & INFN Roma1
Mauro	Sandri	INAF - IASF Bologna
Alessandro	Schillaci	Dip. Fisica Sapienza & INFN Roma1
Giovanni	Signorelli	INFN Pisa
Franco	Spinella	INFN Pisa
Luca	Stringhetti	INAF - IASF Bologna
Andrea	Tartari	Dip. Fisica Università di Milano Bicocca
Riccardo	Tascone	IEIIT - CNR - Torino
Luca	Terenzi	INAF - IASF Bologna
Maurizio	Tomasi	Dip. Fisica Università di Milano
Elisabetta	Tommasi	Italian Space Agency
Carole	Tucker	University of Cardiff
Fabrizio	Villa	INAF - IASF Bologna
Giuseppe	Virone	IEIIT - CNR - Torino
Nicola	Vittorio	Università di Roma TorVergata & INFN Roma2
Andrea	Zacchei	INAF Osservatorio Trieste
Mario	Zannoni	Dip. Fisica Università di Milano Bicocca
Guido	Zavattini	Università di Ferrara & INFN Ferrara

The LSPE-SWIPE Collaboration

Peter	Ade	Dept. Of Phys. And Astronomy, Cardiff Univ. (UK)
Giorgio	Amico	Phys. Dep. Sapienza Roma & INFN Roma
Alessandro	Baldini	INFN Pisa
Elia	Battistelli	Phys. Dep. Sapienza Roma & INFN Roma
Michele	Biasotti	Phys. Dep. Genova & INFN Genova
Corrado	Boragno	Phys. Dep. Genova & INFN Genova
Andrea	Boscaleri	IFAC CNR Firenze
Alessandro	Buzzelli	Phys. Dep. Tor Vergata Roma & INFN Roma 2
Paolo	Cabella	Phys. Dep. Tor Vergata Roma & INFN Roma 2
Fabrizio	Cei	INFN Pisa
Valentina	Ceriale	Phys. Dep. Genova & INFN Genova
Elisabetta	Cesarini	Phys. Dep. Tor Vergata Roma & INFN Roma 2
Stefano	Chiozzi	Dipartimento di Fisica e Scienze della Terra, Università di Ferrara and INFN, Sez. Di Ferra
Eugenio	Coccia	Phys. Dep. Tor Vergata Roma & INFN Roma 2
Fabio	Columbro	Phys. Dep. Sapienza Roma & INFN Roma
Gabriele	Coppi	Phys. Dep. Sapienza Roma & INFN Roma
Gabriele	Coppi	Phys. Dep. Univ. of Manchester (UK)
Alessandro	Coppolecchia	Phys. Dep. Sapienza Roma & INFN Roma
Dario	Corsini	Phys. Dep. Genova & INFN Genova
Angelo	Cotta Ramusino	Dipartimento di Fisica e Scienze della Terra, Università di Ferrara and INFN, Sez. Di Ferra
Giuseppe	D'Alessandro	Phys. Dep. Sapienza Roma & INFN Roma
Sabrina	D'Antonio	Phys. Dep. Tor Vergata Roma & INFN Roma 2
Paolo	de Bernardis	Phys. Dep. Sapienza Roma & INFN Roma
Giancarlo	De Gasperis	Phys. Dep. Tor Vergata Roma & INFN Roma 2
Viviana	Fafone	Phys. Dep. Tor Vergata Roma & INFN Roma 2
Flavio	Fontanelli	Phys. Dep. Genova & INFN Genova
Francesco	Forastieri	Dipartimento di Fisica e Scienze della Terra, Università di Ferrara and INFN, Sez. Di Ferra
Elisa	Fumagalli	Phys. Dep. Genova & INFN Genova
Luca	Galli	INFN Pisa
Flavio	Gatti	Phys. Dep. Genova & INFN Genova
Mauro	Giovannini	Phys. Dep. Genova & INFN Genova
Marco	Grassi	INFN Pisa
Daniele	Grosso	Phys. Dep. Genova & INFN Genova
Alessandro	Gruppuso	Dipartimento di Fisica e Scienze della Terra, Università di Ferrara and INFN, Sez. Di Ferra
Sandeep	Haridasu Balakrishna	Phys. Dep. Tor Vergata Roma & INFN Roma 2
Giuseppe	Iacobellis	Dipartimento di Fisica e Scienze della Terra, Università di Ferrara and INFN, Sez. Di Ferra
Marco	Incagli	INFN Pisa
Luca	Lamagna	Phys. Dep. Sapienza Roma & INFN Roma
Massimiliano	Lattanzi	Dipartimento di Fisica e Scienze della Terra, Università di Ferrara and INFN, Sez. Di Ferrara
Margherita	Lembo	Dipartimento di Fisica e Scienze della Terra, Università di Ferrara and INFN, Sez. Di Ferrara
Matteo	Lorenzini	Phys. Dep. Tor Vergata Roma & INFN Roma 2
Vladimir	Lukovich	Phys. Dep. Tor Vergata Roma & INFN Roma 2
Tommaso	Marchetti	Phys. Dep. Sapienza Roma & INFN Roma
Lorenzo	Martinis	Phys. Dep. Univ. of Manchester (UK)
Silvia	Masi	Phys. Dep. Sapienza Roma & INFN Roma
Andrew	May	Phys. Dep. Univ. of Manchester (UK)
Mark	McCulloch	Phys. Dep. Univ. of Manchester (UK)
Simon	Melhuish	Phys. Dep. Univ. of Manchester (UK)
Marina	Migliaccio	Dipartimento di Fisica e Scienze della Terra, Università di Ferrara and INFN, Sez. Di Ferrara
Andrea	Moggi	INFN Pisa
Diego	Molinari	Dipartimento di Fisica e Scienze della Terra, Università di Ferrara and INFN, Sez. Di Ferrara
Umberto	Natale	Dipartimento di Fisica e Scienze della Terra, Università di Ferrara and INFN, Sez. Di Ferrara
Paolo	Natoli	Dipartimento di Fisica e Scienze della Terra, Università di Ferrara and INFN, Sez. Di Ferrara
Donato	Nicolò	INFN Pisa
Luca	Pagano	IAS Orsay
Alessandro	Paiella	Phys. Dep. Sapienza Roma & INFN Roma
Francesco	Piacentini	Phys. Dep. Sapienza Roma & INFN Roma
Lucio	Piccirillo	Phys. Dep. Univ. of Manchester (UK)
Marco	Piendibene	INFN Pisa
Giampaolo	Pisano	Dept. Of Phys. And Astronomy, Cardiff Univ. (UK)
Linda	Polastri	Dipartimento di Fisica e Scienze della Terra, Università di Ferrara and INFN, Sez. Di Ferrara
Gianluca	Polenta	Agenzia Spaziale Italiana
Alessio	Rocchi	Phys. Dep. Tor Vergata Roma & INFN Roma 2
Alessandro	Schillaci	Phys. Dep. Sapienza Roma & Caltech
Giovanni	Signorelli	INFN Pisa
Franco	Spinella	INFN Pisa
Elisabetta	Tommasi	Agenzia Spaziale Italiana
Carole	Tucker	Dept. Of Phys. And Astronomy, Cardiff Univ. (UK)
Davide	Vaccaro	INFN Pisa
Nicola	Vittorio	Phys. Dep. Tor Vergata Roma & INFN Roma 2
Angela	Volpe	Agenzia Spaziale Italiana
Guido	Zavattini	Dipartimento di Fisica e Scienze della Terra, Università di Ferrara and INFN, Sez. Di Ferrara

MILANO
GENOVA
PISA
FERRARA
ROMA1
ROMA2

LSPE in a nutshell

- The Large-Scale Polarization Explorer is an experiment to measure the polarization of the CMB at large angular scales.
- **Science drivers** :
  - The B-modes from inflation are mainly at large scales (*r*)
  - Polarization signatures from reionization (τ) are mainly at large scales
  - Rotation of the polarization angles (related to new physics)
  - Sensitive polarized dust survey at frequencies close to the CMB ones
  - Sensitive polarized synchrotron survey at f close to the CMB ones
- **Instrumental approach** :
  - The use of a large number of **multimode detectors** promises to improve the sensitivity wrt to Planck-HFI
  - The use of a **polarization modulator** (in SWIPE) promises to solve several systematic effects affecting the performance of Planck-HFI at large scales
  - The use of a **single *large* polarizer, common** for the entire focal plane to definine the main axis of the polarimeter with high precision (<<0.1°) promises to improve the absolute reconstruction of the polarization directions.

LSPE in a nutshell

- The Large-Scale Polarization Explorer is an experiment to measure the polarization of the CMB at large angular scales.
- Frequency coverage: 40 – 250 GHz (5 bands)
- 2 instruments: STRIP & SWIPE covering the same northern sky
- **STRIP** is a ground-based instrument working at 44 and 90 GHz (hear Marco Bersanelli in a while)
- **SWIPE** works at 140, 220, 240 GHz
  - collects 8800 radiation modes
  - uses *a spinning stratospheric balloon payload* to avoid atmospheric noise, flying *long-duration, in the polar night*
  - uses a *polarization modulator* to achieve high stability
  - Angular resolution: 1.3^{o} FWHM
  - Sky coverage: 20-25% of the sky per flight / year
  - Combined sensitivity: 10 μK arcmin per flight
- See astro-ph/1208.0298, 1208.0281, 1208.0164 and forthcoming updates

LSPE – Experiment Strategy

STRIP

Ground telescope at 43 and 95 GHz located in Tenerife. Will measure for two years. Based on coherent polarimeters

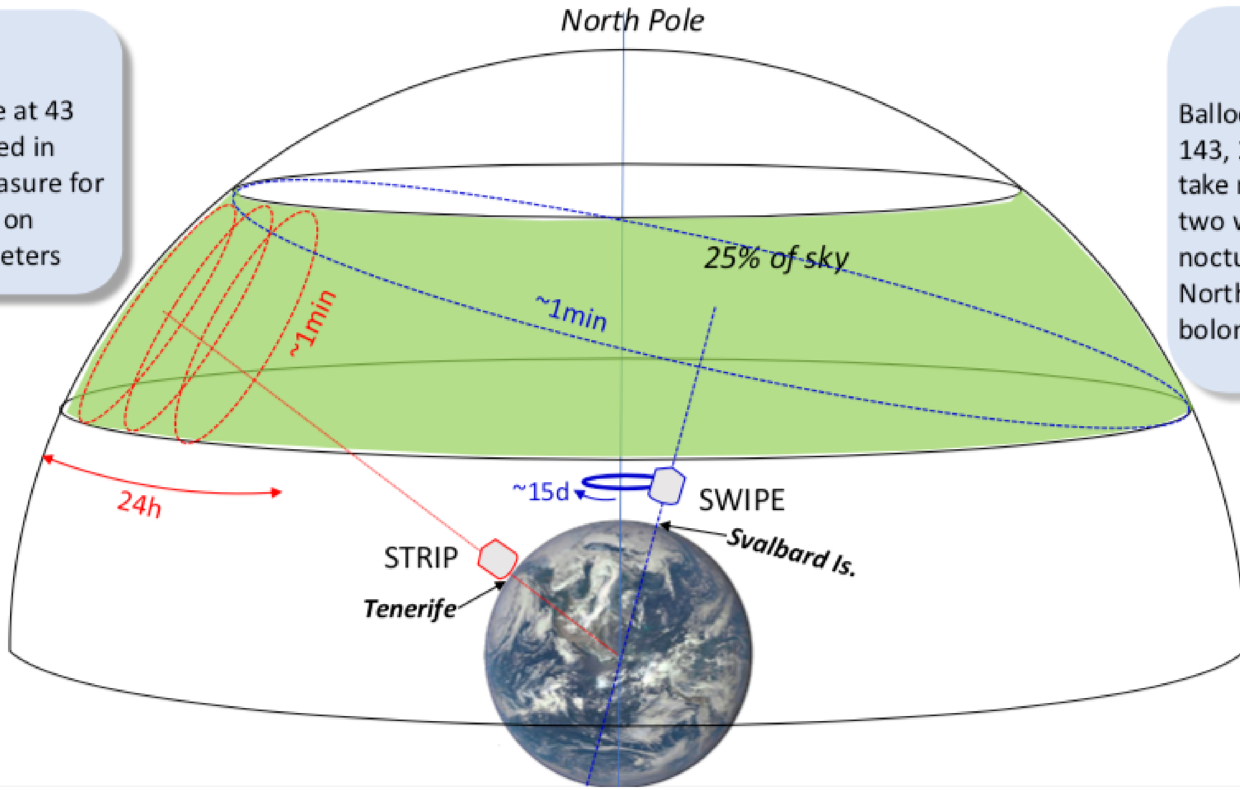

SWIPE

Balloon borne telescope at 143, 220 and 240 GHz. Will take measurements for two weeks during a LDB nocturnal flight around the North Pole. Based on TES bolometers

Credit A. Mennella

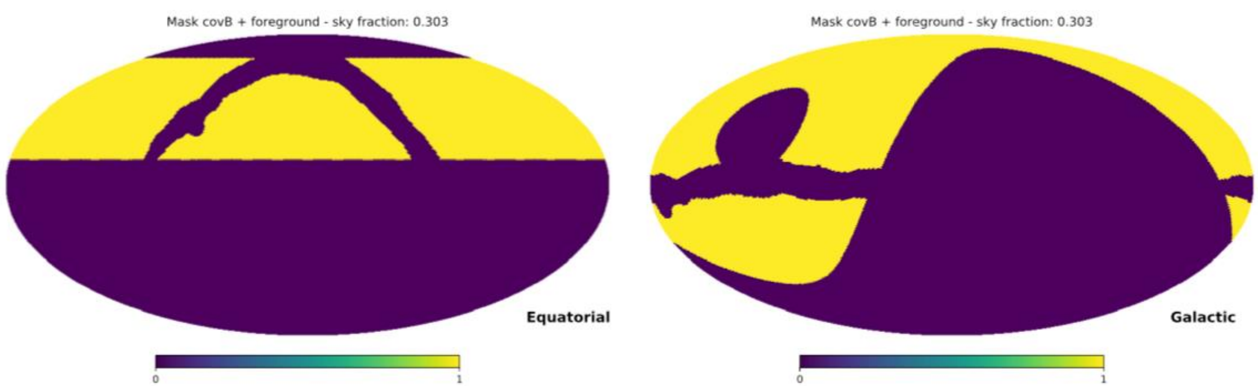

Credit L. Pagano, F. Piacentini

LSPE : Foregrounds cleaning strategy

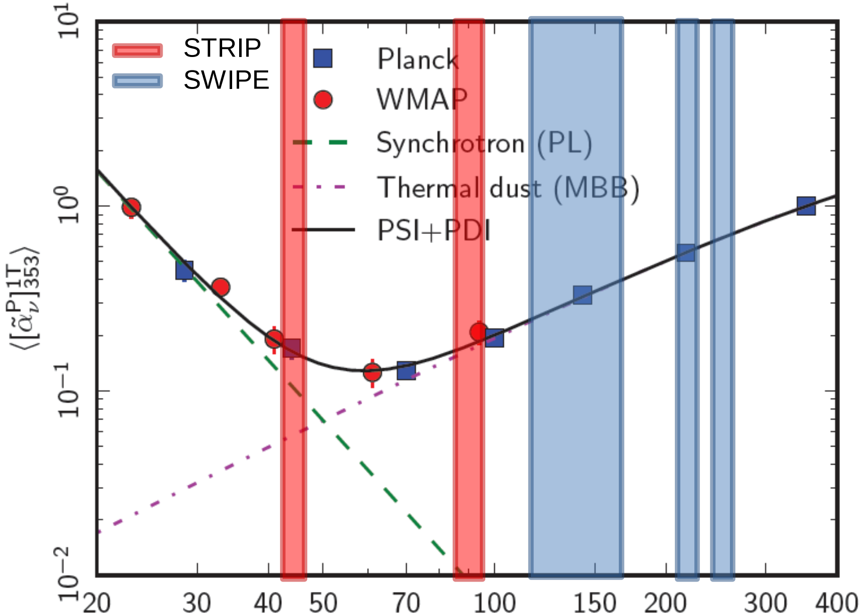

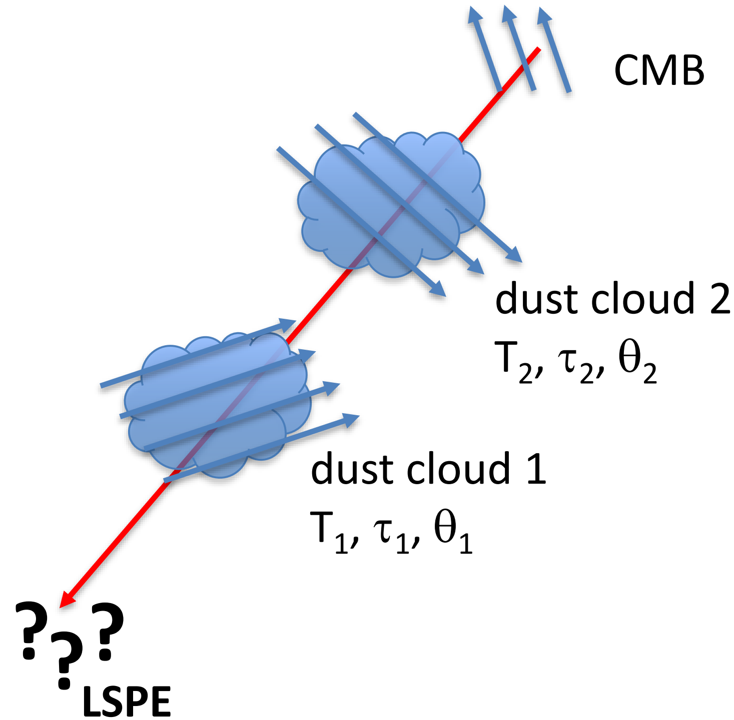

44 GHz
Monitor polarized synchrotron

90 GHz
Atmospheric monitor

140 GHz
Main CMB channel

220 + 240 GHz
Monitor **level, slope and possible rotation** of polarized dust emission.
To date - extrapolated from 350 GHz

SWIPE : general design

Ferrara
Genova
Pisa
Roma1
Roma2

- SWIPE is a Stokes Polarimeter, based on:
  - a simple 50 cm aperture refractive telescope,
  - a cold HWP polarization modulator,
  - a beamsplitting polarizer, and
  - two large focal planes,
  - filled with multimode bolometers at 140, 220, 240 GHz.

- Everything is cooled by a large L^4He cryostat and a ^3He refrigerator, for operation of the bolometers at 0.3K

- The instrument is flown at 40 km altitude to mitigate the effects of earth's atmosphere, and scans the sky spinning in azimuth.

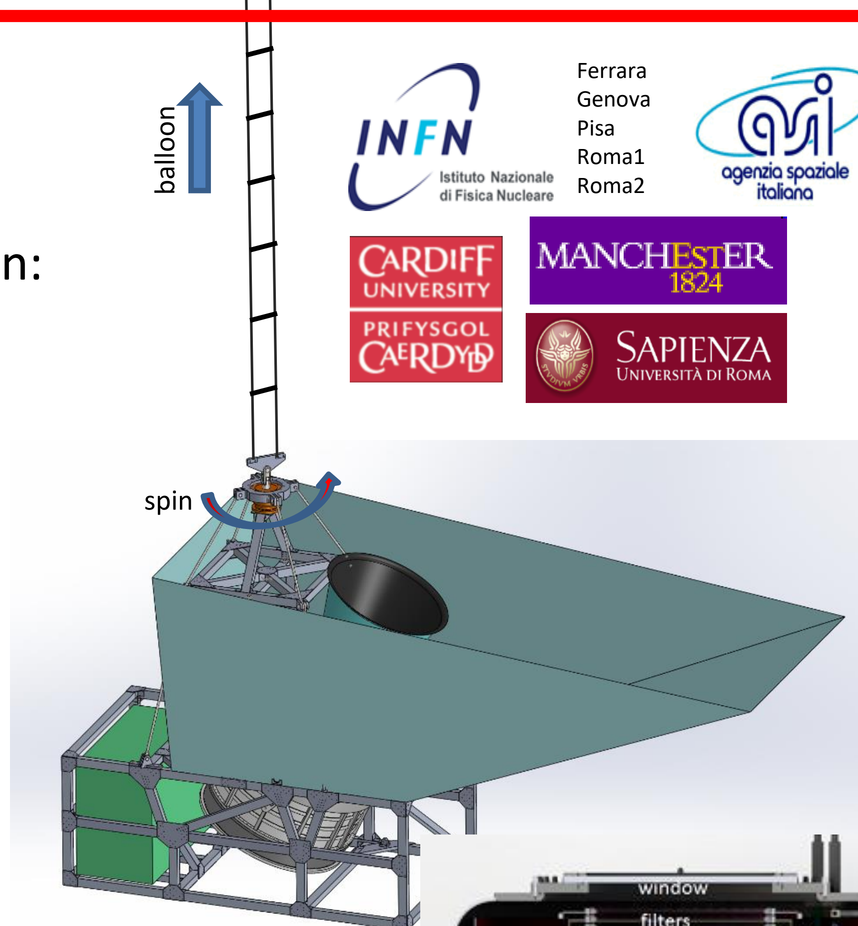

SWIPE gondola

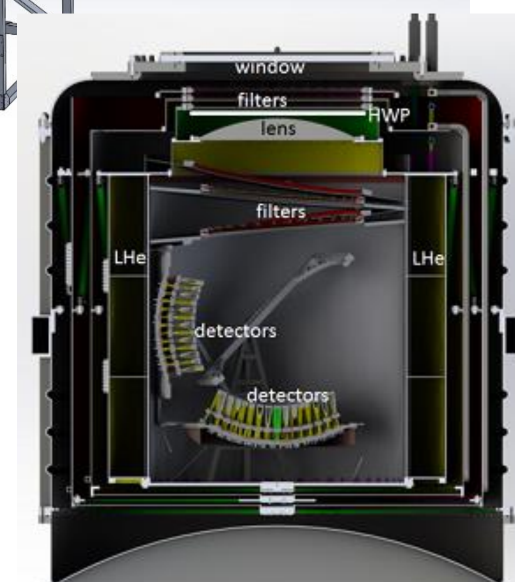

SWIPE receiver

SWIPE: ground/sun shield

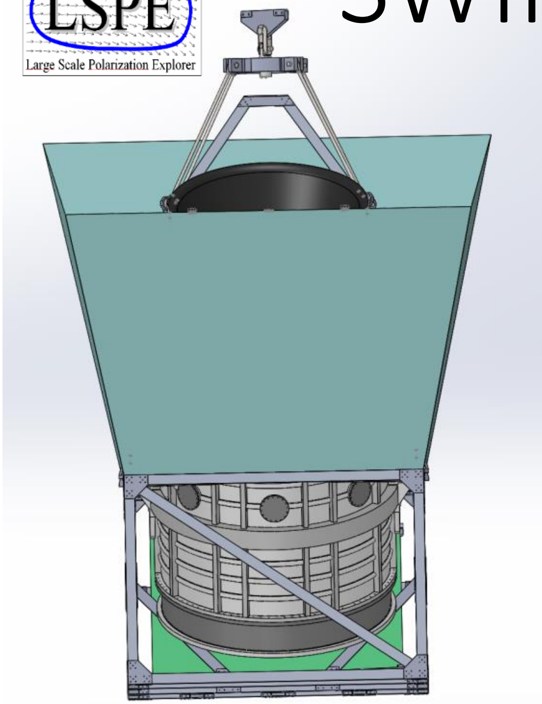

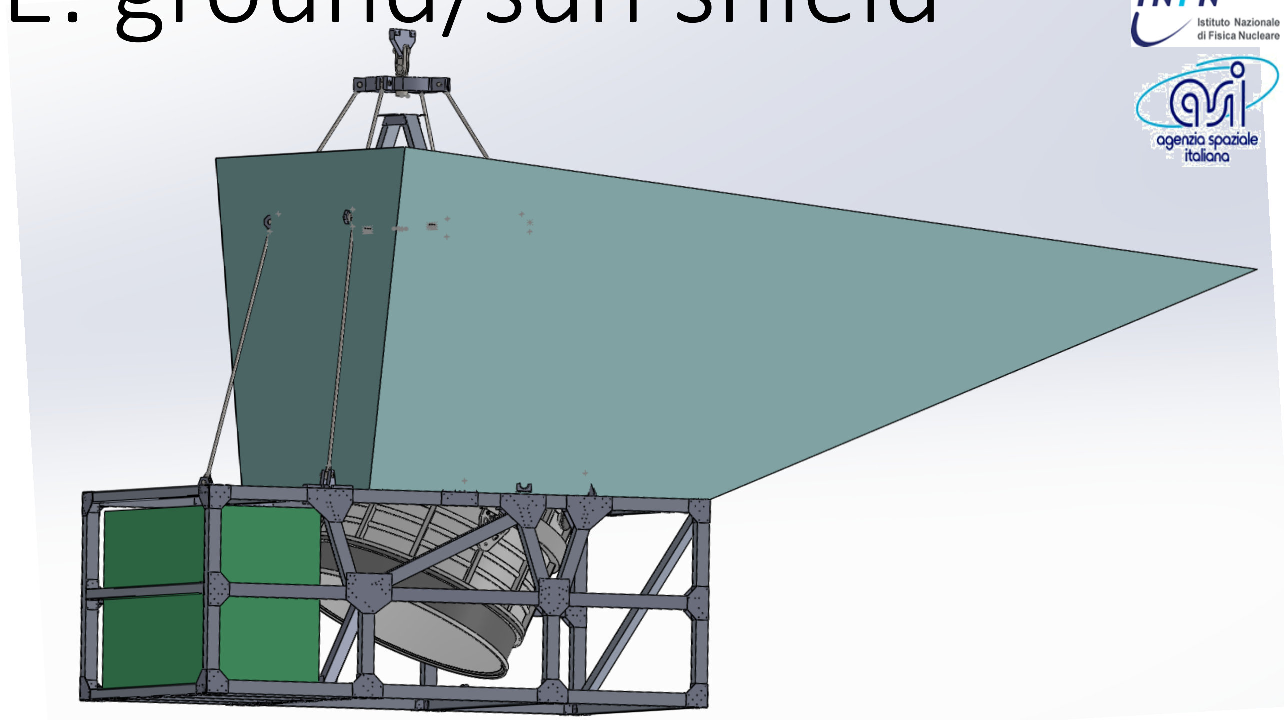

The ground shield is very large ..
.... but not impossible :

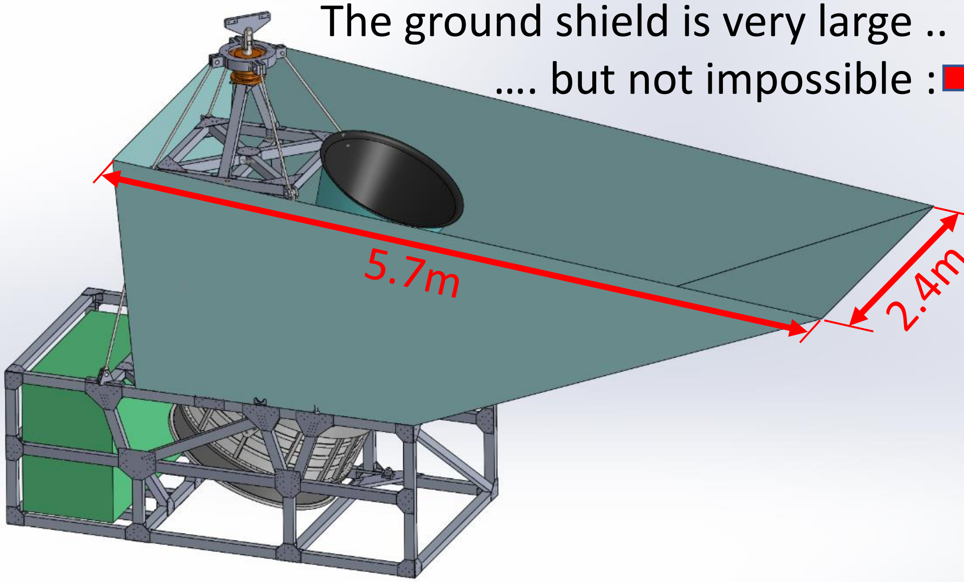

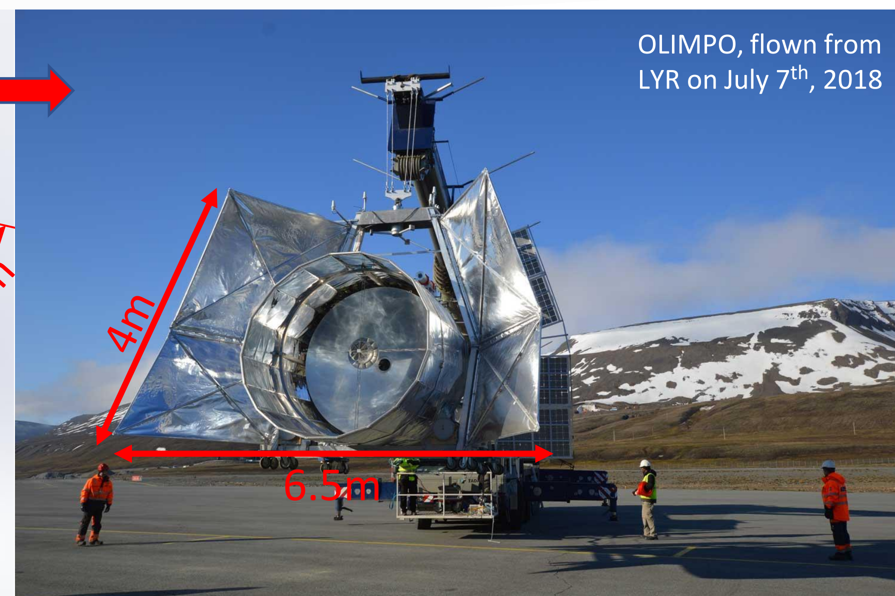

LSPE/SWIPE

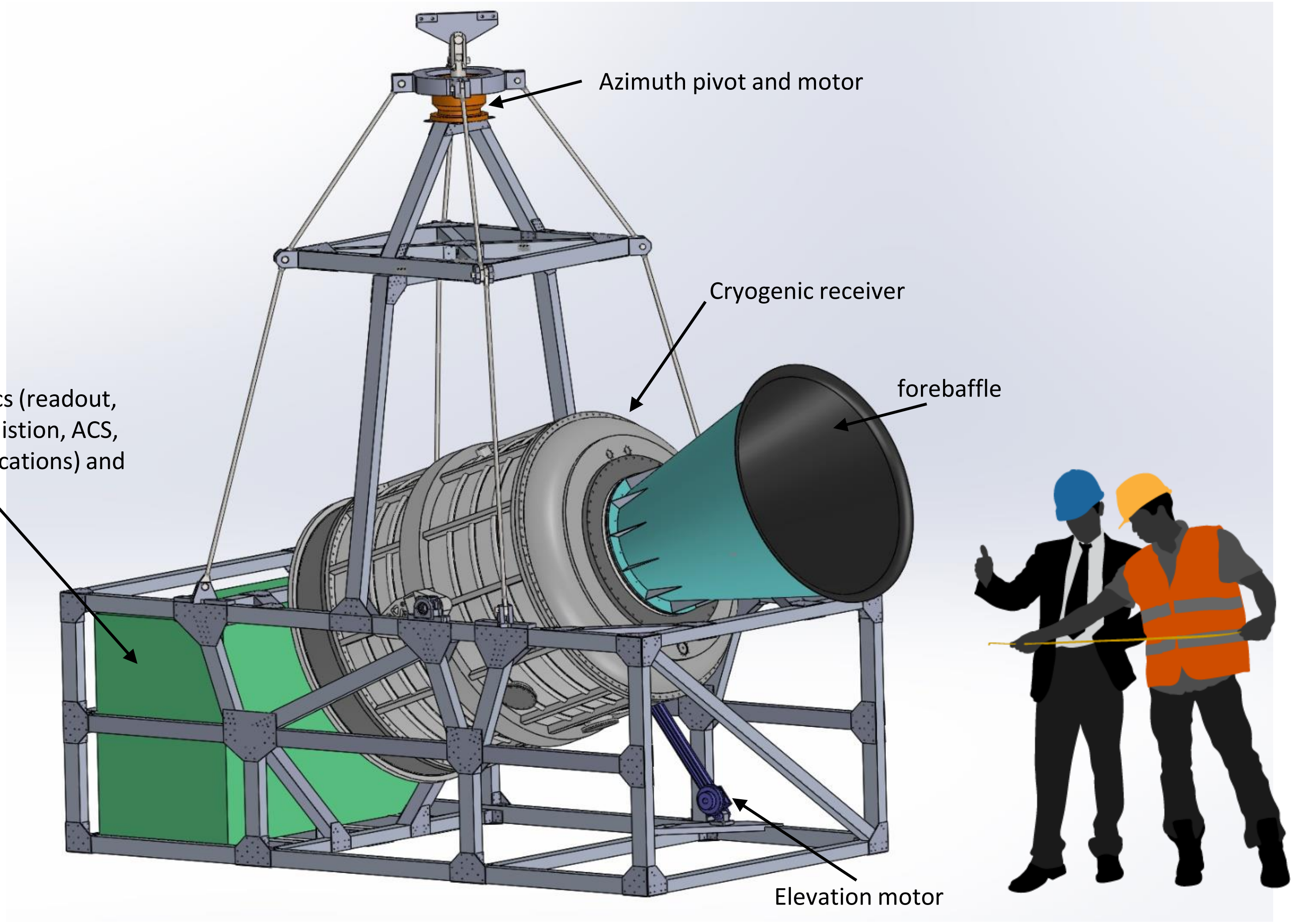

Rendering without ground/sun shields – a 1.6 tons payload

SWIPE: Simple ACS

- ACS based on the successfull pivot flown on BOOMERanG and OLIMPO.
- Azimuth spin of the entire payload up to 3 rpm (with 3A current for a 1600kg load).
- Attitude determination from the same gyros and star sensors flown on Archeops (Nati et al. *A fast star sensor for spinning balloon payloads* Review of Scientific Instruments, 74, 4169-4175, (2003))

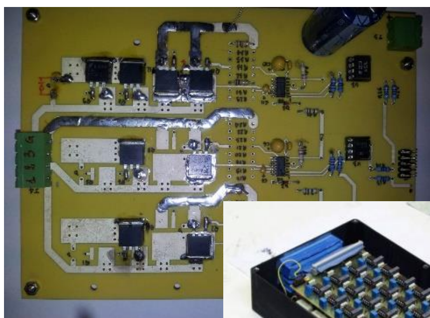

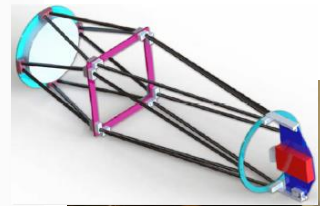

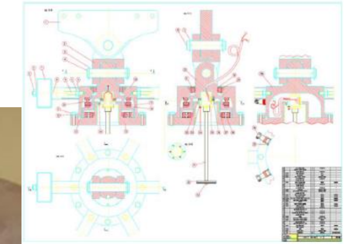

SWIPE - receiver

- A Stokes (HWP + polarizer + power detector) polarimeter, panoramic
- Simple implementation
- Two large focal planes (8800 modes), at 0.3K, in a large cryostat, cooling also the lens (490mm diam. and a 460 mm diam. cold stop) and the polarization modulator (HWP at about 10-15 K).
- FOV: 20° split by a 500mm diam., 45° tilted wire grid into 2 Focal Planes 300 mm diam (f/1.75)
- **Most components being machined, some ready**

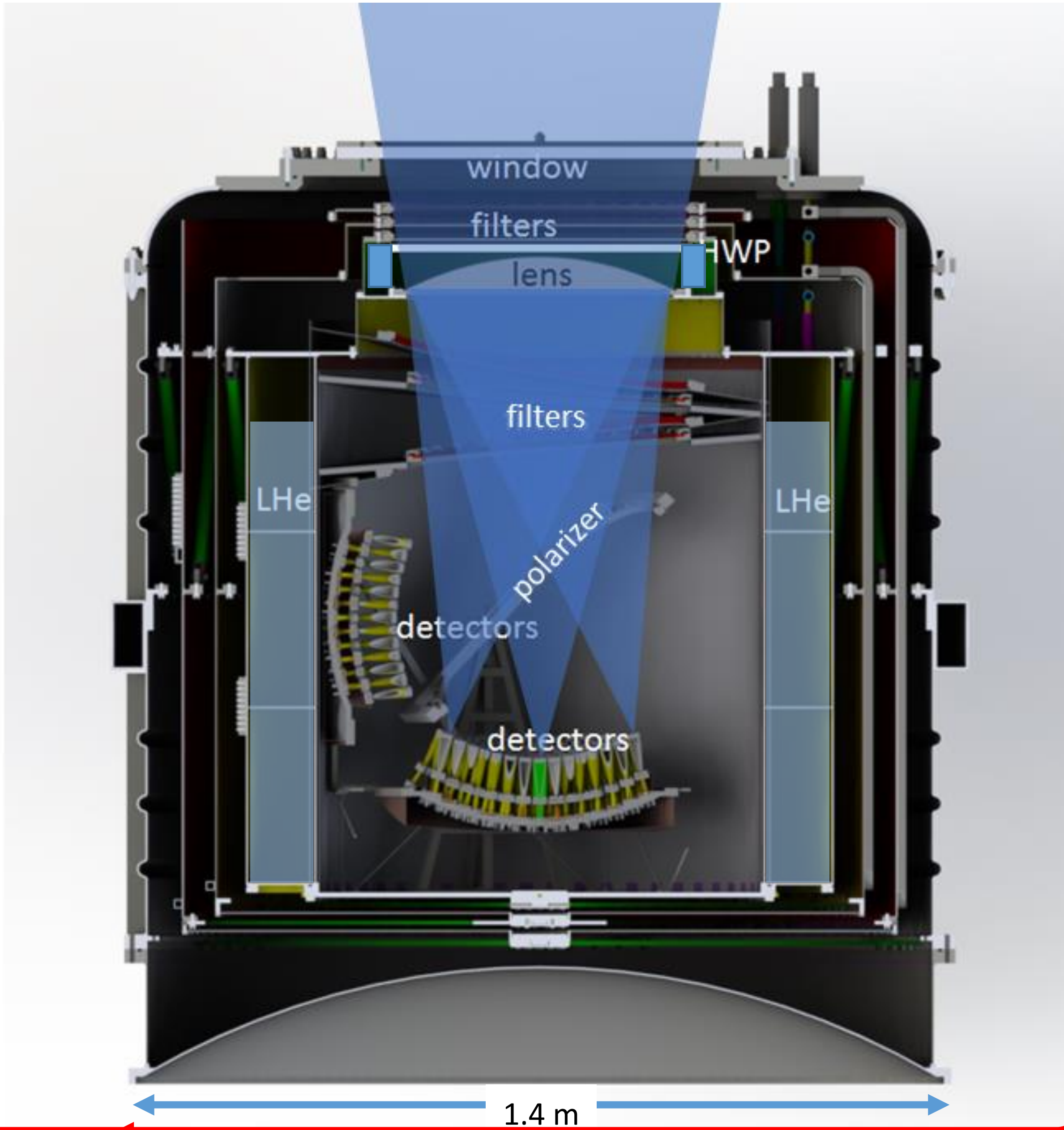

LSPE/SWIPE: Receiver

LSPE-SWIPE polarimeter and cryostat

LSPE-SWIPE polarization modulator

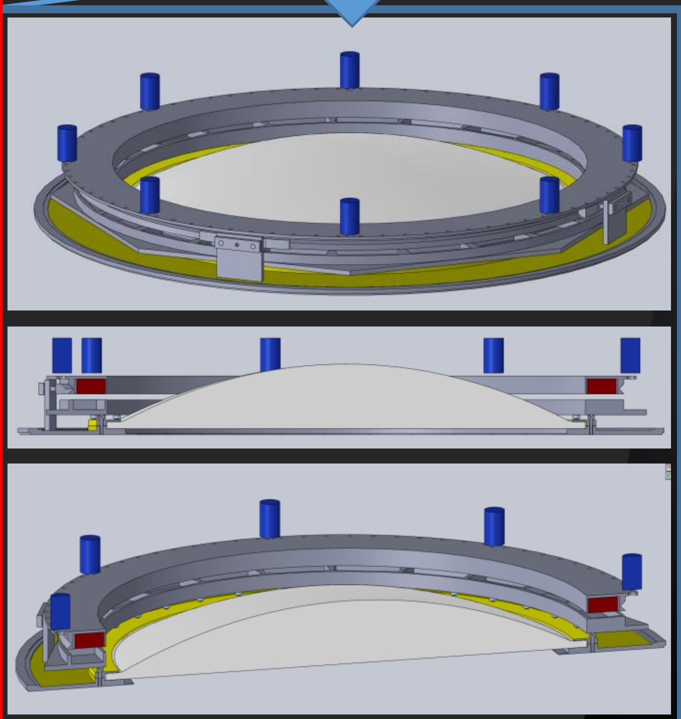

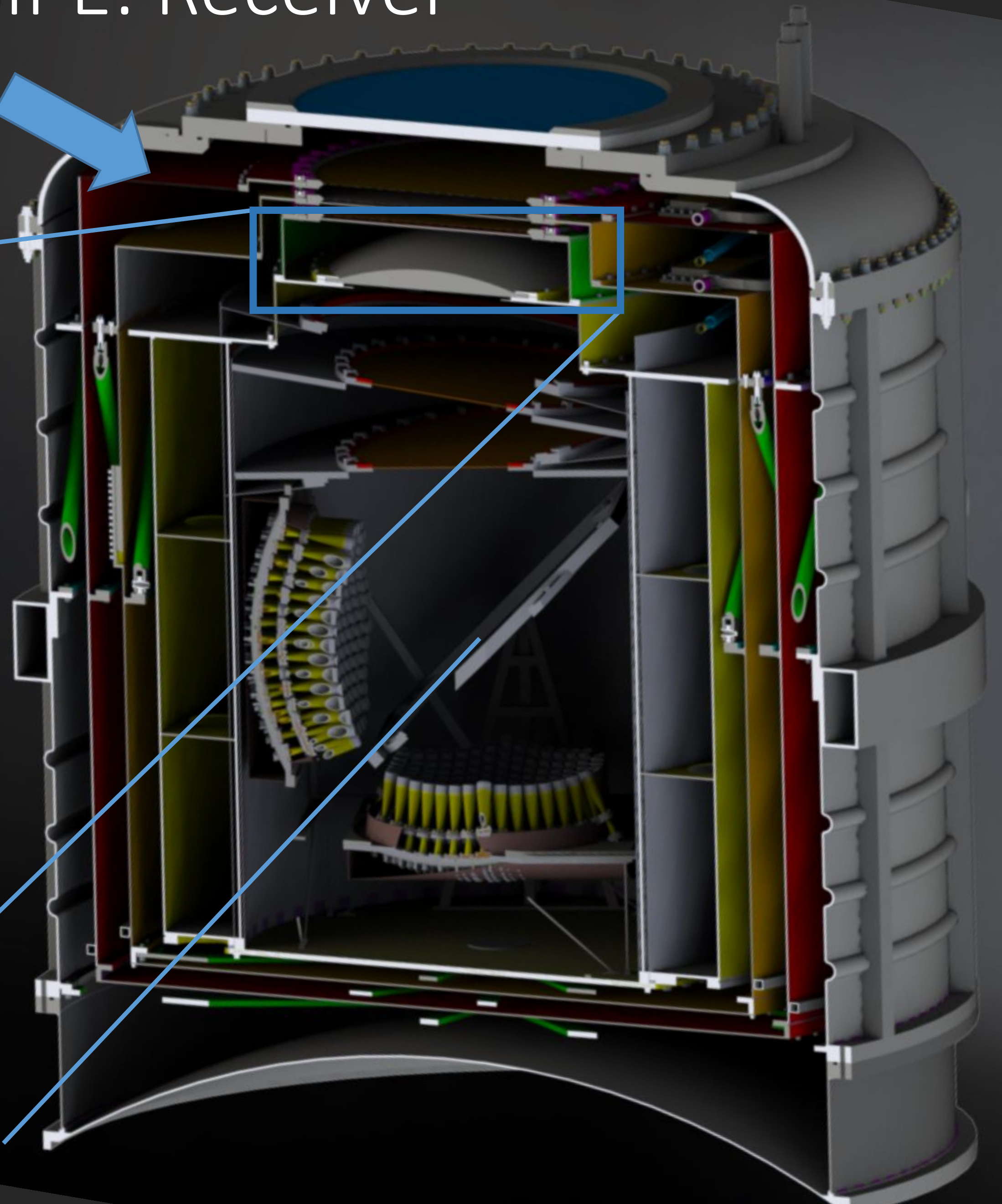

Fast (1-2 rps) levitating HWP rotator and HDPE lens

Large polarizer, common to all bolometers

Advantage of large polarizer

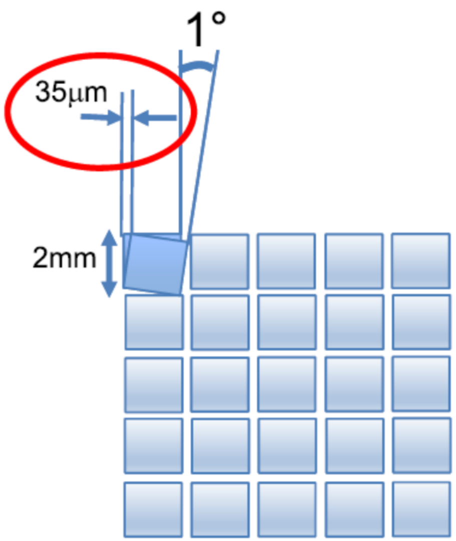

array of
discrete
elements.
$\Delta\theta = O(1°)$

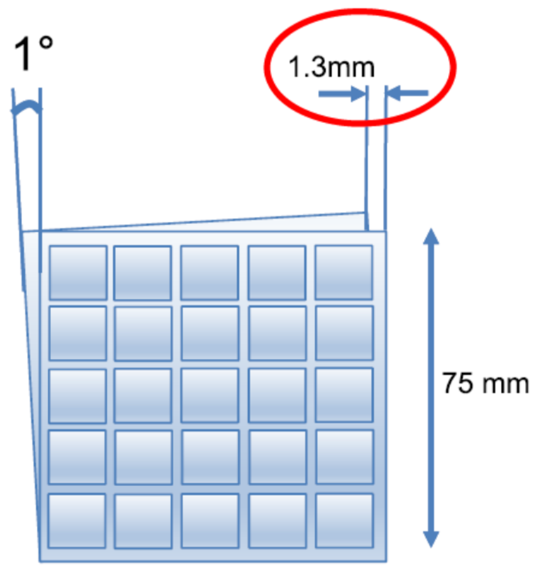

photolitograph
array – high
precision
within the tile.
$\Delta\theta = o(0.1°)$

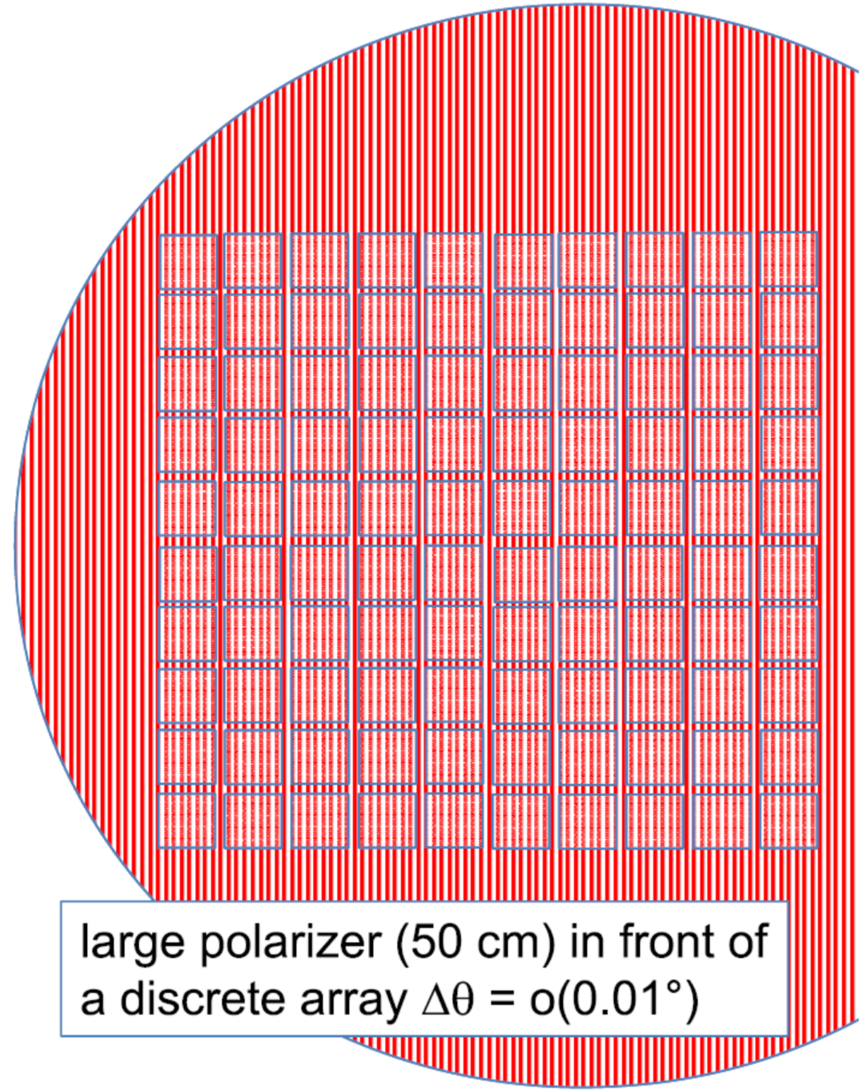

large polarizer (50 cm) in front of
a discrete array $\Delta\theta = o(0.01°)$

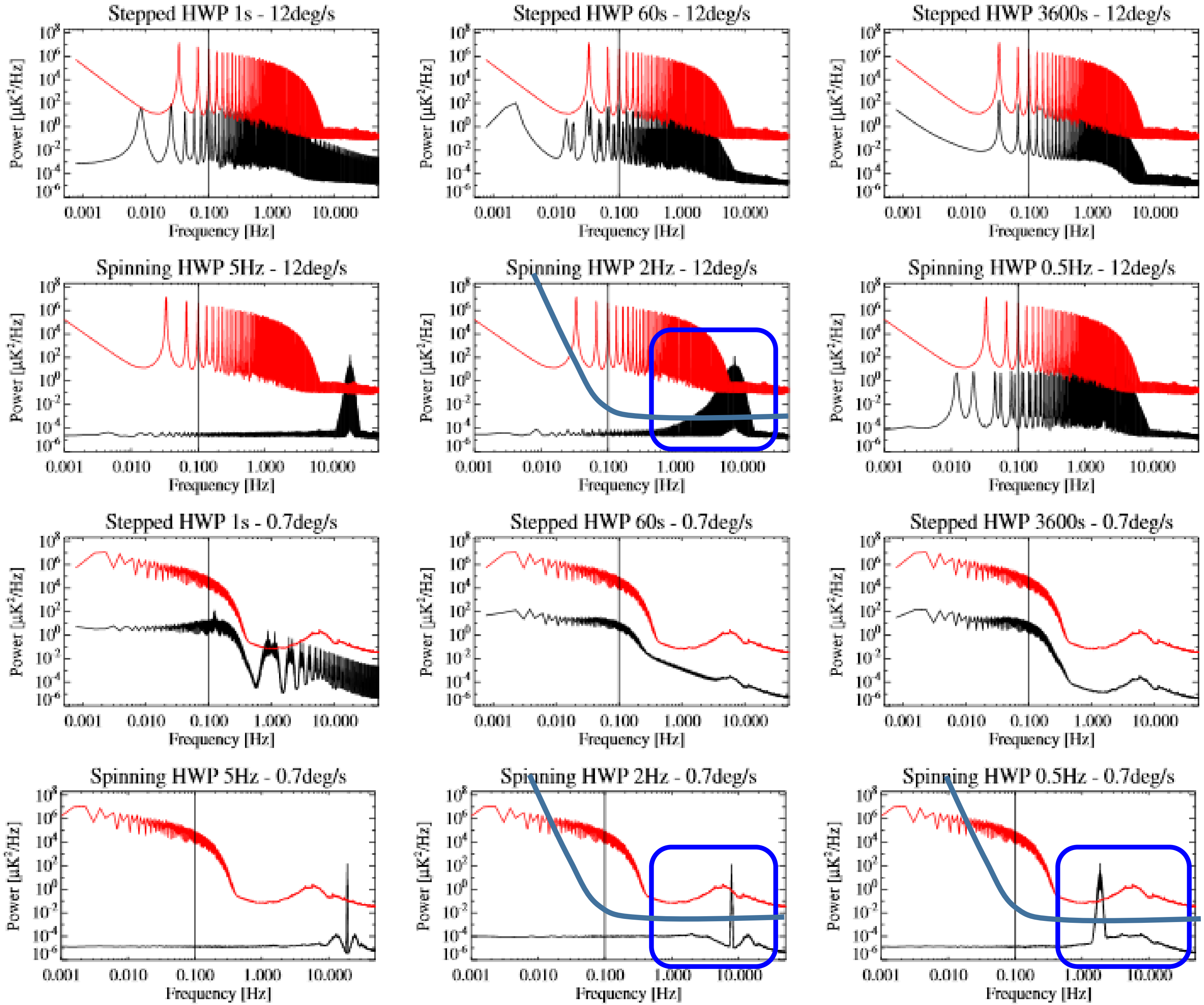

Buzzelli et al., A&A 609, A52 (2018)

SWIPE – HWP

- Is a cold (2K), large (50 cm useful dia.), wide-band meta-materials HWP, placed immediately behind the window and thermal filters stack.
- HWP characteristics for the ordinary and extraordinary rays are well matched: $(T_o\text{-}T_e)/T_o < 0.001$, $X_{pol}<0.01$, over the 100-300 GHz band.
- Simulations show that continuous rotation has advantages in terms of 1/f noise mitigation and angles coverage.
- A custom superconductive rotator has been developed.

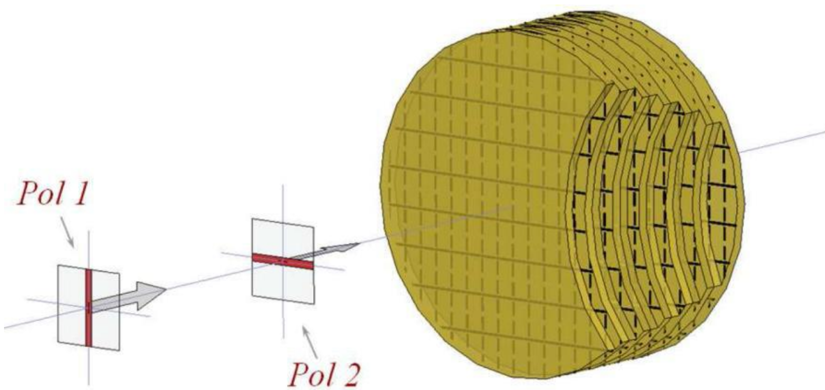

Pisano et al., Proc. SPIE, Vol. 9153, id. 915317 (2014)

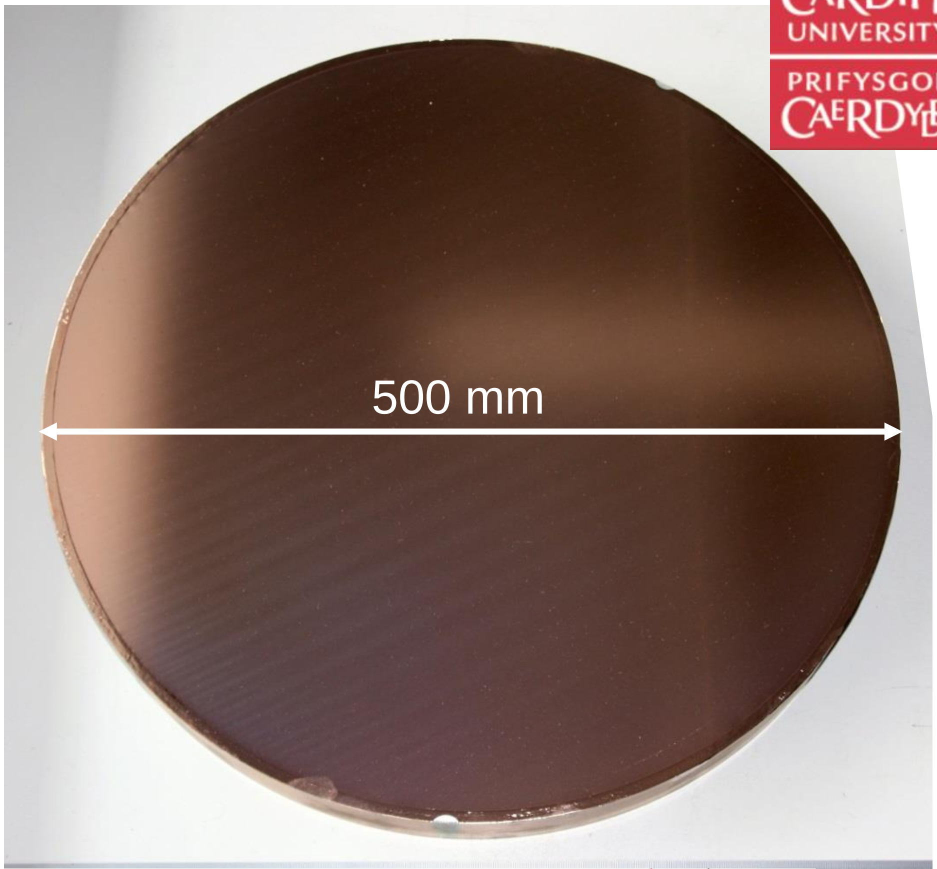

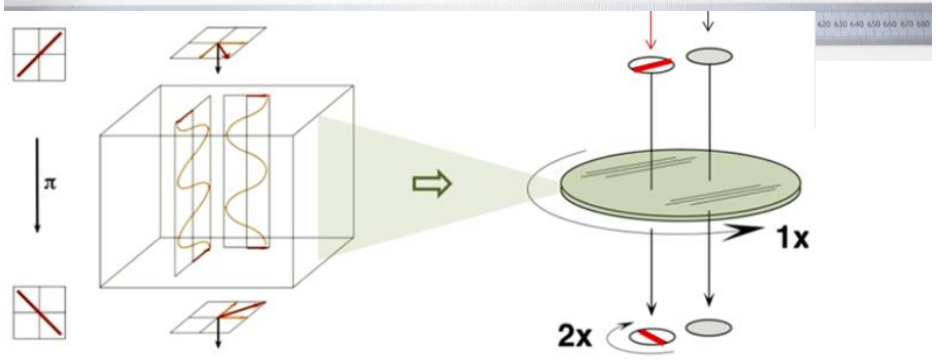

SWIPE – HWP rotator

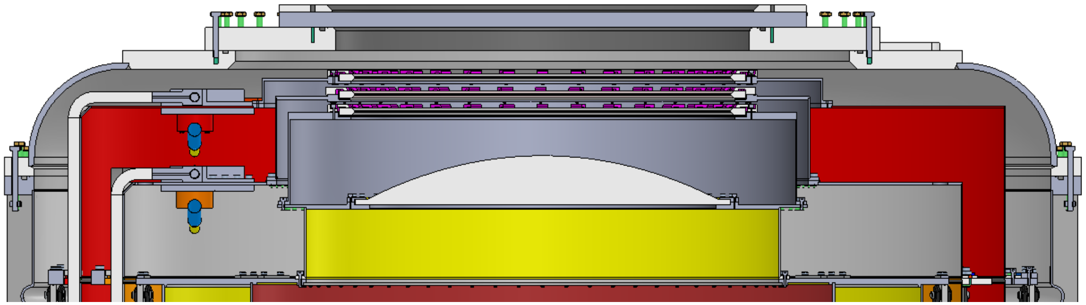

~670mm

Permanent magnet ring

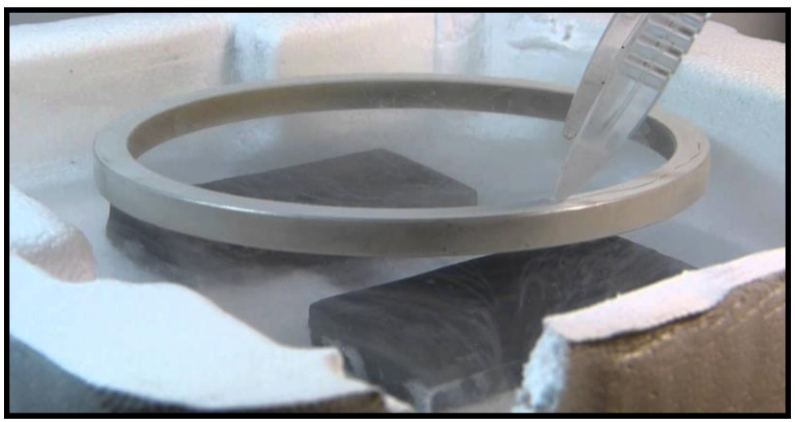

High Temperature Superconductors

Pros

- NO stick-slip friction
- NO extra-effort to cool HTSs
- Passive stable levitation
- Low Coefficient of friction
- Continuous rotation (0-10Hz)

Cons

- Variable magnetic field
- Clamp mechanism at 4K

S. Hanany et al., IEEE Trans.Appl.Supercond. 13 (2003) 2128-2133

T. Matsumura et al., IEEE Trans.Appl.Supercond. 26 (2016)

SWIPE – HWP rotator - General layout

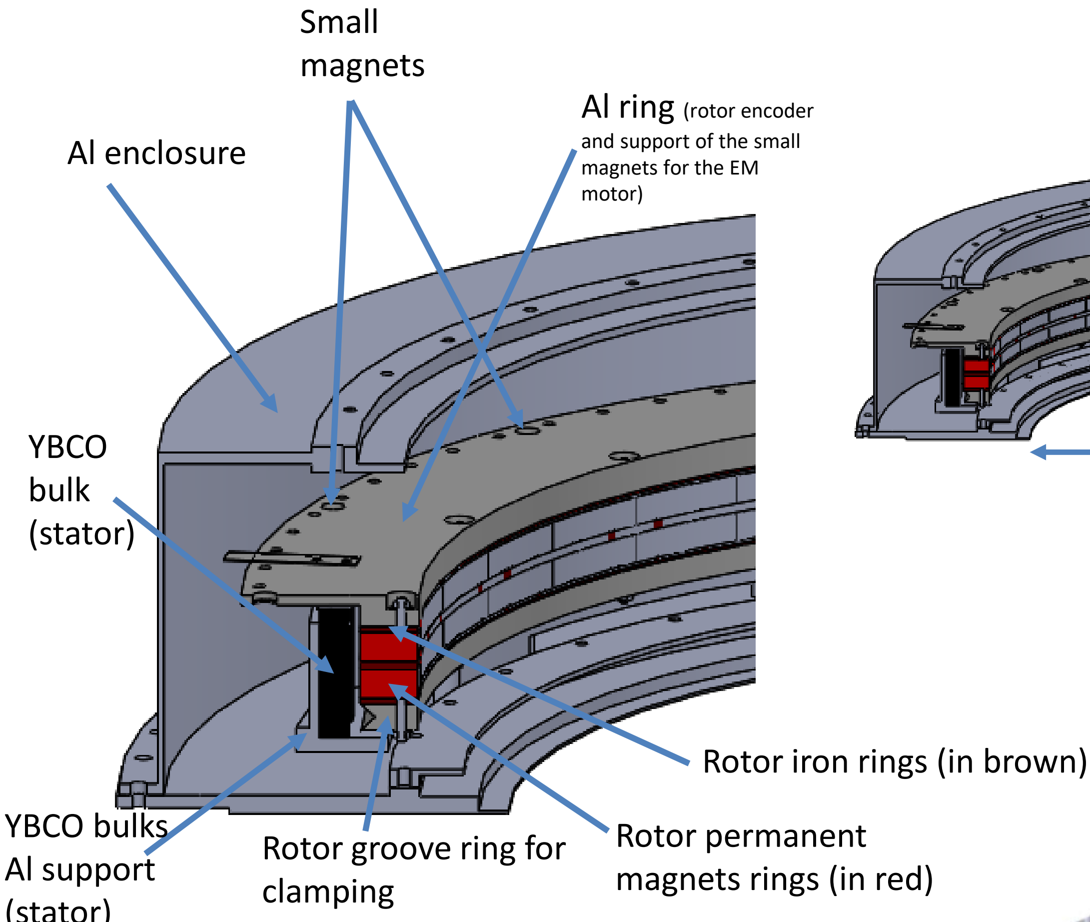

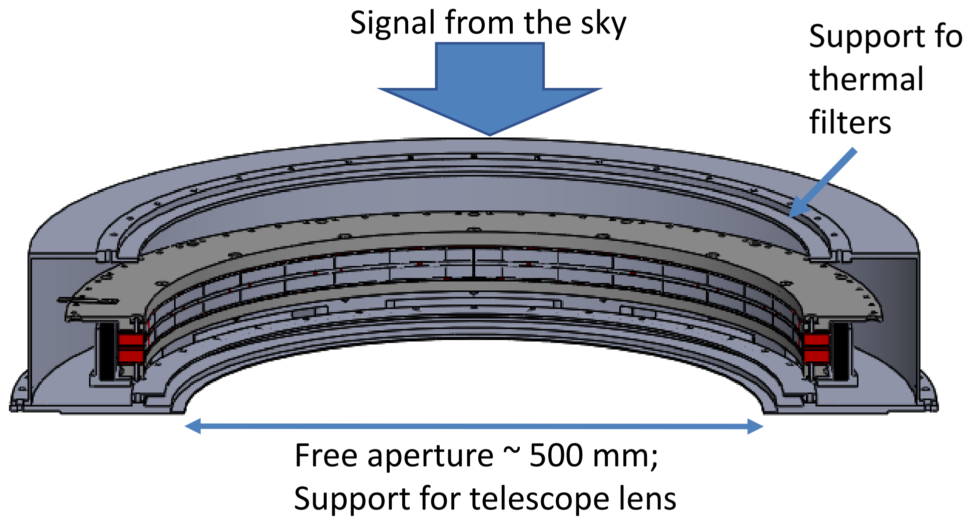

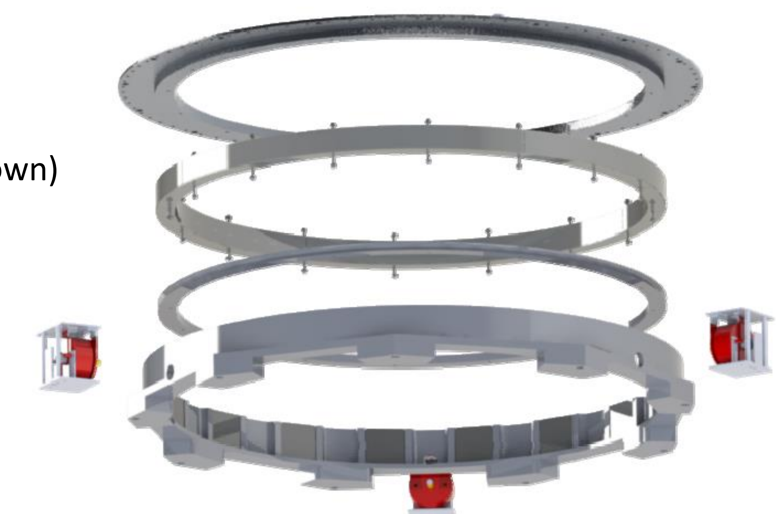

1T field strength in the gap. Total mass 9 kg.

SWIPE – HWP rotator – parts procured

LSPE Large Scale Polarization Explorer

INFN Istituto Nazionale di Fisica Nucleare

asi agenzia spaziale italiana

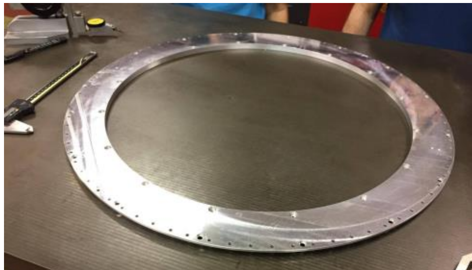

Groove ring for C/R

Stator with YBCO bulks

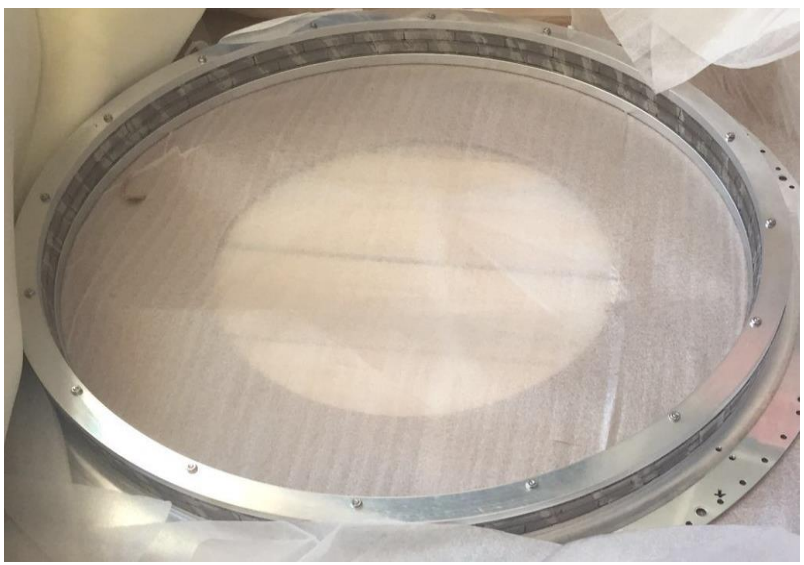

Rotor with permanent magnets

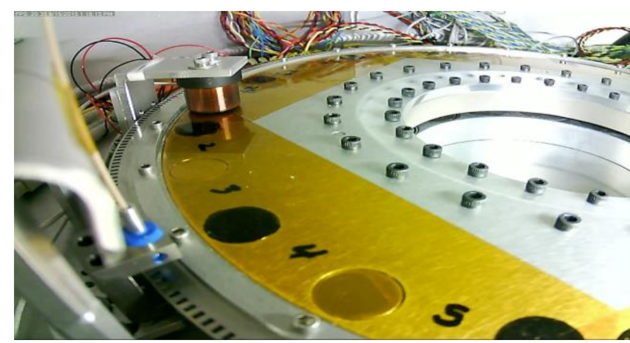

smaller diameter Prototype arXiv:1706.05963v3

SAPIENZA UNIVERSITÀ DI ROMA

SWIPE – HWP rotator – clamp/release

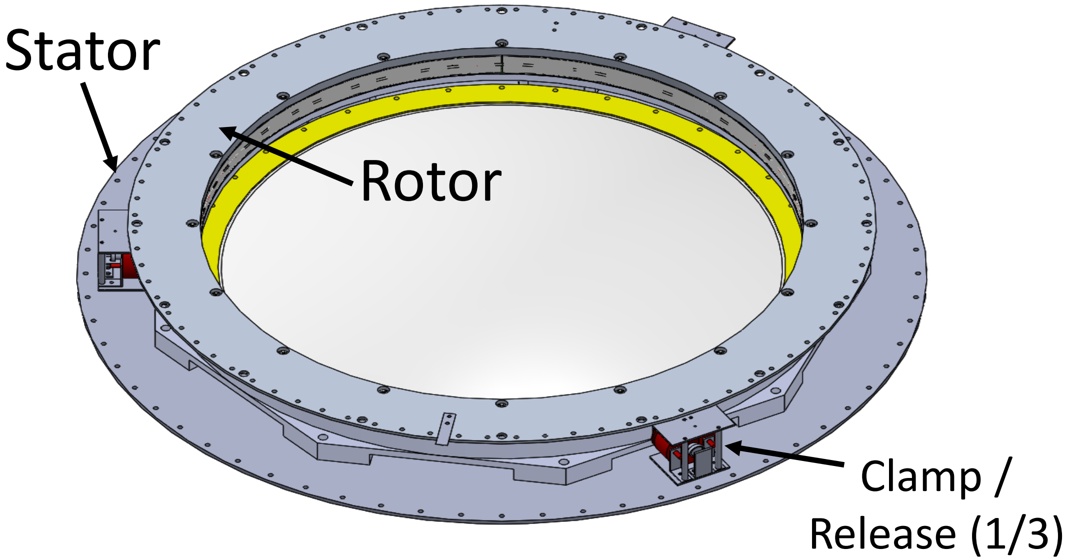

Frictionless actuator for operation @ 2K

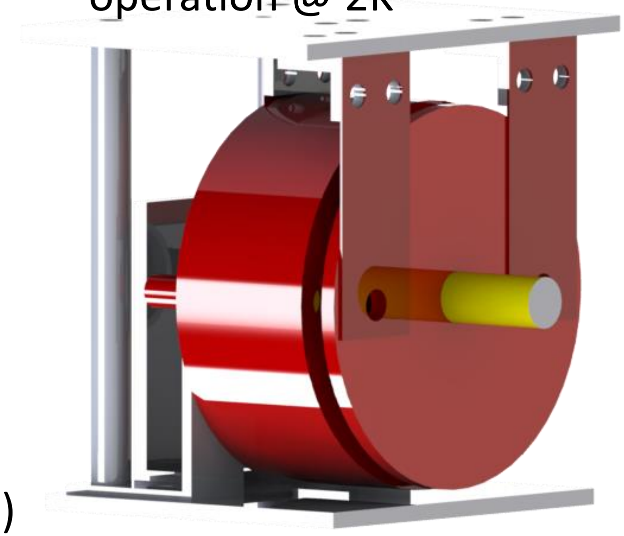

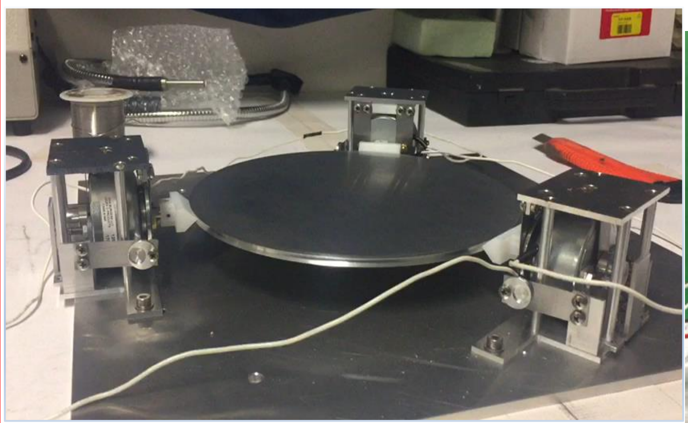

Fabio Columbro, Paolo de Bernardis, and Silvia Masi
A clamp and release system for superconducting magnetic bearings
Review of Scientific Instruments 89, 125004 (2018)

SWIPE: Cryogenic Testbed

Based on a pulse-tube cooler

A. Rocchi

Cryogenic PMU rotator – Control Electronics

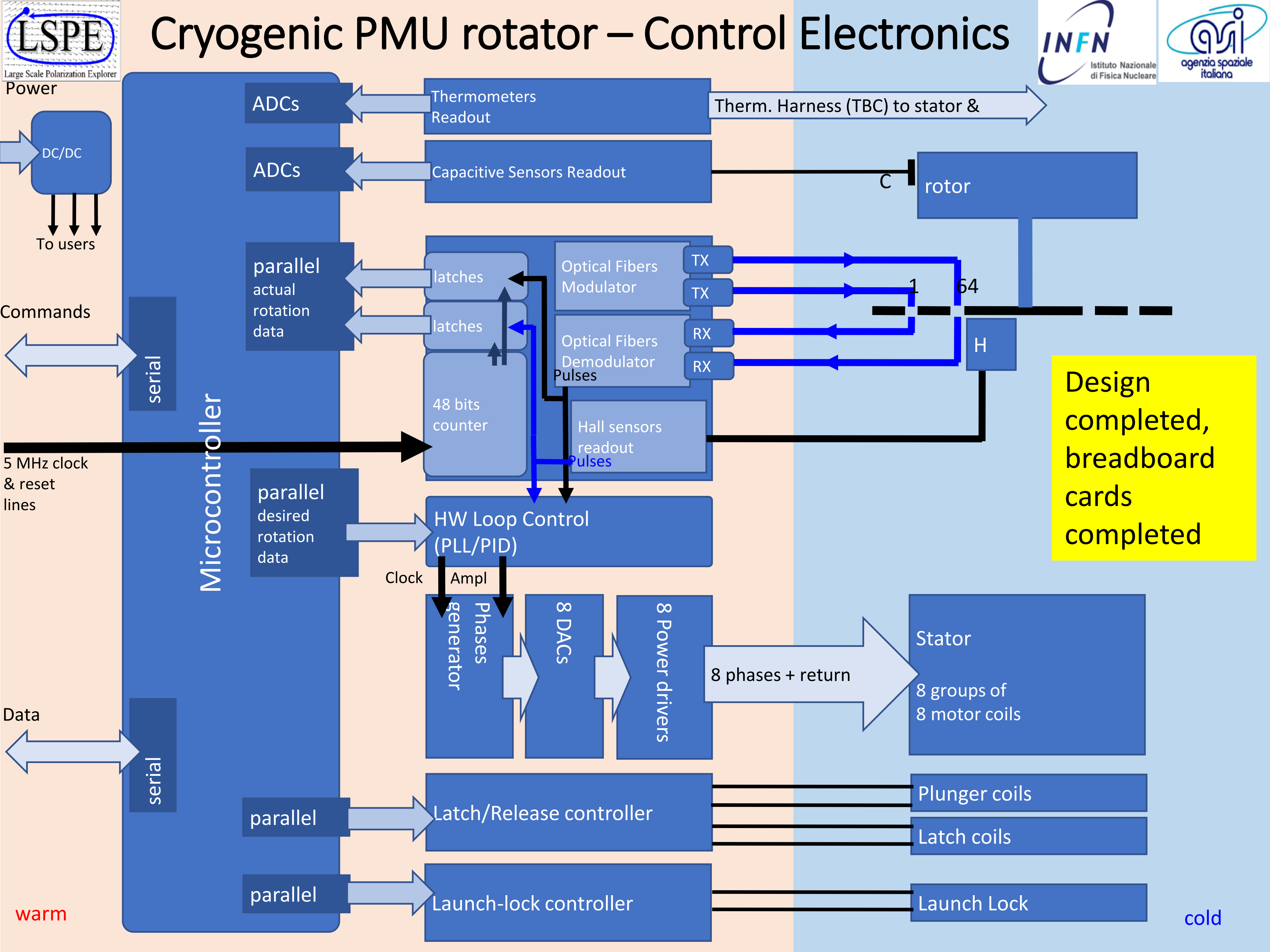

Single lens 490mm in dia: plano-convex lens curved focal plane

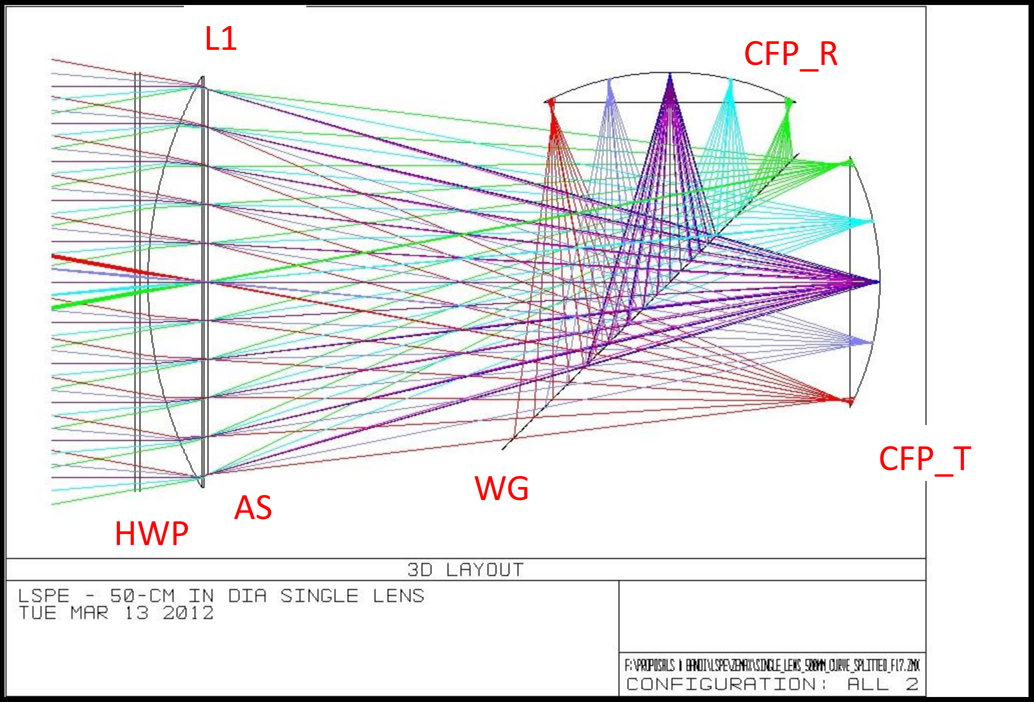

Dimensions:

HDPE Lens (L1) diameter = 480 mm
Aperture Stop (AS) = 440 mm
Entrance Pupil = 450 mm
FOV = 20 deg
f/1.88
Curved Focal plane (CFP_T o CFP_R) diameter = 300 mm
Lens thickness = 65 mm
HDPE lens with AR by porous PTFE

Constraints:

Thermal filters max c.a. diameter = 500 mm
Wire Grid (WG @45 deg tilt) max c.a. diameter = 500 mm
HWP max c.a. diameter = 500 mm

Single lens 490mm in dia: plano-convex lens curved focal plane

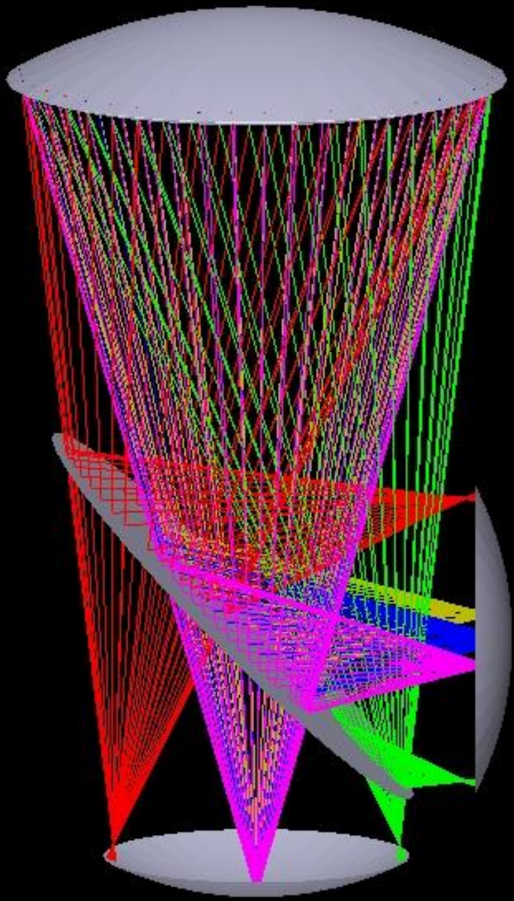

Corrected focal plane *vs* bands

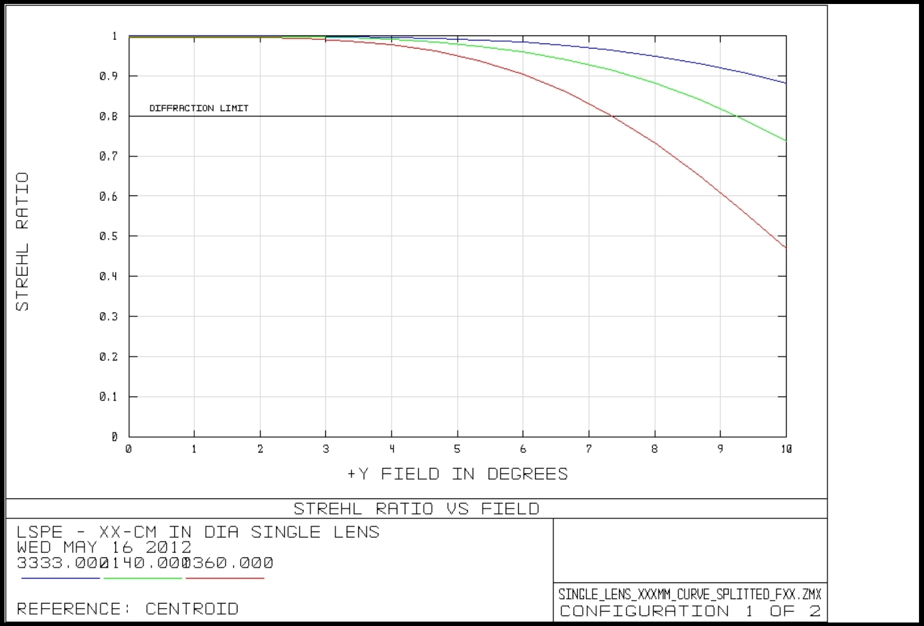

SWIPE: Simple Optical Design

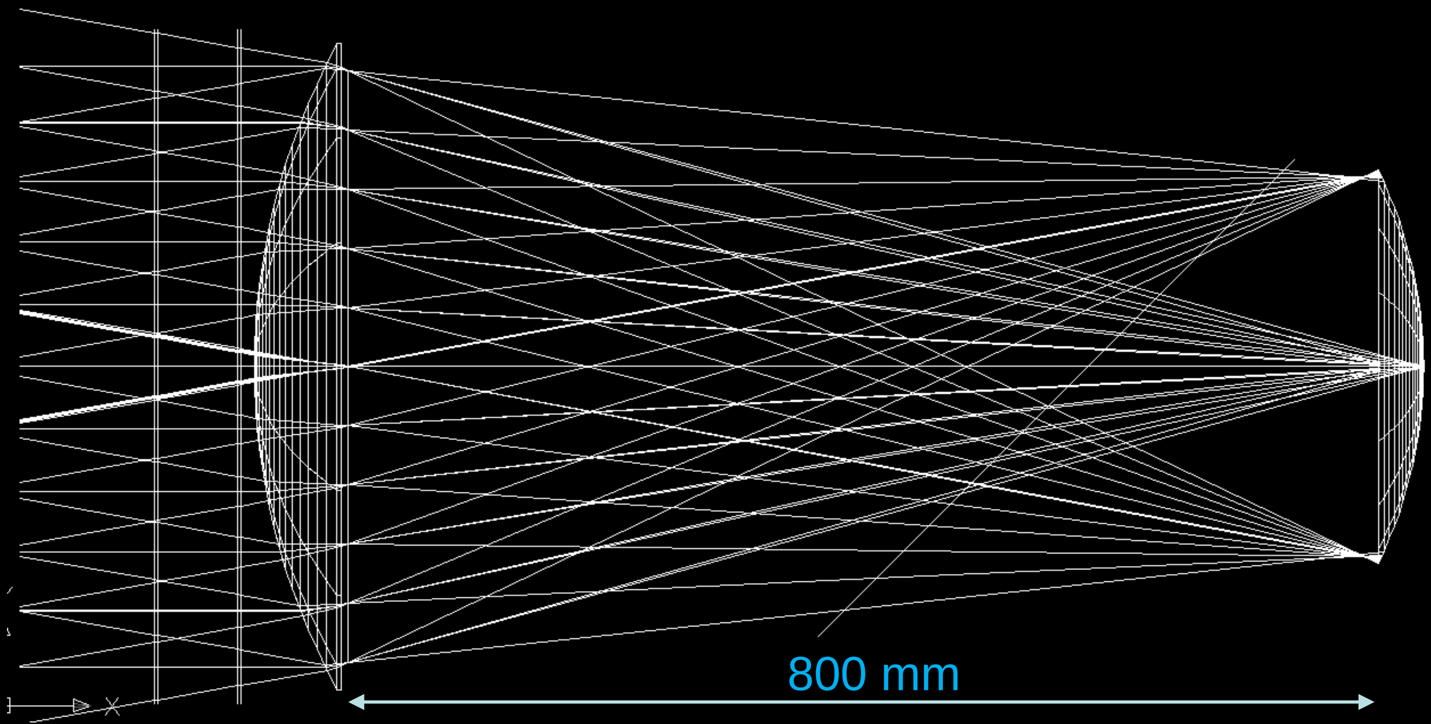

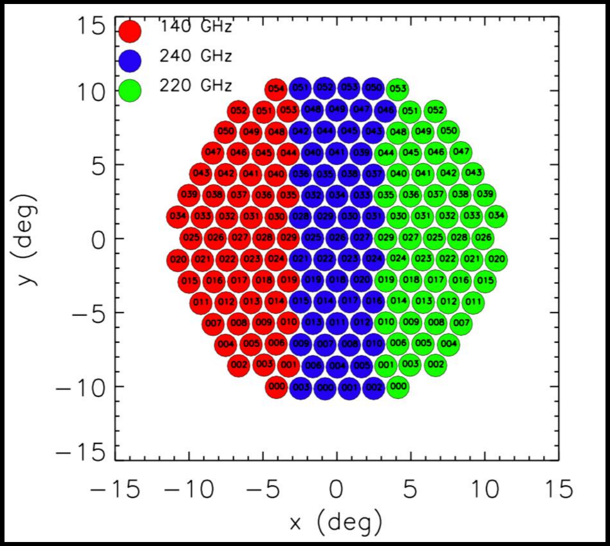

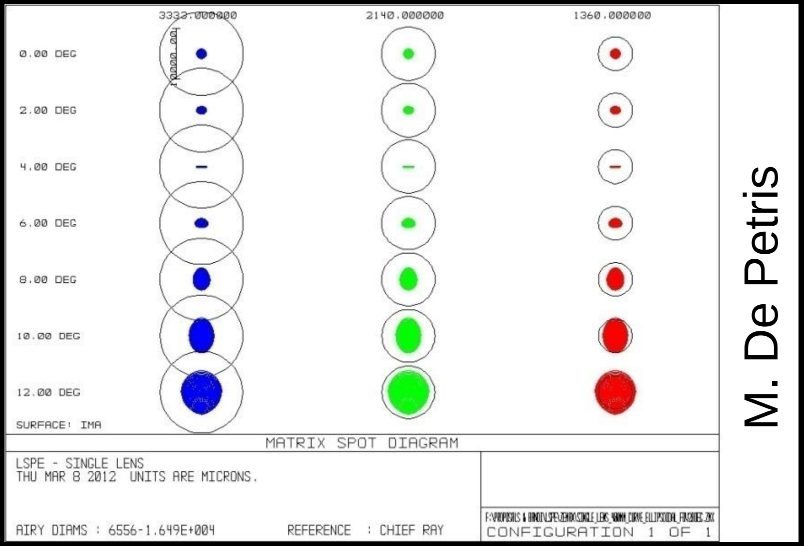

M. De Petris

Single-Mode vs Multi-Mode design: how, when and why go Multi-Mode

- Diffraction- and photon-noise limited operation over quite a broad band demonstrated
- Solid modeling techniques
- Reliable methods for assessing real-life performance.
- Instrument design is complicated but huge experience accumulated by community over the last few years.
- Large numbers of detectors needed to break photon noise limit

- Reduce the number of individual sensitive elements each hitting the photon noise limit more easily
- Sensitivity per individual device scales like $N_{modes}^{1/2}$
- Comparatively larger detector units and coarser angular resolution.
- Viable and cost-effective when sensitivity is a stronger requirement than diffraction-limited operation (e.g. Planck 545 and 857 GHz)
- CMB spectral distortion and large scale B-mode searches can fully take advantage of m-m design (PIXIE, LSPE)

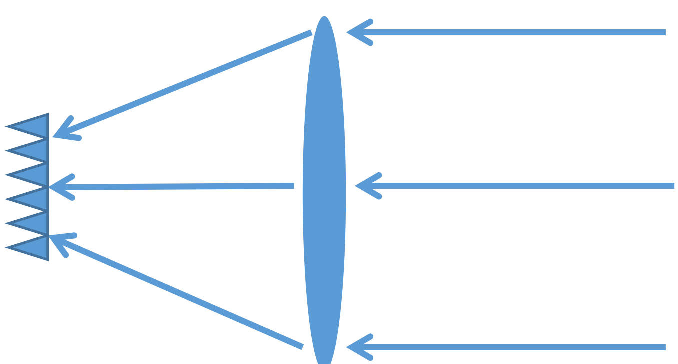

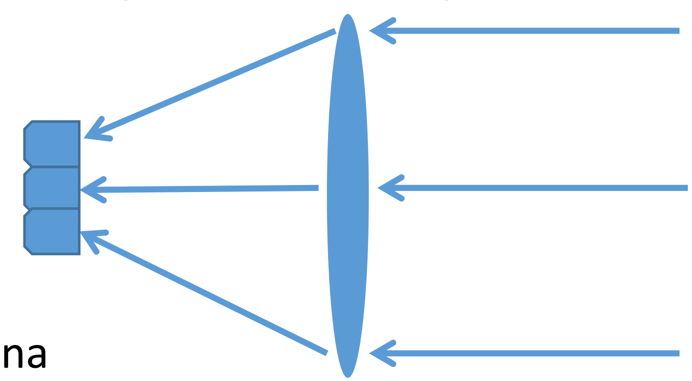

L. Lamagna

LSPE/SWIPE: multimode optics

- Whole system multi-mode
- Full EM simulation
  described in: Legg, Lamagna, Coppi, de Bernardis, Giuliani, Gualtieri, Marchetti, Masi, Pisano, Maffei, *Development of the multi-mode horn-lens configuration for the LSPE-SWIPE B-mode experiment* Proc. SPIE 9914, Millimeter, Submillimeter, and Far-Infrared Detectors and Instrumentation for Astronomy VIII, 991414 doi:10.1117/12.2232400
- Resulting beam approximately top-hat. 1.5° FWHM.
- Good polarization properties.

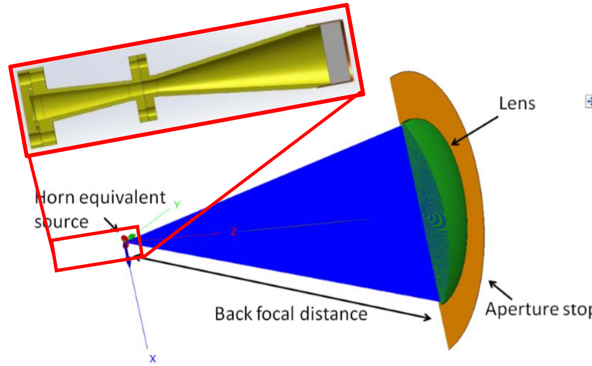

Diameter (mm)	428
Centre thickness (mm)	60
Focal length (mm)	805
Refractive index	1.57
Conic constant	-0.54
Cold stop diameter (mm)	420

L. Lamagna, S. Legg

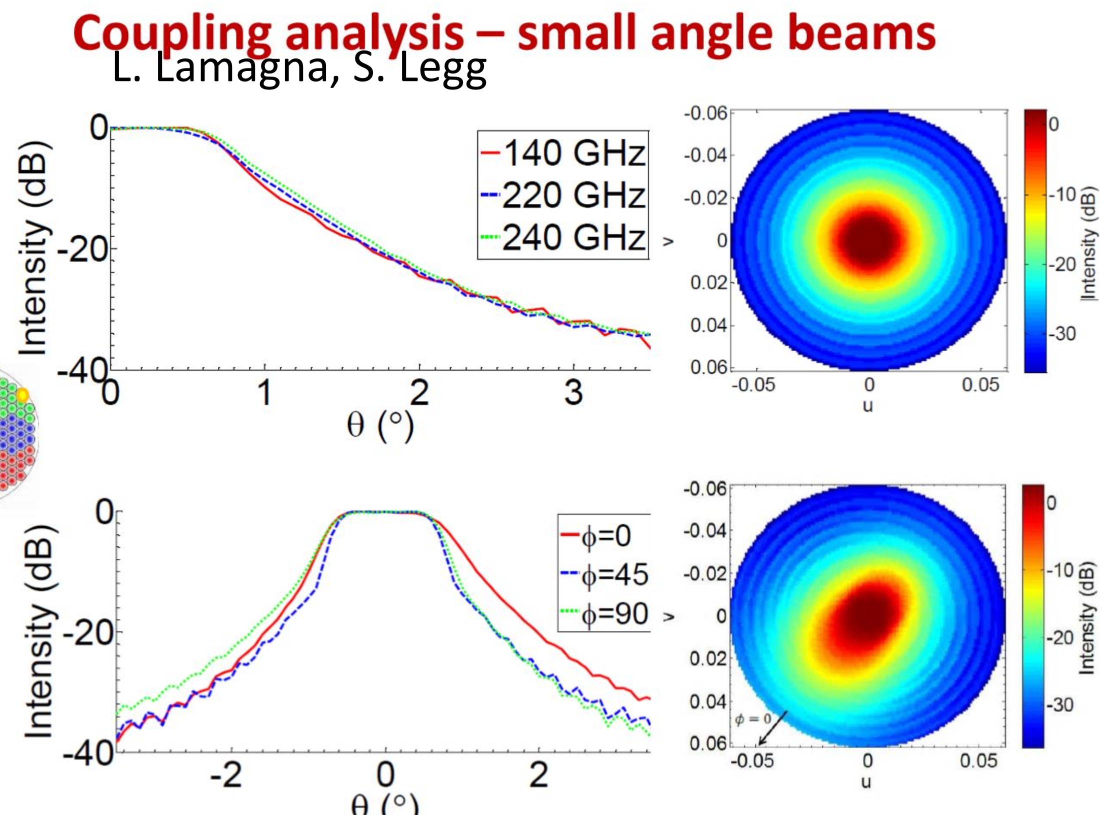

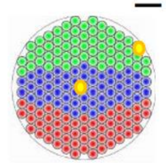

L. Lamagna. M. De Petris

The SWIPE pixel assembly

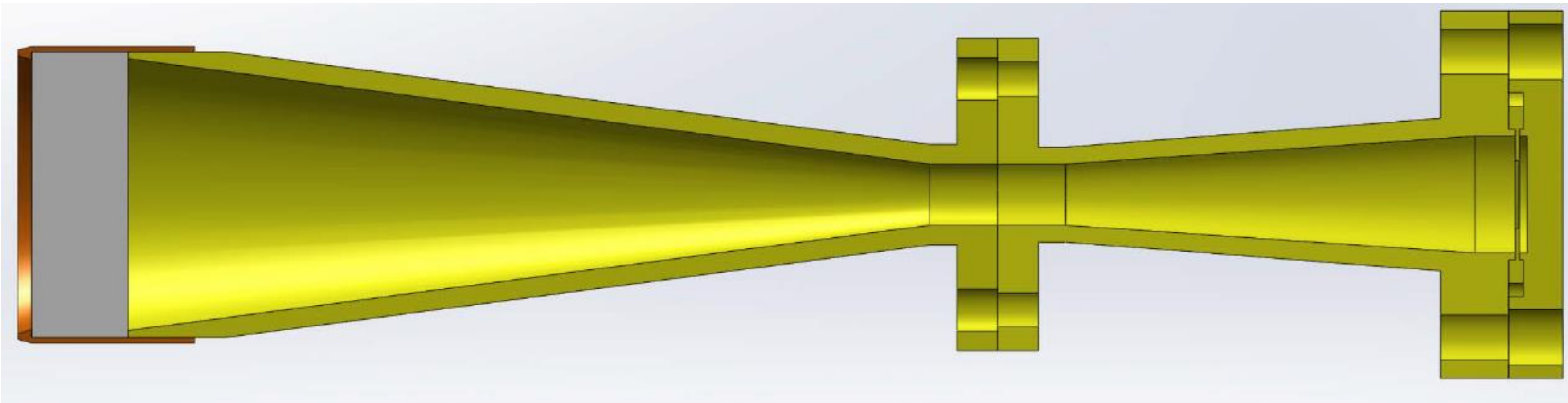

Nominal freq (GHz)	Bandwidth	Min freq (GHz)	Max freq (GHz)
140	30%	119	161
220	5%	214.5	225.5
240	5%	234	246

Table 1 – main features of the SWIPE bandpasses (source: C. Tucker, Cardiff Univ.)

Channel	ν_{min}(GHz)	$N_{modes}(\nu_{min})$	ν_{max}(GHz)	$N_{modes}(\nu_{max})$	ν_{eff}(GHz)	$N_{modes}(\nu_{eff})$
140	119	10	161	17	140	12
220	214	28	226	31	220	30
240	234	32	246	35	240	34

Table 2 – number of coupled modes N_{modes} at the center and at the edges of each SWIPE band. The total optical throughput at frequency ν is $N_{modes}c^2/\nu^2$.

L. Lamagna

SWIPE: Horn beam

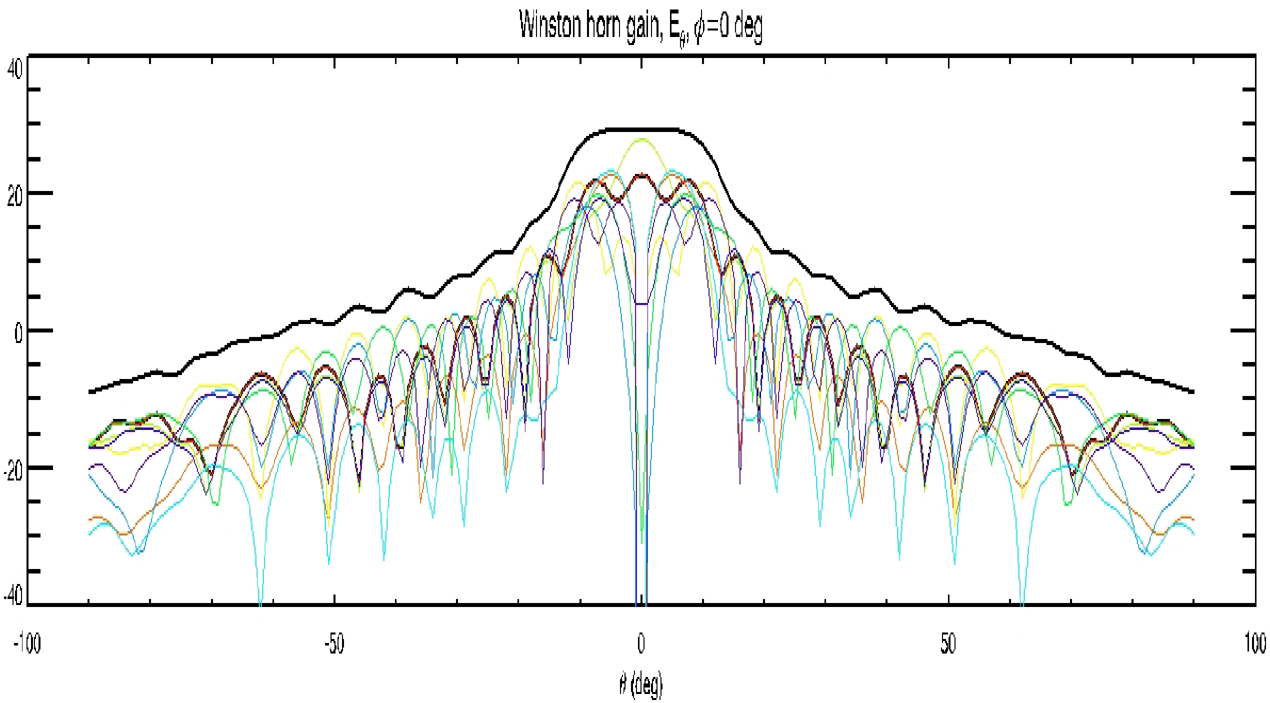

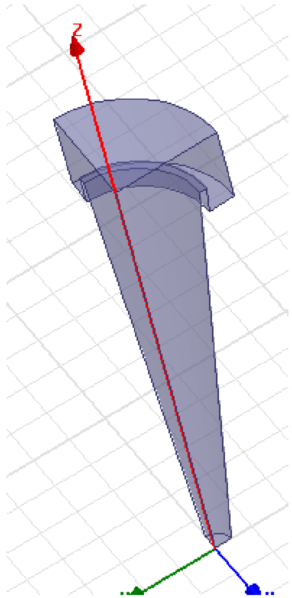

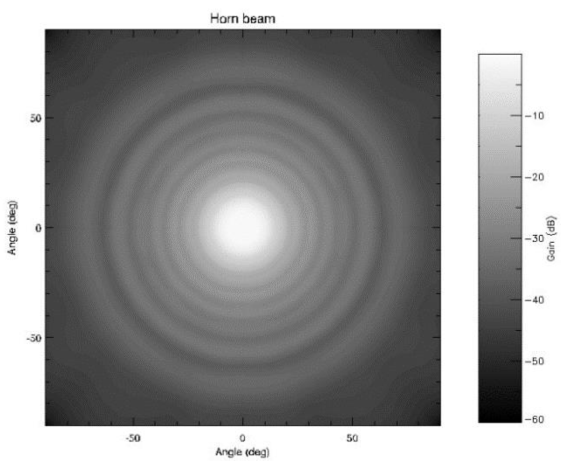

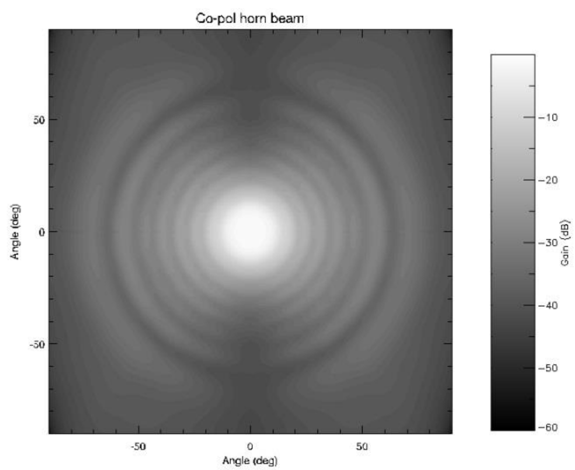

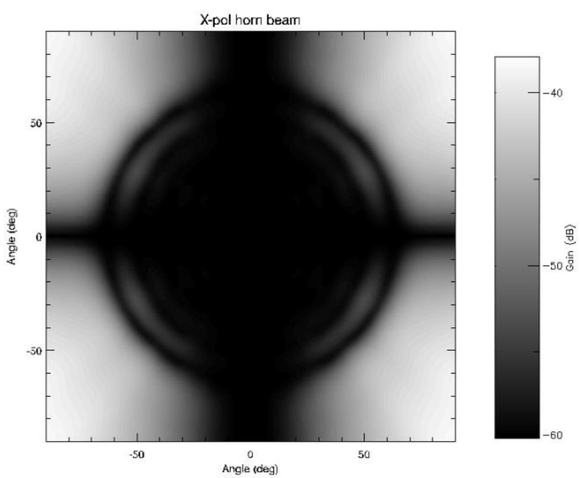

Lamagna et al., Proc. 36° ESA Antenna Workshop, manuscript 110138 (2015)

SWIPE focal planes : 33% 140 GHz, 33% 220 GHz, 33% 240 GHz
Total 330 detectors, with $A\Omega = 10\lambda^2, 21\lambda^2, 23\lambda^2$ @140,220,240

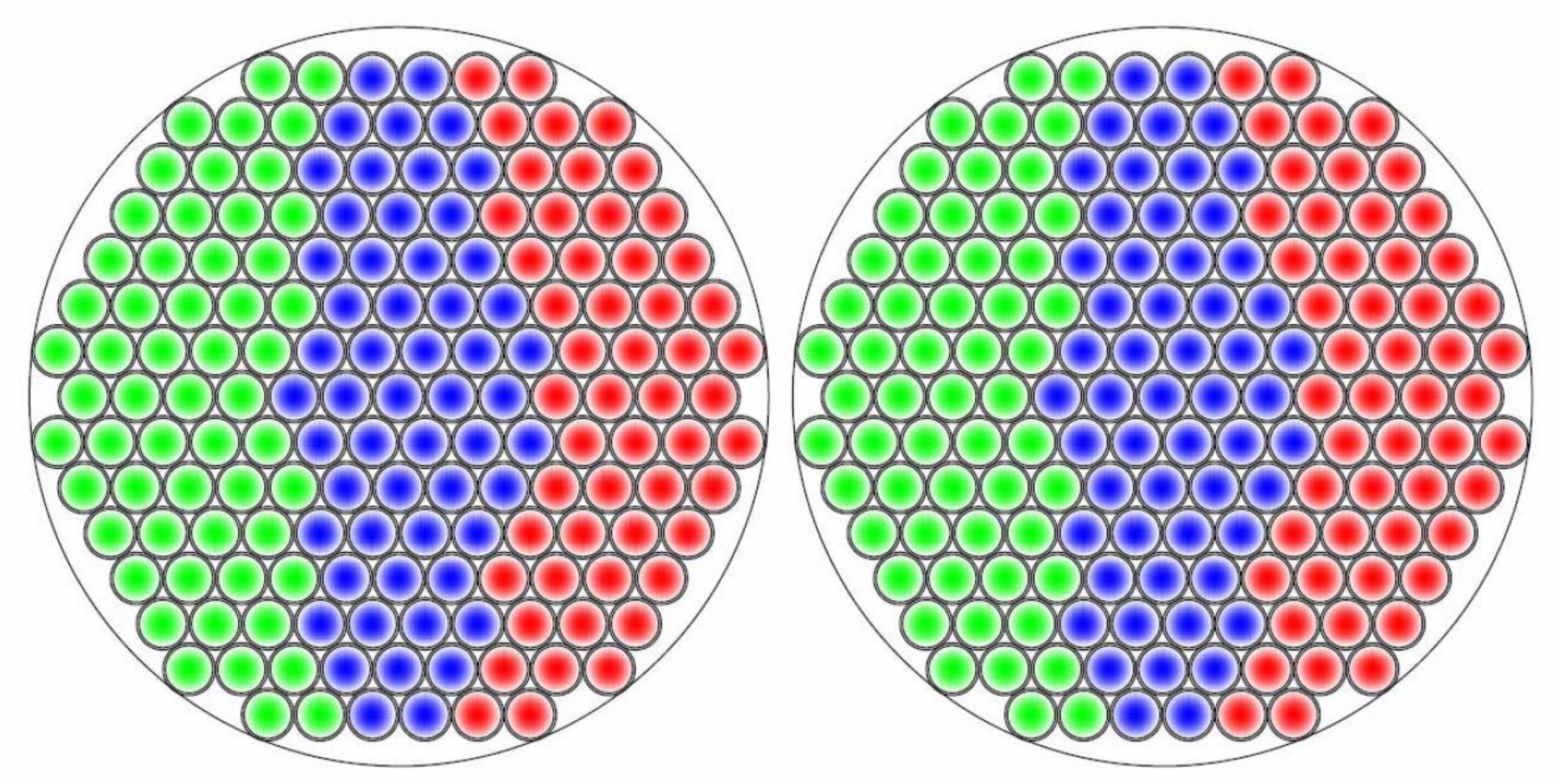

Reflected focal plane

transmitted focal plane

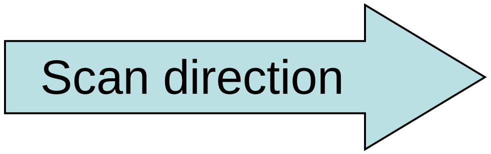

SWIPE: Focal Planes real estate

- The distribution of colors in the pixels has been optimized with a simplified scheme for foregrounds (dust) removal.
- A roughly equal number of pixels in the three bands provides sufficient precision to extrapolate the dust signal from high frequency down to 150 GHz
- This configuration totalizes 4400 radiation modes for each focal plane (transmitted and reflected).

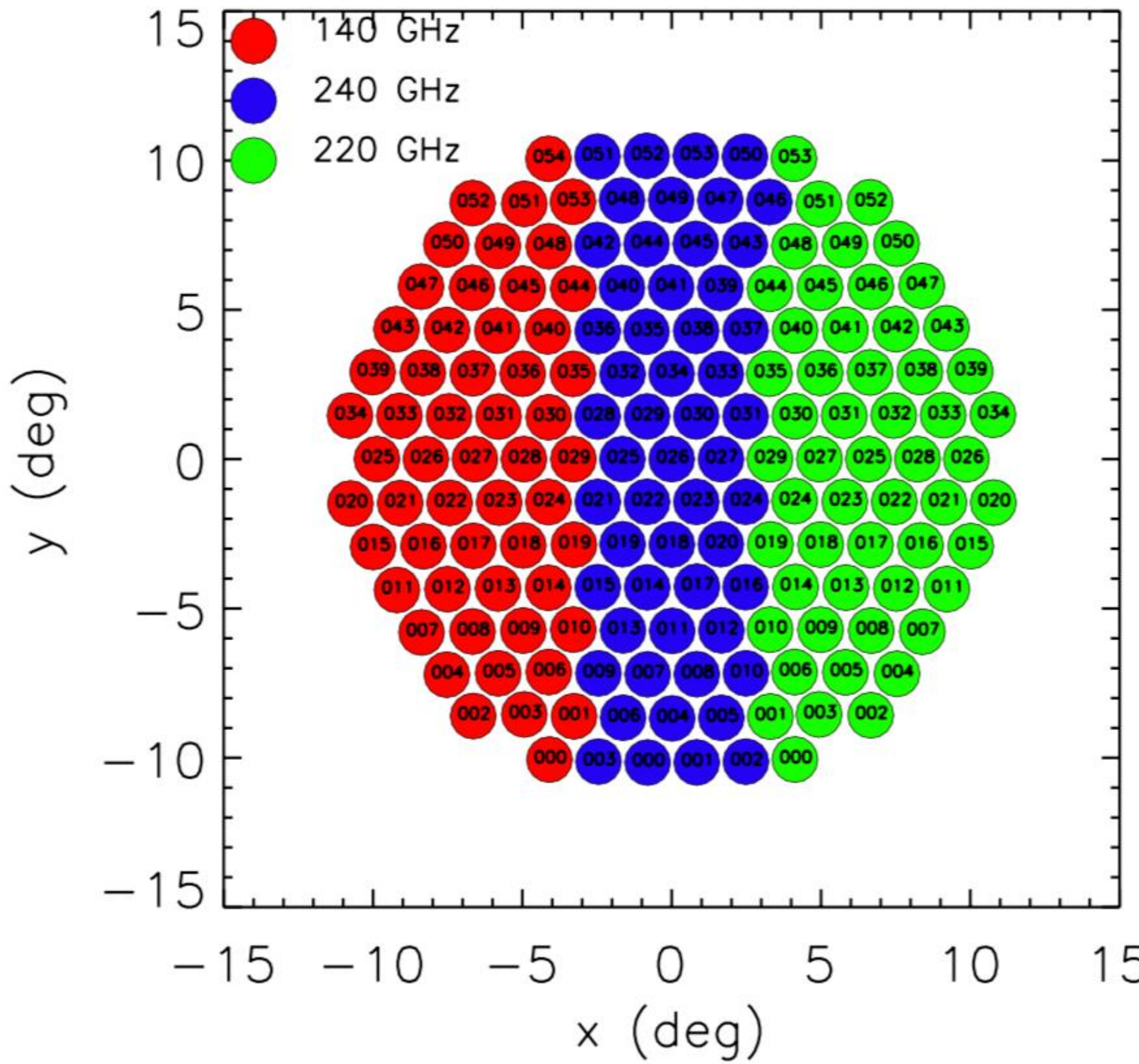

INFN Istituto Nazionale di Fisica Nucleare
Sezione di Roma

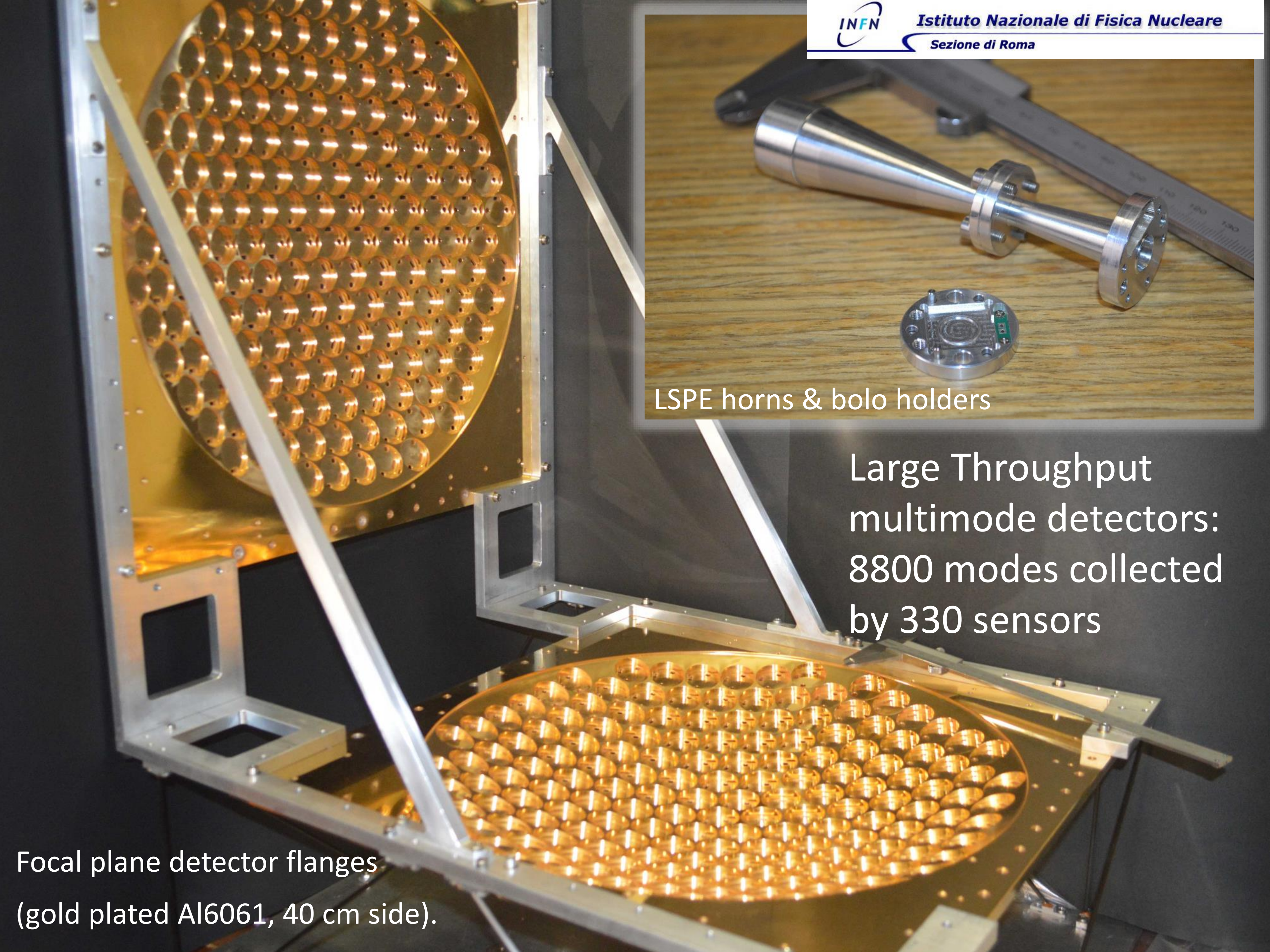

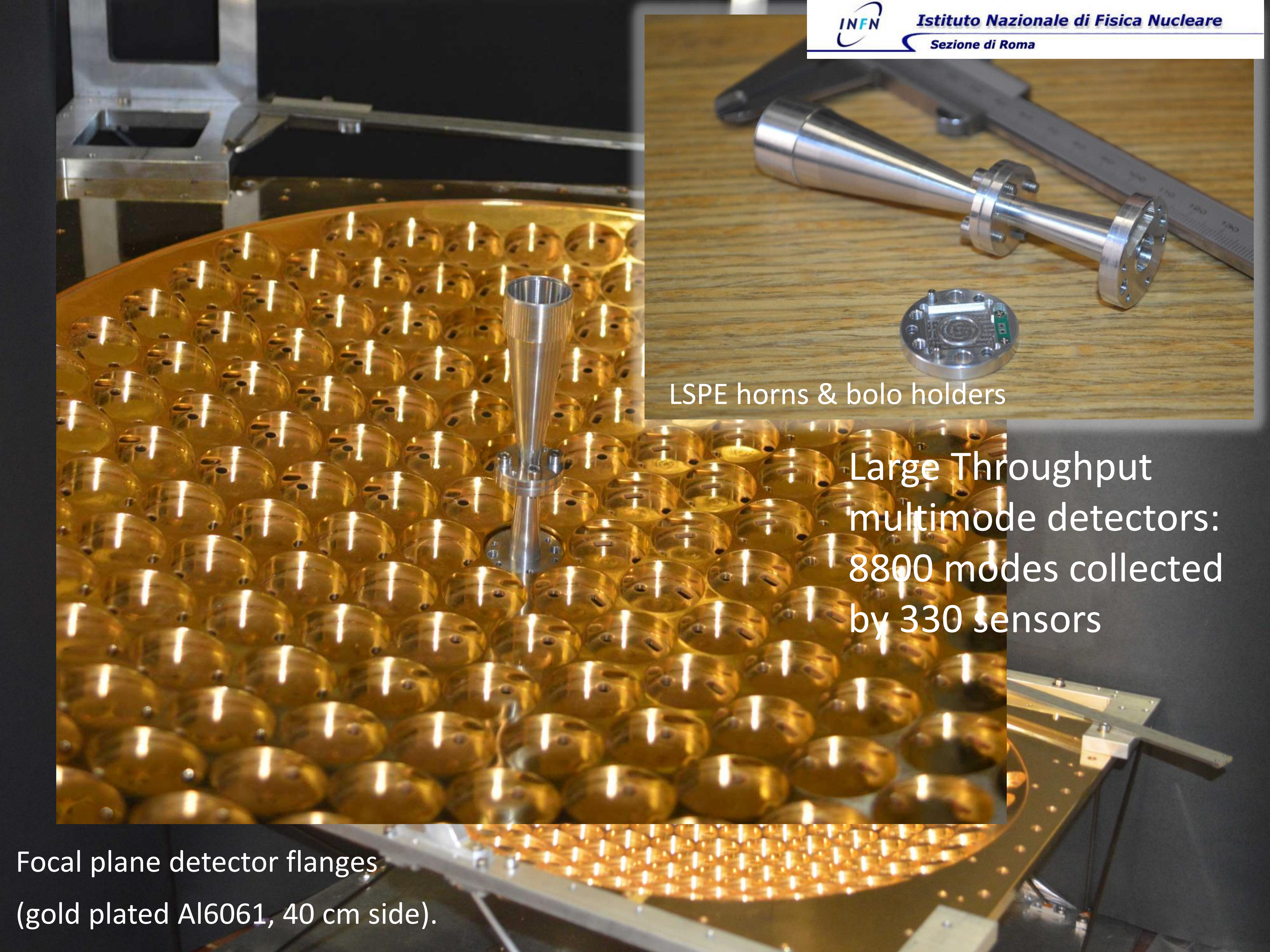
INFN
Istituto Nazionale di Fisica Nucleare
Sezione di Roma
LSPE horns & bolo holders
Large Throughput
multimode detectors:
8800 modes collected
by 330 sensors
Focal plane detector flanges
(gold plated Al6061, 40 cm side).

SWIPE - multimode absorbers & TES

- The absorbers are large Si_3N_4 spider-webs (8 mm diameter, multimode)
- Sensors are Ti-Au TES
- Photon noise limited
- τ = 10 ms

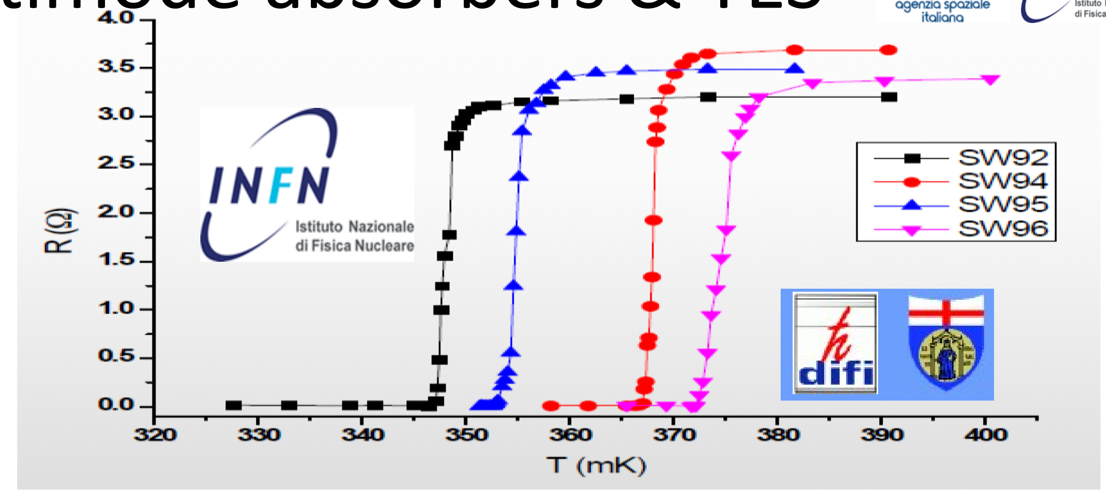

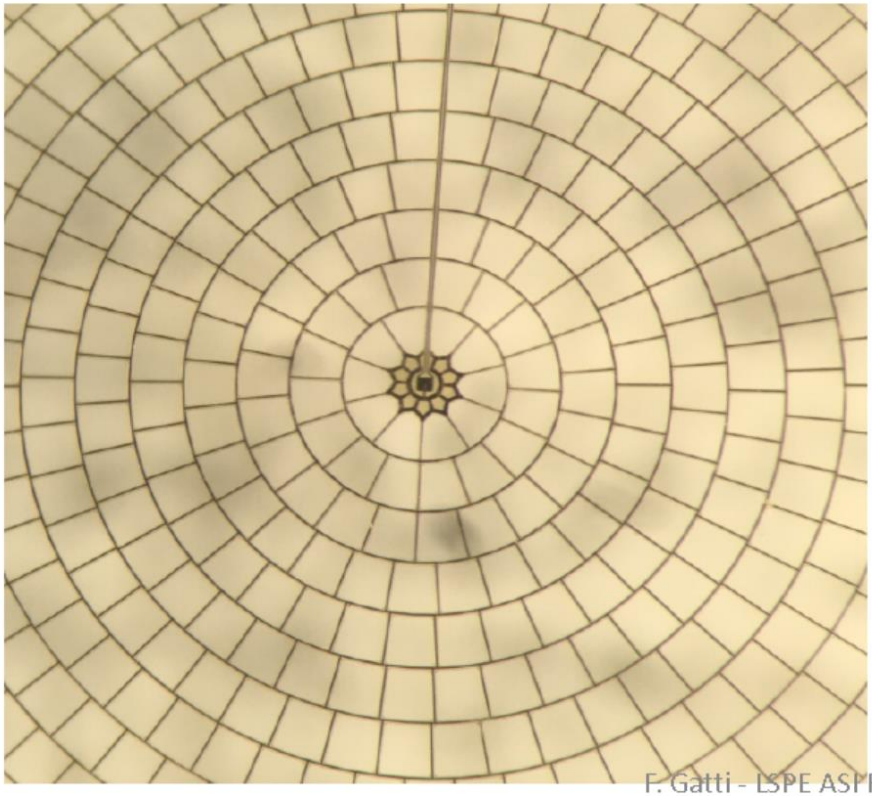

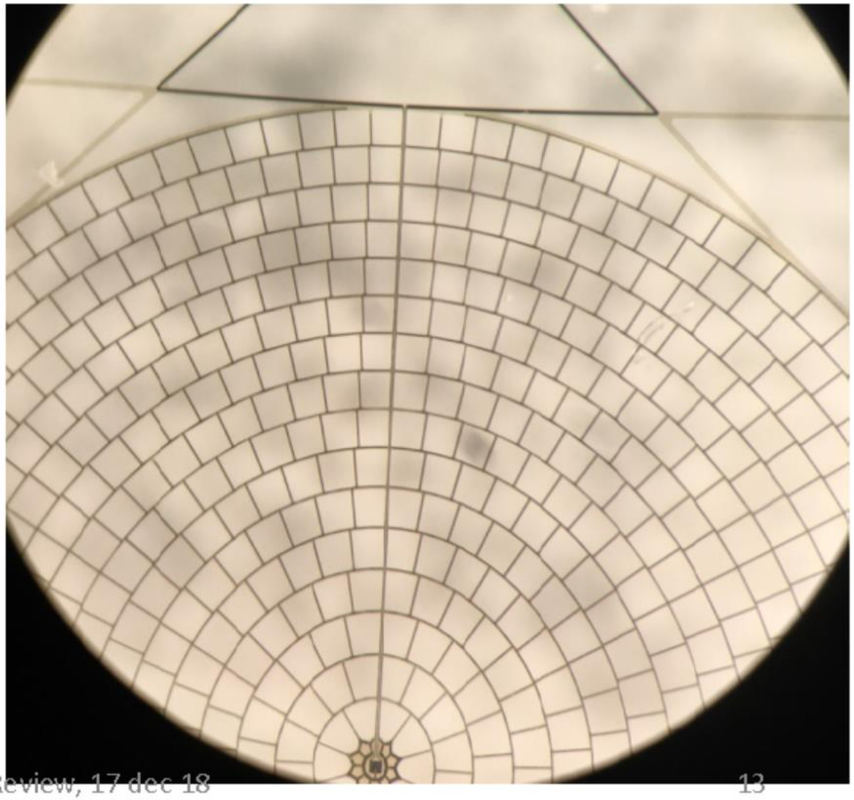

SWIPE - multimode absorbers & TES

- IV curves acquired with SQUID VTT J3, with M=36 μA/ϕ
- Voltage bias generated onto a shunt resistor of 7.34 mΩ
- The analysis allows to calculate the effective thermal conductance G and the NEP, including the electro-thermal feedback

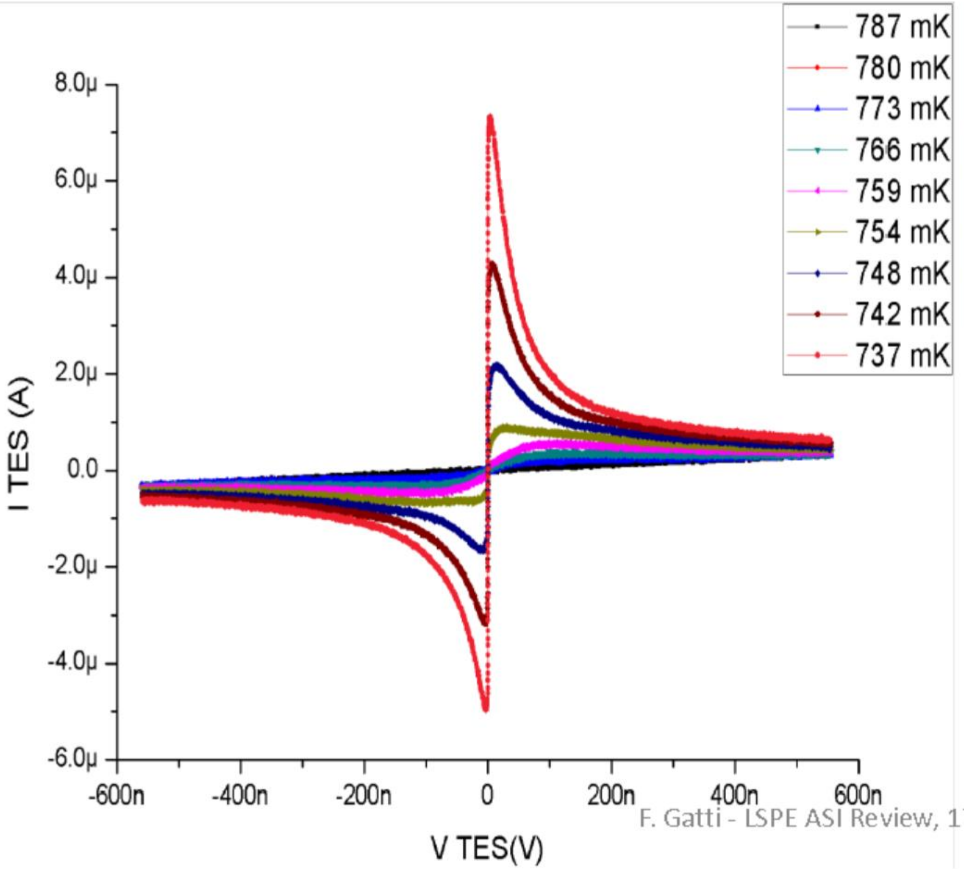

Vbias (uV)	G (10^{-11} W/K)	NEP 10^{-17} W/$Hz^{0.5}$
0.5	5	2.6
1.0	10	3.8
1.5	20	5.3
2.0	28	6.3

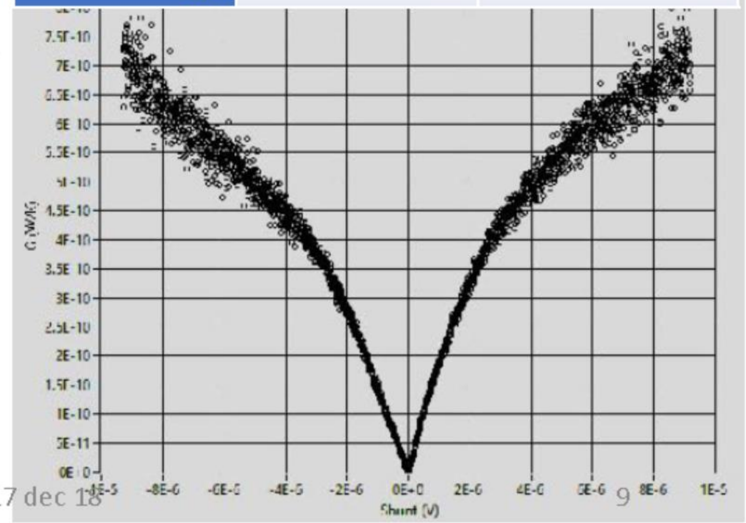

F. Gatti

SWIPE - multimode absorbers & TES

- Very large spider-web absorbers: long time constant, even with large electrothermal feedback
- Minimize heat capacity by using Bi metalization of the spider-web
- Optimization of resistance per square versus heat capacity
- Expected around 10-20 ms

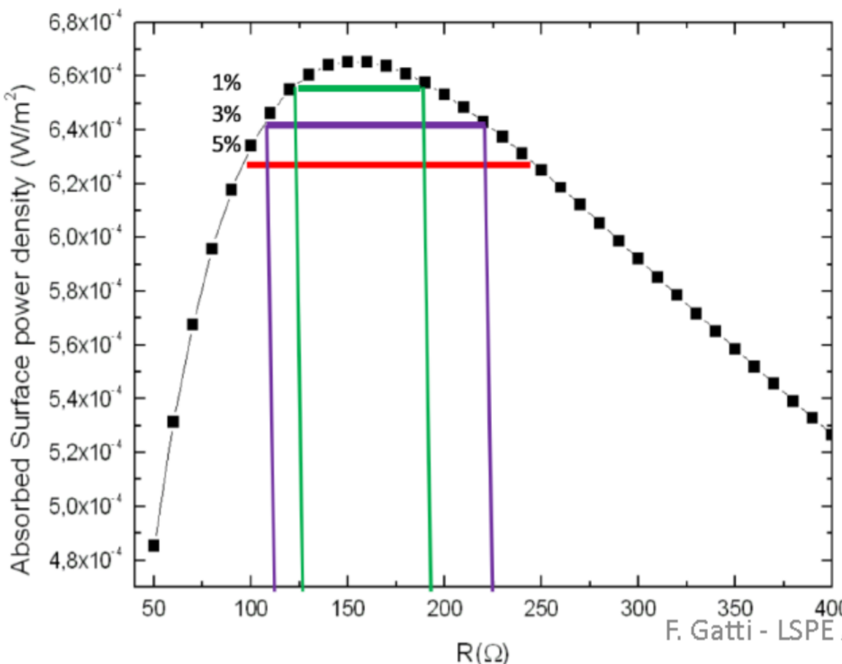

Parameters for Gold	Expct/meas. factor	Effect on heat capacity
RRR	1.5	1.5
3% Match. Fact.	1.8	1.8
G factor	2	-
Expctd Tau fact.	5	

Parameter for Bi over Gold	Expctd/meas . factor	Effect on heat capacity
Resistivity Ratio	50(expec.) - 70(meas.)	3,4(expec.)- 2,4(meas.)
Specific heat ratio	1/170	
G fact.	2	
Expectd. Tau fact	5(meas.)- 7(expec.)	

F. Gatti

Absorber properties

- **EM simulations of absorber illumination, mode by mode, for several off-axis angles**

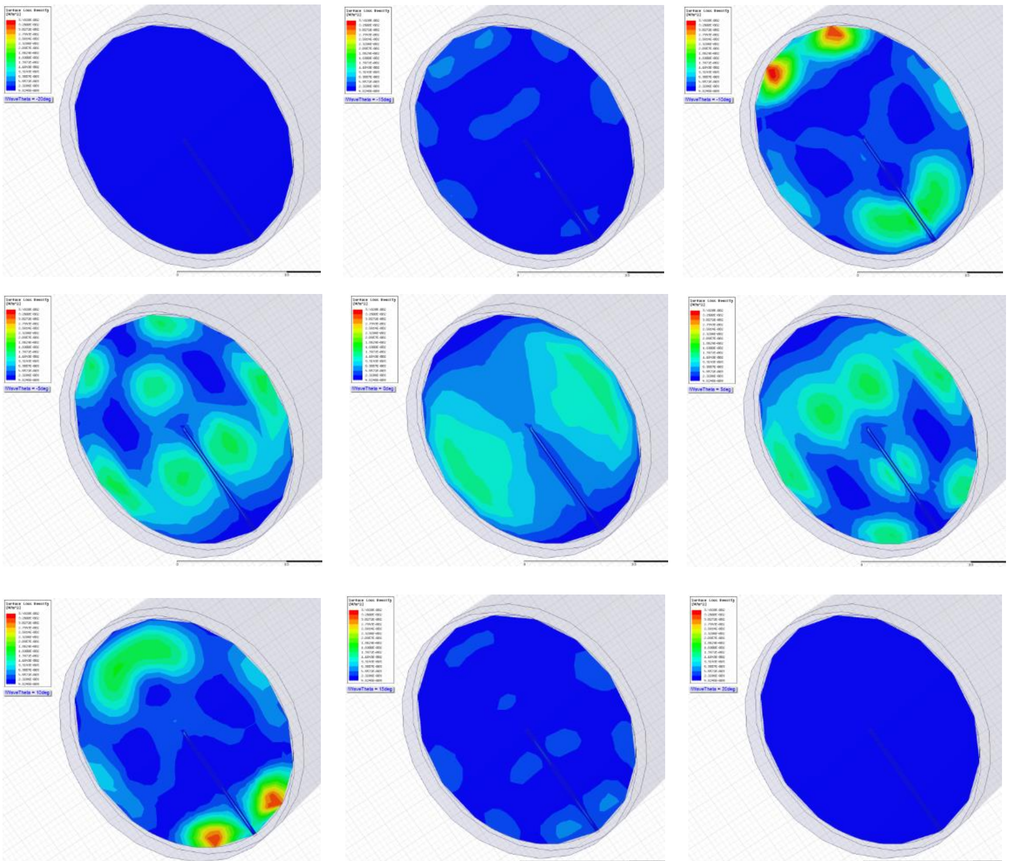

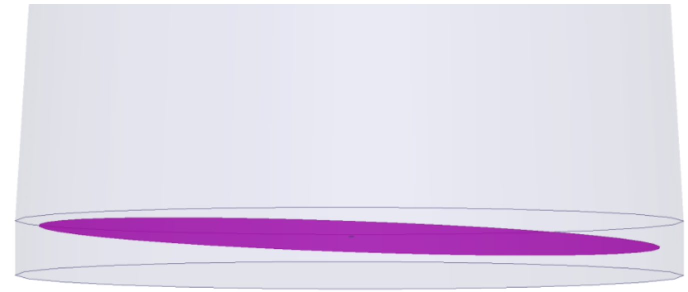

L. Lamagna

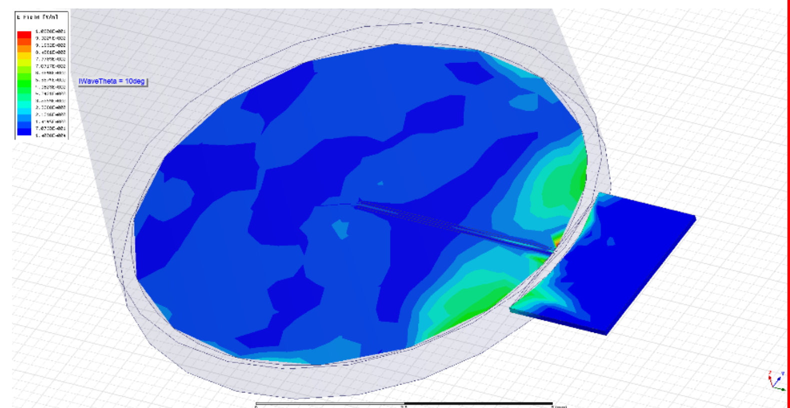

- **Despite of the different shapes, the integral is regular.**
- **Uniformity of absorption is very important to obtain a regular beam pattern.**
- **Internal conductivity of the absorber mesh also very important.**
- **RA measurements are warranted to be significant only in cold operating conditions**

SWIPE - TES readout (mux)

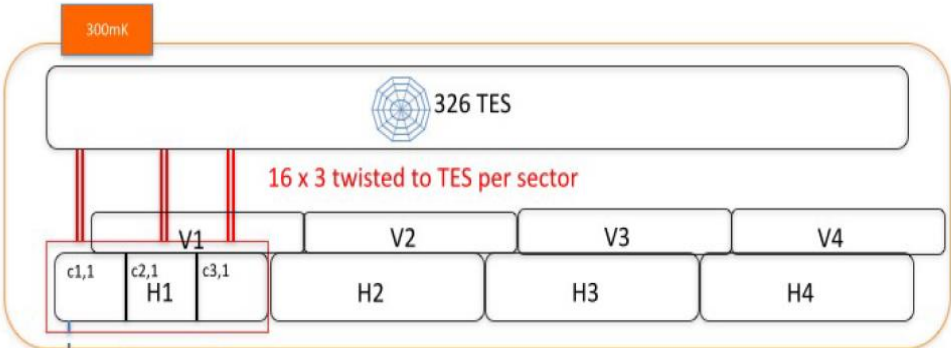

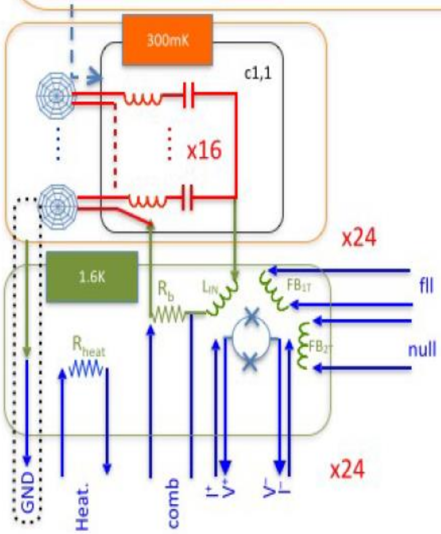

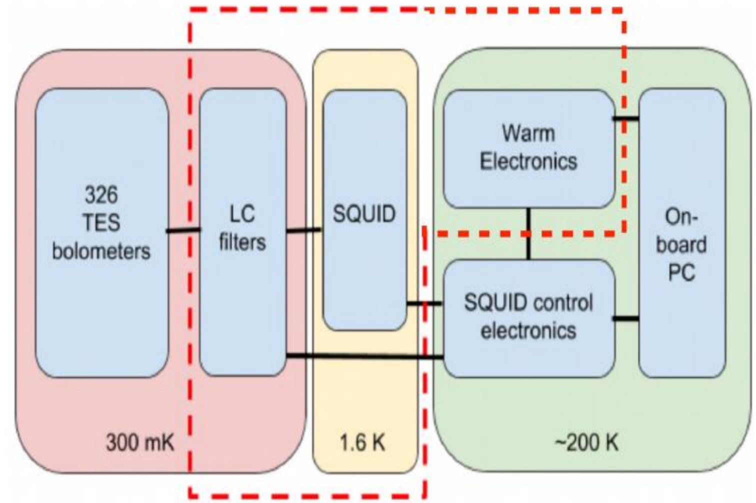

Wiring and connections
from 300 mK to 250 K

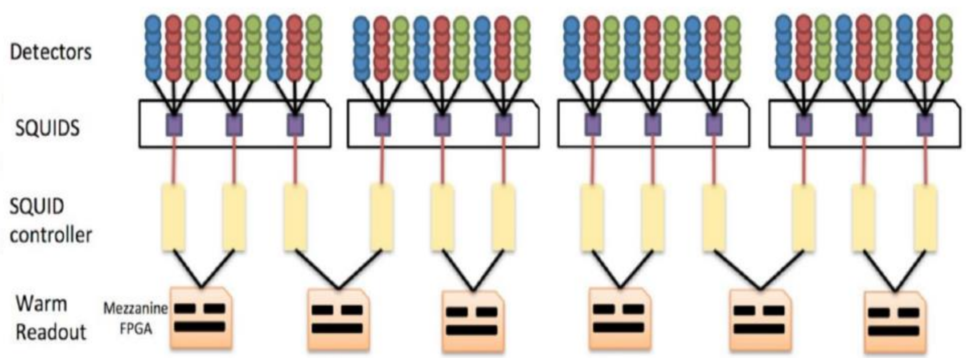

G. Signorelli

INFN
PISA
Istituto Nazionale di Fisica Nucleare
Sezione di Pisa

SWIPE - TES readout (mux)

- 14 Si chips, 2 Nb $15\ \mu\mathrm{H}$ inductors each, 5 open-circuited
- 28 SMD capacitors, ranging from $220\ \mathrm{pF}$ to $100\ \mathrm{nF}$
- SMD resistors with $\mathrm{R} = 1\ \Omega$, $\mathrm{R}_{\mathrm{shunt}} = 100\ \mathrm{m}\Omega$
- Readout with SQUID in FLL
- Tested @ 4 K

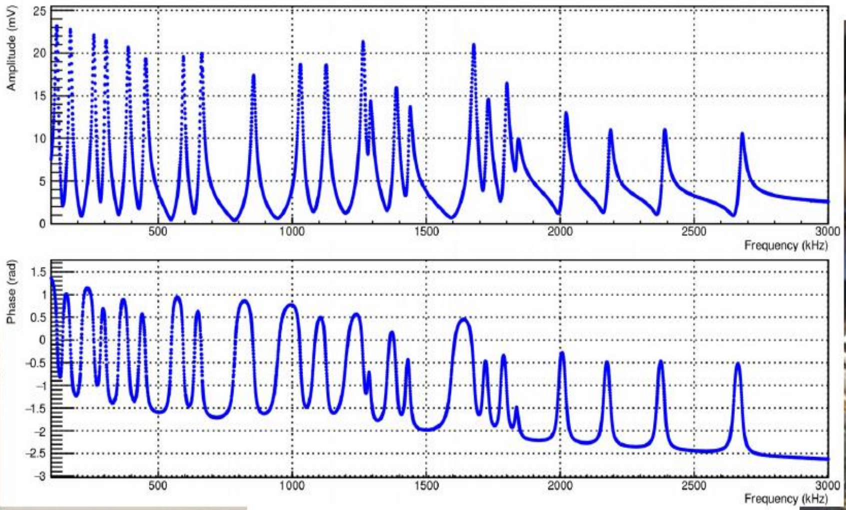

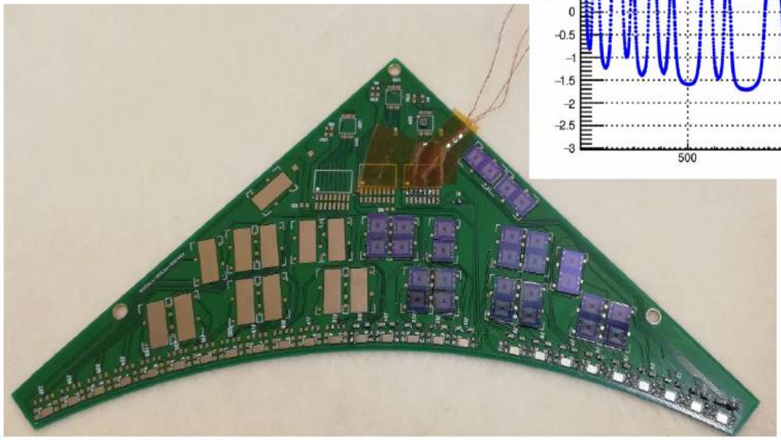

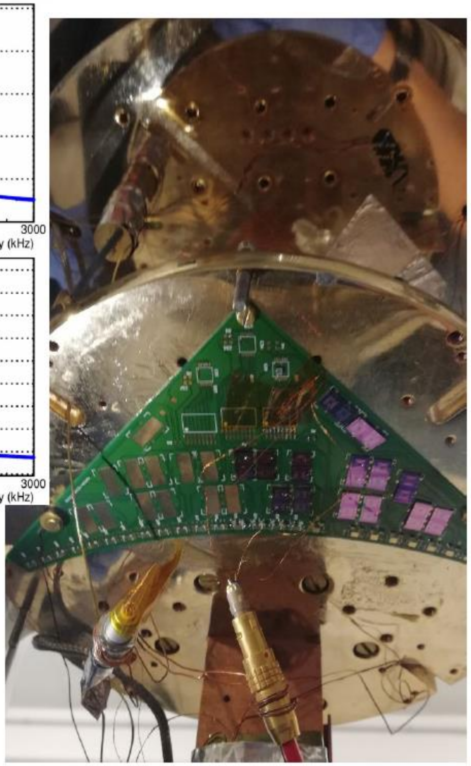

Test of a readout channel

G. Signorelli

INFN PISA Istituto Nazionale di Fisica Nucleare Sezione di Pisa

SWIPE - TES readout (mux)

- Altera Cyclone V SoC
  - FPGA with 110'000 logic elements
  - 925 MHz dual-core micro-controller
- Mezzanine plug-ins for DAC and ADCs
  - 2 LTC1668 DACs (low noise, low power consumption)
  - 1 LTM9001-GA ADCs (16-bit, 25 MSPS)
- Gbit interface for data communication
- CAN & I2C interfaces to control low noise amps

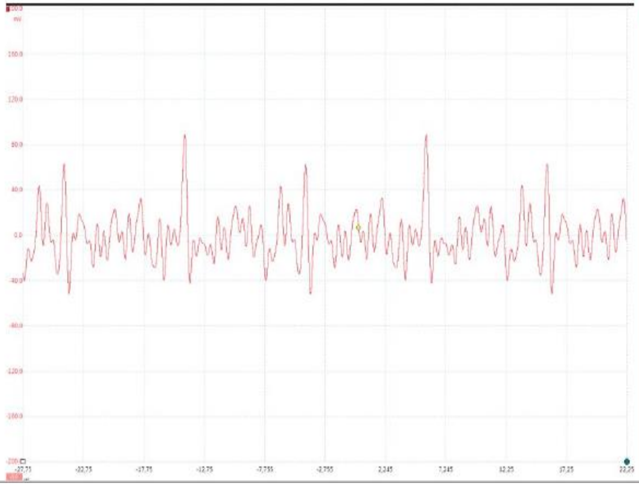

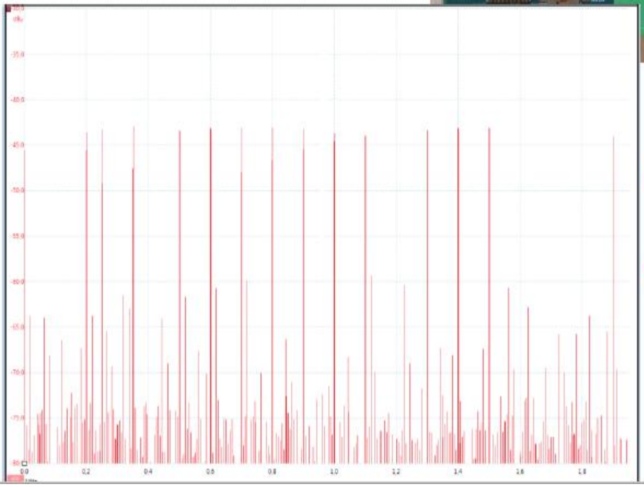

FDM board tested and working

First comb generation algorithm

G. Signorelli

INFN PISA
Istituto Nazionale di Fisica Nucleare
Sezione di Pisa

LSPE/SWIPE: cryogenic system

LSPE-SWIPE

- Aluminum cryostat
- Large cold volume (1m^3)
- 2 vapor cooled shields
- Fiberglass support system
- 250L of superfluid ^{4}He @ 1.6K
- > 15 days hold time
- ^{3}He refrigerator 0.28K

  (Coppi et al. 2016SPIE.9912E..65C)

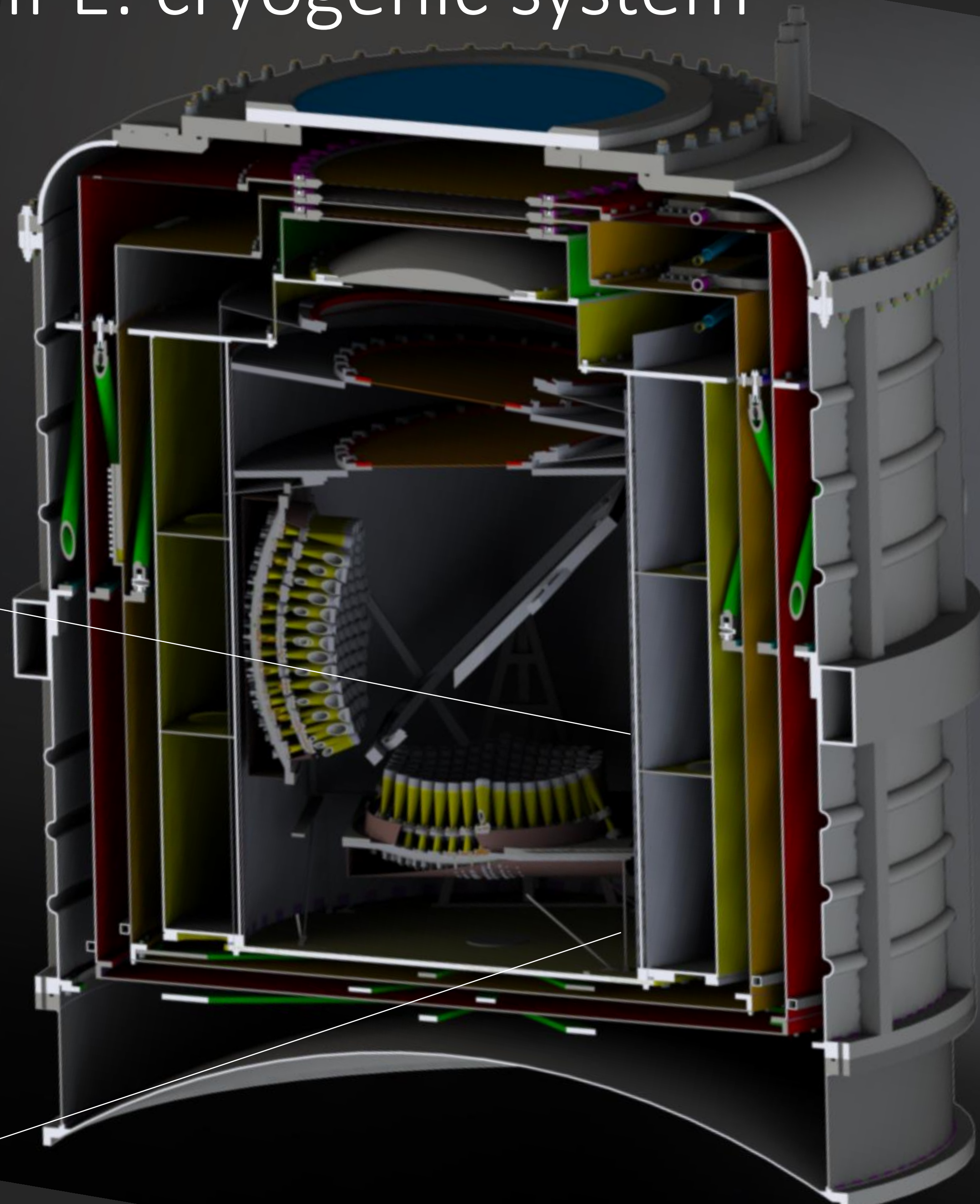

LSPE/SWIPE: cryogenic system

Expected performance versus gas exchange efficiency (30 s.i. shields)

T_{ext}(K)	Efficiency	$T_{shield1}$ (K)	$T_{shield2}$ (Kelvin)	Hold time (days)
290	0.7	90	251	30
290	0.8	90	247	30
290	0.9	90	244	30
220	0.7	75	183	41
220	0.8	71	180	45
220	0.9	67	178	50

Cryostat development
parts being machined

S. Masi, 3/12/2018

Cryostat development

parts being welded

S. Masi, 3/12/2018

Expected performance of SWIPE-LSPE , from realistic simulations, in a single flight

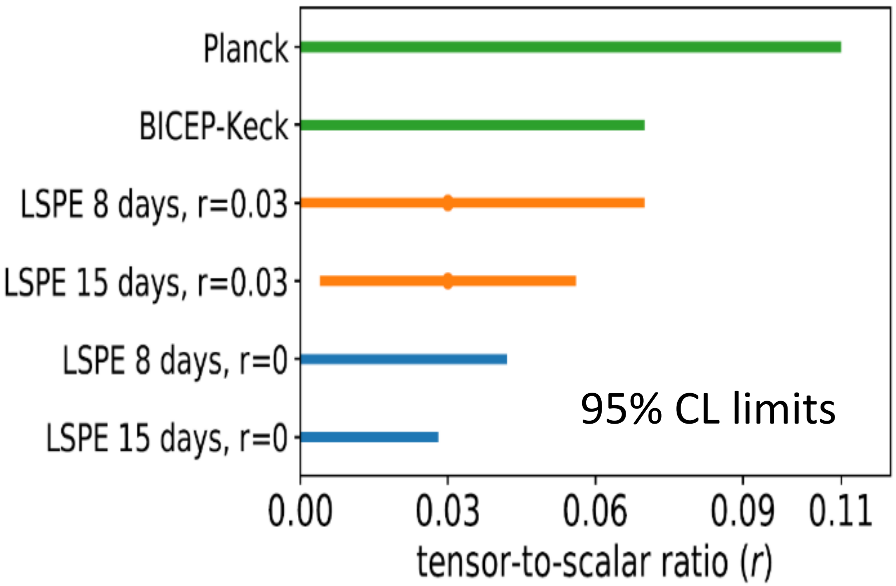

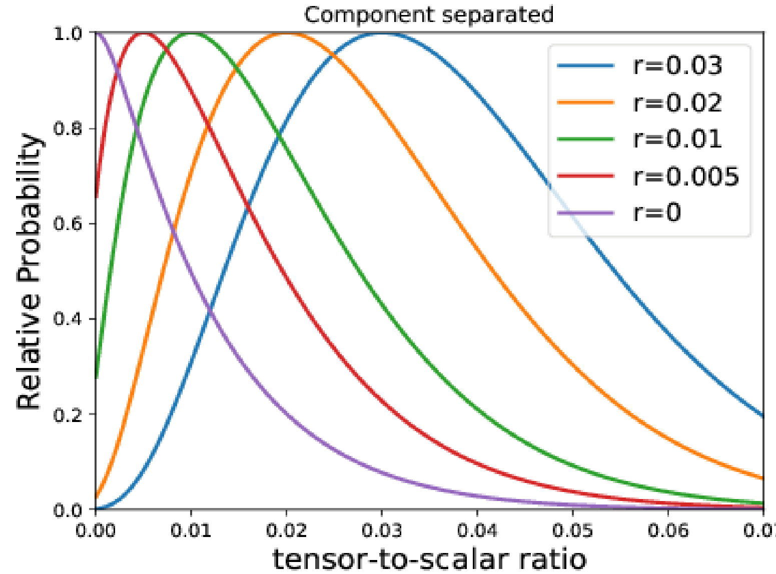

- If r << 0.01 LSPE-SWIPE provides a 95% CL U.L. r < 0.03
- If r > 0.01 LSPE-SWIPE provides a significant detection of r
- The measurement of the optical depth to recombination is improved significantly wrt Planck:

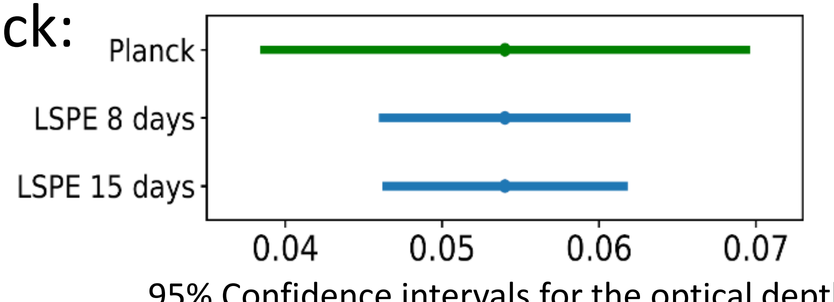

L. Pagano, F. Piacentini

Mission Requirements:

SWIPE limits (68% CL) to the tensor to scalar ratio versus integration time:

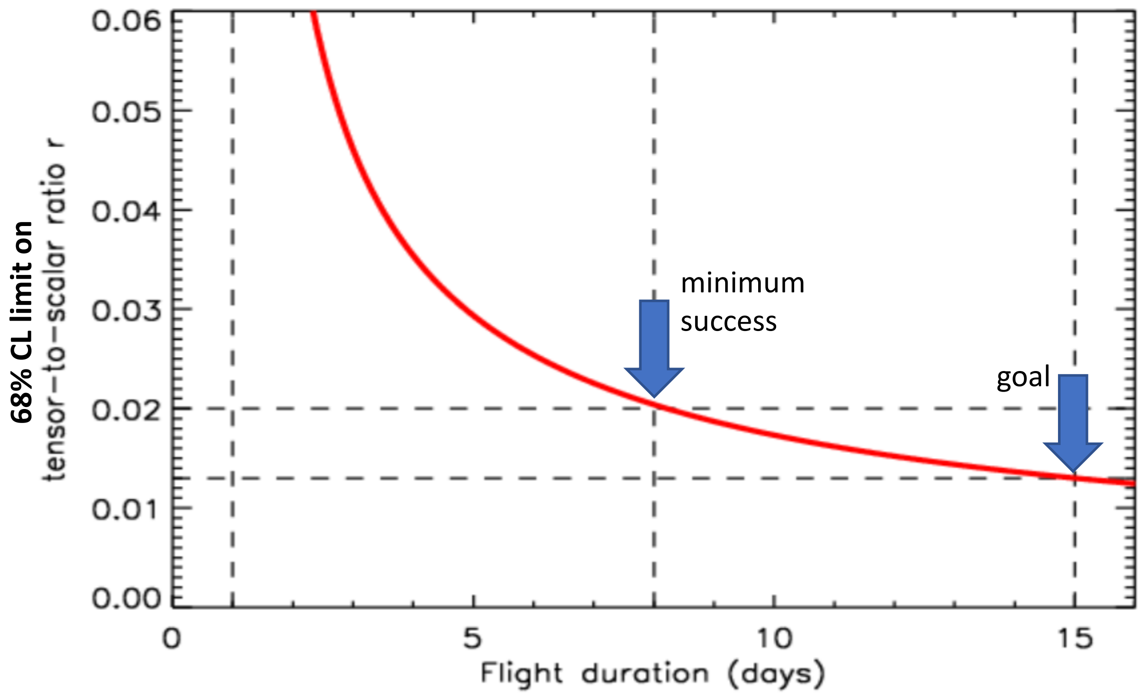

- Long integration time (8 days minimum, 15 days goal)
- Night flight (to cover all azimuths with a telescope spinning in azimuth)

SWIPE : night flight

Flight managed by ASI, scheduled for end of 2020
Longyearbyen - Svalbard




SWIPE: solar illumination issues

- With a careful choice of the launch date and launch site the length of the illuminated portions of the flight can be minimized (see forecast document *Analysis of Winter Polar stratospheric balloon trajectories, 23/10/2018*).
- We do not plan to carry out science measurements during these periods, but the instrument should be prepared to survive short solar illumination periods.

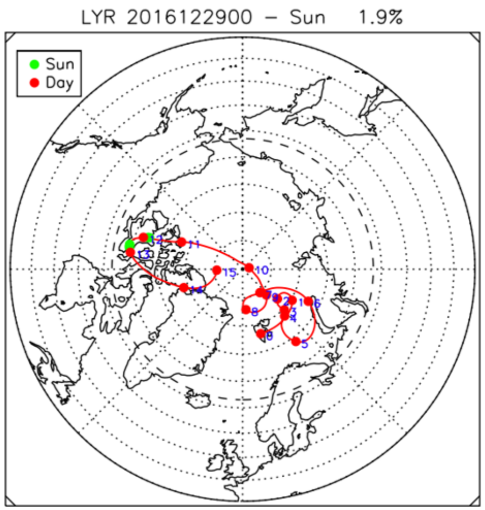

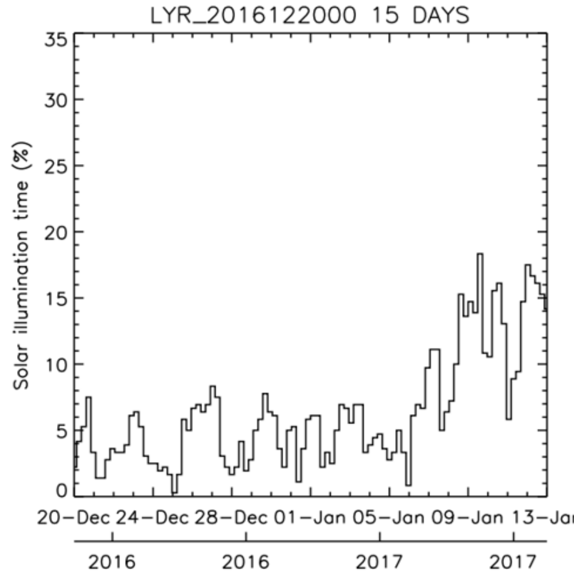

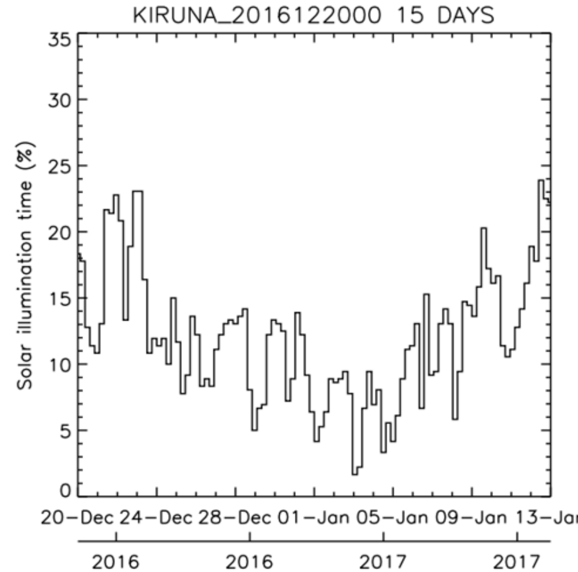

F. Piacentini

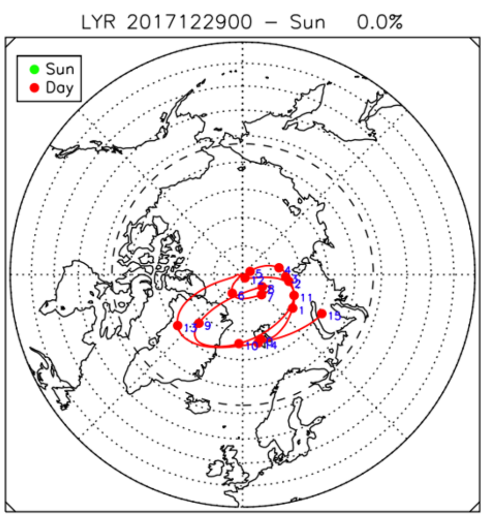

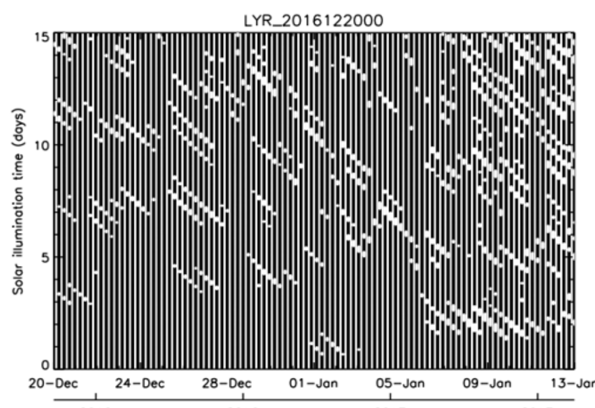

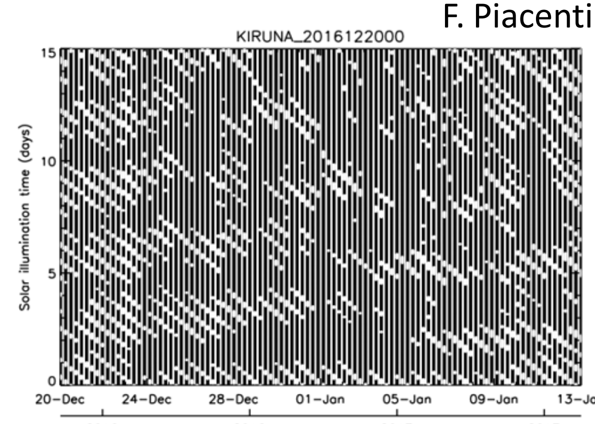

COSMO
(COSmic Monopole Observer)

A measurement of the largest spectral distortion of the CMB at mm wavelengths, with a DFTS in Dome-C, fast atmospheric modulation and removal. Expected result :

The COSMO collaboration: *Masi S., Battistelli E., Bersanelli M., Castellano M.G., Cibella S., Columbro F., Coppolecchia A., D'Alessandro G., de Bernardis P., De Petris M., Franceschet C., Gervasi M., Lamagna L., Paiella A., Pettinari G., Piacentini F., Pisano G., Tucker C., Zannoni M.*

Spectral Distortions of the CMB

- In the primeval fireball, CMB photons are frequently scattered by free electrons, and efficiently thermalized, thus acquiring their blackbody spectrum.
- After recombination, CMB photons do not interact with matter anymore, and the blackbody spectrum is maintained, with its temperature scaling as the inverse of the scale factor.
- The dependences of the number density and the wavelength on the scale factor conspire to maintain a Planck spectrum for CMB photons. And this has been measured by COBE-FIRAS: **a perfect Planck spectrum**, within deviations, if any, < 100 ppm of its maximum brightness.
- All this is *very delicate*: if there is any deviation from any of the hypothesis above, the result will be a *spectral distortion*, a deviation from a pure Planck spectrum.
- **Spectral deviations are expected, at a level of 20 ppm or lower.** See e.g. J. Chluba, R. A. Sunyaev MNRAS (2012) 419 1294

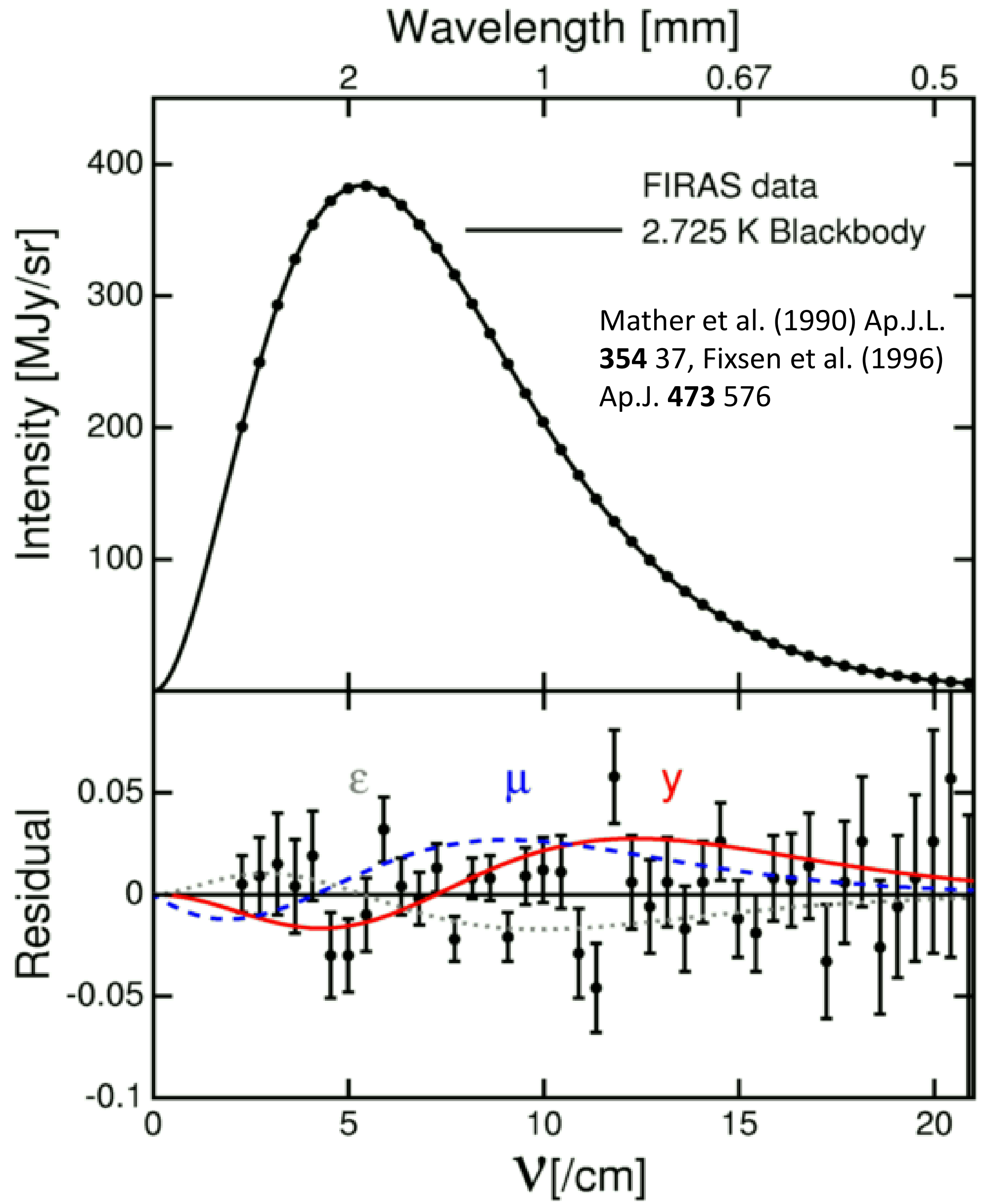

The observable is small, compared to … everything.

- Great scientific importance of measuring spectral distortions in the CMB – Cosmology and Fundamental Physics.
- Distortion signals are *guaranteed to exist*, but are *very small* compared to
  - detector noise,
  - instrument emission,
  - atmospheric emission and fluctuations,
  - foregrounds,
  - the CMB itself.
- Intelligent measurement methods required. Experimentalists way behind theorists. Final measurement certainly to be carried out from space.
- Here focus on a pathfinder experiment, ground-based, which does not target at the smallest distortions, but tries to exploit at best existing, relatively cheap opportunities.

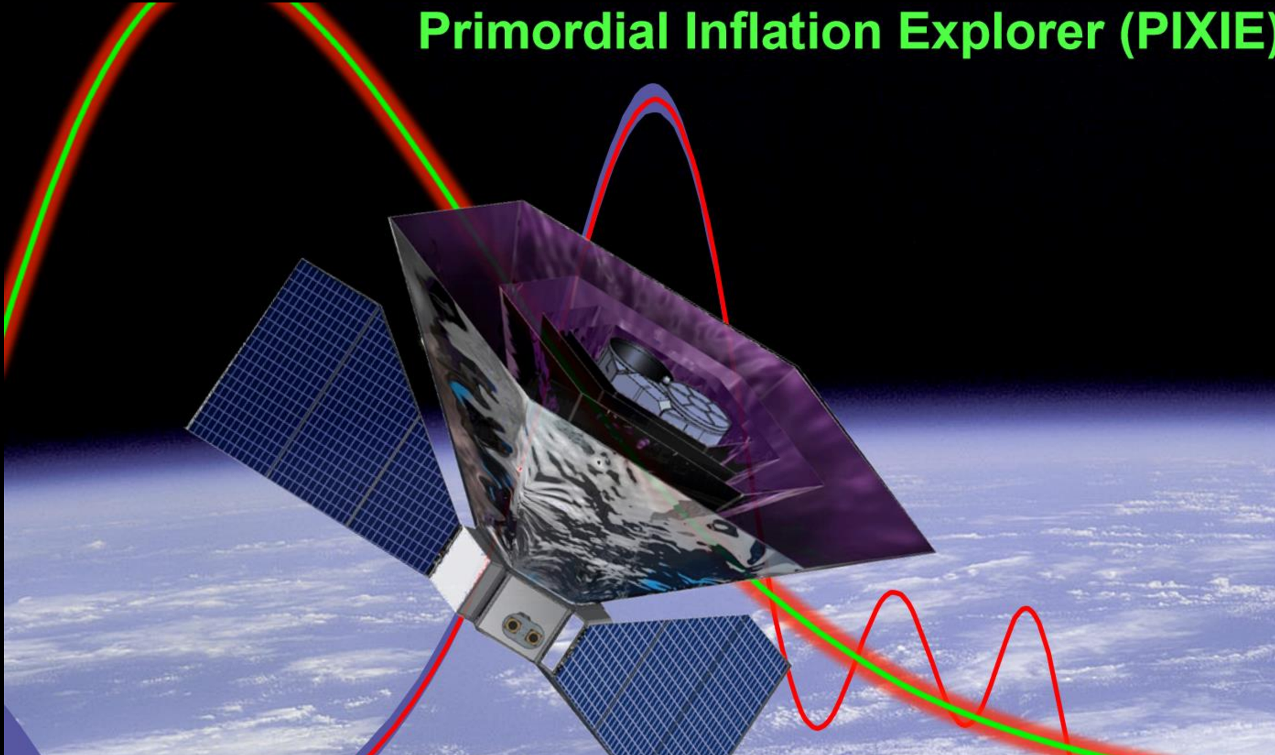

Satellite measurements can sample the CMB spectrum over the entire range 0-600 GHz.
PIXIE !!!
(*https://asd.gsfc.nasa.gov/pixie/*).

Ground based measurements are surely limited to frequencies in the atmospheric transmission windows.

If a ground-based measurement can be attempted from the ground, the site should be the high Antarctic Plateau (e.g. Dome-C or South Pole).

COSMO (COSmological Monopole Observer) targets this observable from Dome-C

Absolute measurement approach

- The Martin-Pupplett Fourier Transform Spectrometer used un FIRAS and PIXIE has two input ports.
- The instrument is intrinsically differential (DFTS), measuring the spectrum of the difference in brightness at the two input ports. Normally one port looks at the sly, the other one at an internal reference blackbody

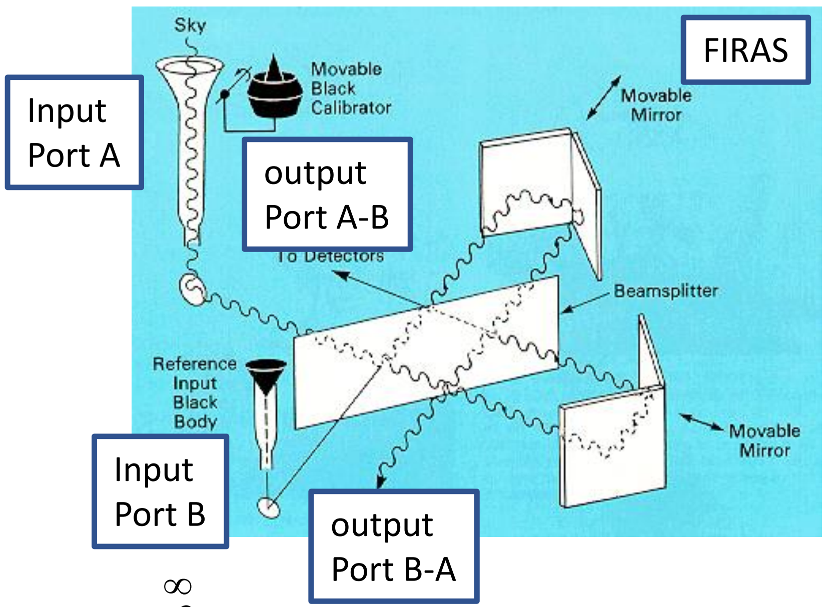

Sky measurement

$$I_{SKY}(x) = C\int_0^\infty [S_{SKY}(\sigma) - S_{REF}(\sigma)] rt(\sigma)\{1+\cos[4\pi\sigma x]\} d\sigma$$

Calibration measurement

$$I_{CAL}(x) = C\int_0^\infty [S_{CAL}(\sigma) - S_{REF}(\sigma)] rt(\sigma)\{1+\cos[4\pi\sigma x]\} d\sigma$$

A ground-based measurement ?

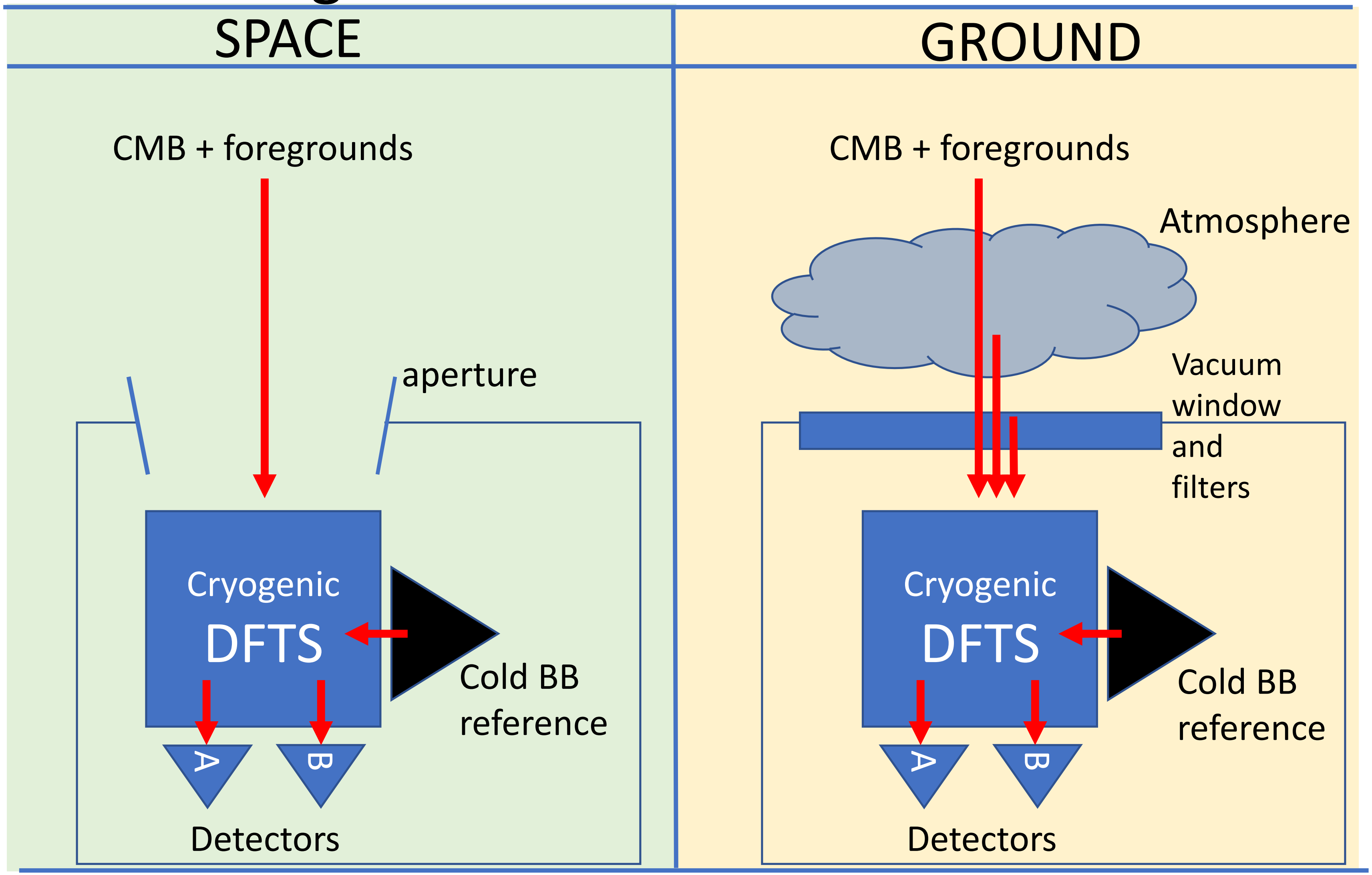

In a space-based instrument there is nothing between signal to be measured (CMB + foregrounds) and the DFTS

In a ground-based instrument the signal to be measured (CMB + foregrounds) is dominated by the emission of the Earth atmosphere and the emission of the warm part of the cryogenic system (vacuum window & filters). **They must be *minimized* AND *subtracted*.**

A ground-based measurement ?

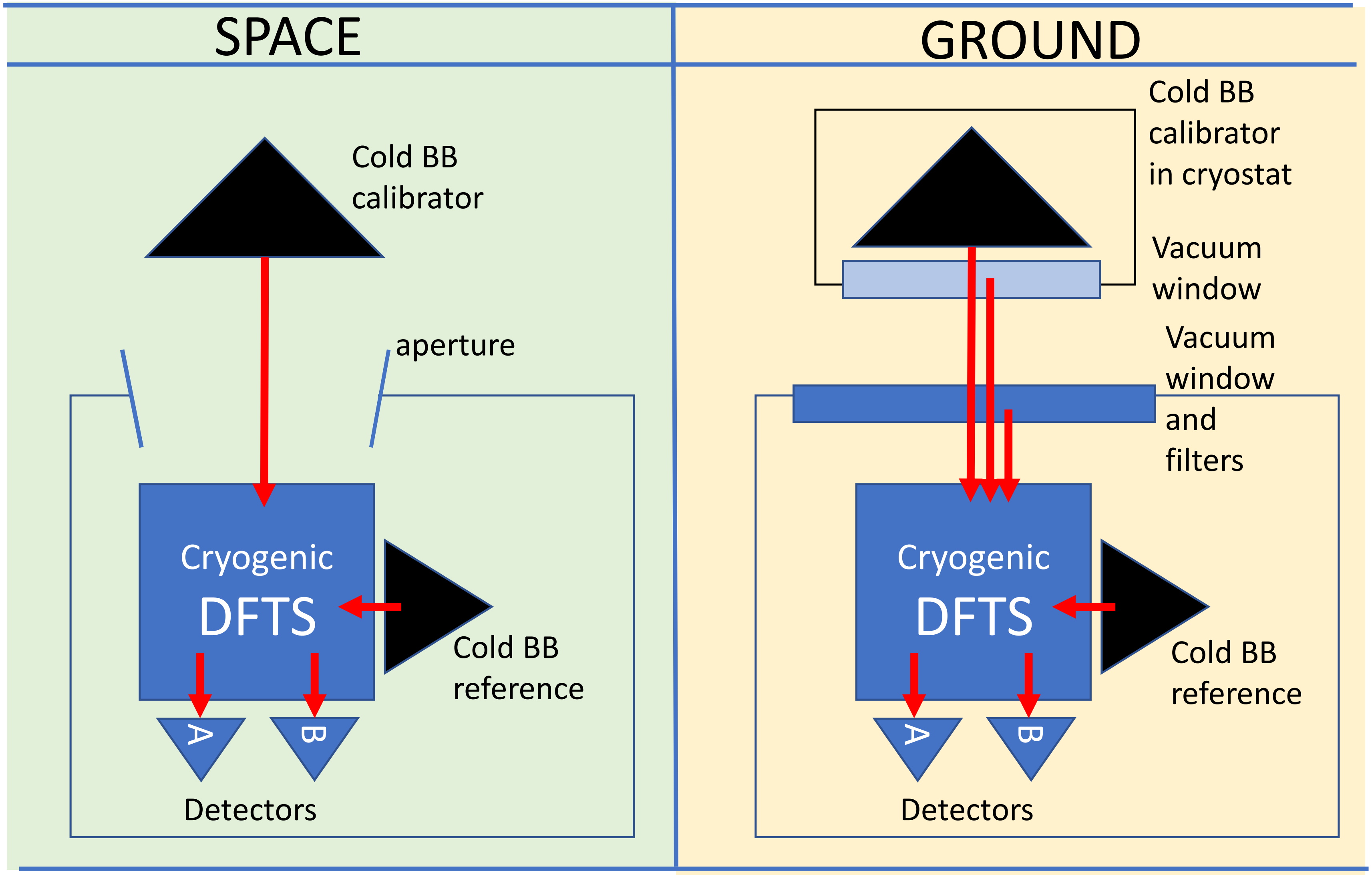

Even the Calibration measurement cannot be carried out on the ground in the same way as is done in space. A vacuum window is necessary to keep the calibrator BB cold. **Its emission must be *minimized* AND *subtracted*.**

Feasibility of a ground-based measurements

- Let’s analyze the different nuisances:
  - Atmospheric emission
  - Window emission
- And try to cope with them optimizing the conditions.

Why Dome-C : optical depth of the atmosphere (credits : AM code)

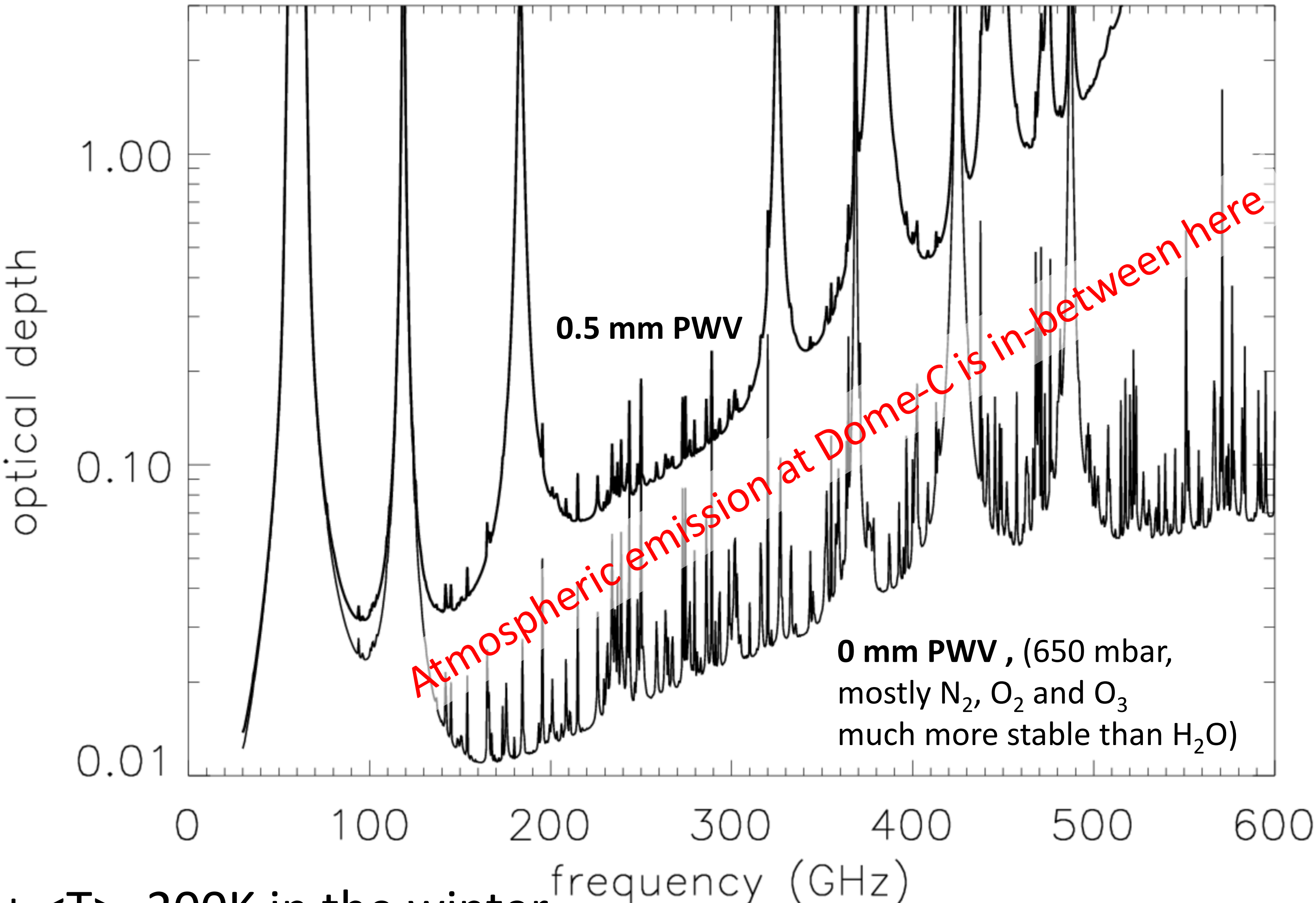

+ <T>=200K in the winter

Why Dome-C : optical depth of the atmosphere (credits : AM code)

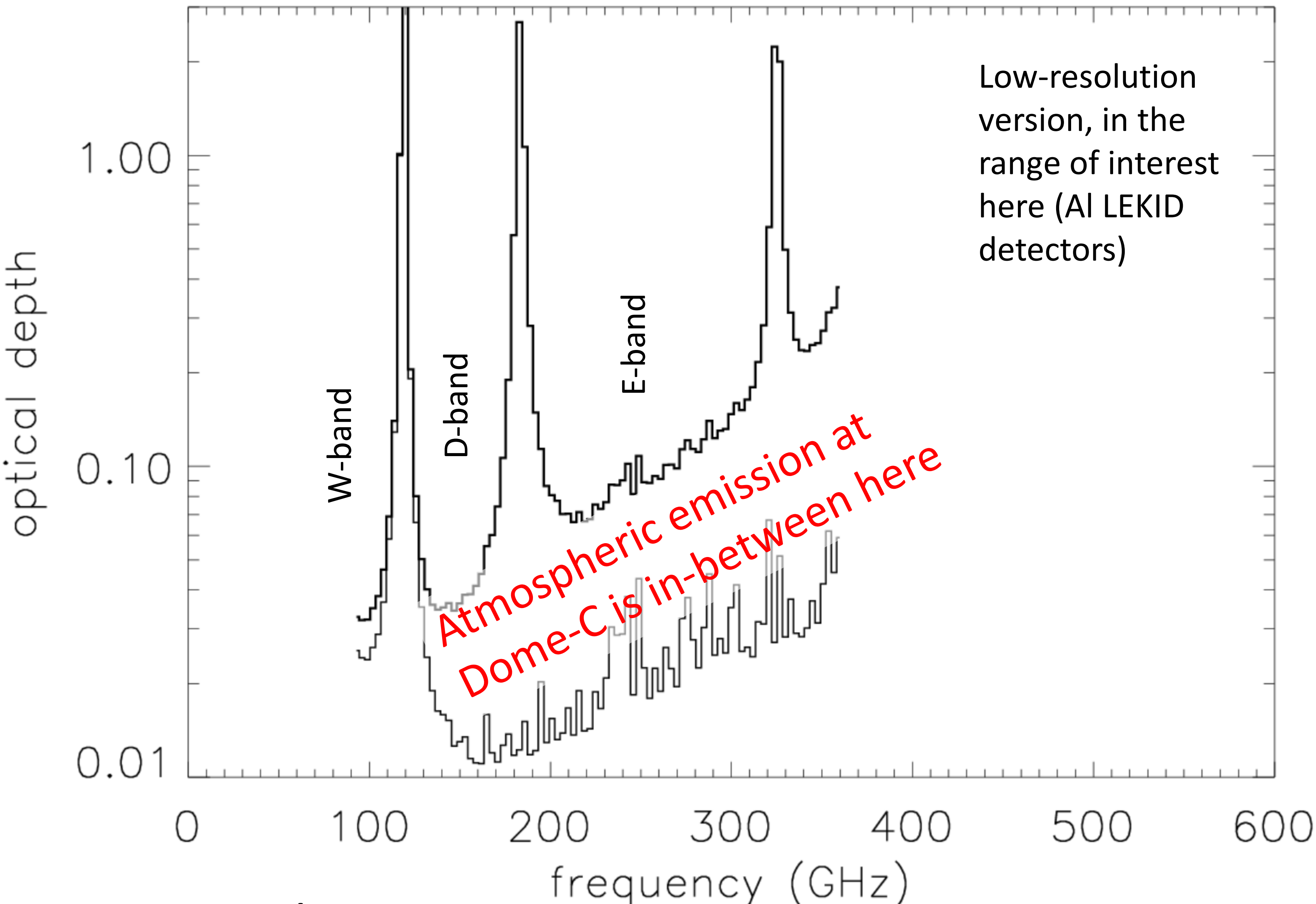

Low-resolution version, in the range of interest here (Al LEKID detectors)

+ <T>=200K in the winter

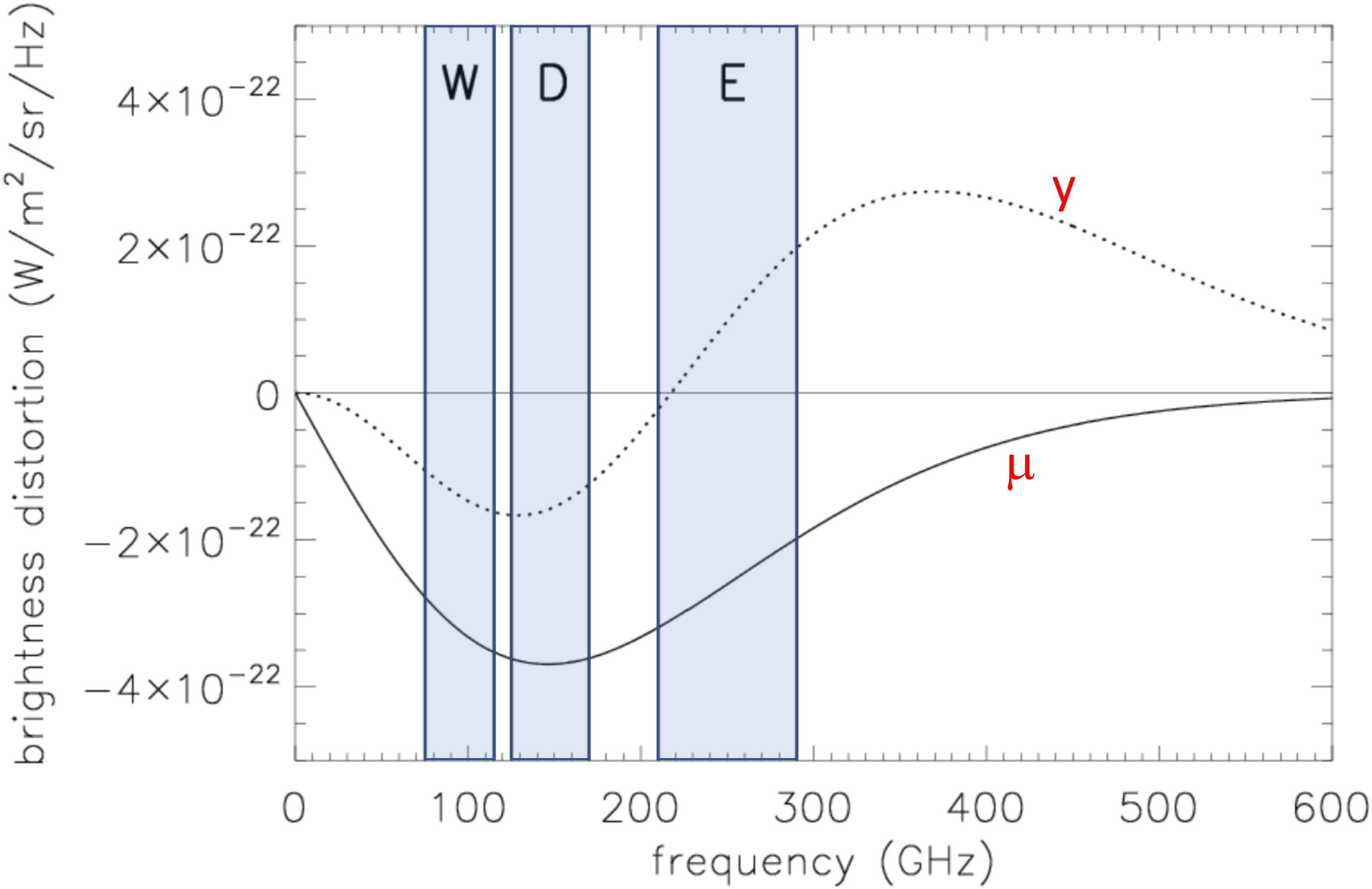

The signals to be measured are way smaller !

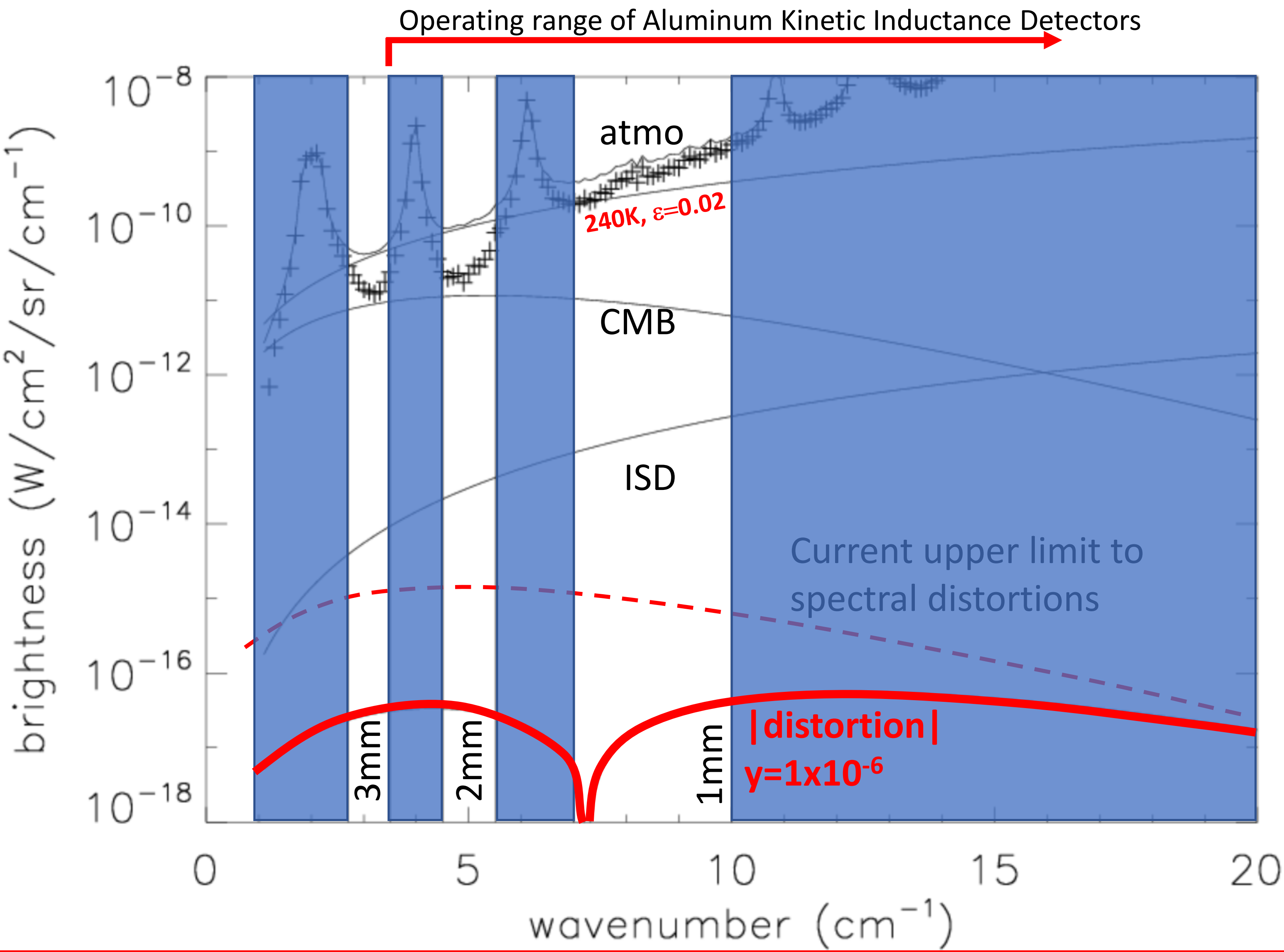

Consider the 2 mm and 1 mm atmospheric windows, which are very transparent (low emission) and where Aluminum KIDs work efficiently. Simulate measurements, mask lines, and attempt spectral template fitting for y, since it has a characteristic shape:

$$\text{meas} = \text{atmo} + \text{CMB} + \text{ISD} + \text{distor}(y=10^{-6}) - B_{ref}\,(300\text{K}, \varepsilon=0.02) + \text{noise (BLIP)}$$

Atmospheric separation

- Bulk atmospheric emission follows a cosec law with zenith angle.
- Can be estimated making sky dips, and subtracted.
- However, due to turbulence, atmospheric emission is not stable, and follows water vapour and temperature fluctuations.
- Main characteristics of the fluctuations:

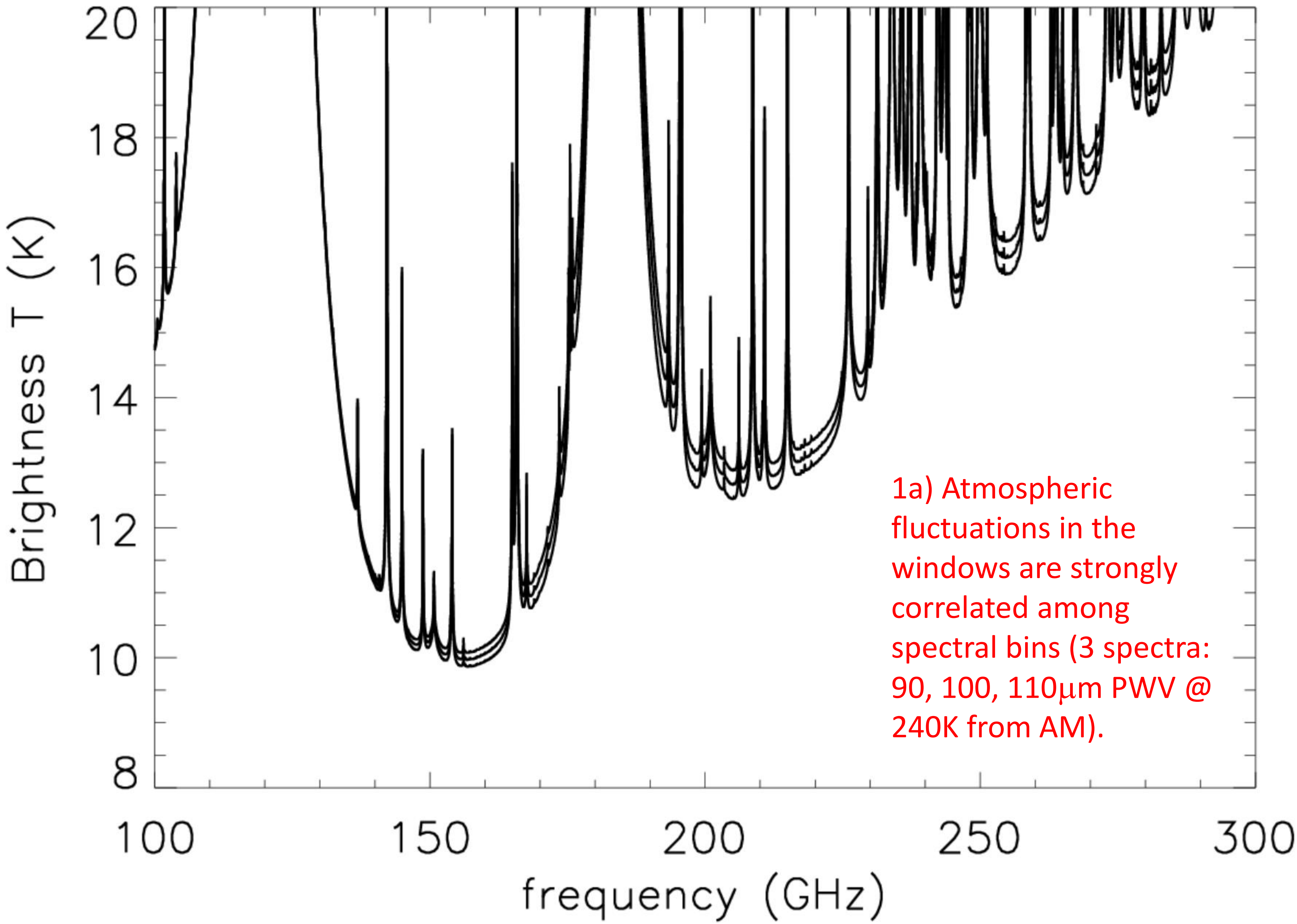

20
18
16
14
12
10
8
Brightness T (K)
100
150
200
250
300
frequency (GHz)
1a) Atmospheric fluctuations in the windows are strongly correlated among spectral bins (3 spectra: 90, 100, 110μm PWV @ 240K from AM).

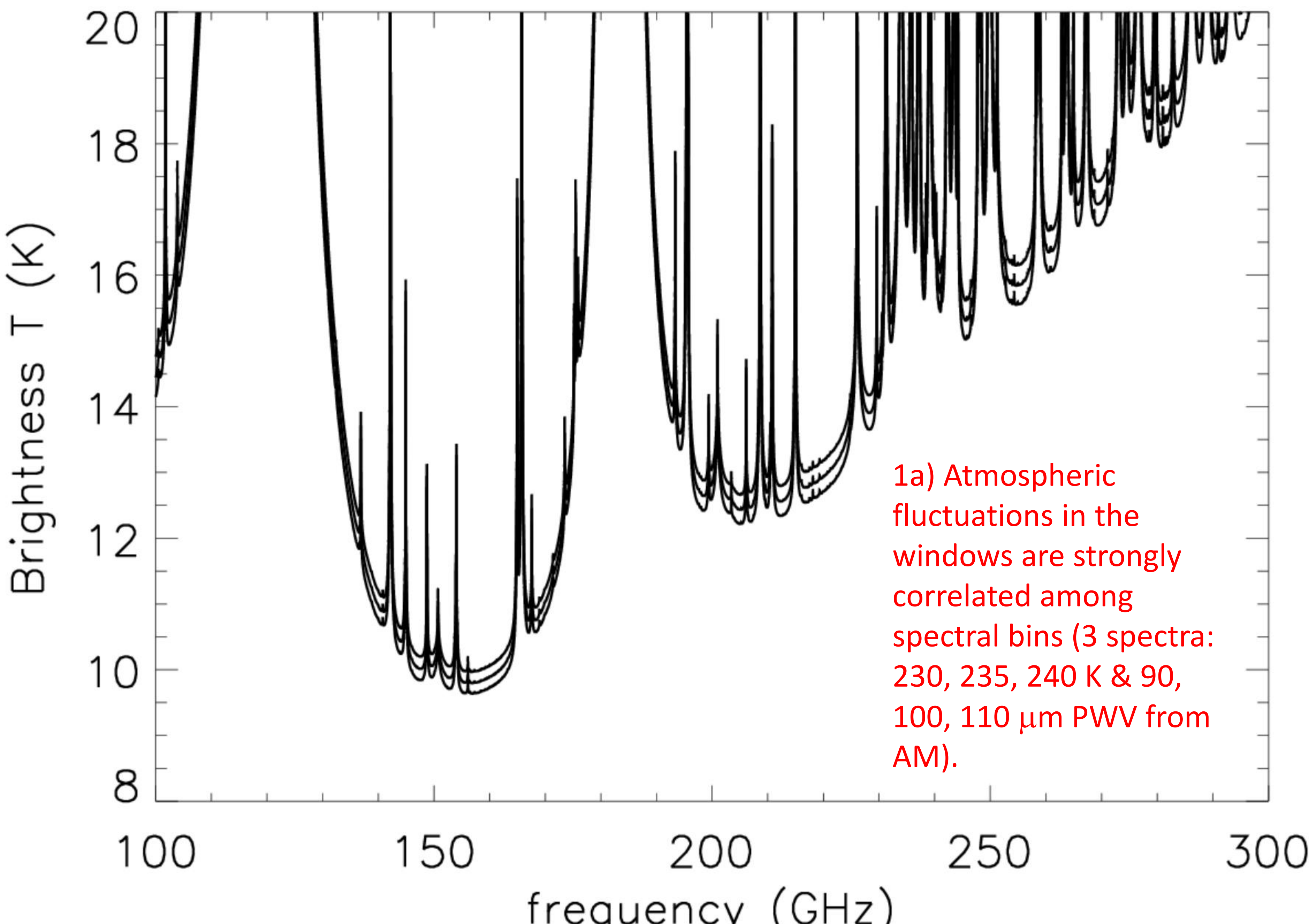

1a) Atmospheric fluctuations in the windows are strongly correlated among spectral bins (3 spectra: 230, 235, 240 K & 90, 100, 110 μm PWV from AM).
Brightness T (K)
frequency (GHz)
20
18
16
14
12
10
8
100
150
200
250
300

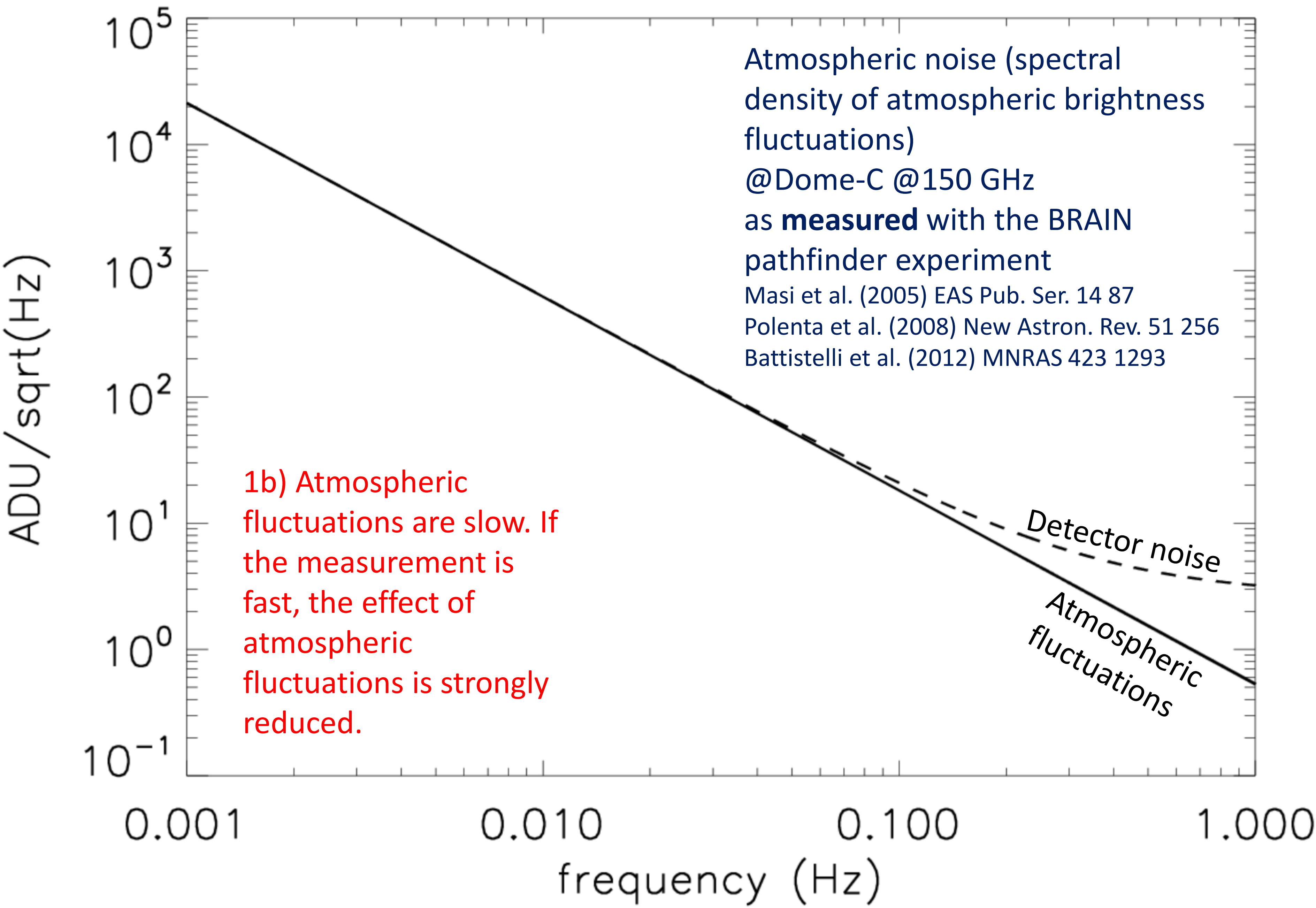

Atmospheric noise (spectral density of atmospheric brightness fluctuations)
@Dome-C @150 GHz
as **measured** with the BRAIN pathfinder experiment
Masi et al. (2005) EAS Pub. Ser. 14 87
Polenta et al. (2008) New Astron. Rev. 51 256
Battistelli et al. (2012) MNRAS 423 1293
1b) Atmospheric fluctuations are slow. If the measurement is fast, the effect of atmospheric fluctuations is strongly reduced.
Detector noise
Atmospheric fluctuations
ADU/sqrt(Hz)
frequency (Hz)
10^5
10^4
10^3
10^2
10^1
10^0
10^{-1}
0.001
0.010
0.100
1.000

Atmospheric separation

- Bulk atmospheric emission follows a cosec law with zenith angle.
- Can be estimated making sky dips, and subtracted.
- However, due to turbulence, atmospheric emission is not stable, and follow water vapour and temperature fluctuations.
- For this reason we would like to avoid modelling, and only use the hypothesis that on short time scales atmospheric emission is stable.
- If the sky-dip is performed faster than the typical timescale of atmospheric emission, the separation is effective.

COSMO : coping with the atmosphere

- We have to measure and subtract atmospheric emission, and we have to do it very quick.
- Recipe to mitigate the problem:

1. Work from a high altitude, cold and dry site (Dome-C, Antarctica) to minimize the problem
2. Measure the specific spectral brightness of atmospheric emission while measuring the brightness of the sky, modulating the optical depth
3. Use fast, sensitive detectors, and fast modulators.

COSMO sky/atmosphere scan strategy

Oversized (1.6m diameter), spinning flat mirror, 10° wedge (red/blue)
To scan circles (D=5°-20°) in the sky modulating atmospheric emission.
Center elevation ranges between 30° and 80° depending on cryostat tilt.

Cryostat tilt = 0°	Cryostat tilt = 20°	Cryostat tilt = 40°	Cryostat tilt = 50°
PT tilt = 40°	PT tilt = 20°	PT tilt = 0°	PT tilt = -10°
Min. elev. = 20°	Min. elev. = 40°	Min. elev. = 60°	Min. elev. = 70°
Max. elev. = 40°	Max. elev. = 60°	Max. elev. = 80°	Max. elev. = 90°

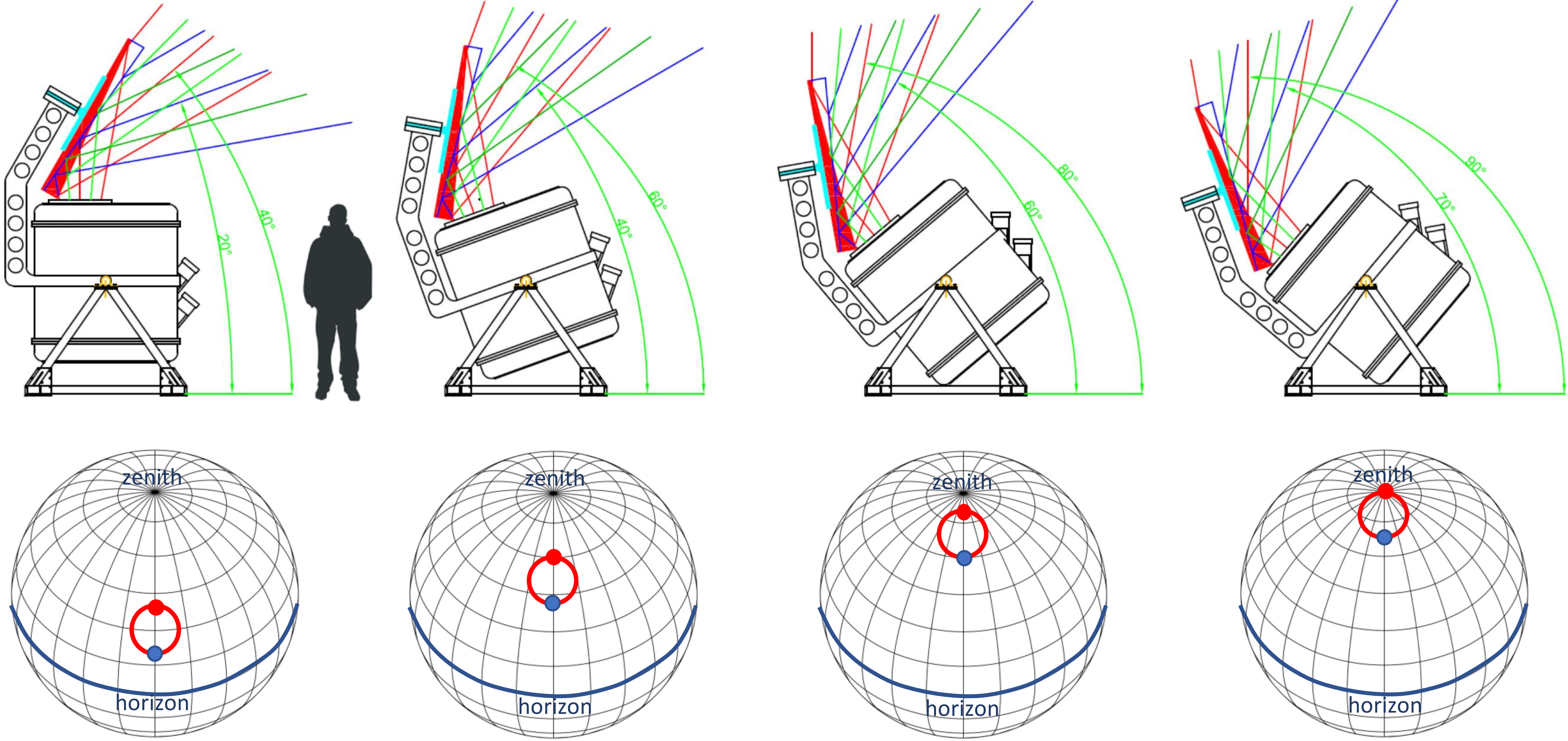

COSMO measurement timing

Exploits the availability of fast detectors (Kinetic Inductance Detectors - KIDs) and the know how of racing cars to beat atmospheric noise

detector performance		
detector time constant	**5.00E-05**	**s**
5 time constants	2.50E-04	s
NET	100	uK/sqrt(Hz)
noise per sample	6.3	mK

interferogram scan fast		
maximum wavenumber (Nyquist)	20	cm-1
sampling step	0.0125	cm
resolution	6	GHz
resolution	0.200	cm-1
number of frequency samples	100	
number of samples in double-sided interferogram	256	
time to complete an interferogram	0.064	s
interferograms per second	15.6	
mirror scan mechanism period	0.13	s
sky scan slow		
circle radius	5	deg
circle length	31.4	deg
beam size	0.5	deg
number of samples per circle (3 per beam)	188	
time per beam	0.192	s
time for 2 sky dips (downwards + upwards)	36.19	s
wedge mirror rotation rate	1.66	rpm
sky stability required for	18.10	s

sky scan fast		
circle radius	5	deg
circle length	31.4	deg
beam size	1	deg
number of samples per circle (3 per beam)	94	
time per beam	2.50E-04	s
time for 2 sky dips (downwards + upwards)	2.36E-02	s
wedge mirror rotation rate	2546	rpm
interferogram scan slow		
maximum wavenumber (Nyquist)	20	cm-1
sampling step	0.0125	cm
resolution	6	GHz
resolution	0.200	cm-1
number of frequency samples	100	
number of samples in double-sided interferogram	256	
time to complete an interferogram	6.032	s
interferograms per second	0.2	
mirror scan mechanism period	12.06	s
sky stability required for	**6.03**	**s**

- This configuration requires a fast cryogenic mirror scanning mechanism
- High dissipation in the cryo system

- This configuration requires a fast room-temperature mirror rotation device
- **Not impossible.**

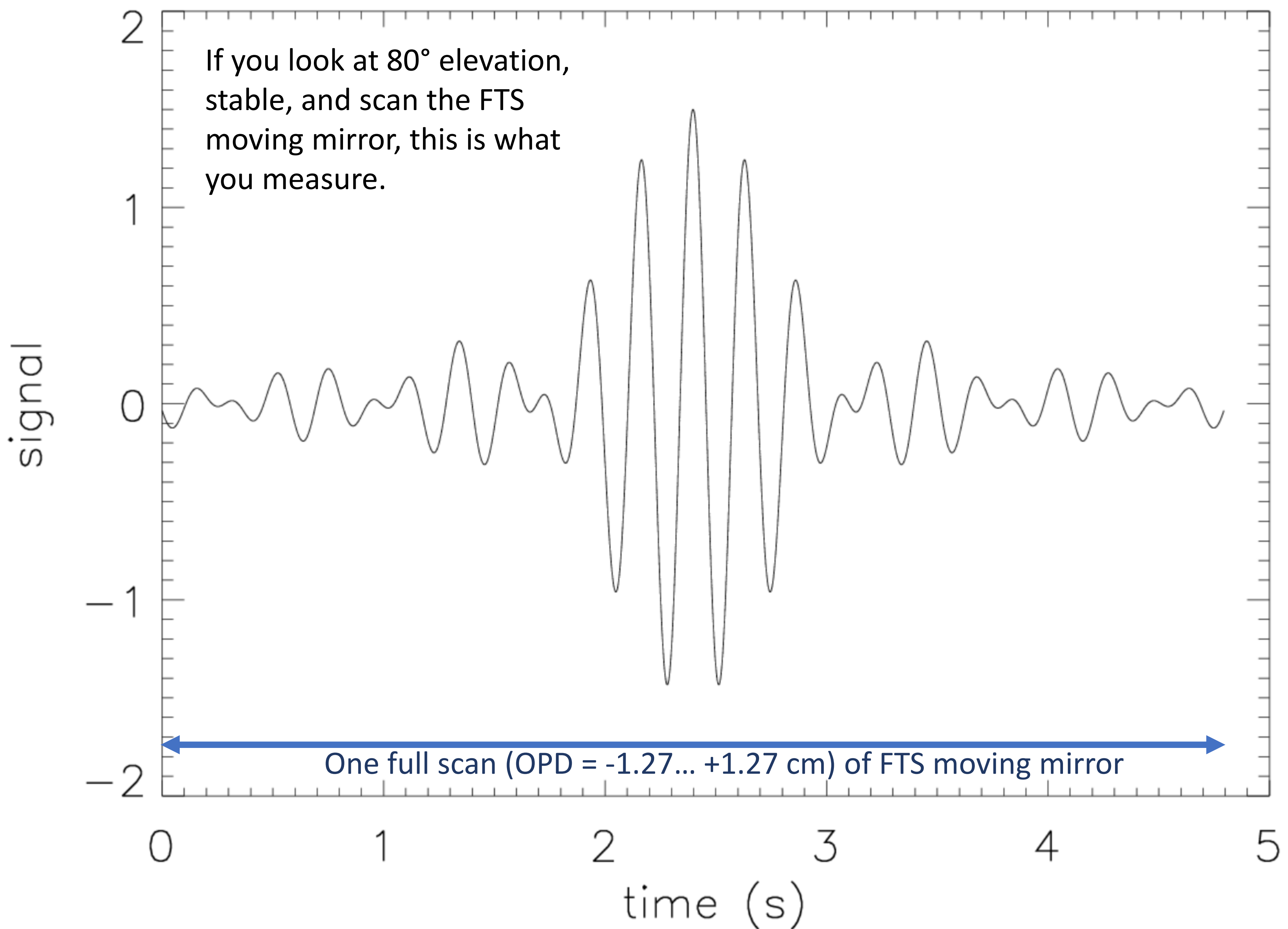

If you look at 80° elevation, stable, and scan the FTS moving mirror, this is what you measure.
One full scan (OPD = -1.27… +1.27 cm) of FTS moving mirror
signal
time (s)
2
1
0
−1
−2
0
1
2
3
4
5

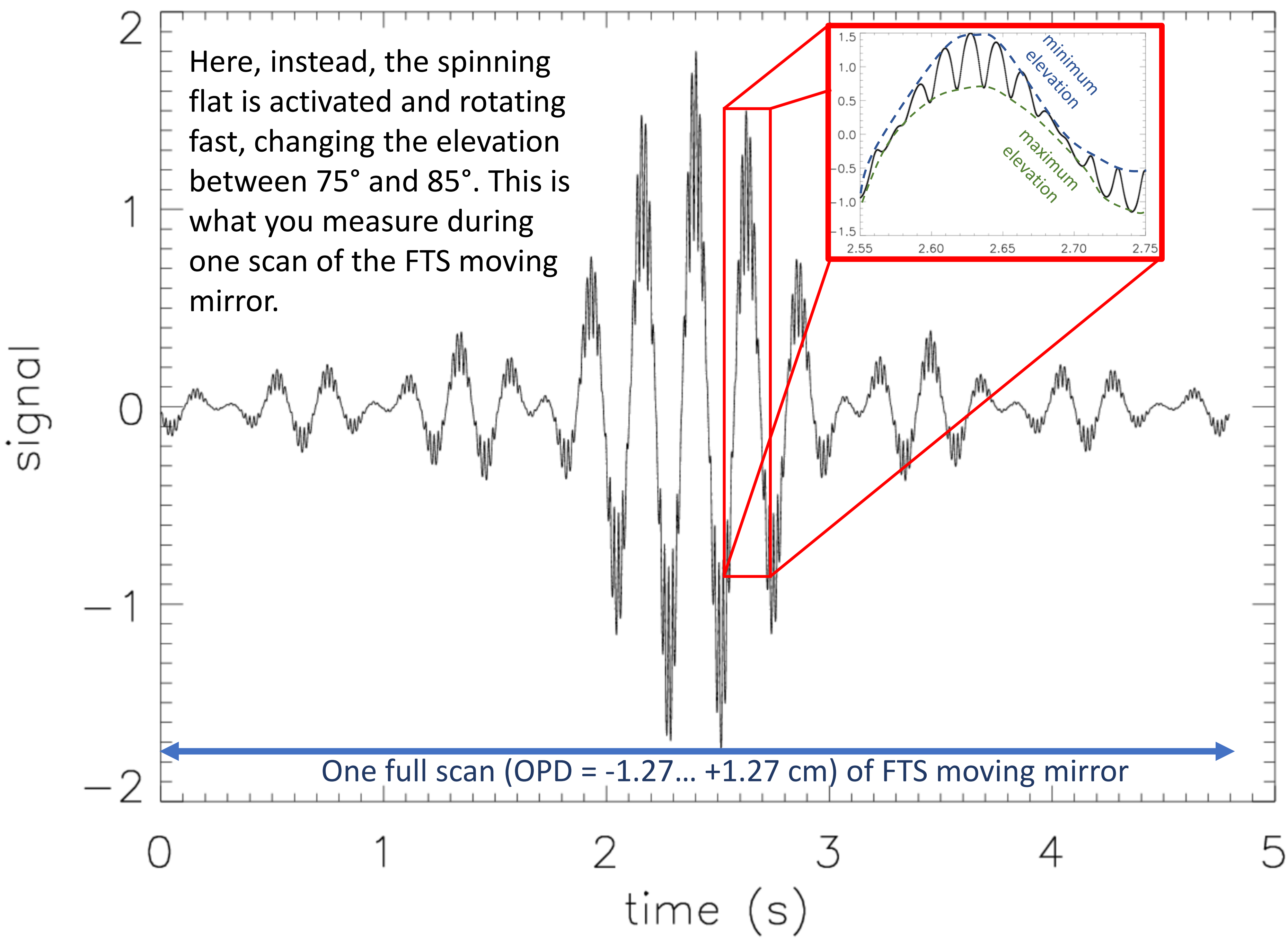
Here, instead, the spinning flat is activated and rotating fast, changing the elevation between 75° and 85°. This is what you measure during one scan of the FTS moving mirror.
minimum elevation
maximum elevation
One full scan (OPD = -1.27… +1.27 cm) of FTS moving mirror
signal
time (s)

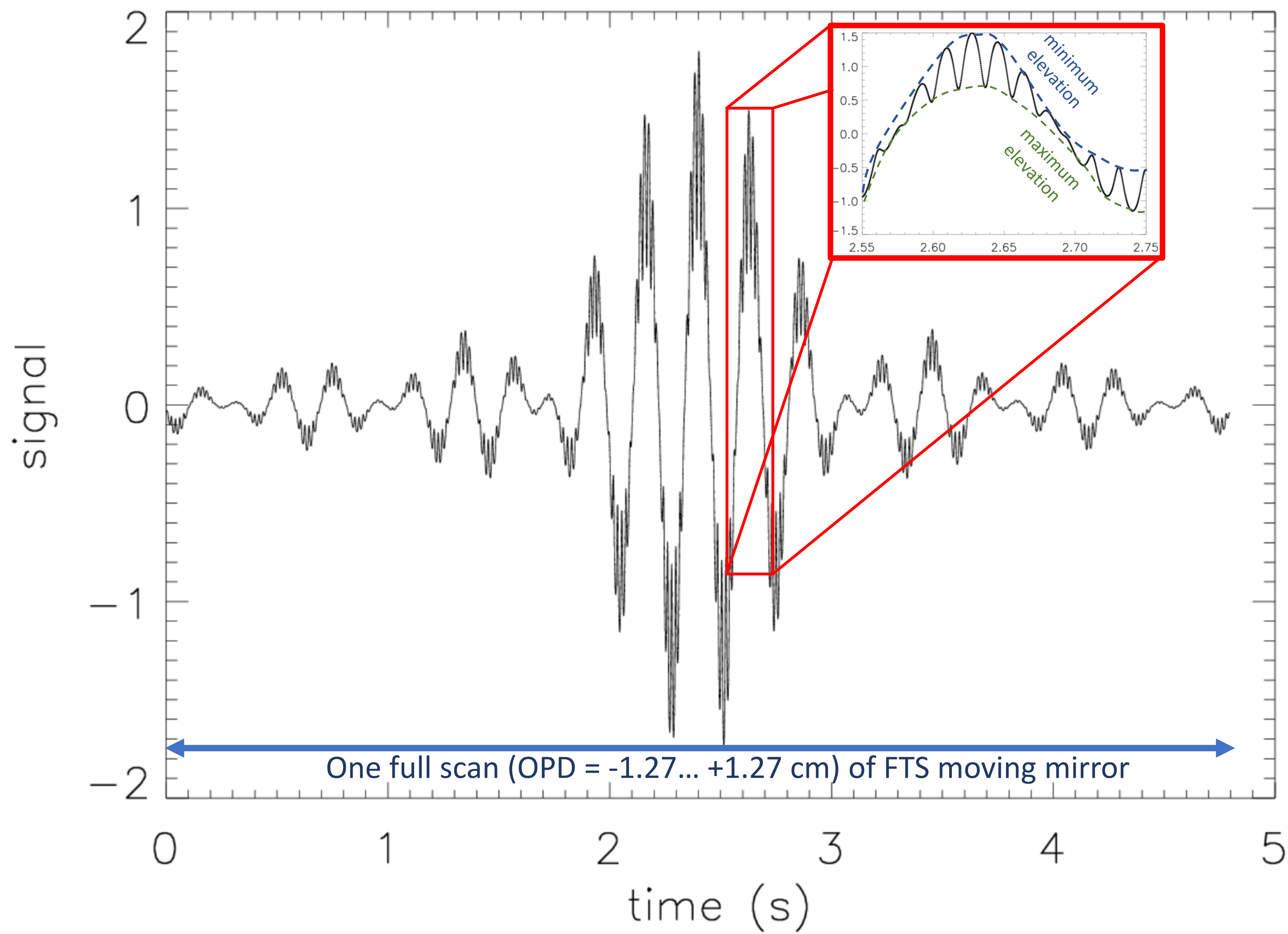

signal
time (s)
minimum elevation
maximum elevation
One full scan (OPD = -1.27… +1.27 cm) of FTS moving mirror

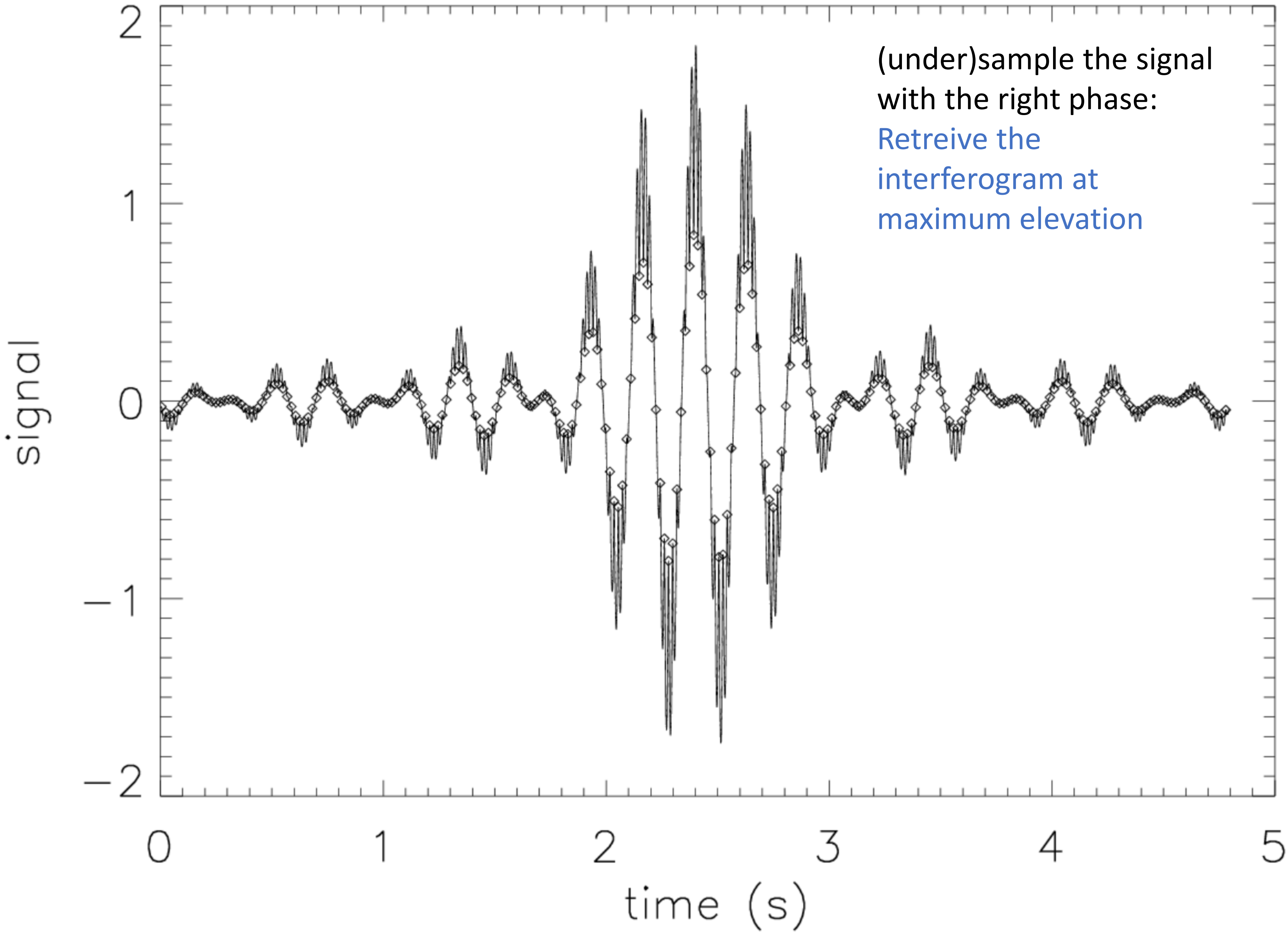

(under)sample the signal with the right phase:
Retreive the interferogram at maximum elevation

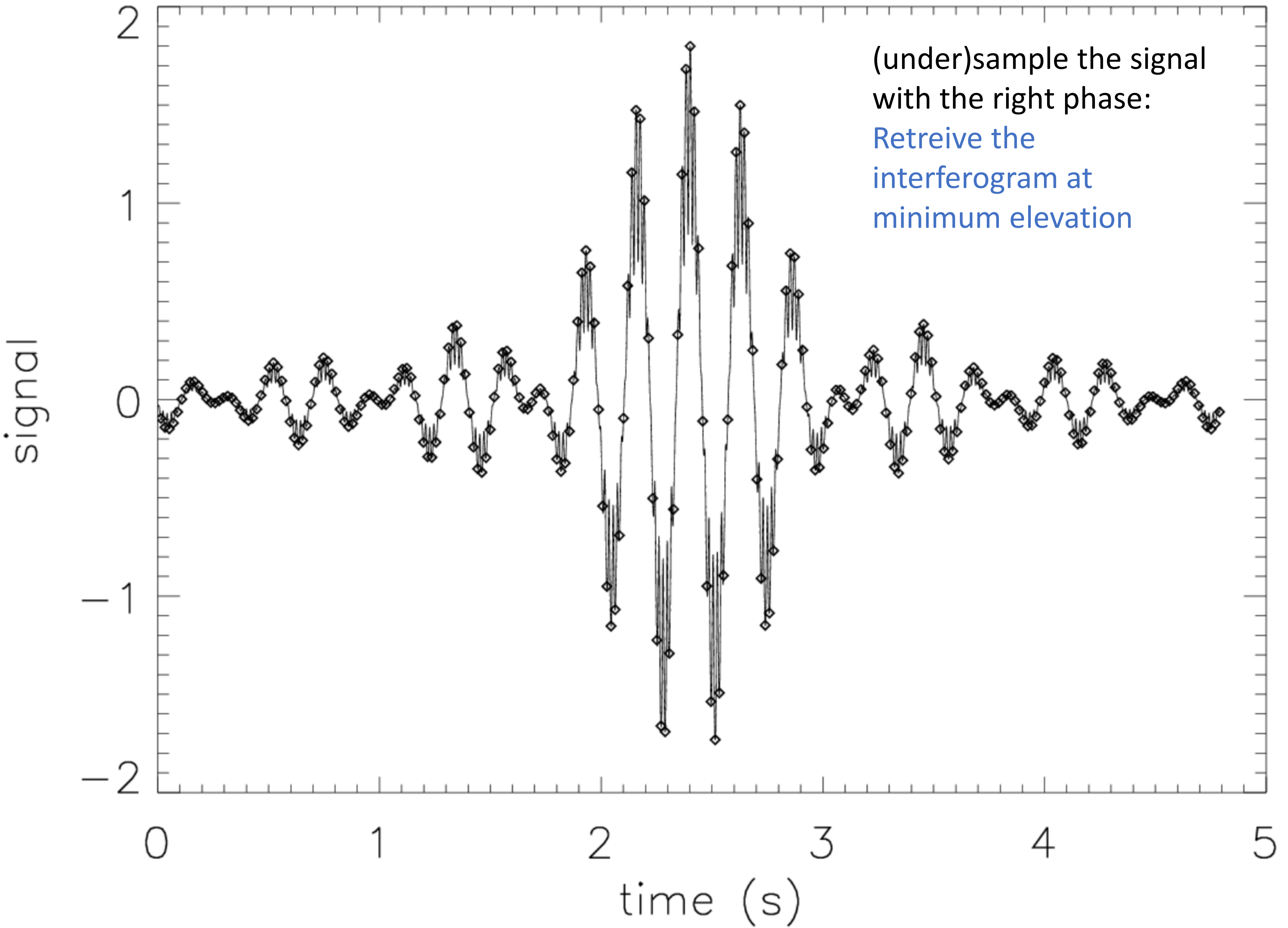

(under)sample the signal
with the right phase:
Retreive the
interferogram at
minimum elevation
signal
time (s)
2
1
0
−1
−2
0
1
2
3
4
5

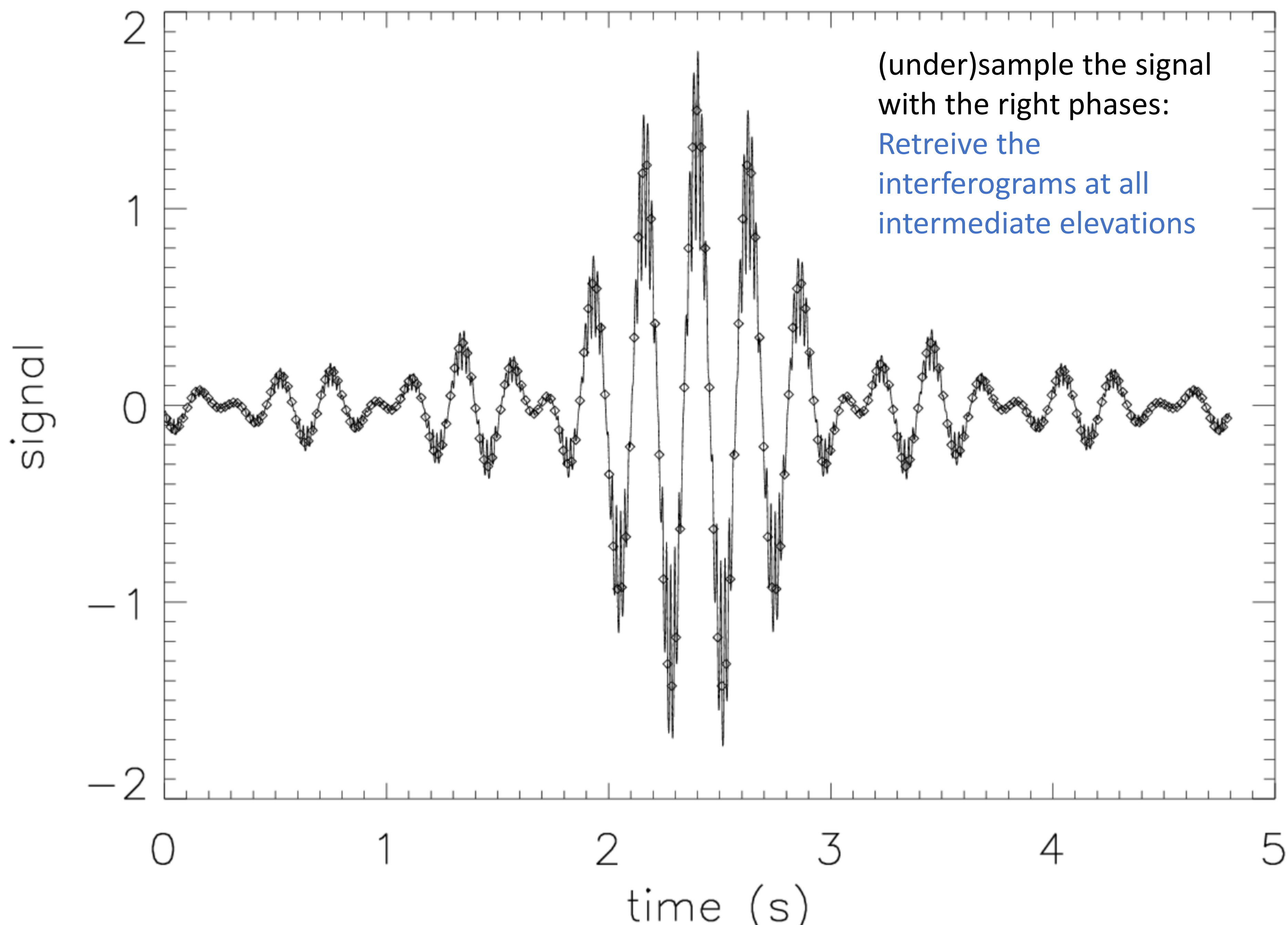

(under)sample the signal
with the right phases:
Retreive the
interferograms at all
intermediate elevations
2
1
0
−1
−2
signal
0
1
2
3
4
5
time (s)

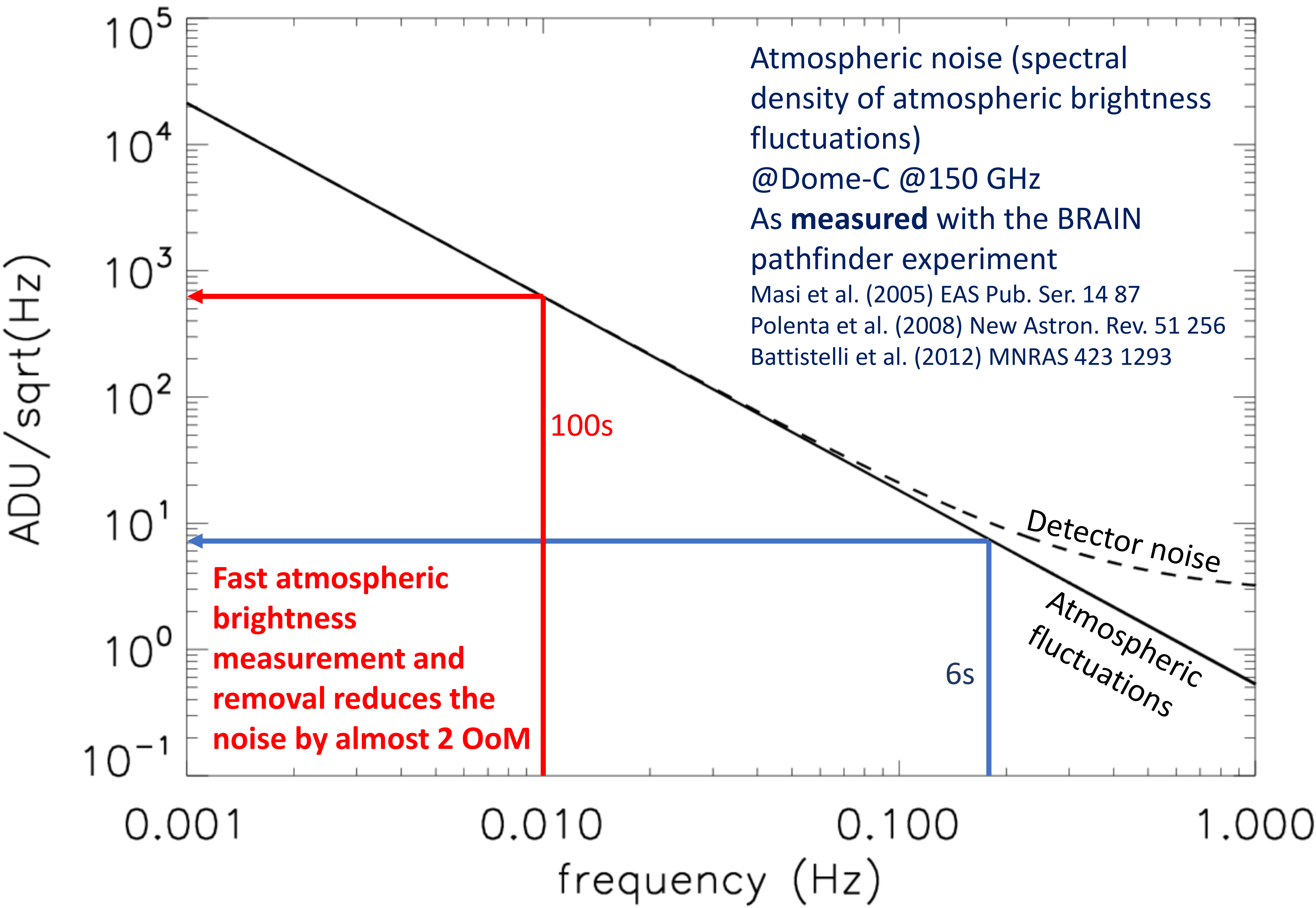

Atmospheric noise (spectral density of atmospheric brightness fluctuations)
@Dome-C @150 GHz
As **measured** with the BRAIN pathfinder experiment
Masi et al. (2005) EAS Pub. Ser. 14 87
Polenta et al. (2008) New Astron. Rev. 51 256
Battistelli et al. (2012) MNRAS 423 1293
100s
6s
Detector noise
Atmospheric fluctuations
Fast atmospheric brightness measurement and removal reduces the noise by almost 2 OoM
ADU/sqrt(Hz)
frequency (Hz)
0.001
0.010
0.100
1.000
10^5
10^4
10^3
10^2
10^1
10^0
10^{-1}

COSMO window emission

- Window (& mirror) common mode emissions must be measured and removed with high accuracy.
- Special calibration procedure based on the comparison of the emission from 1 or 2 windows stacked.
- PhD thesis, Lorenzo Mele
- Preliminary results:

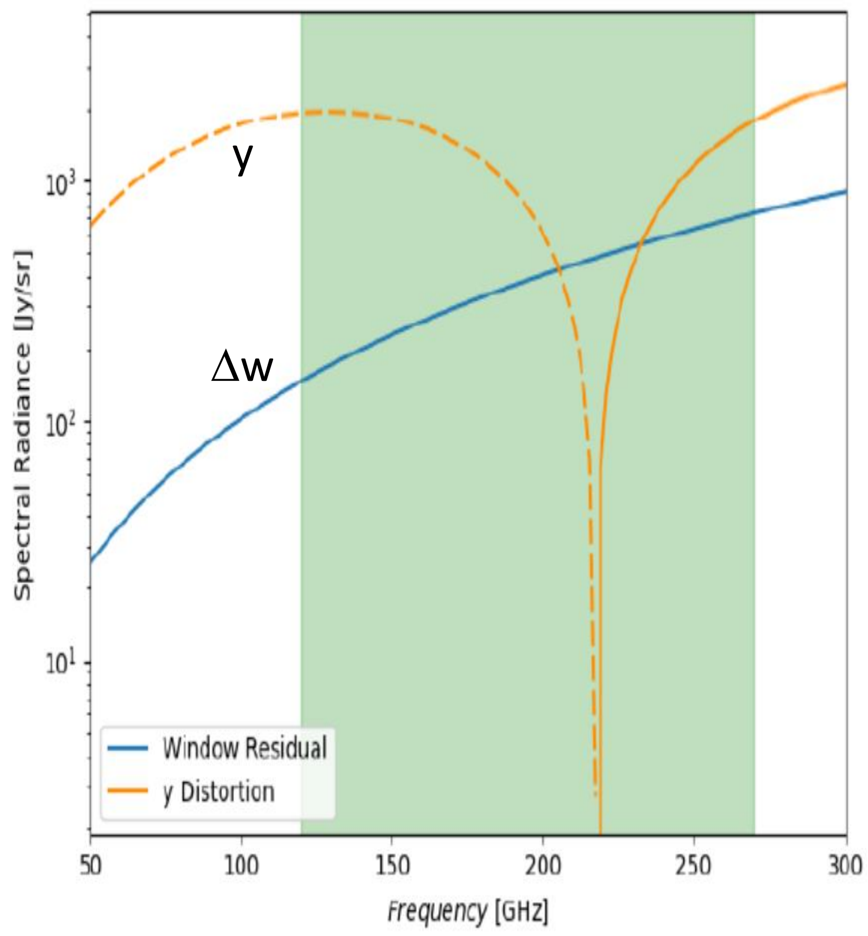

Naive Forecast Simulation

- Retreive all the interferograms at all different elevations, and Fourier transform them to obtain the measurements of the specific spectral brightness at all elevations. This is a very fast *sky-dip* measurement.
- The atmospheric contribution depends on the optical depth and on the temperature profile.
- For a naive single isothermal layer, the measured brightness at elevation ***e*** is

$$B(\nu, e) = B(T_{atm}, \nu)\left(1 - e^{-\tau(\nu,e)}\right) + B_{sky}e^{-\tau(\nu,e)} - B(T_{ref}, \nu).$$

- which can be rewritten $B(\nu, e) = a(\nu)x(\nu, e) + b(\nu)$
- where

$$x = 1 - \exp(-\tau_z(\nu)/\cos(e))$$

$$B_{sky}(\nu) - B(T_{ref}, \nu) = b(\nu)$$

$$B(T_{atm}, \nu) - B(T_{ref}, \nu) = b(\nu) + a(\nu)$$

- So, for each frequency, a simple linear fit will provide the measurement of the sky brightness, with atmospheric emission removed.
- Since the length of the data record used for this procedure is very short (few seconds) slowly fluctuating atmospheric emission is continuously removed.
- The SNR of this determination will be low, but many measurements can be stacked to gain SNR for the monopole of sky emission.

COSMO sky / atmosphere scan simulations

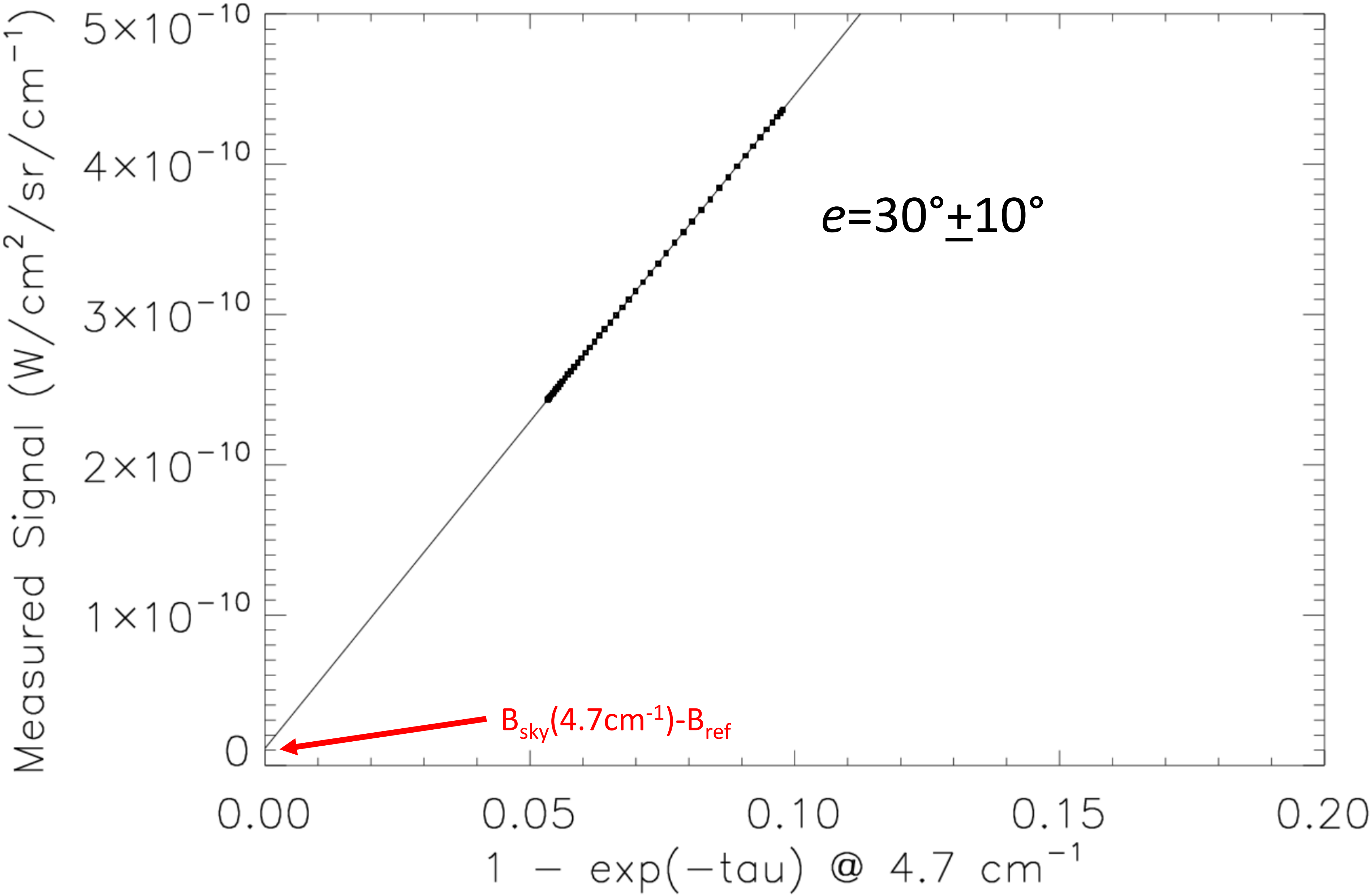

COSMO sky / atmosphere scan simulations

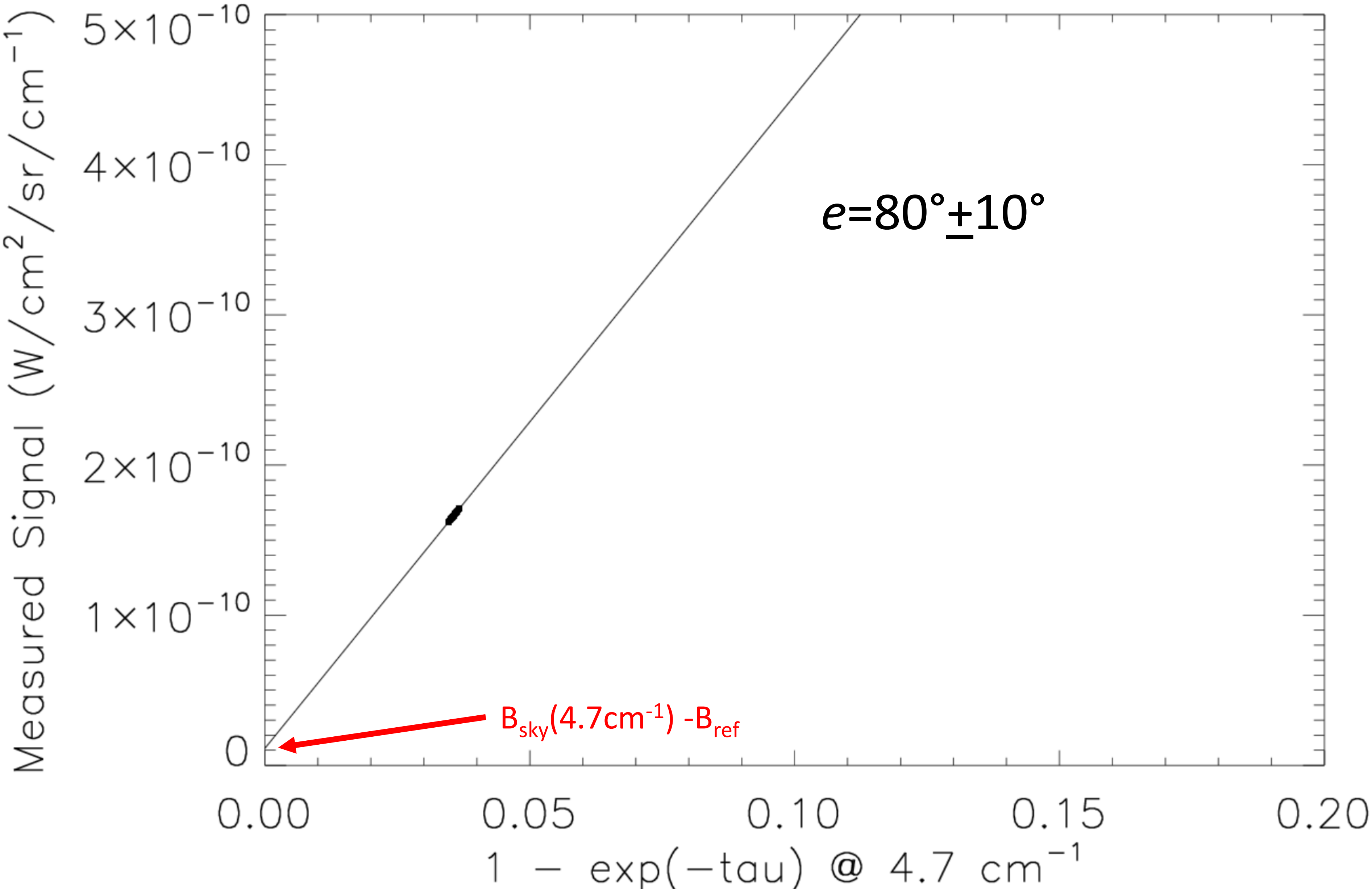

COSMO sky / atmosphere scan simulations

Result of «vanilla» simulation:

- **assumed small atmospheric fluctuations** (0.01% in 6s)
- **no spatial gradients in atmosphere**
- **no foregrounds (including window)**
- Photon noise limited detector array (100 dets)
- Long integration time (1000 hours)

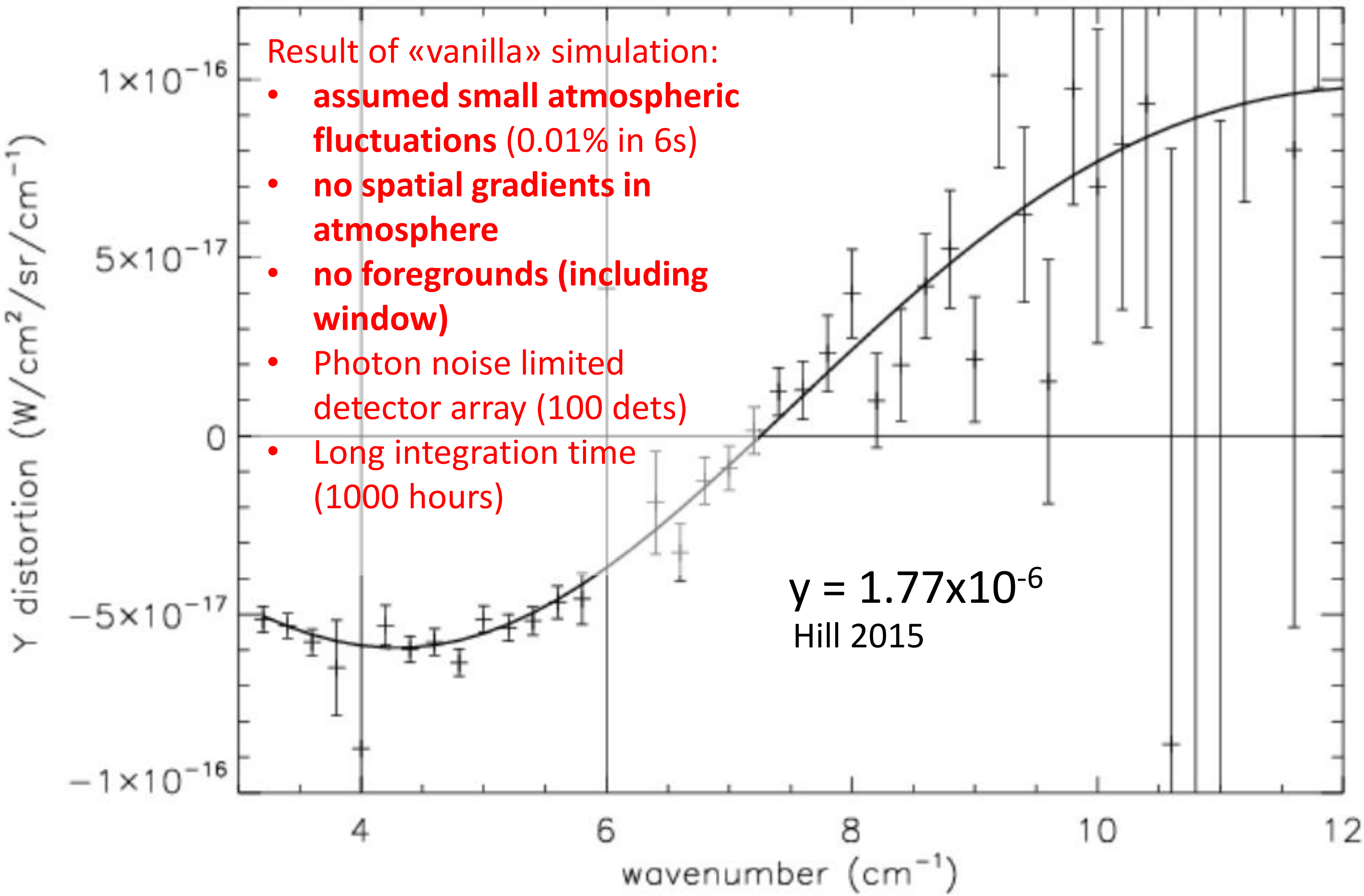

***COSMO'*s successor: a balloon-borne instrument ?**

- **LSPE** LDB payload
  http://planck.roma1.infn.it/LSPE
- Works in the polar night
- Suitable cryogenic system
- Possible to add (slower ?) modulator, if needed
- Might gain a factor 10.

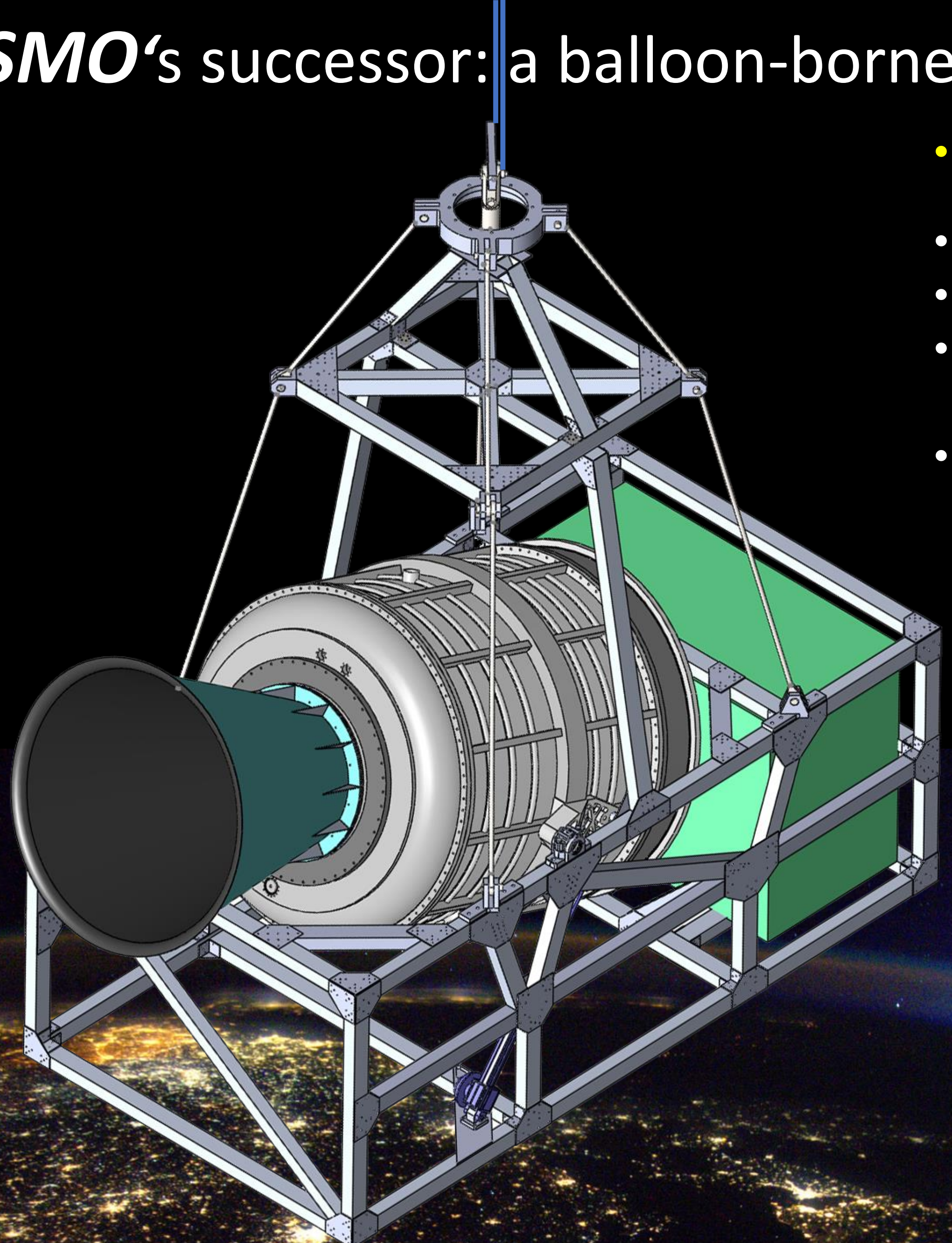

COSMO on a balloon:

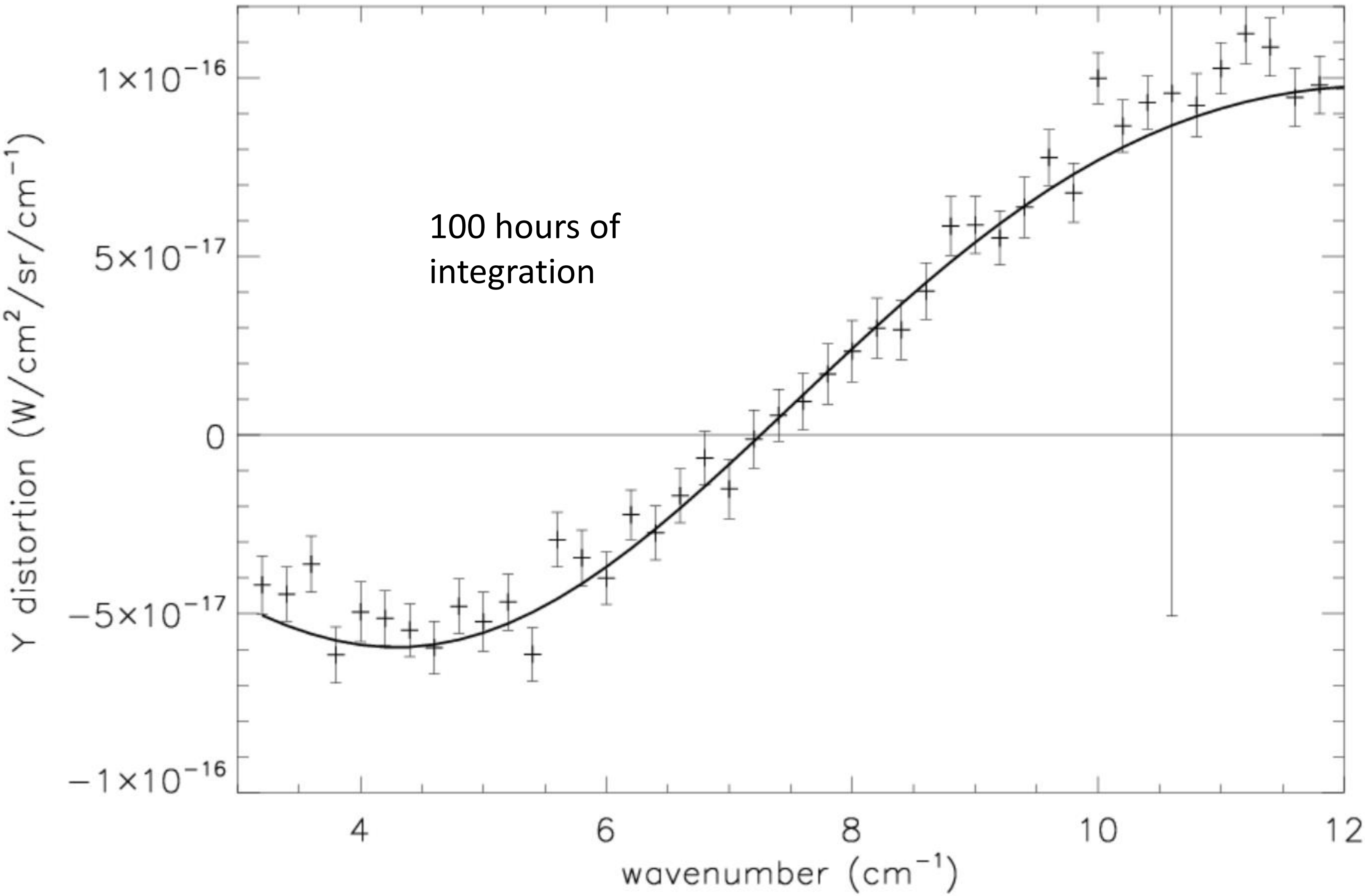

See also recent CNES study proposal BISOU (Balloon Interferometer for Spectral Observations of the primordial Universe) - Maffei et al. 2019.

Conclusions

- CMB research is expanding towards large and global experiments, with very high discovery potential
- Stratospheric balloons offer a great deal of opportunities for CMB research, covering the high-frequency range of CMB measurements and dust-related polarized foregrounds.
- Balloon-borne **Stokes Polarimeters** represent very useful pathfinders for the measurement solutions of LiteBIRD:
  - Polarization Modulator Unit (rotation and optical performance)
  - Detectors in close to representative environment
- Balloon-borne **spectrometers** (differential and absolute) represent a way to investigate spectral distortions, opening a new window on the early universe, and paving the way to a dedicated satellite mission.